CHAPTER 3 GEOCHEMICAL SURVEY OF TUNCELİ AREA

3. Geochemical survey of Tunceli area

3-1 Introduction

Geochemical investigation of soil samples was performed in 1978 in an area covering 115 km^2. As a result, a large anomaly area, widely extending in Mamlis area, was found, and observed to extend eastward between the Düzpelit Formation and the Bulanık quartz diorite. Therefore, geological and geochemical investigation was carried out in the Mamlis-Kört-Mehmet area including the above-mentioned mineralization area, which covered 50 km^2. Soil samples for geochemical survey were taken in the course of geological field survey conducted on the scale of 1:10,000, collected by Ridge and Spur method, the same as in 1978. They were collected at constant intervals whenever possible. In the strong alteration areas east of Mamlis and Kört areas, soil samples were taken at 150 meter intervals and detailed geological investigation was carried out on the scale of 1 : 2,000, in order to study the ore deposits and mineralized zone in detail. In other areas samples were taken at an interval of 300 meters. Sampling density was 12 samples/km^2, covering an area of over 50 km^2. Total of 620 samples were collected.

The samples were sieved through 80 mesh in the field. Topographical maps on a scale of 1 : 10,000 were used for positioning of soil samples.

3-2 Chemical analysis

Analysis of soil samples was performed by the chemical section of the Diyarbakır branch office of M.T.A. Components which were analyzed by atomic absorption spectroscopic method were Cu, Pb, Zn and Mo, the same as in 1978. Results of chemical analysis are shown in Appendix 8.

3-3 Results of chemical analysis

The soil samples taken in the investigated area did not contain humus soil, and are considered to indicate the composition of the weathered parent material. As a result of chemical analysis in 1979, parent material was divided into three groups as follows.

a. Granitic rocks .... Gt
(Bulanık quartz diorite)

b. Düzpelit Formation (Miocene) .... Dmd
(Dacite, and dacitic pyroclastic rocks)

c. Atadoğdu ~ Kamışlık Formation (Eocene) .... Aem, Kem
(Calcareous mudstone and sandstone)

Based on the results of chemical analysis, no noteworthy difference based on the above-mentioned lithofacies classification was found, because the area where soil samples were taken was small in the range of 50 km^2. Background values of copper and lead in the Bulanık quartz diorite are higher than those in the Eocene and Miocene sediments. The relationship between background and rock types is similar to that found last year, but the background of Eocene sediment zone is higher than that of the other

Fig. 3-1 Location map of soil samples in Tunceli area

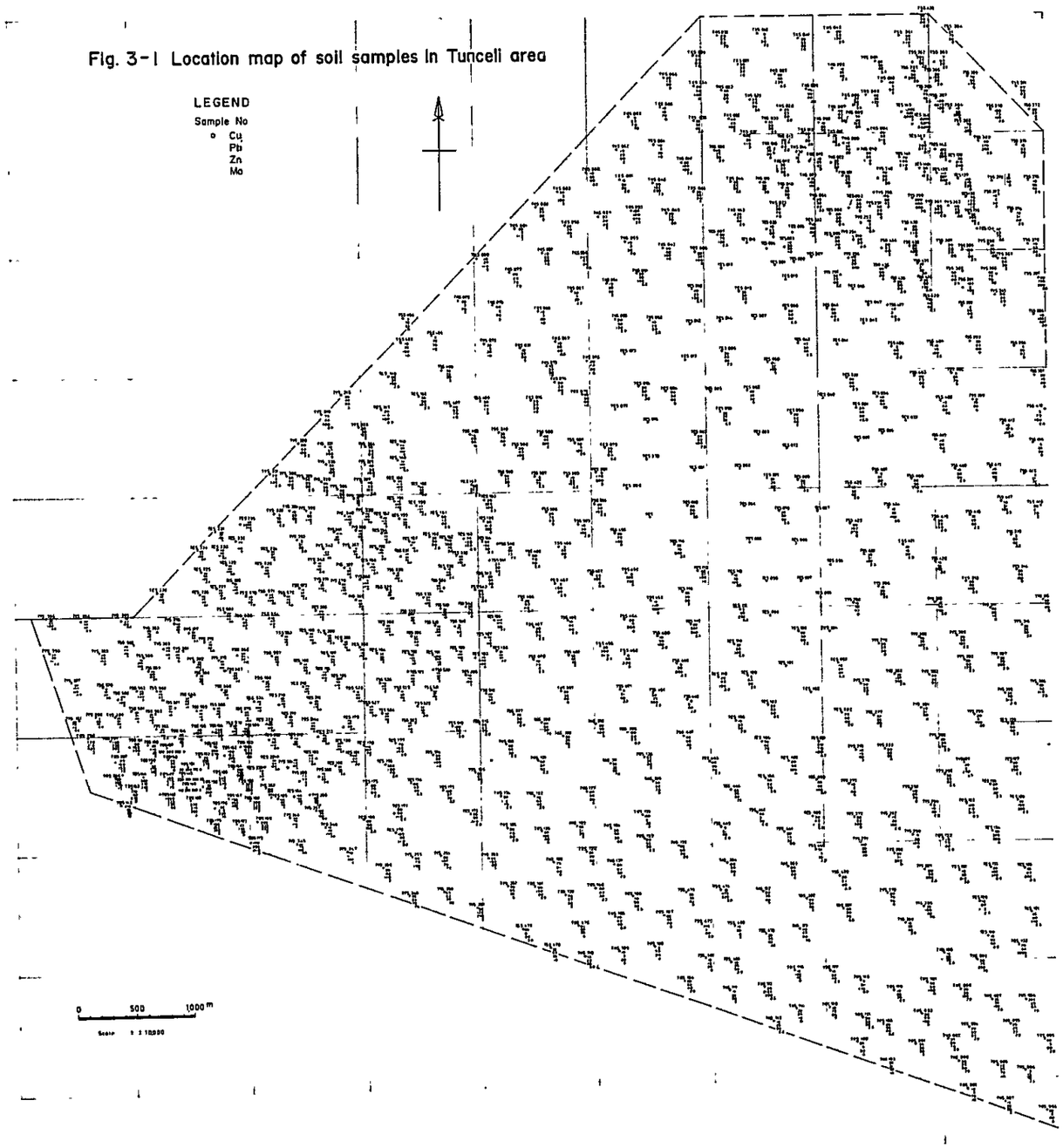

Table 3-1 Pattern of Dispersion

Geological Unit	Cu		Pb		Zn		Mo	
	Deviation	Pattern	Deviation	Pattern	Deviation	Pattern	Deviation	Pattern
Soil(in all)	H	excess of high value	M	excess of high value	M	excess of high value	M	two groups mixture
Quartz diorite	M	two groups mixture	M	excess of high value	M	excess of high value	H	excess of low value
Miocene (includes dacite)	H	two groups mixture	M	excess of high value	H	two groups mixture	M	excess of low value
Eocene	H	excess of high value	H	excess of high value	H	two groups mixture	M	excess of low value

Deviation
Very High (VH): standard deviation $S \geqq 0.7$
High (H) : " $0.7 > S \geqq 0.3$
Moderate (M) : " $0.3 > S \geqq 0.2$
Low (L) : " $0.2 > S$

Table 3-2 Correlation coefficient of geochemical elements

Geological Unit	ρ					
	Cu-Pb	Cu-Zn	Cu-Mo	Pb-Zn	Pb-Mo	Zn-Mo
Soil samples (in all)	0.4809	0.3706	0.1882	0.5245	0.0745	0.0817
Quartz diorite	0.4018	0.2291	0.2217	0.5469	0.2485	0.1159
Miocene (includes dacite)	0.3221	0.2020	0.2306	0.3208	0.0067	Δ0.0079
Eocene	0.4964	0.5571	0.1398	0.6714	0.0732	0.1577

Table 3-3 Background and Threshold Value

Geological Unit		Soil (in all)	Quartz diorite	Miocene	Eocene
Population (N) *1		655	142	133	139
Background value (b) ppm	Cu	35	65	24	35
	Pb	54	61	51	46
	Zn	89	70	86	95
	Mo	3.7	2.7	4.8	3.4
Geometric deviation:(S')	Cu	2.400	1.615	2.042	2.200
	Pb	1.889	1.607	1.862	2.109
	Zn	1.854	1.771	1.628	2.000
	Mo	1.973	2.222	1.646	1.853
Standard deviation (S)	Cu	0.380	0.208	0.310	0.342
	Pb	0.276	0.206	0.270	0.324
	Zn	0.268	0.248	0.212	0.301
	Mo	0.295	0.347	0.216	0.268
Threshold value (t) ppm	Cu	175	170	98	110
	Pb	105	130	105	133
	Zn	220	187	154	274
	Mo	12.0	10.4	12.5	14.0
Supplementary threshold value (t') *2 ppm	Cu	91	117	54	77
	Pb	104	100	95	97
	Zn	165	130	140	190
	Mo	8.2	6.7	8.4	7.1
Supplementary threshold value (2t) ppm	Cu	350	340	196	220
	Pb	210	260	210	266
	Zn	440	374	308	548
	Mo	24.0	20.8	25.0	28.0

*1: Total number of specimens (655)

*2: t' is the value either equal to or less than 10% of cumulative frequency percentage of "t value" or corresponds to less than 16% of the highest value of total number of cumulative frequency.

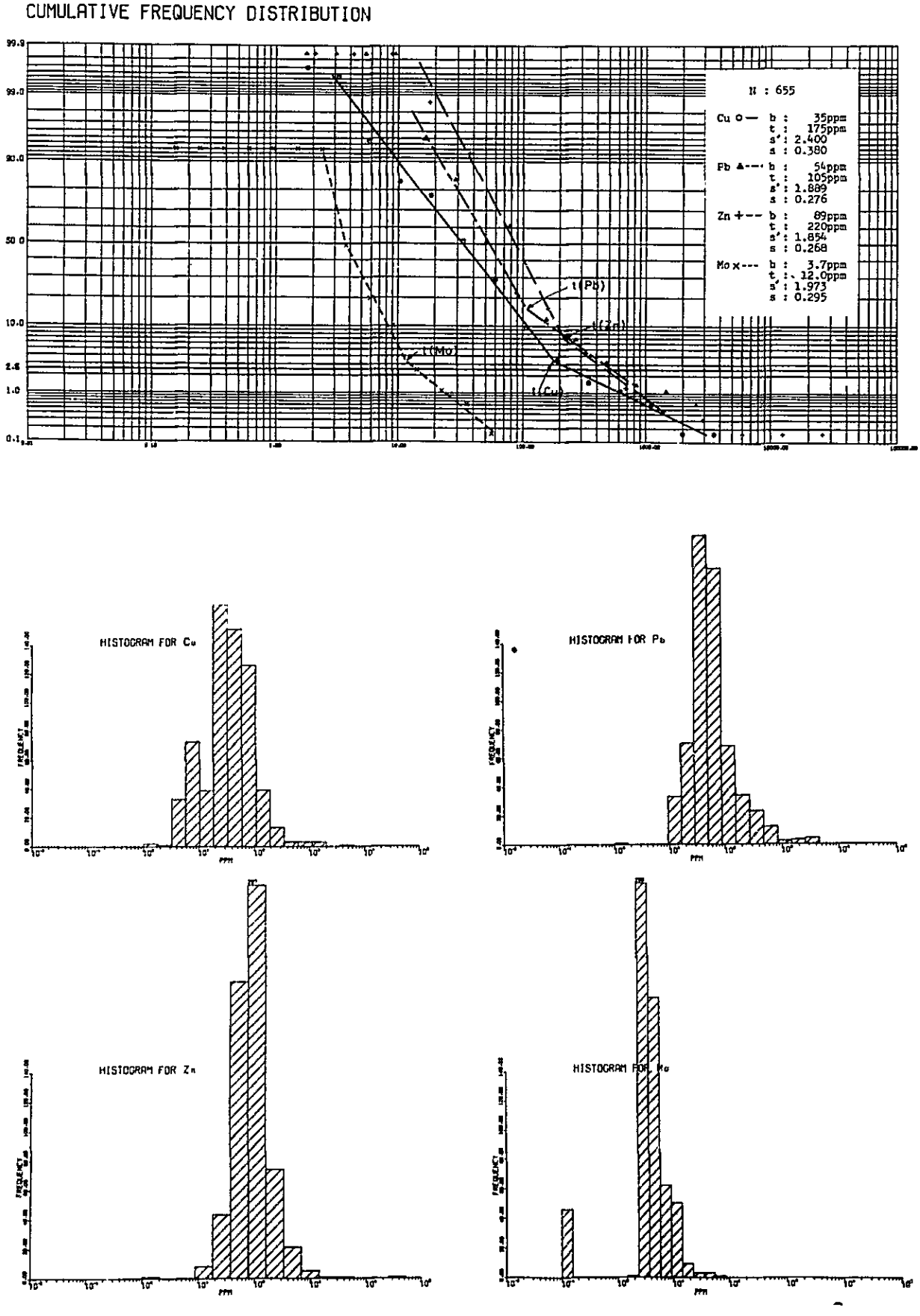

Fi. 3-2 Cumulative frequency distribution and histogram for the soil samples

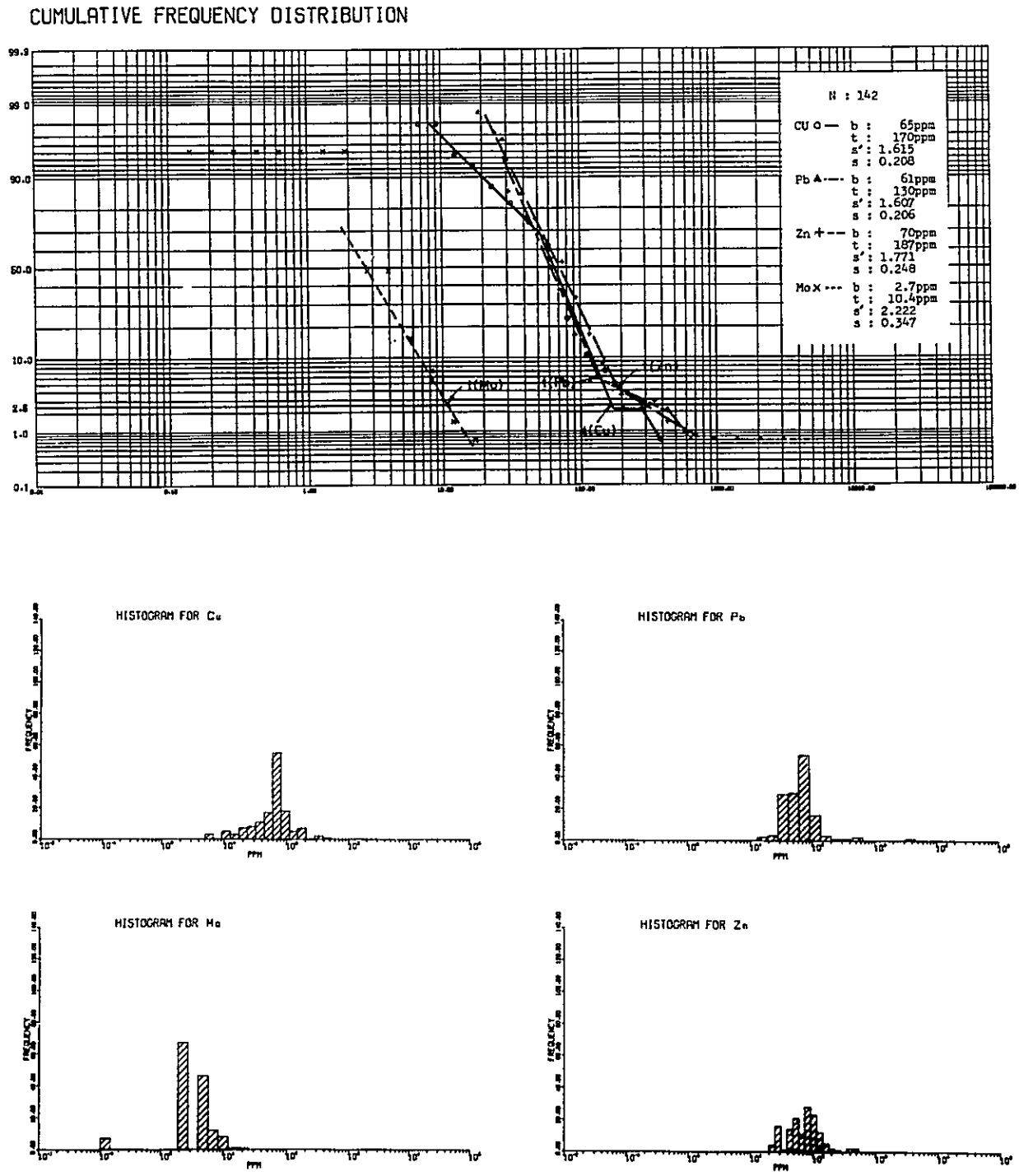

Fig. 3-3 Cumulative frequency distribution and histogram for the Bulanık quartz diorite

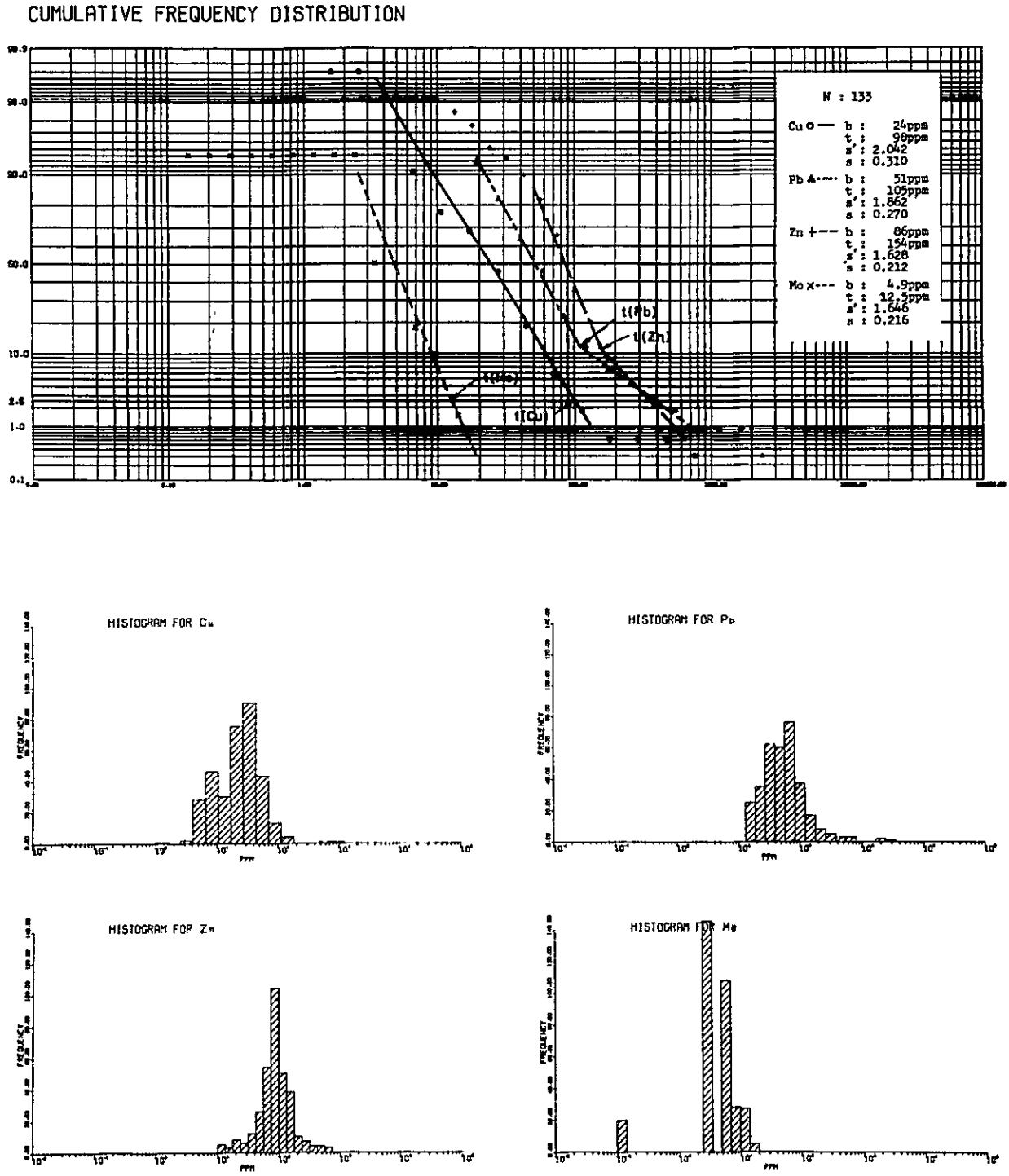

Fig. 3-4 Cumulative frequency distribution and histogram for the Düzpelit Formation (including dacite)

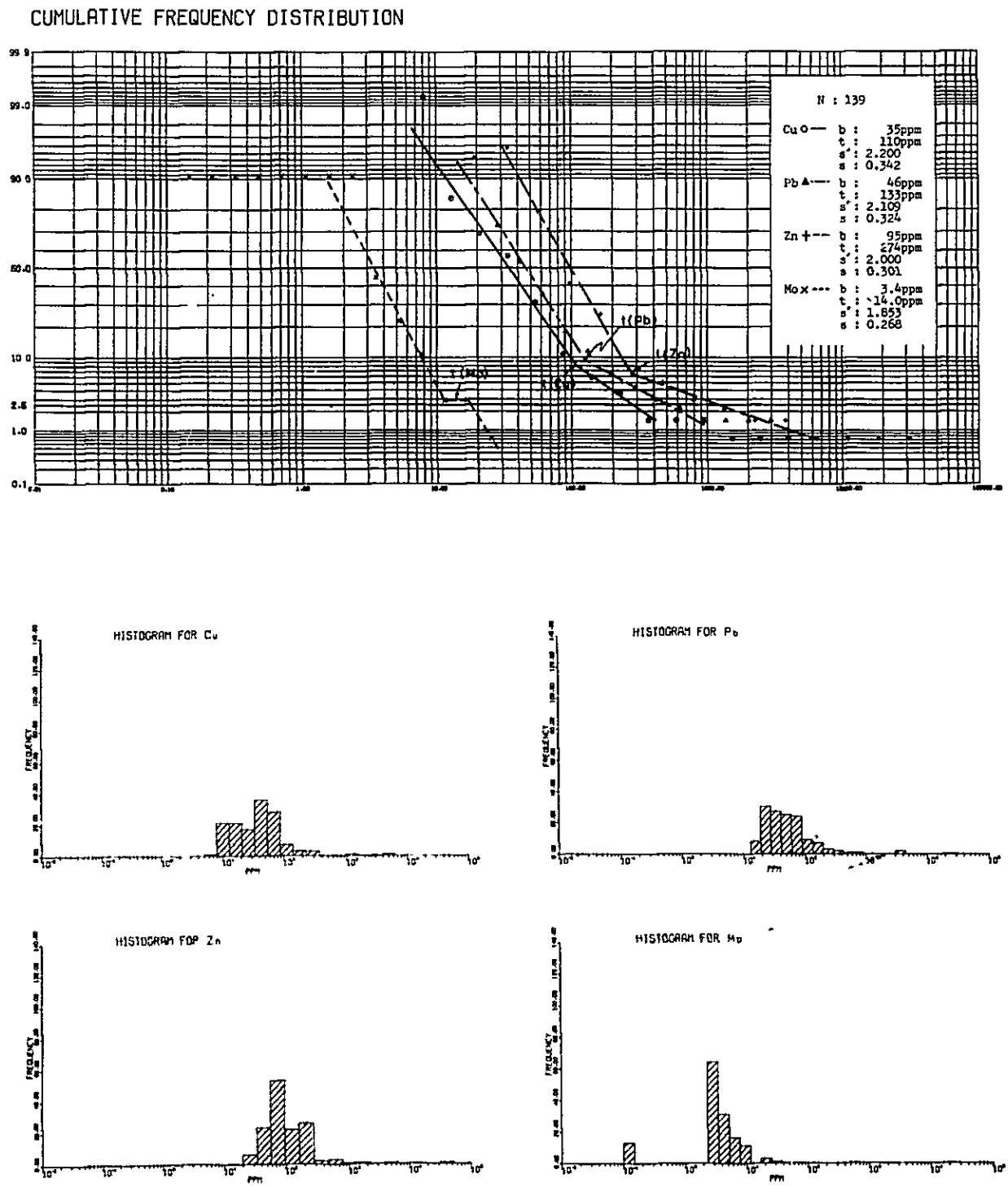

Fig. 3-5 Cumulative frequency distribution and histogram for Eocene sediments

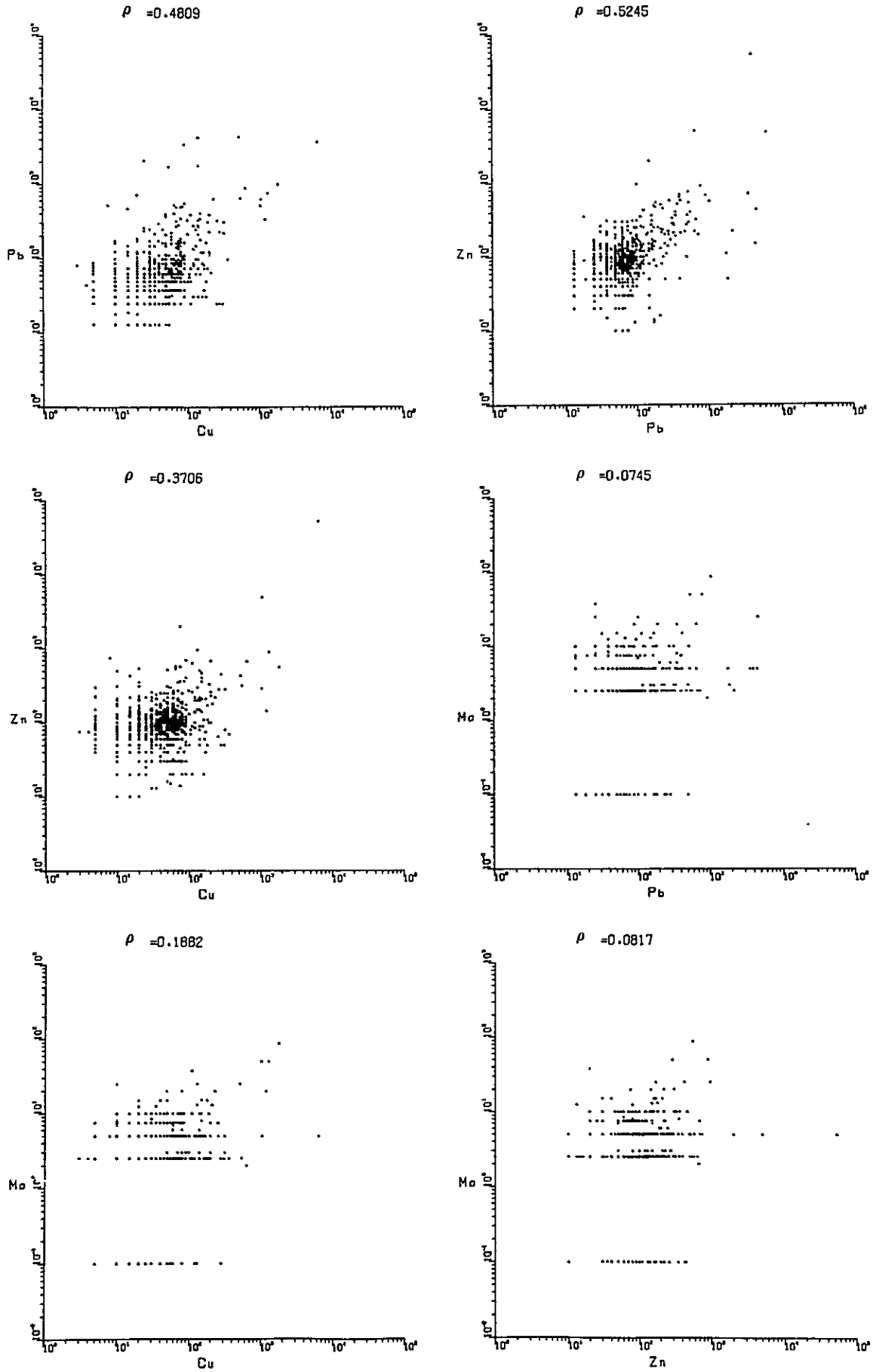

Fig. 3-6 Correlation of geochemical elements

zones. This is considered to be due to the influence of exogenic halo of Kört ore deposits. Anomaly map was made on the basis of all samples, but 35 samples which had been taken last year (1978) in this area, were added to 620 samples taken this year (1979), and therefore the total number of samples used for statistical analysis is 655.

3-4 Statistical analysis

The statistical treatment of geochemical data followed the method of Cloude LEPELTIER (1969). On the basis of the above-mentioned three lithofacies classification, data on the four indicator elements from soil samples were treated statistically. Cumulative frequency distribution for copper, lead, zinc and molybdenum in each geological unit is shown in Fig. 3-2 ~ 3-5. Dispersion patterns which were obtained from the diagrams are shown in Table 3-1, coefficient of correlation of the four elements is given in Table 3-2, and background, deviation, and threshold values in Table 3-3.

3-4-1 Dispersion (Frequency distribution)

Cu: (1) The frequency distribution curve of copper appears to be a mixture of two different types of anomalies and it is positively skewed (excess of high value).

(2) Although standard deviation is generally high, it is moderate in granodiorite.

Pb: (1) The frequency distribution curve of lead generally shows "excess of high value".

(2) Standard deviation is moderate, except for Eocene sediments which show high value.

Zn: (1) Frequency distribution curve is generally high, and the Eocene and Miocene sediments appear to be a mixture of two different types of anomalies.

(2) Standard deviation is moderate, except for Miocene sediments, which show high value.

Mo: (1) Molybdenum content is lower than the determined limit, and therefore the reliability of the pattern is low in comparison with other elements.

(2) Frequency distribution curve is negatively skewed.

(3) Standard deviation is large in quartz diorite, otherwise moderate.

3-4-2 Correlation

Correlation between the four indicator elements for each geological unit is shown in Table 3-2. Correlation charts of the all soil samples are shown in Fig. 3-6.

Coefficient of correlation is positive except for Zn - Mo in Miocene, and is particularly large for Cu - Pb and Pb - Zn except for Miocene. Cu - Zn is large in Miocene. Otherwise there is no correlation.

3-5 Anomaly areas

3-5-1 Selection of anomaly areas

The criterion for selection of an anomaly area is a set of threshold values on a graph in Claude LEPELTIER's method.

That is:

1st class anomaly value ..... values higher than 2t

2nd class anomaly value .... values between t and 2t

3rd class anomaly value .... values between t' and t

where "t'" is the value of either equal to or less than 10% of cumulative frequency percentage of "t value", or corresponds to less than 16% of the highest value of total number of cumulative frequency (in other words, it is almost equal to background plus two times standard deviation).

Selection of an anomaly area is based on the following tentative standard (the same method as in 1978).

(a) one point higher than 2t

(b) two adjacent points higher than t

(c) four adjacent points higher than t'

3-5-2 Evaluation of anomaly areas

Evaluation of anomaly areas is usually based on the number of anomaly points which are included within the area. For this, it is necessary that the sampling interval is the same, but practically,

it is difficult to satisfy this condition. The sampling pattern was homogeneous, and evaluation of anomaly was the same as in 1978, as follow:

That is, in the evaluation of an anomaly area the following was considered: Number of anomaly values for each indicator element, its continuity, and the maximum analysis value are included in it. The density of samples is 30 samples/km^2 in Garipuşağı and Kört areas in order to cover the mineralized zone in detail.

A rank: Unit area which contains more than ten values which are higher than t and two higher than 2t for adjacent sample localities.

B rank: The unit area which contains more than five values which are higher than t and one higher than 2t.

C rank: (1) Unit area which contains two points higher than t and ten higher than t'.

(2) Unit area which contains three points higher than t and five higher than t'.

(3) Unit area which contains four points higher than t.

D rank: (1) Unit area which contains one point higher than 2t.

(2) Unit area which contains five points higher than t' and one higher than t.

(3) Unit area which contains ten points higher than t'.

E rank: (1) Unit area which contains four points higher than t'.

(2) Unit area which contains two points higher than t.

All of these areas for the adjacent sample localities.

3-5-3 Relation between anomaly area and its geology and mineralization

Ultimately, twenty-five anomaly unit areas were drawn on the map. Those anomaly areas are shown in Fig. 3-7.

The classification of each rank is as follows:

	rank / component	A	B	C	D	E
Soil Sample	Cu	1	-	-	2	1
	Pb	2	2	1	10	3
	Zn	1	3	-	5	2
	Mo	-	-	-	3	2

The relation between geochemical anomaly areas, stratigraphy, intrusive rocks, alteration zone and mineralized area are indicated in Table 3-4. Those anomaly areas are classified on the basis of the following.

		Mineralized zone	Altered zone	Others
(1)	Anomaly areas related to dacite	1,	10, 11, 12	
(2)	Anomaly areas related to quartz diorite	1, 21, 22	3, 5, 6, 7, 8, 9, 12, 13, 16, 17, 18, 19, 20, 23, 24, 25	
(3)	Anomaly areas due to different rock in geological unit		2,	4, 13, 14, 15, 16

In the above-stated,

(1): The ore deposits related to dacite are represented by Sin mine in the area investigated in 1978. Mineralization of the Garipuşağı area and the area south of Kört mine are similar to Sin mine which is related to dacite. Notable mineralization except for silicification and pyritization was not observed in Garipuşağı by geochemical survey.

(2): The ore deposits related to quartz diorite are represented by Mamlis mine. The mineralizations related to the Bulanık quartz diorite were observed at the Kört mine, Doludibek Mah and west of Varsilli yayla, in the area surveyed in 1979.

(3): The anomaly areas in this group coincide with limestone in the pyroclastic rocks of Miocene (for example, 13) and are assumed to be due to metallic minerals disseminated in country rock. It cannot be called a mineralization.

Table 3-4 Geological anomaly areas of the soil samples

No. of Unit Anomaly	Locality	Classification	Area km²	Cu						Pb						Zn						Mo						Geological unit	Relation of the Geology		Name of mine or mineralized area	Remarks
				Classification	Area km²	No. of anomaly point t'	t	2t	Max. value ppm	Classification	Area km²	No. of anomaly point t'	t	2t	Max. value ppm	Classification	Area km²	No. of anomaly point t'	t	2t	Max. value ppm	Classification	Area km²	No. of anomaly point t'	t	2t	Max. value ppm		Intrusive rock	Alteration and mineralization		
1	Kort			E	0.2	3	1	-	200						400						690						10	Kamışlık F.		Cu-Pb-Zn-Qtz vein siliceous zone	Kört mine	
1	Körr	A	1.0	D	0.1	1	-	2	6,400	A	0.6	-	5	10	4,375	B	0.8	7	7	5	53,000	D	0.2	2	-	2	25	Kamışlık & Bentepe F.	Dacite Diorite	Cu-Pb-Zn-Qtz vein Malachite-Qtz vein	Kört mine	
2	West Aynalpozverk		0.2	-	0.1	1	-	-	130	-	0.1	-	1	-	163	D	0.2	-	1	1		D	0.1	-	-	1	25	Kamışlık F.				
3	Leşkan		0.5	-		-	-	-	50	-		-	-	-	75	-		-	-	-	90	E	0.5	6	-	-	10	Düzpelit F.	Diorite	Argillaceous zone		
4	South Aşlıca		0.1	-		-	-	-	80	D	0.1	-	-	1	113	-		-	-	-	116	-		-	-	-	2.5	Düzpelit F.				
5	Leşkan Yaylası		0.1	-		-	-	-	10	-	0.1	-	1	-	175	D	0.1	-	-	1	500	-	0.1	-	-	-	5	Düzpelit F.		Argillaceous zone		
6	Yeşilsivri T.	C'	0.5	-		-	-	-	65	B	0.5	1	6	5	413	D	0.2	2	-	1	590	-		-	1	-	15	Düzpelit F.		Argillaceous zone		
7	West south Yeşilsivri T.		0.1	-		-	-	-	50	D	0.1	-	-	1	213	-		-	-	-	16	-		-	-	-	2.5	Düzpelit F.		Argillaceous zone		
8	Kurtepe		0.1	-		-	-	-	55	D	0.1	-	-	1	1,750	-		-	-	-	110	-		-	-	-	5	Düzpelit F.		Argillaceous zone		
9	North Kavak T.		0.1	-		-	-	-	90	D	0.1	-	-	1	3,500	D	0.1	-	-	1	700	-		-	-	-	5	Düzpelit F.		Argillaceous zone		
10	North Varsekli		0.1	-		-	-	-	50	D	0.1	-	-	1	400	-	0.1	-	-	-	50	-		-	-	-	5	Düzpelit F.	Dacite	Siliceous & argillaceous zone		
11	North Varsekli		0.1	-		-	-	-	40	E	0.1	-	2	-	113	-		-	-	-	100	-		-	-	-	2.5	Düzpelit F.	Diorite	Siliceous & argillaceous zone		
12	East Garipuşağı	C'	0.3	D	0.1	-	-	2	1,200	B	0.3	-	5	2	675	-	0.1	-	1	-	350	E	0.2	3	2	-	20	Düzpelit F.	Dacite Diorite	Strong siliceous & argillaceous zone		
13	Buyuktepeler	C'	1.3	-	0.1	1	-	-	110	C	0.4	-	2	3	537	B	1.0	2	7	2	750	-		-	-	-	5	Düzpelit F.		Weak siliceous & argillaceous zone		
14	Atöglu T.		0.1	-		-	-	-	20	-	0.1	-	1	-	187	D	0.1	-	-	1	540	-		-	-	-	2.5	Düzpelit F.		Weak argillaceous zone		
15	East Atöglu T.		0.3	-		-	-	-	60	-		-	-	-	63	E	0.3	3	1	-	310	-		-	-	-	2.5	Kamışlık F.				
16	North Dikenlitarla	C'	1.0	-		-	1	-	140	D	0.2	-	1	2	375	B	1.0	3	5	2	520	-		-	-	-	5	Kamışlık & Bentepe F.	Diorite	Weak argillaceous zone		
17	Dikenlitarla		0.2	-		-	-	-	75	-	0.1	-	1	-	150	E	0.2	-	1	1	2,000	-		-	-	-	7.5	Bentepe F.		Weak argillaceous zone		
18	Mehmet Suh		0.3	-	0.2	2	-	-	100	D	0.1	-	-	1	475	-	0.1	-	1	-	220	-		-	-	-	5	Bentepe F.		Siliceous & argillaceous zone		
19	East Gobunkulesi T.		0.2	-		-	-	-	25	D	0.2	-	1	1	2,125	-		-	1	-	220	-		-	-	-	2.5	Düzpelit F.		Siliceous & argillaceous zone		
20	North Cincik T.		0.2	-		-	-	-	85	E	0.2	-	2	-	175	-		-	-	-	160	-		-	-	-	7.5	Bulanık diorite	Diorite	Siliceous zone (weak)		
21	West Varzilli Yayla		0.3	C	0.2	3	1	1	365	-	0.1	-	1	-	165	-	0.1	2	-	-	190	-	0.1	-	-	-	10	Bulanık diorite	Diorite	Cu-Pb-Zn-Qtz vein		
22	Doludibek	A	1.5	A	0.8	13	12	5	1,800	A	1.3	-	16	24	4,500	A	0.8	9	13	5	900	D	0.2	3	1	1	25	Bulanık diorite	Diorite	Pyritization Argillaceous & siliceous zone		
23	Hamlis T.		0.1	-		-	-	-	30	E	0.1	-	2	-	125	-		-	-	-	60	-		-	-	-	7.5	Düzpelit F.		Siliceous & argillaceous zone		
24	West Hamlis T.		0.1	-		-	-	-	70	D	0.1	-	-	2	325	-		-	-	-	210	-					5	Düzpelit F.	Dacite	Siliceous & argillaceous zone		
25	Nalatma T.		0.1	-		-	-	-	20	D		-	-	1	725	-	0.1	1	-	-	200	-					2.5	Düzpelit F.	Diorite	Siliceous & argillaceous zone		

3-6 Discussion of main anomaly areas

Kört area △1 Pb: A-rank [1] Zn: B-rank

The anomaly areas consisting of copper, lead and zinc cover about 1 km^2. Interesting values were obtained by geochemical investigation. Maximum values in this area are 6,400 ppm copper, 3,875 ppm lead, and 53,000 ppm zinc, which are more than double the threshold of lead and zinc. These high values are due to the exogenous halo of Kört mine. As a result of geological and geochemical investigation, the anomaly of Kört area is considered to be partly primary and partly due to exogonous halos influenced by topography. Geochemical anomaly map of Kört area is shown in Fig. 3-8.

It has been made clear that mineralizations occur in two kinds of fissure patterns, N20°E fissure system of Kört mine and a quartz vein of the N60°W fissure system.

Those mineralizations are inferred to have been caused by fissures accompanying the intrusion of the Bulanık quartz diorite. In addition, there is disseminated mineralization related to dacitic lava dome in the Düzpelit Formation. The observed mineralizations in the area are complicated, as shown in the following table.

		Maximum value (ppm)			
		Cu	Pb	Zn	Mo
Anomaly related to Kört ore deposits		6,400	3,875	53,000	5
Anomaly related to quartz vein with malachite	(N60°W)	140	4,375	350	5
	(N20°E)	140	397	640	10
Anomaly related to limonite-quartz vein	(N40°W)	90	63	130	5
Anomaly within altered mudstone	(N20°E)	170	88	310	25
Anomaly related to altered dacite		200	563	690	75

Yeşilsivri T. area (6) Pb: B-rank

The anomaly area is located between Leşkan and Garipuşağı hamlets, and consists of a lead anomaly. Dacitic pyroclastic rock of the Düzpelit Formation is distributed in this anomaly area. It is correlated with the alteration from Mamlis, Garipuşağı and Leşkan to Kört. Alteration of Yeşilsivri T. is more weak than that of Leşkan and Garipuşağı areas.

The maximum anomalous value, which is lower than that of other anomalous areas, is 65 ppm copper, 413 ppm lead, 590 ppm zinc, and 15 ppm molybdenum.

East of Garipuşagı area (12) Pb: B-rank

The anomaly area east of Garipuşağı hamlet consists mainly of lead, copper, and a little zinc, and is distributed in dacitic pyroclastic rock and dacite in the Düzpelit Formation and is partly in contact with the Bulanık quartz diorite. It is pyritization accompanied by silicification and argillization. Maximum values are 1,200 ppm copper, 675 ppm lead, 350 ppm zinc and 20 ppm molybdenum. The anomaly is of small extent.

Altered dacite lava is predominant around the Garipuşağı hamlet, and is accompanied by silicification. It contains disseminated hematite, but no remarkable anomaly was found by geochemical means in this area.

Büyüktepeler area [13] Zn: B-rank

The anomaly area is located in the central part of 1979 geological survey and lies in the Düzpelit Formation between two blocks of the Bulanık quartz diorite batholith.

Silicification and argillization are partially recognized, but generally speaking, are weak in the anomaly area.

Maximum value is 110 ppm copper, 537 ppm lead, 750 ppm zinc and 5 ppm molybdenum. This anomaly is assumed to be caused by the supply of the elements from limestone at the topographical top of the area, also it is possible that it is a primary halo due to concealed mineralization. Mineralization in the area was not observed by geological investigation..

East of Dikenli area [16] Zn: B-rank

The anomaly area consists of zinc, it is located about 1 km east of Dikenli hamlet, and lies in the Kamışlık and Bentepe Formations. The anomaly area is wide spread, but only a weak alteration, resulting from quartz diorite intrusion, was found by geological investigation.

The anomalies are inferred to be a halo due to concealed mineralization, because maximum value is 140 ppm copper, 375 ppm lead, 520 ppm zinc and 5 ppm molybdenum, and alteration is weak.

Doludibek area (East of Mamlis) (22) Cu, Pb, Zn: A-rank

These anomalies are located in an eastward extension of Gp - 4 and Gp - 3 anomaly areas reported in 1978, and lie in the Düzpelit Formation and marginal part of the Bulanık quartz diorite. The classification of the anomalies more than double the threshold value, taking into consideration topography and detailed geological evidence, is as follows:

		Definite dimension	Maximum value (ppm) Cu	Pb	Zn	Mo
(1)	Anomaly related to limonite-quartz vein	length: 15 m	1,800	4,500	1,033	88
(2)	Anomaly related to silicified zone with limonite-hematite	500 m and 200 m long parallel to silicification zone	1,300	1,830	900	50
(3)	Other than the above mentioned anomalies (formed by network of limonite-pyrite with silicification and argilization, and a thin malachite-quartz vein)	300m x 1,000m 300m x 1,300m	1,030	650	360	50

Fig. 3-9 shows anomalies of copper, lead and zinc over the double threshold, delineated with consideration to topography and detailed geological evidence. Based on Fig. 3-9 mineralization is inferred to be developed along the fissure of the NE-SE system.

3-7 Conclusion

Many geochemical anomaly areas were found in the surveyed area. These anomalies in Kört area △1 [1] Doludibek (22) and East of Garipuşağı area [16] coincide with ore deposits and mineralization zones found by geological survey. In spite of the fact that the anomaly areas investigated in 1979 are smaller than those of the Mamlis and Sin areas investigated in 1978, there are two anomalies worth noting in Doludibek and Kört areas.

The Doludibek area is located east of Mamlis anomaly, and belongs to the same mineralized zone, whose extent was clarified by geochemical survey in 1978 and 1979. The mineralization of Kört mine is located in fissures. Further investigation of fissure pattern in the area is recommended.

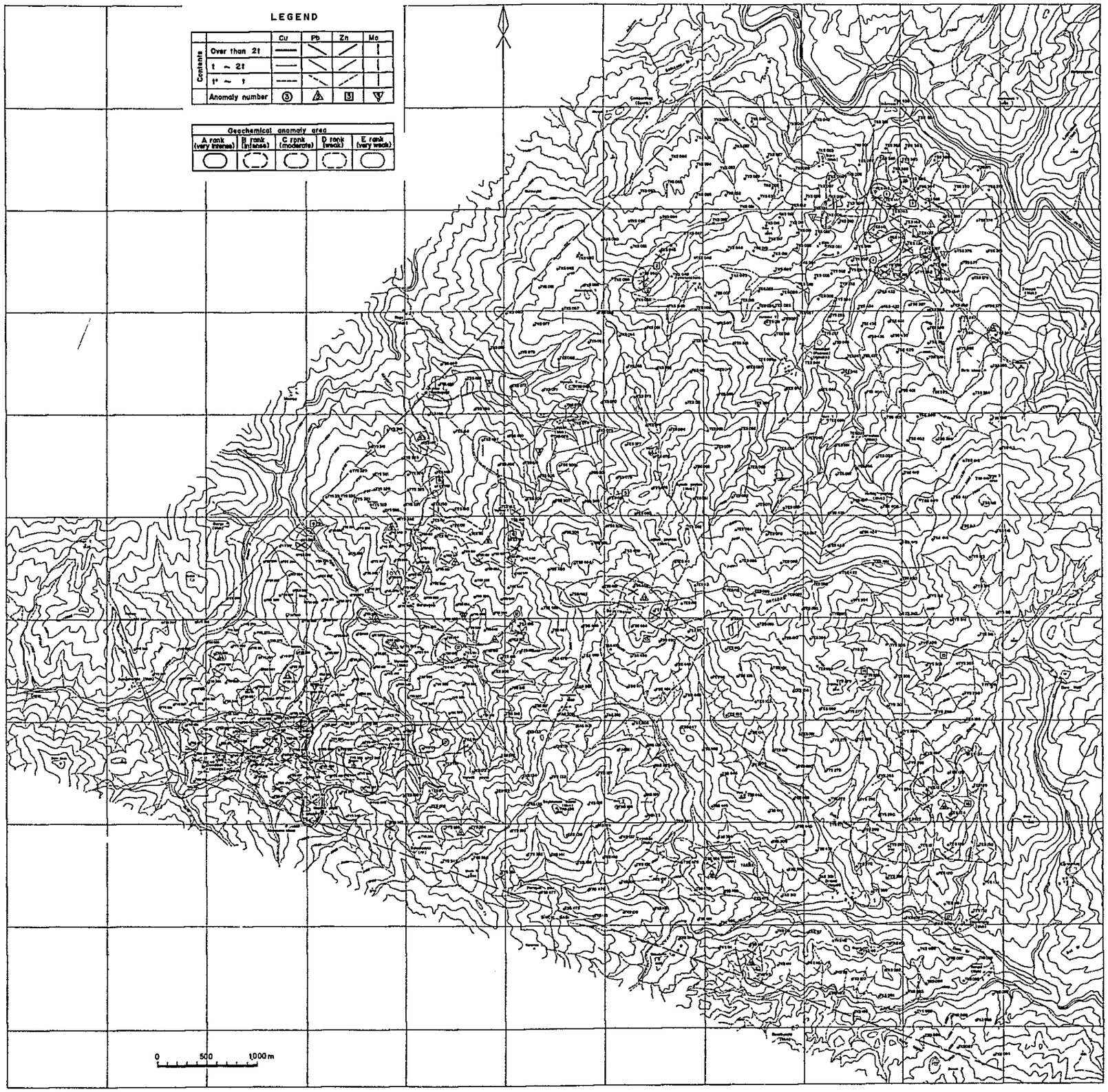

Fig. 3-7 Geochemical Anomaly Map

Fig. 3 - 8 Geochemical anomaly map in Kört area

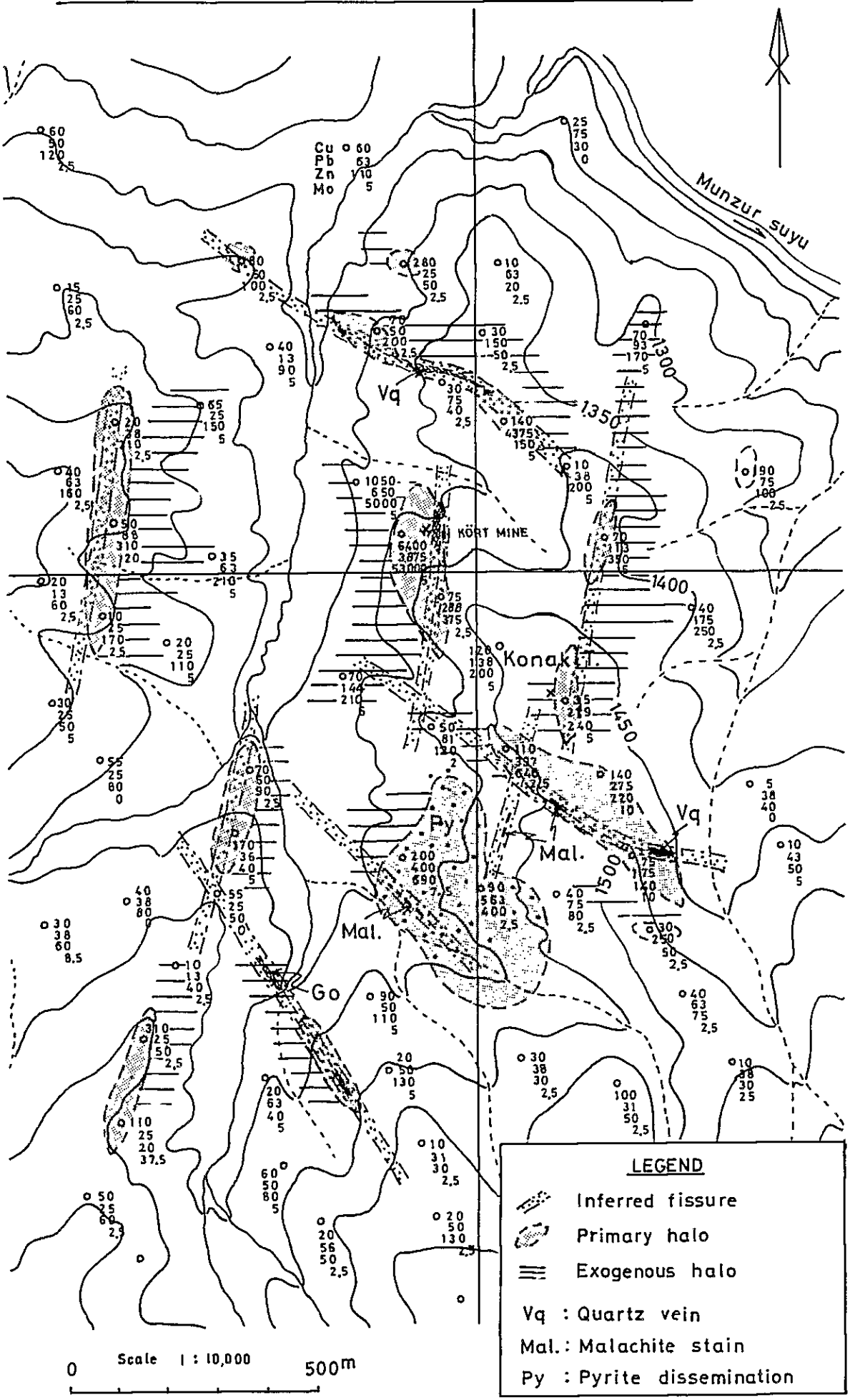

Fig. 3-9 Geochemical anomaly map in Mamlis area

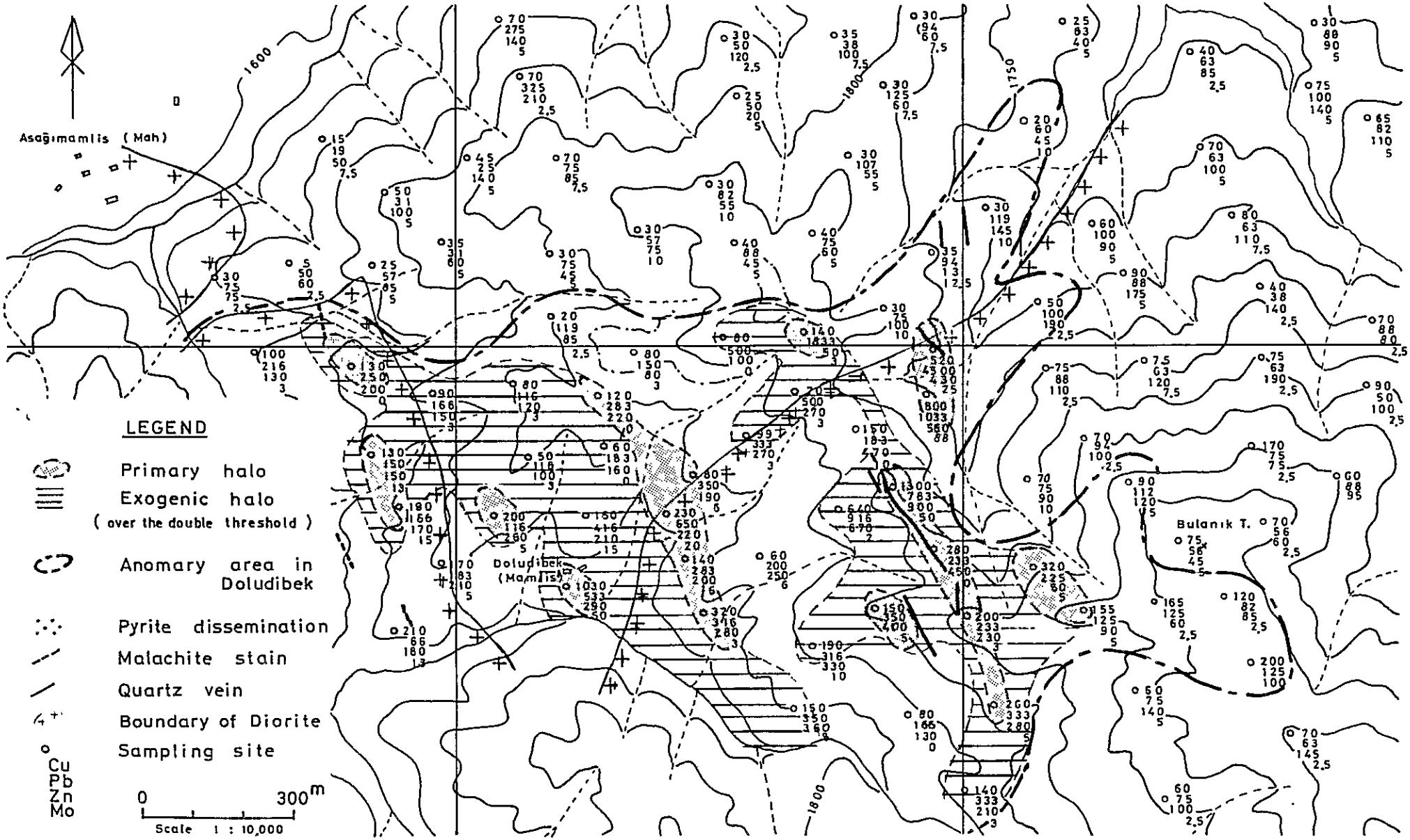

CHAPTER 4 GEOPHYSICAL SURVEY OF MAMLIS AND SIN AREAS (INDUCED POLARIZATION METHOD)

Chapter 4 Geophysical Survey of Mamlis and Sin Areas (Induced Polarization Method)

4-1 Introduction

In the Mamlis and Sin areas, promising mineralized zones have been discovered by the 1978 preliminary geological and geochemical surveys. In the Mamlis area, the Vein-type mineralization was found in quartz diorite, and the network-type mineralization was found in dacitic pyroclastic rocks (Düzpeliz Formation) surrounding quartz diorite, outcrops of the network are fully limonitized due to the strong oxidation, it is considered to be primary sulfide minerals underneath the surface. In the Sin area, field evidence has suggested some mineralization of the Sin dacite and the alternative sedimentary environment accompanied with the dacite intrusion. A promising mineralized zone including chalcopyrite, sphalerite and pyrite has been recognized around an open pit of the Sin Mine about one km southeast of Sin hamlet.

On the basis of the above survey results, an Induced Polarization (IP) survey has been planned for exploring the further extension of the mineralized zone and for presuming ore-mineral content. This survey covers an area of about 6 km^2 including 28 survey lines. The total length of the lines amounts to 53.6 km.

The field work has been launched in June 19, 1979, and performed in Sept. 27, 1979. Field data processings have been carried out at both the Tunceli Camp and the Araklı Branch, while computations of terrain

correction for apparent resistivity, laboratory IP tests of rock specimens, and simulation analyses have been completed in Tokyo, Japan.

4-2 IP method

There are two types of IP field survey: frequency domain method and pulse method. The former is in more general use than the latter because of the fact that the measuring technique is much easier. Moreover, the former is applicable to poorly-disseminated ore deposits such as porphyry-copper deposits, so that it has been adopted as the present survey method.

For expressing IP characteristics, the following variables are taken into account: FE (frequency effect), AR (apparent resistivity) and MF (metal conduction factor). FE is expressed as a different between apparent resistivities measured at a low and a high frequency in percentage, which Wait (1959) defined as

$$FE = \frac{\rho(\infty) - \rho(0)}{\rho(0)} \times 100\%, \qquad (1)$$

where $\rho(\infty)$ and $\rho(0)$ indicate ARs when the frequency f becomes infinity and zero respectively. In the present survey, the measurements have made at frequencies of 0.3 and 3 Hz instead of f = 0 and ∞, respectively. Then Eq. (1) becomes

$$FE = \frac{\rho(0.3\ \text{Hz}) - \rho(3\ \text{Hz})}{\rho(3\ \text{Hz})} \times 100\% \qquad (2)$$

AR for a dipole-dipole electrode configuration is calculated from the following formula:

$$\rho = \pi a n (n + 1) (n + 2) \frac{V}{I} \tag{3}$$

in the unit of ohm - m, where 'a' is the electrode spacing (m), 'n' the electrode-separating coefficient, 'V' the input voltage of a receiver (volt), 'I' the output current of a transmitter (amp.) and 'π' the circular constant (= 3.14159). In the present survey, ρ(3 Hz), AP at a frequency of 3 Hz, is calculated.

Most of sulfide ore deposits indicate a high FE and a low AR. In order to emphasize such characteristics, MF is defined by taking Eqs. (2) and (3) into account, i.e.

$$MF = \frac{FE}{\rho(3\ Hz)} \times 1,000 \tag{4}$$

4-2-1 Method of Operation

The dipole-dipole electrode configuration arranges a coaxial array on a survey line with a given separation (a) between transmitter and receiver electrodes. As shown in Fig. 4-1, a receiver is located at stations 0 and 1, and electric currents are supplied to a transmitter located at stations na and (n + 1) a, where 'n' indicates an integer number. The current electrodes are transferred station by station from n = 1 to 5 in most cases.

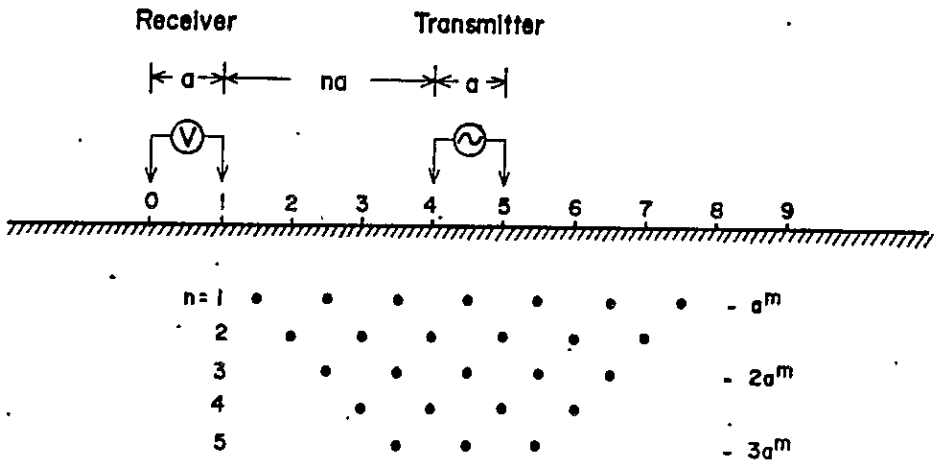

Fig.4-1 IP measurements of dipole-dipole configuration

The followings are specification of the present IP survey:

Table 4-1 Specification of IP survey

	Mamlis area	Sin area
Direction of traverse line	N 6.5° W	N 66.5° W
Direction of baseline	N 83.5° E	N 23.5° E
Method of measurement	frequency domain method	
Transmitting frequencies	3.0, 0.3 Hz	
Electrode configuration	dipole - dipole	
Electrode separations	100 m, 50 m*1	100 m
Spacing of traverse lines	200 m	100 m
Electrode separating coefficient	n = 1 - 5	n = 1 - 5
Shifting of measuring stations	100 m, 50 m*1	100 m

*1 Note: used for Line W_3 (8-18) and Line W_4 (8-18)

4-2-2 Plotting of results

Results of measurement are plotted on cross sections and plan maps. On a cross section as indicated in Fig. 4-1, the obtained data are plotted at the intersection of 45 degree diagonals drawn from the midpoints of receiver dipole (0 - 1) and transmitter dipole (4 - 5). In a practical case, the interval between points of data plotting is not always equal due to topographic irregularities as shown in Fig. 4-2.

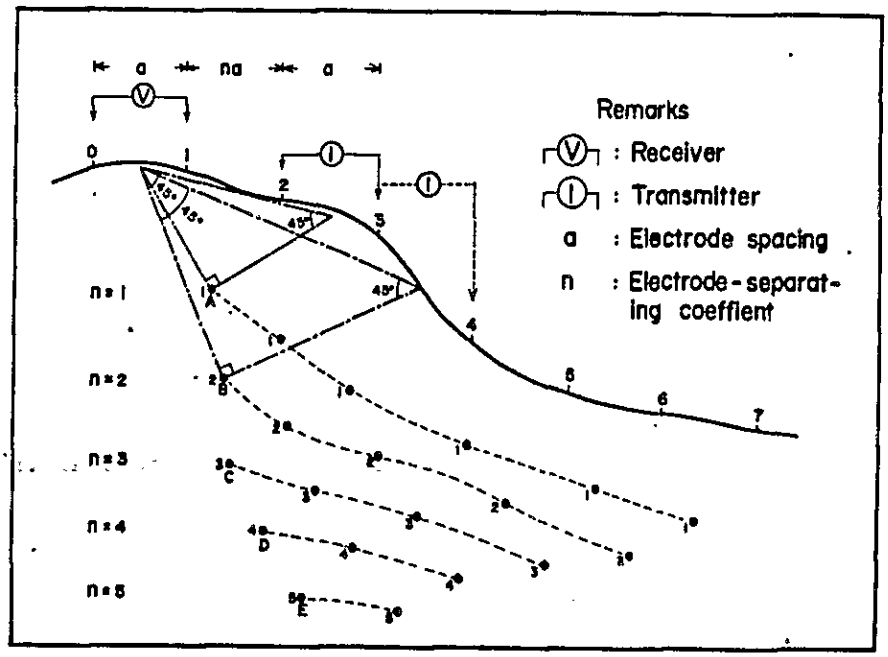

Fig.4-2 Illustration of IP measurements

A plan map represents the areal distribution at a given level, say 200 m (n = 3) below the ground surface.

All the present survey results are plotted on the cross sections along each of the traverse lines. The data of FE, AR and MF are presented on plan maps at levels of 100 m (n = 1), 200 m (n = 3) and

300 m (n = 5) deep below the ground surface. Contour intervals used here are as follows. If necessary, auxiliary contours are drawn.

Mamlis Area

FE : 0.5, 1.0, 1.5, 2.0, 2.5, 3.0 .....

AR : 10, 30, 50, 70, 100, 300, 500, ...

MF : 5, 10, 15, 20, 25, 30, ...

Sin Area

FE : 2, 4, 6, 8, 10, 12, ...

AR : 10, 30, 50, 70, 100, 300, 500, ...

MF : 20, 40, 60, 80, 100, 120, ...

4-3 Data Processing

4-3-1 Terrain correction to AR

In a dipole-dipole electrode configuration, the terrain effect on AR is so sensitive that terrain corrections are necessary for expressing local features of AR distribution. Without terrain corrections, AR has a tendency to increase at a top of mountain, and to decrease in a valley (see Fig. 4-3-a). The terrain effects are explicitly recognized in the rugged mountainous areas of Mamlis and Sin, so that the computations of terrain correction are performed.

There are three methods of terrain corrections for AR: the experimental determination using a three-dimensional model of topographic relief in a water-tank, the two-dimensional method using an analyzer-paper, and the computer simulation method. We adopt here the analyzer-paper method, by which terrain correction values can easily be obtained along arbitrary-shaped sections of topography.

(Method of Terrain Correction)

(1) Modeling sections of topographic relief along traverse lines and 500 m extension from both the sides in order to eliminate edge effects.

(2) Experimental determinations of AR (ρ_1) of analyzer-papers using a pulse generator and receiver which can control a weak electric current in laboratory tests.

(3) Similar determinations of AR (ρ_0) for a terrain model having a flat surface. The correction coefficient K is given by

$$K = \frac{AR\ (\rho_1)}{AR\ (\rho_0)} \quad \text{or} \quad AR\ (\rho_0) = \frac{AR\ (\rho_1)}{K}\ .$$

(4) Finally, field data are divided by K to obtain corrected values of AR.

a : AR of Analyzer-paper

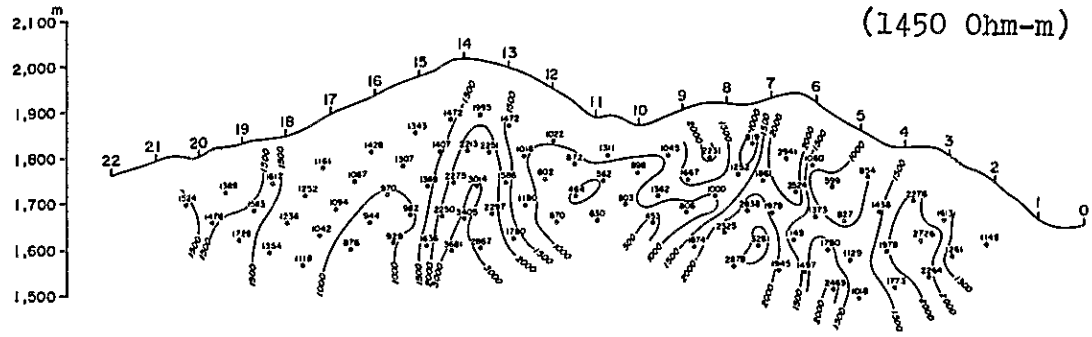

b : Coefficient value of correction (K)

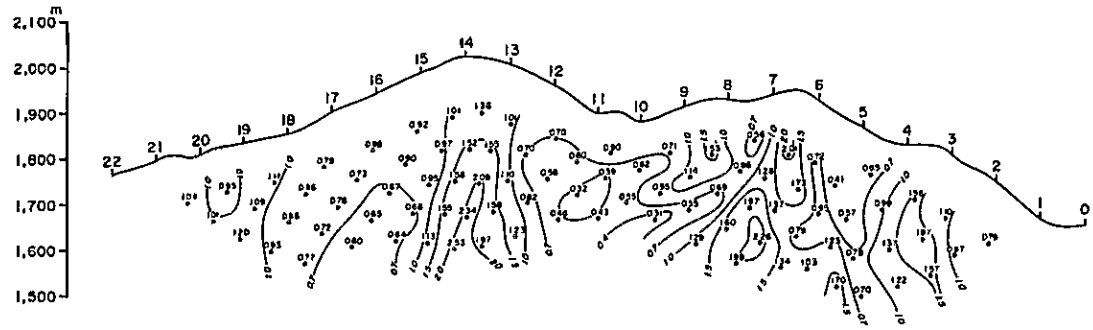

c : AR of Field Measurements (Ohm-m)

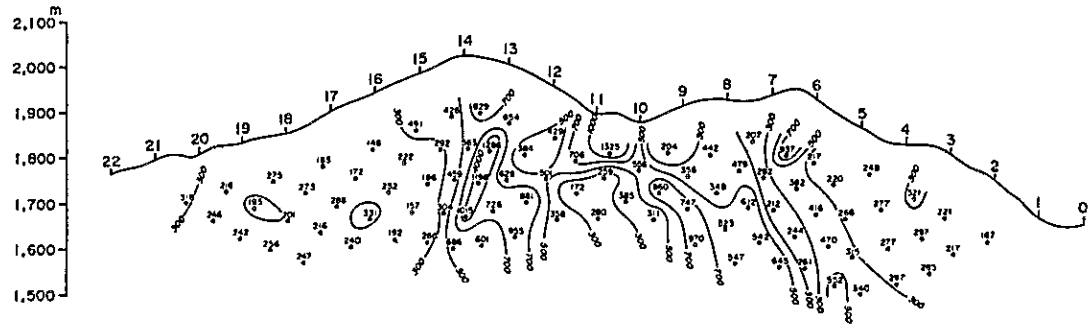

d : AR after the correction (Ohm-m)

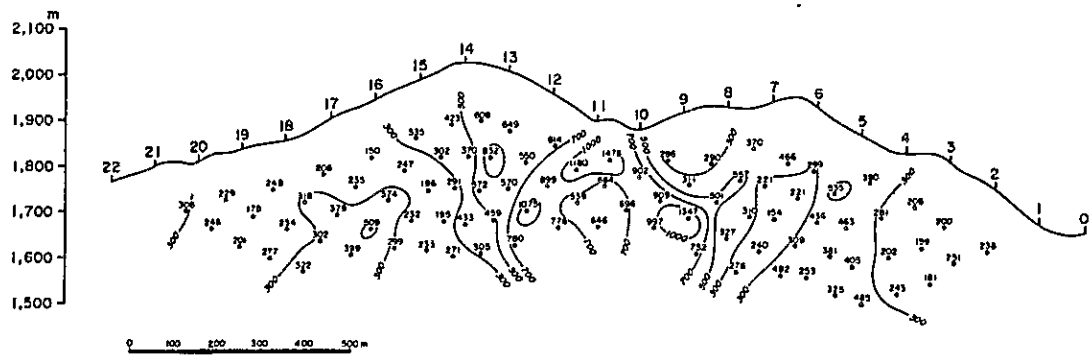

Fig.4-3 Terrain Correction to Apparent Resistivity

(Instruments used for correction)

The followings are instruments used for terrain corrections.

(1) Pulse Generator

Type:	Constant Current Pulse Generator Model 801
Manufacturer:	Burr-Brown Research Corporation
Input Voltage:	115 ± 10 (V)
Input Frequency:	50 ∿420 (Hz)
Output Frequency:	0.01 ∿ 1,100 Hz 5 steps with a fine adjustor
Output Current:	1μA ∿ 11 mA 4 steps with a fine adjustor

(2) Receiver

Type:	IP Receiver Model YDC - 434
Manufacturer:	Yokohama electric research Co.
Input Voltage:	0.3, 1, 3, 10, 30, 100, 300, 1,000 mV 8 steps with a fine adjustor
Frequency:	0.1, 0.3, 1, and 3 Hz
Time Constant:	2, 6, 15, 60, and 150 sec.
Input Impedance	10 M ohm
Power:	two 15.6 V Mercury Cells

(3) Analyzer Paper

Name:	Analyzer Paper
Manufacturer:	Tomoegawa Manufacture Co.
Size:	Length 50 m
	Width 1,000 mm

Fig. 4-4 illustrates a block diagram of experimental determinations of terrain correction using the analyzer-paper method.

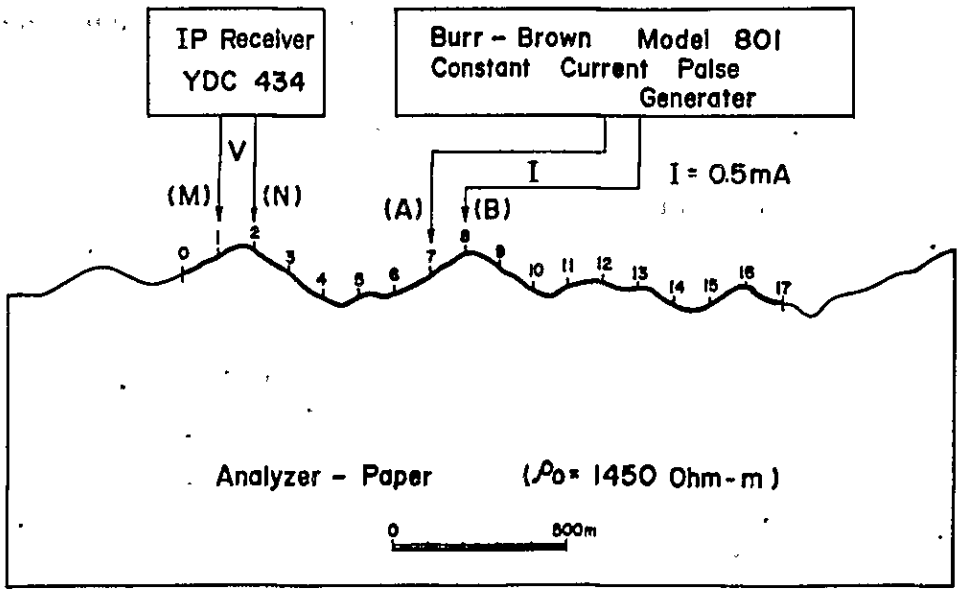

Fig.4-4 Illustration of topographic effects measuring

4-3-2 Rock sample tests

The laboratory measurements of FE and resistivity of rock specimens sampled from the survey area give us important informations for the interpretation of the field IP results. These data are indispensable especially for a computer simulation analysis. Statistical considerations of the results obtained from many typical rock specimens also play an important role for discriminating IP characteristics related to ore implacement.

(Method of rock specimen tests)

An outline of the method of rock specimen tests is briefly explained as follows:

Fig. 4-5 shows a block diagram of the apparatus. The measurements are made with rock specimens which keep an original state of nature as possible in order to obtain reliable results. The specimens are processed in order before tests as follows.

(1) Form: Form a specimen into a 3 x 3 x 3 cm cube.

(2) Water saturation: Dip a specimen into water during 24 hours or longer up to a state of water saturation.

(3) Preliminary process: Set a specimen on the sample holder under the temperature control with a vacuum pump. Two-hour setting makes the specimen in a stable condition to obtain reliable results.

(4) Measurement: Measure IP with a current density as low as possible (about 2 μA).

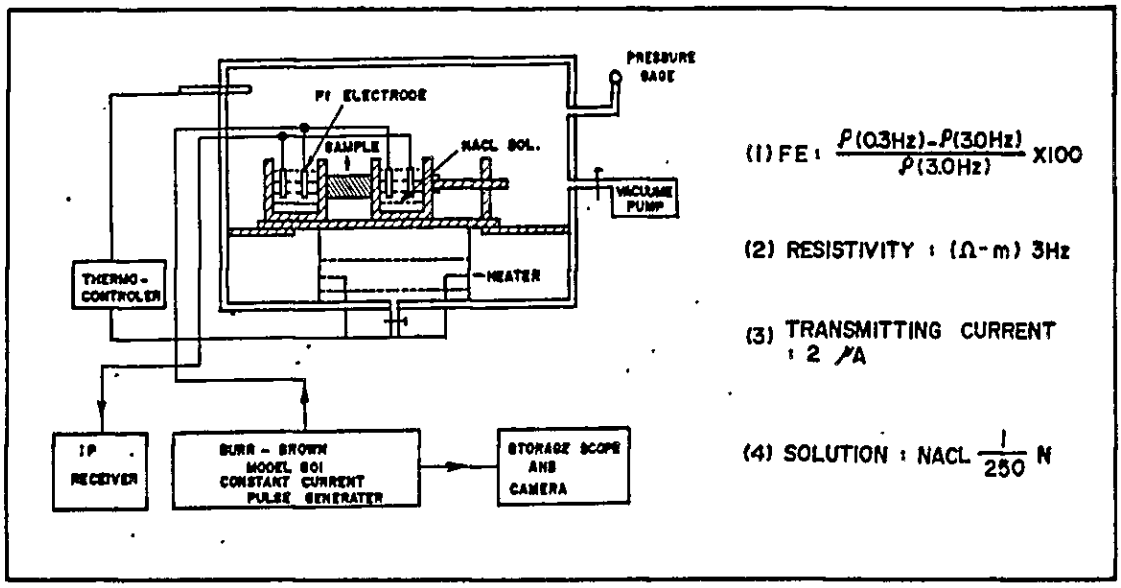

Fig.4-5 A block diagram of the laboratry measuring apparatus

4-4 Method of Field Data Analyses

Qualitative analyses of IP field data are made for the interpretations of cross sections along traverse lines and of FE, AR and MF plan maps at various levels. As a result, the spatial dimensions of the anomaly generating source can be presumed by taking geological and geochemical data as well as results of rock specimen tests into consideration.

The computer simulation gropes about for geological structures to be disclosed. Assuming model structures based on FE and AR field data, the computations are repeatedly made to determine the optimum model by comparing with field data. Such computer trial-and-error approaches obtain the final determinations of dimension and depth of resultant bodies corresponding to the FE and AR anomalies.

The flow chart representing the jobs of data processings and analyses is given in Fig. 4-6.

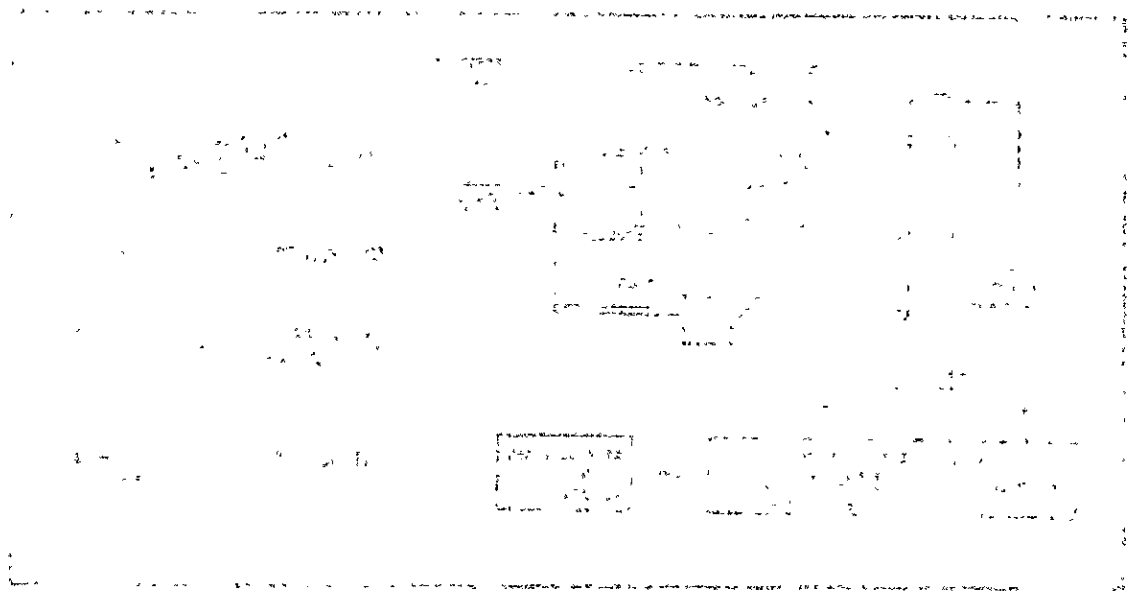

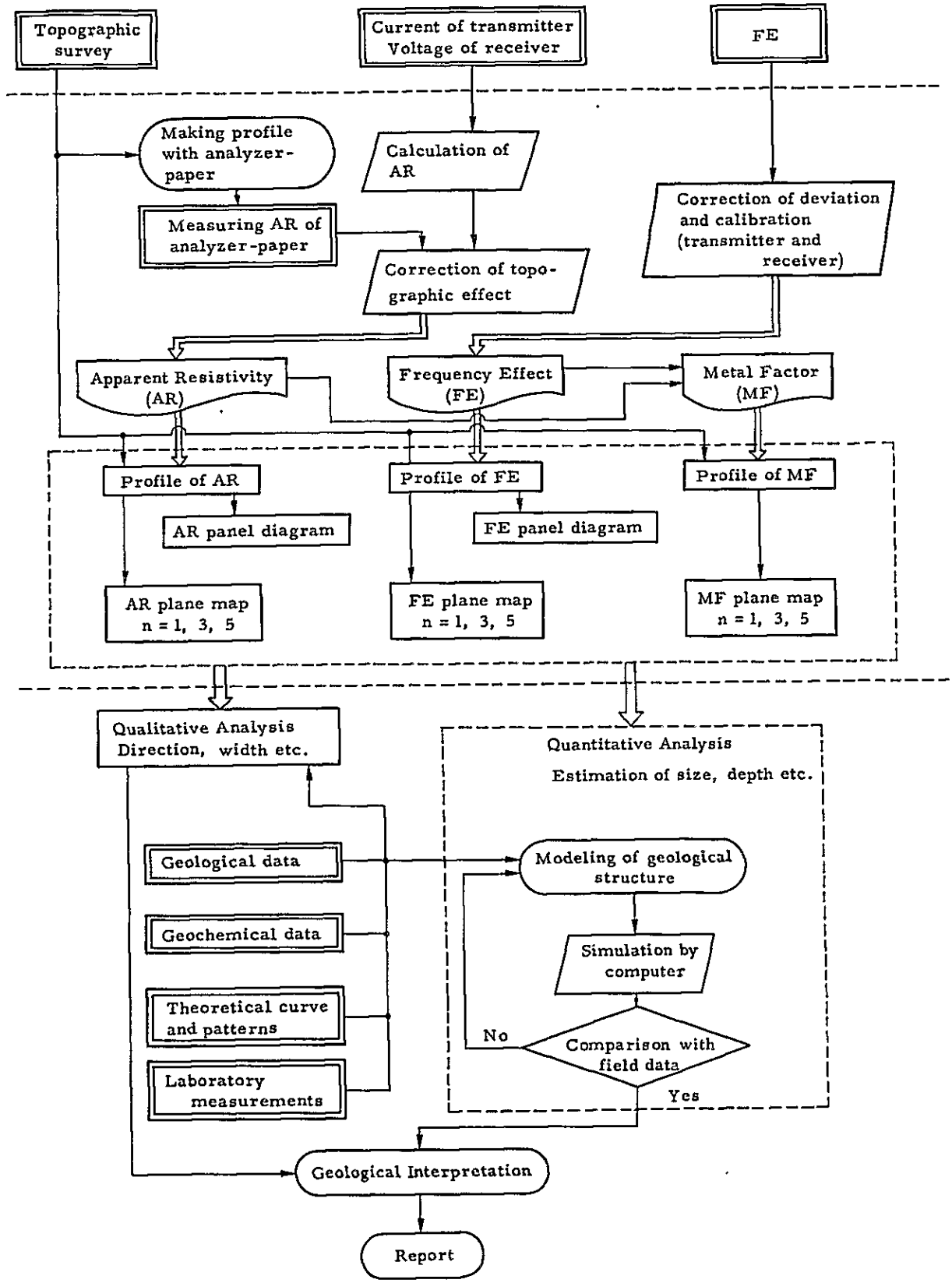

Fig. 4-6 Flow chart of IP data processing and interpretation

4-5 Mamlis Area

4-5-1 Survey area (PL. 4-1)

Mamlis area is located about 30 km NW of Tunceli City. It takes about three hours to go to Ağtaş hamlet by jeep from Tunceli City via Ovacık, and takes further one hour to go to an advanced camp at Aşağı Mamlis hamlet on foot.

The survey covers an area of 4.1 km^2 including 12 survey lines, the total extension of which amounts to 26.6 km.

No.	Line	Length (m)	No. of Survey stations
1	E_6	2,200	90
2	E_5	"	"
3	E_4	"	"
4	E_3	"	"
5	E_2	"	"
6	E_1	"	"
7	00	"	"
8	W_1	"	"
9	W_2	"	"
10	W_3	1,400	50
11	W_4	"	"
12	B(8)	2,000	80
13	W_3(8-18)	1,000	"
14	W_4(8-18)	"	"
Total		26,600 m	1,150

4-5-2 Survey period

Land Survey	:	July 30 to September 20, 1979
Field IP Measurements	:	August 16 to September 27, 1979

4-5-3 Outline of geology

Geology of Mamlis area consists mainly of dacitic pyroclastic rocks of Düzpelit Formation and Bulanık quartz diorite intrusions. Dacitic pyroclastic rocks cover almost all over the area except for the northwest part, and quartz diorite is recognized in the northwest and east of the area. In the northern part of the area is observed the porphyry intrusions penetrating with a width of 10 ~ 20 m in the direction of N 40° - 60°E.

The mineralized zones are recognized in an area of 1 km NS by 1.4 km EW centered at Mt. Sivrikaya. The dacitic pyroclastic rocks are silicified and argillized by the strong alteration, so that limonite zones of sulfide mineral origin are distributed widely in the survey area. It is especially noteworthy that many NS-oriented strong silicification zones are distributed over the north slope of Mt. Sivrikaya and the east foot of Mt. Haydar.

The Mamlis Mine is located about 0.6 km WNW of Mt. Haydar. The ore deposits in quartz veins include chalcopyrite, galena and sphalerite, which are situated at the margins of the quartz diorite intrusions.

The mineralized quartz diorite is white due to the strong argillization, but the alterations are restricted to a relatively narrow area.

On the east and west ridges of Mt. Haydar, there are several outcrops of limonite-rich gossan trending with a width of about 10 m in the N 60° ~ 80°E direction. They are described in detail in the 1978 Geological Survey Report of Tunceli Area.

4-5-4 Survey apparatus

The field apparatuses used in the present survey are as follows:

Transmitter

Type	:	IP square-wave generator Model T2800
Manufacturer	:	Geotronics Co., USA
Input Voltage	:	95 - 120 V, 400 Hz
Output Voltage	:	95 - 800 V
Output Current	:	0.05 - 2.0 A
Frequency	:	0.1, 0.3, 1, 3 and 10 Hz

Receiver

Type	:	Phase Lock IP Receiver Model 5280
Manufacturer	:	Geotronics Co., USA
Input Voltage	:	10 μV ~ 1 V, 11 steps
Input Impedance	:	10 M ohm
Time Constant	:	2, 6, 15, 60, 150, and 600 sec.

Electrode

Current Electrode	:	Stainless steel stick
Potential Electrode	:	Porous electrode pot saturated with copper sulfate solution

Engine Generator

Type	:	Mark 11 - 400
Manufacturer	:	McCullch, USA
Output	:	115 V, 400 Hz, 2 kW

4-5-5 Results of rock sample tests

FE and resistivity laboratory tests are made with 33 rock specimens sampled in the Mamlis area (see the sampling location map in PL. 4-2). The results are given in Table 4-2. The statistical distribution of resistivity values is plotted in Fig. 4-7.
Fig. 4-8 shows the FE-resistivity relation.

The statistical distribution ranges of FE and resistivity together with the mean values except for both the maximum and minimum values are given below.

Rocks	FE (%)	Mean (%)	Resistivity (ohm-m)	Mean (ohm-m)
Ore	18.7 ~ 49.2	35.0	10 ~ 64	37
Gossan	3.8 ~ 5.2	4.5	525 ~ 1,910	1,010
Diorite	2.6 ~ 4.3	3.2	634 ~ 3,850	1,750
Dacite	2.5 ~ 3.1	2.8	142 ~ 493	318

Rocks	FE (%)	Mean	Resistivity (ohm-m)	Mean
Siliceous rock	1.1 ~ 2.3	1.5	192 ~ 674	336
Tuff	0.8 ~ 1.7	1.2	76 ~ 332	162
Porphyry	4.9		3,470	

The followings can be inferred from Figs. 4-7 and 4-8.

Table 4-2 Results of Rock Sample Tests in Mamlis Area

No.	Rocks	FE (%)	Resistivity (ohm-m)	Metal Factor	Remarks
M-4	Gossan	5.2	959	5	Druse
M-9	"	6.8	1,910	4	"
M-21	"	4.2	147	29	"
TAR-119	"	4.7	5,650	1	"
TAR-120	"	2.4	525	5	"
TSR-347	"	3.8	645	6	"
M-22B	Granodiorite	18.7	10	1,870	Cu-Pb-veinlet
TSR-365	Ore	49.2	64	768	Cu-Pb-Zn vein
M-19	"	114.7	10	11,470	"
M-14	Granodiorite	2.6	2,900	1	Py poor imp.
M-15	"	4.3	4,250	1	Hem, Mag imp.
M-16	"	3.2	634	5	"
M-22A	"	2.8	291	10	Weathered
M-23	"	6.6	1,490	4	
M-28	Siliceous Diorite	3.6	3,850	1	Py poor imp.
M-32	" "	1.9	763	2	"
M-27	Siliceous microdiorite	2.7	876	3	"
M-24	Dacite	2.5	142	18	Hem-Qtz veinlet
M-26	Siliceous Dacite	3.1	493	6	
M-6	Siliceous Rock	1.1	250	4	Hem-Qtz veinlet
M-10	" "	1.3	142	9	
M-25	" "	1.2	387	3	Drasey
M-29	" "	0.8	196	4	
M-30	" "	2.5	674	4	Py poor imp.
M-31	" "	2.3	235	10	Thin Hem-Qtz veinlet
M-3	" "	1.7	345	5	"
M-11	" "	1.7	262	6	Argillaceous
M-12	" "	1.4	825	2	Hem-Qtz vein
M-18	Dacitic Tuff	1.0	76	13	Hem-Qtz veinlet Sili-arg zone
M-19	" "	1.7	99	17	"
M-7	Dacitic Tuff Brec	0.8	140	6	
M-8	" " "	1.1	332	3	
M-13	Porphyry	4.9	3,470	1	Py imp.

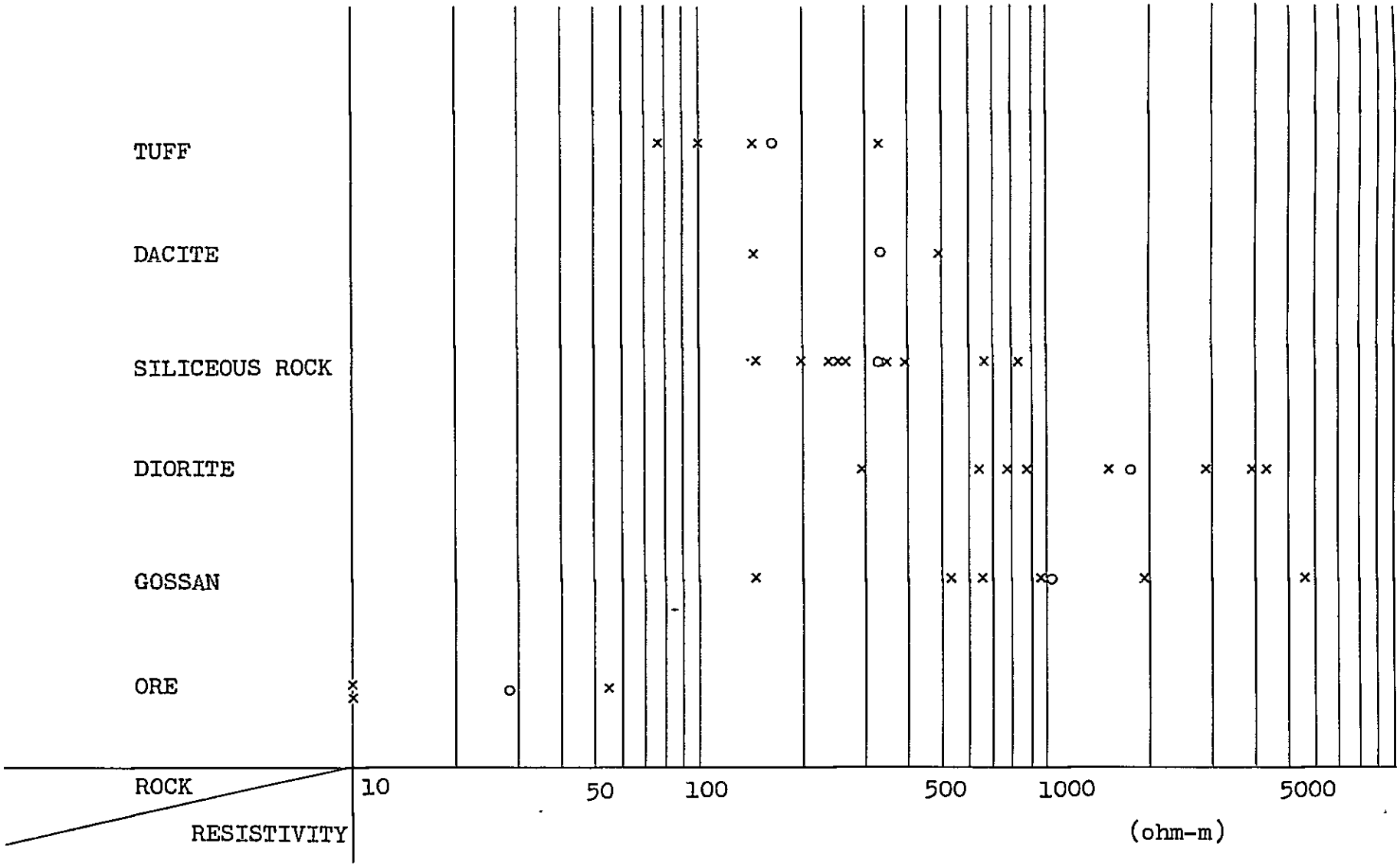

Fig.4-7 Distribution range of resistivity in laboratory measurements (Mamlis area)

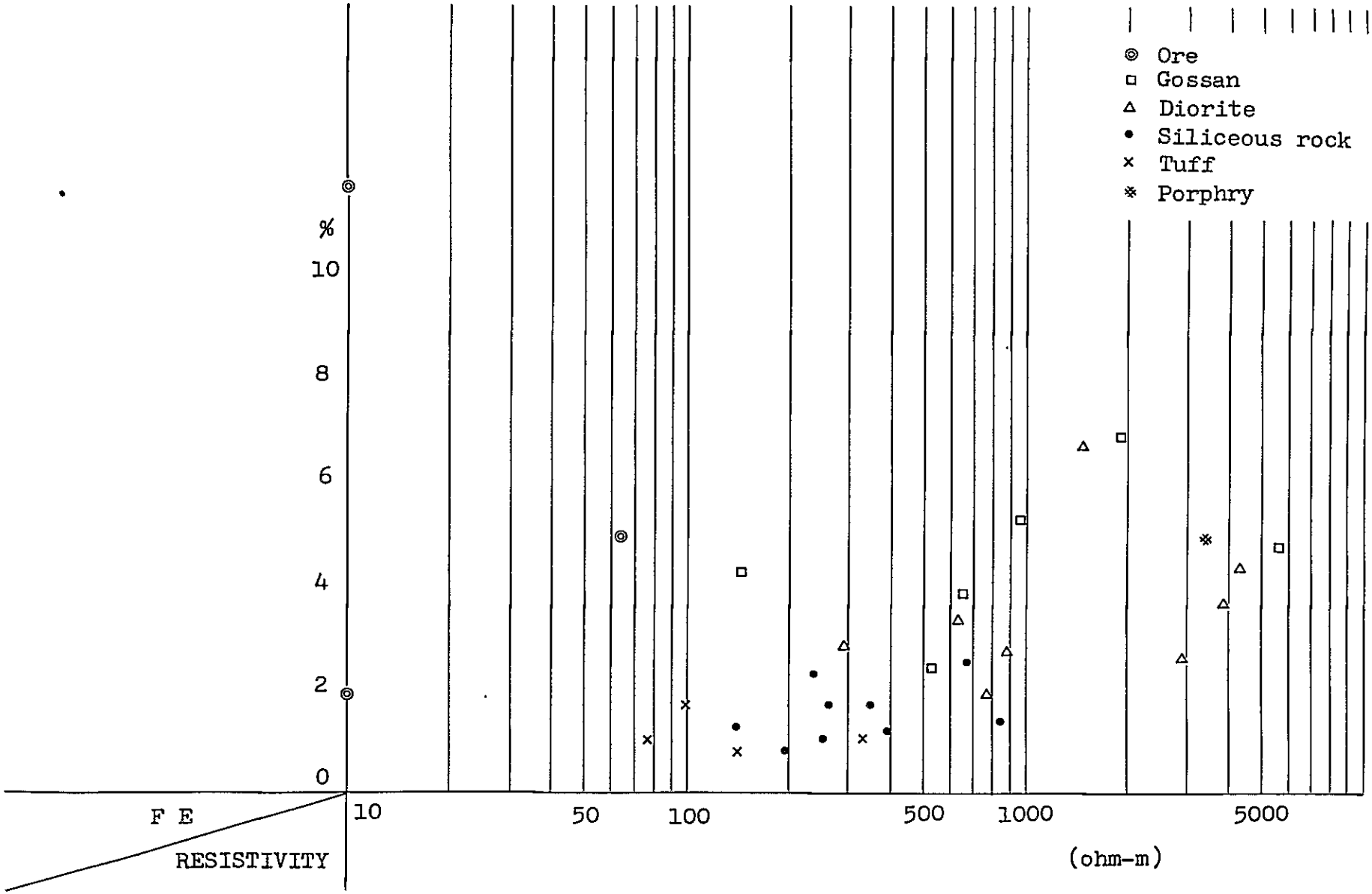

Fig.4-8 Correlation between FE and resistivity in laboratory measurements (Mamlis area)

FE: (1) The mean FE of ore specimens is 35%, very high as compared with the other kinds of specimens. Even in case of a granodiorite sample including Cu — Pb veinlets, the mean FE is not higher than 20%.

(2) The FE percentage of gossan is relatively low, ranging 2.6 ~ 5.2%, but slightly higher than those of host rocks.

(3) The mean FE of diorite is 3.2%, high relatively to the other kinds of host rocks. The pyrite dissemination of diorite samples may give rise to such a high FE.

(4) Specimens of widely distributed tuff indicate FEs ranging 1 ~ 2%.

(5) Only one specimen of porphyry indicates a 4.9% FE, relatively high. The siliceous dacite specimen, which was sampled at the site of the above porphyry specimen was sampled, also has a high FE amounting to 3.1%, and slightly higher than the other siliceous dacite specimens. This fact may imply that the mineralization was occurred around the sampling site.

Resistivity:

(1) As shown in Fig. 4-7, resistivities of the ore specimens have lower than 50 ohm-m, as compared with the other kind of specimens having resistivities ranging 75 ~ 5,600 ohm-m.

(2) The mean resistivities of gossan and diorite are 1,010 and 1,750 ohm-m, respectively. Those of dacite and siliceous rocks are 318 and 336 ohm-m, respectively.
The tuff specimens have a low resistivity, 162 ohm-m on average.

(3) The relatively low resistivity of siliceous rock may indicate that the silicification is not effective on AR.

(4) The statistical distributions of resistivity are overlapped each other, that is, there are no significant differences in resistivities between any kinds of rocks. Accordingly, it may be difficult to identify rocks on the basis of the differences in resistivity.

The FE-resistivity relation (Fig. 4-8) shows the following results.

(1) The ore specimens indicate very high FE and low resistivity, it is significantly different from those of host rocks.

(2) The gossan specimens have relatively high FE and resistivity.

(3) The diorite specimens have an FE slightly lower than the gossan specimens, but have a slightly higher resistivity.

(4) Both the FE and resistivity are low for the siliceous rock and tuff specimens.

4-5-6 Survey results

The field survey results processed as previously mentioned in 4-3 are represented in the cross sections of FE, AR and MF (PL. 4-3 ~ 4-16). The areal distribution of FE, AR and MF is also indicated in the plan maps at various levels of 100 m (n = 1), 200 m (n = 3) and 300 m (n = 5) as shown in PL. 4-17 ~ 4-25. The panel diagram representation (PL. 4-26, PL. 4-27) makes it easy to consider a three-dimensional distributions of FE and AR.

As a result of the survey, taking into consideration of the geological data and the rock specimen tests, the features of FE, AR and MF are interpreted as below.

1) FE

For the purpose of determining the standard level of FE which can identify an anomaly with background noise, a histogram (Fig. 4-9) and a cumulative distribution curve (Fig. 4-10) are made on the basis of statistics of all the FE survey results.

The distribution curve of the FE values, ranging $0.2 \sim 5.0\%$ is governed by a Gaussian distribution law as shown in Fig. 4-9. Denoting the mean and the standard deviation by μ and σ respectively, the cumulative frequency becomes 50% at μ, 84% at $\mu + \sigma$, and 98% at $\mu + 2\sigma$. If the values of background noise, weak and marked anomalies are respectively defined as μ, $\mu + \sigma$ and; $\mu + 2\sigma$ the corresponding standard levels of FE become 1.8%, 2.8% and 4.0% as shown in Fig. 4-10.

However, a small value of FE should not necessarily be neglected in the interpretation of the plan map. The pattern of FE anomaly contours sometimes indicates an important criterion of estimating FE anomalies. Deepseated ore deposits are indicated as feeble FE anomalies as compared with shallowseated ones. The contour pattern also varies with a depth to the resultant deposit. The appearance of FE depends on geological features and physical properties of surrounding rocks.

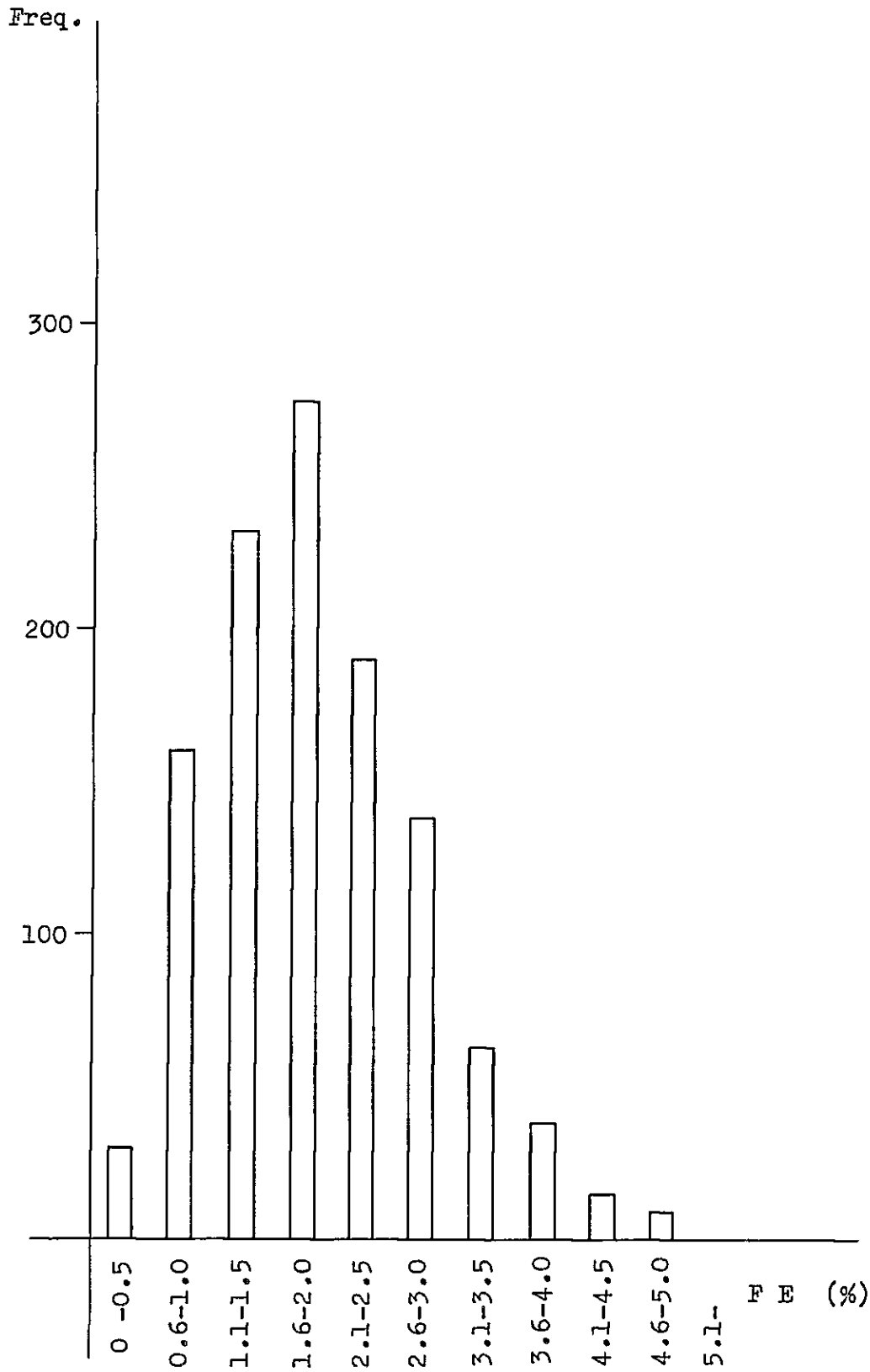

Fig.4-9 Histogram of FE (Mamlis area)

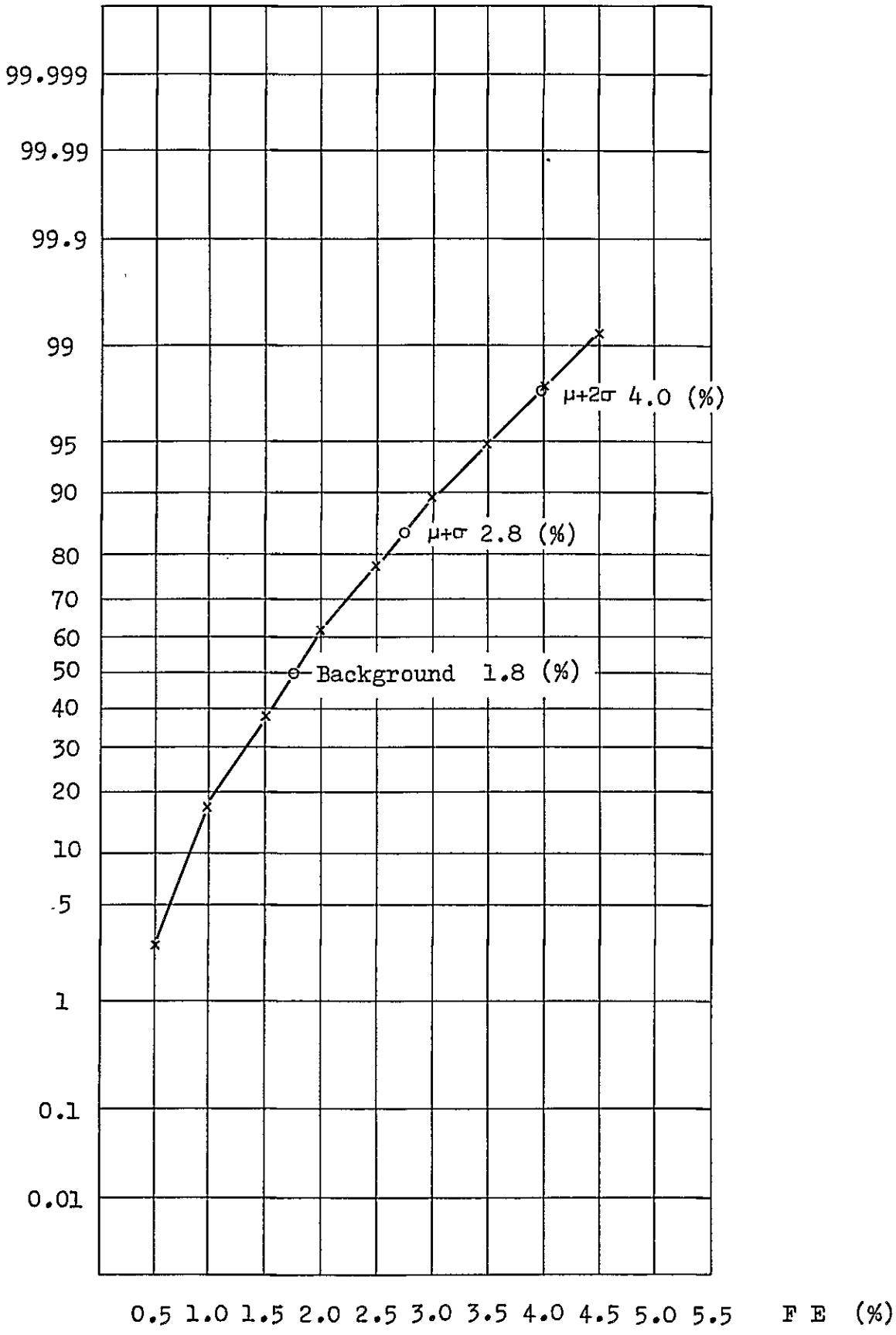

Fig.4-10 Cumulative frequency distribution of FE (Mamlis area)

Judging from these various conditions, the standard level of extracting anomalies from background noises is defined as:

	Fig. 4-10	Standard value
Background noise	1.8%	1.5%
Weak FE anomaly	> 2.8%	> 2.5%
FE anomaly	> 4.0%	> 3.0%

The followings are the results of the quantitative analysis of the FE anomalies with respect to each level.

n = 1 Plan Map (PL. 4-17)

(1) The FE values range 0.2 ~ 4.9%

(2) The FE anomalies are recognized in the following five locations.

a) Aşağı Mamlis hamlet and its neighborhood (FE - I Anomaly).

b) The northern part of Sivri Kaya (FE - II Anomaly)

c) The southeastern part of Haydar Tepe (FE - III Anomaly)

d) The southwestern part of Haydar Tepe (FE - IV Anomaly)

e) The southern part of Mamlis Maden (FE - V Anomaly)

The distribution and the geological features of these anomalies can be described as follows:

FE - I Anomaly:

A NW-SE or N-S trending high FE zone centered at Line E_5 No. 5 and Line E_4 Nos. 1 ~ 3 stations. The further extension of this zone is prolonged northwestwards. An anomalous area above 2.5% coincides with the distribution of quartz diorite (hereafter called Gt). It is especially noticeable that an area above 4.0% coincides with that of pyrite disseminated and/or siliciferous alteration zones.

FE - II Anomaly:

A circular anomalous area centered at Line 00 and Line E_1 Nos. 6 ~ 7 stations. It coincides with the limonite and silicified zone of dacitic pyroclastic (hereafter called Dmd) distributing over the north slope of Mt. Sivrikaya.

FE - III Anomaly:

An E-W trending high FE zone located around Line E_1 ~ Line E_4 and south of Line E_6. A good agreement is found with the gossan distribution. According to the geological survey results, the gossan distribution is prolonged zigzag in the west direction. The FE pattern lower than 1.5%, which is recognized across Lines W_1 to W_3, seems not to be a promising anomaly.

FE - IV Anomaly:

An anomaly detected at Line W_4 Nos. 17 ~ 20 stations. The entire picture of this anomaly is not known because of its

location at the southwest corner of the survey area, where gossan outcrops are found. The southwestern extension can be expected for a future object of geophysical prospecting.

FE - V Anomaly:

A NE-SW trending small-sized weak anomaly located south of Mamlis Mine.

(3) The quartz diorite distribution over the northwestern part of the survey area coincides with FE anomalies below the background noise level of 1.0 ~ 1.5%. The Dmd distribution over there is related to a feeble FE of 0.5 ~ 1.5% east of the Gezik stream. A 0.5 ~ 1.5% feeble FE also corresponds to the Dmd distribution over the southern part of the survey area.

n = 3 Plan Map (PL. 4-18)

(1) The FE pattern of this plan map has a tendency similar to that of the n = 1 plan map. However, FE anomalies over 3% occupy a smaller area as compared with that of the n = 1 map.

(2) The FE - I anomaly of this map covers Line E_5 No. 4, but smaller in size than the corresponding anomaly of the n = 1 plan map. The anomaly of over 4% distributed over the northern part of Line E_3 ~ E_4 in the n = 1 map

is diminished to be swallowed up by the anomaly located at Line E_5 No. 4. The FE - I anomaly source may be rather shallow-seated.

(3) The FE - II anomaly occupies a smaller-sized area as compared with the corresponding pattern of the n = 1 map. This anomaly seems to be split into two parts in both the sides of Mt. Sivrikaya. The resultant source may also be shallow-seated.

(4) The FE - III anomaly as low as 2.5% expands slightly in a N-S trend. On the other hand, a part larger than 3.0% seems to be shifted eastwards as a whole. An anomaly amounting to 3.3% is newly discovered around Line E_5 No. 16 station.

(5) The FE - IV and -V anomalies are diminished into small-sized patterns.

(6) An anomaly amounting to 4.5% is newly detected at Line E_5 Nos. 11 ~ 12 stations.

n = 5 Plan Map (PL. 4-19)

(1) The FE range of this map is 0.7 ~ 3.7%, i.e. the low FE area is expanded. The anomalous areas are generally diminished, and their locations shift to some extent.

(2) FE - I Anomaly: The E-W trend seems to be conspicuous, but an FE anomaly higher than 4% is disappeared in this map.

(3) FE - II Anomaly: The 2.5% area is expanded to the south of Mt. Sivrikaya. In the north, the 3% and higher area is combined with the FE - I anomaly.

(4) FE - III Anomaly: The center of this anomaly of over 3% seems to be shifted south of Line E_4 and E_5 Nos. 17 ~ 19 stations. The high FE zone found at Line E_3 on the n = map is disappeared.

(5) FE - IV Anomaly: The location of this anomaly shifts slightly to the north. The 3% or larger anomaly still remains at the Line W_4 No. 16 station.

(6) FE - V Anomaly: This anomaly is diminished below the background noise level.

2) AR

The results of AR are complied into a histogram (Fig. 4-11), which shows the range as wide as 54 ~ 2,090 ohm-m with a symmetric log-normal distribution. The cumulative frequency distribution of AR (Fig. 4-12) indicates that the median of AR is 270 ohm-m. The standard levels discriminating between high and low anomalies, and background noise are estimated as 500 and 100 ohm-m by taking the results of rock specimen tests into account. The local features of AR results are summarized below.

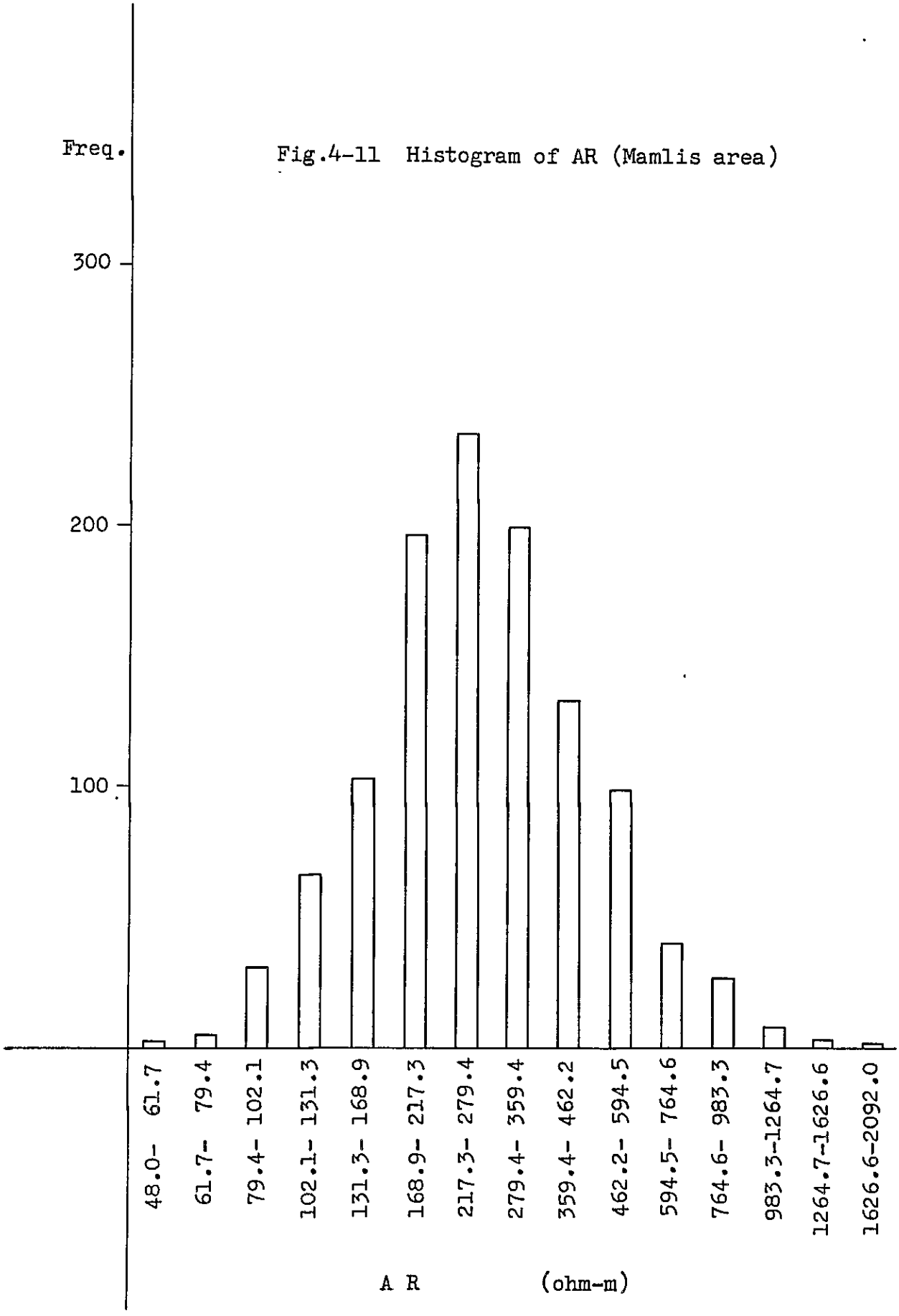

Fig.4-11 Histogram of AR (Mamlis area)

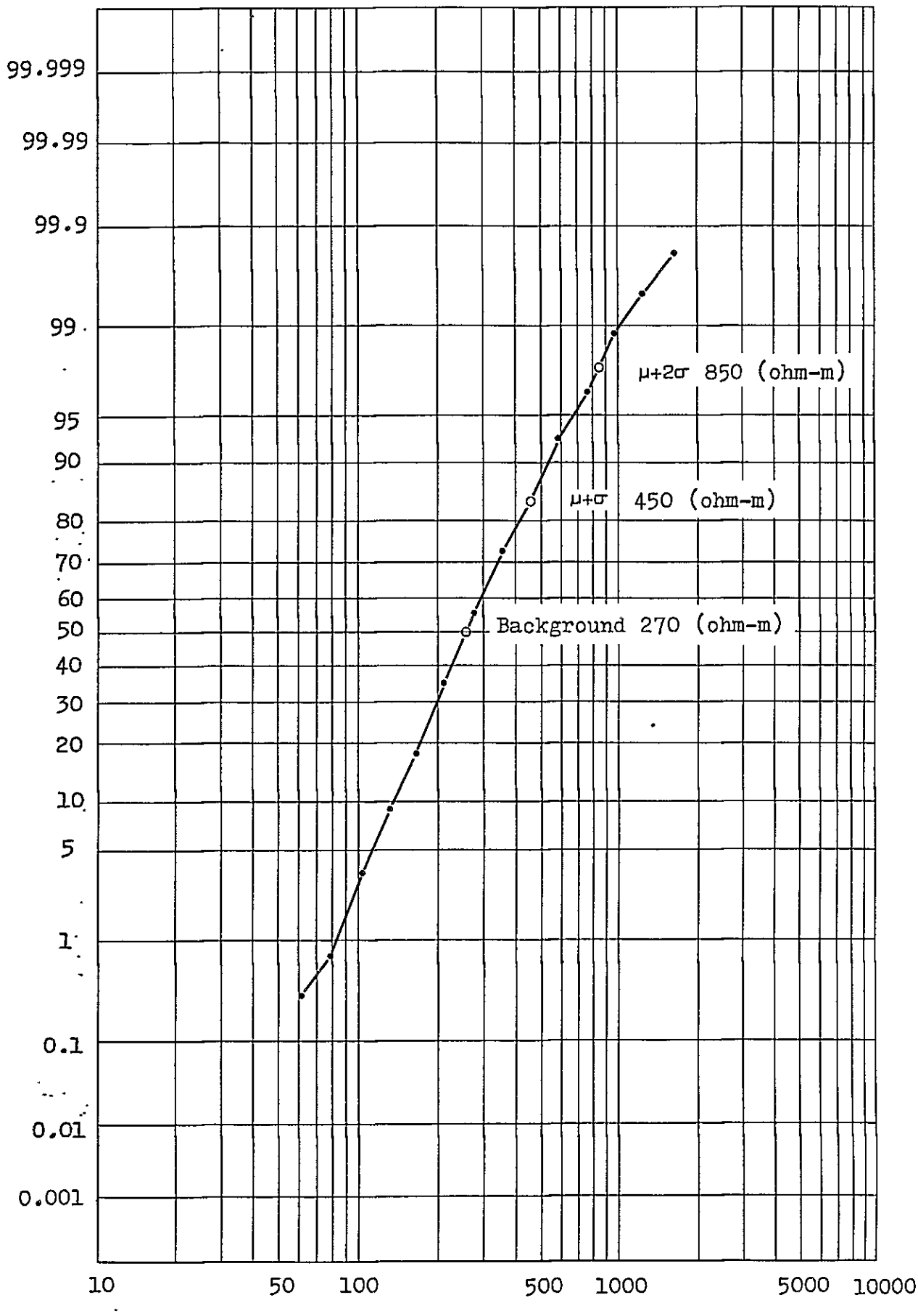

Fig.4-12 Cumulative frequency distribution of AR
(Mamlis area)

n = 1 Plan Map (PL. 4-20)

(1) AR values range from 74 to 1,480 ohm-m in this plan map.

(2) An E-W trending high AR zone, which is well correlated the Gt outcrops, is found in the northwestern and central part, south of Mt. Sivri kaya, of the survey area.

(3) Small-sized high AR zones exsist on Lines E_3, E_4 and E_5. They almost correspond to the Dmd distribution except at Line E_4 No. 12 and Line E_5 No. 10 stations.
The other highs correspond to the FE-III anomaly which is caused by gossan at Line E_4 No. 17 and Line E_5 No. 16 stations. Such a tendency as gossan shows a high AR can be inferred from the IP measurements of rock specimens.

(4) A small-sized high AR anomaly coincides with the FE-II anomaly corresponding to hematite outcrops.

n = 3 Plan Map (PL. 4-21)

(1) The contour pattern of this map is very similar to that of the n = 1 map. The range of AR is 81 ~ 1,810 ohm-m.

(2) A high AR zone trends E-W around Line E_4 and E_5 Nos. 10 ~ 11 stations in the eastern part of the survey area.

(3) The distribution of a high AR over Line E_4 No. 15 station, the southern part of the survey area, is diminished in this map. The marginal area of this high is dotted with spots of anomaly lower than 100 ohm-m.

(4) The high FE zone north of Mt. Sivri kaya in the n = 1 map is completely vanished in this map. This fact may indicate that the corresponding oxidized body is not deep seated.

n = 5 Plan Map (PL. 4-22)

(1) The general aspect of AR, ranging from 86 to 997 ohm-m, is similar to those of the n = 1 and 3 plan maps.

(2) In the southeastern part of this map, an AR zone as low as 100 ohm-m is extended wider than in the n = 1 map.

(3) The distribution pattern of a high AR in the central and northwestern parts of the survey area is very similar to those of the n = 1 and 3 map. The related underground structure is interpreted as deepseated quartz diorite.

3) MF

Similarly to the cases of FE and AR, a histogram and a cumulative frequency distribution chart of MF are also made as indicated in Figs. 4-13 and 4-14. The MF, ranging from 1 to 50, is presumed to have a log-normal distribution curve with the median of 6. The frequency is very high within the range 0 ~ 5.

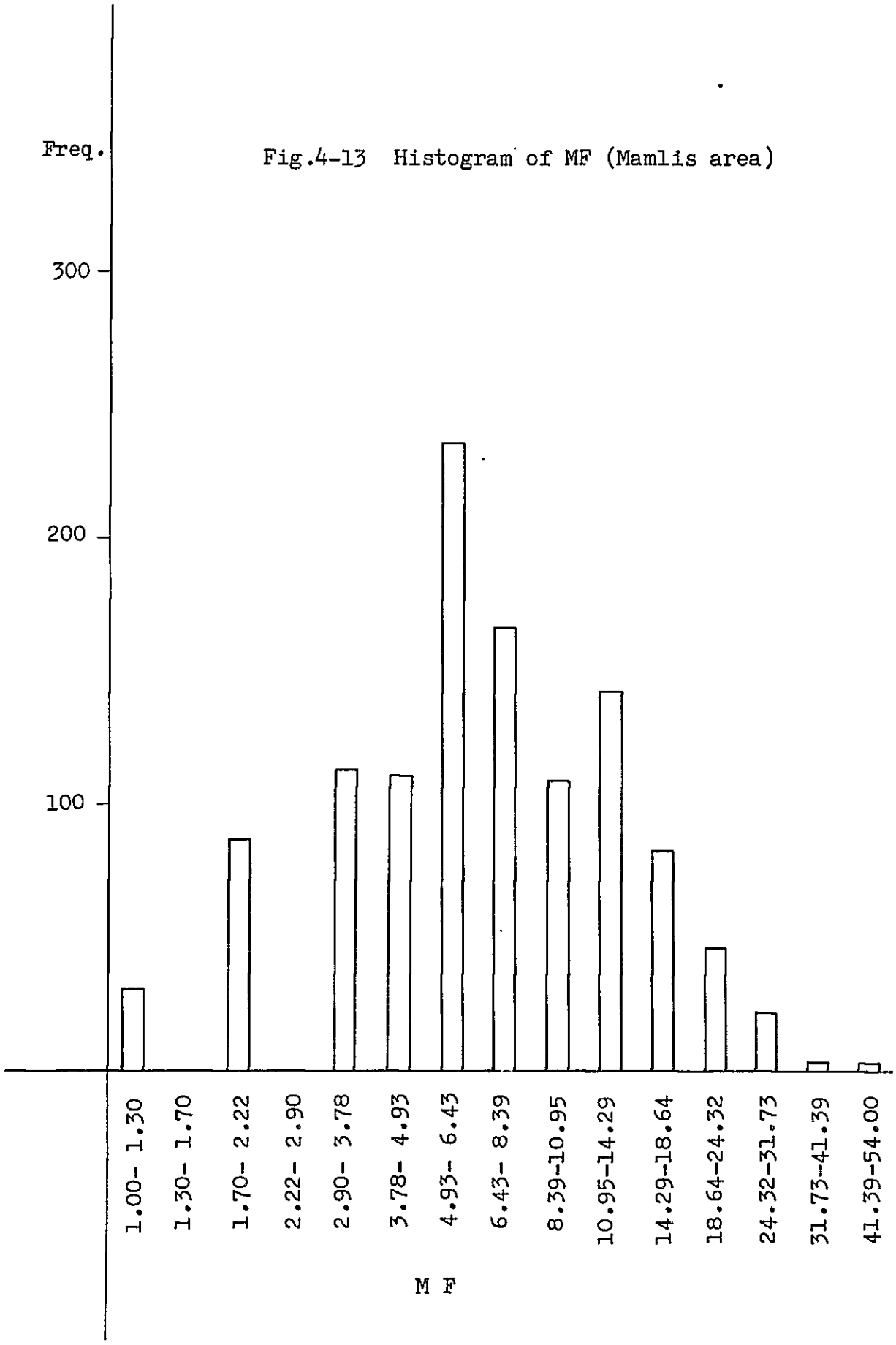

Fig.4-13 Histogram of MF (Mamlis area)

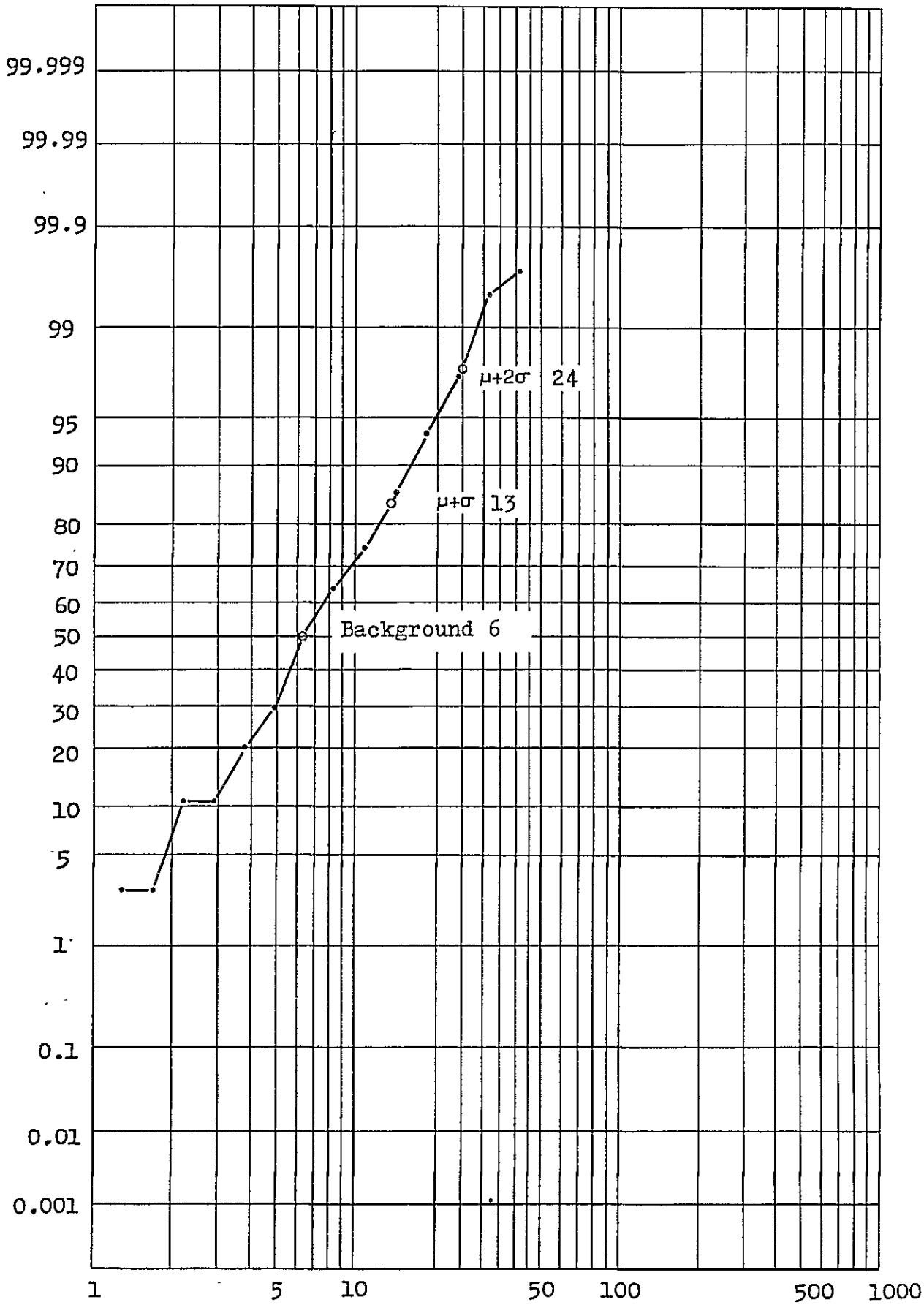

Fig.4-14 Cumulative frequency distribution of MF (Mamlis area)

The points $\mu + \sigma$ and $\mu + 2\sigma$ fall on 13 and 24. Judging from the rock specimen results that mineralized specimens take MF values higher than 15, the level discriminating between anomaly and background is determined as 15.

The features of MF noticeable in the n = 1, 3 and 5 maps are summarized in the followings:

n = 1 Plan Map (PL. 4-23)

(1) MF ranges from 1 to 31 in this map. An E-W trending low MF zone covers the central part.

(2) High MF zones are widely distributed over Line $E_2 \sim E_5$, No. 1 ~ 4, though somewhat higher in the north. Smallsized high MFs trending E-W are found in the south of Guzik stream of the southeastern part of the map. They agree well with the FE-III anomaly due to gossan outcrops.

(3) A high MF zone also covers at Line W_4 No. 18 ~ 20 stations in the southwestern part of the mapped area.

(4) No MF anomaly is found at and around the Mamlis Mine.

(5) The Dmd region has MF ranging from 5 to 10 in the north but from 1 to 5 in the south. The quartz diorite zone covering the northwestern and central part of the mapped area shows MF ranging from 1 to 5.

n = 3 Plan Map (PL. 4-24)

(1) The range of MF is 1 ~ 31

(2) The high MF anomaly, which is widely found in the north-eastern part of the n = 1 map, is split into three small-sized anomalies.

(3) A MF zone higher than 15, covering the northern foot of Mt. Sivri kaya, trends NE-SW. This may suggest that the trend of the mineralized zone is related to the FE-II anomaly.

(4) A wide distribution of high MF in the southern part of the map may be generated from an extensive deepseated mineralized deposits overlaid by gossan. The maximum MF value amounting to 31 is detected near Line E_5 No. 19 station.

n = 5 Plan Map (PL. 4-25)

(1) The range of MF is 2 ~ 33 in this plan map.

(2) The general aspect of the MF pattern is very similar to that of the n = 3 map, although we recognize newly a small-sized high MF in the northeastern area and another high trending E-W in the southeastern area.

4-5-7 Results of simulation analysis

In 4-5-5, the qualitative analysis is made with regard to FE, AR and MF plan map, the correlations are discussed between FE anomalies, AR, MF patterns and the distribution of geology and mineralization. The five anomalous zones are found by the qualitative analysis, the three anomalies in these are applied simulation analysis for the purpose of estimating FE and resistivity values and the depth of anomaly sources.

A) FE-1 Anomaly (Fig. 4-15)

This anomaly locates northern part of Line E_5 and continues to west and east lines. Simulation analysis is applied to the part from No. 2 station to No. 12 station of the Line E_5 where a clear FE pattern is detected. This part, covered quartz diorite, is fully disseminated with pyrite, and silicified near No. 4-5 stations in particular. Malachite is found in the neighborhood of No. 4-5 stations. The Feature of FE profile is that high FE zone (4%) distributes from shallow part to deep part below No. 2-9 stations in a reciprocal triangle and 2.5% zone dipping south from No. 8-9 stations and 4.5% zone below 200 m from the ground surface at No. 11-12 stations are detected.

The following model is built in consideration of pattern of field measurements, geology and rock sample tests, etc. The high FE zone (FE 10%, resistivity 300 ohm-m, code 5) is set below 100 m from the ground surface at No. 4-5 stations. Two slightly high FE zones are set, the one is FE 5%, resistivity 500 ohm-m, code 4 which is at the sharrow

part below No. 6-8 stations, the other is FE 5%, resistivity 200 ohm-m, code 3 which is at No. 9-10 stations. Quartz diorite covered fully in this line is set FE 1%, resistivity 500 ohm-m, code 2.

The result of simulation shows good FE and AR patterns except that FE value is lower than field data and that the low FE zone at No. 7-9 stations is not clear. The FE values of simulation show 50-75% of field data. The simulation result will be better than this in case that the FE values of code 3,4 and 5 increase 10, 7 and 7% respectively.

B) FE-111 Anomaly (Fig. 4-16)

This anomaly corresponds to the gossan which is distributed E-W direction at the SE of Mt. Haydar. A depth of the FE anomaly is at a shallow part between the Line E_2 and Line E_3, and is at a middle deep part of Line E_4 and Line E_5. For the purpose of searching the primary sulfide minerals, the part from No. 11 to No. 21 stations of the Line E_5 is simulated. In this part, two high FE values are detected, the one is FE 3.3% below 300 m from the ground surface at No. 15-16 stations and the other is FE 3.7% below 400 m from the ground surface at No. 18 station. 2.5% zone, around the high FE values above mentioned, is distributed to the extent of No. 15-20 stations. Dacitic pyroclastic rocks (Dmd) distribute widely as the host rocks. The model is made as followings; two high FE zones are set, the one is FE 4%, resistivity 400 ohm-m, code 3 below 200 m from the ground surface at No. 16 station,

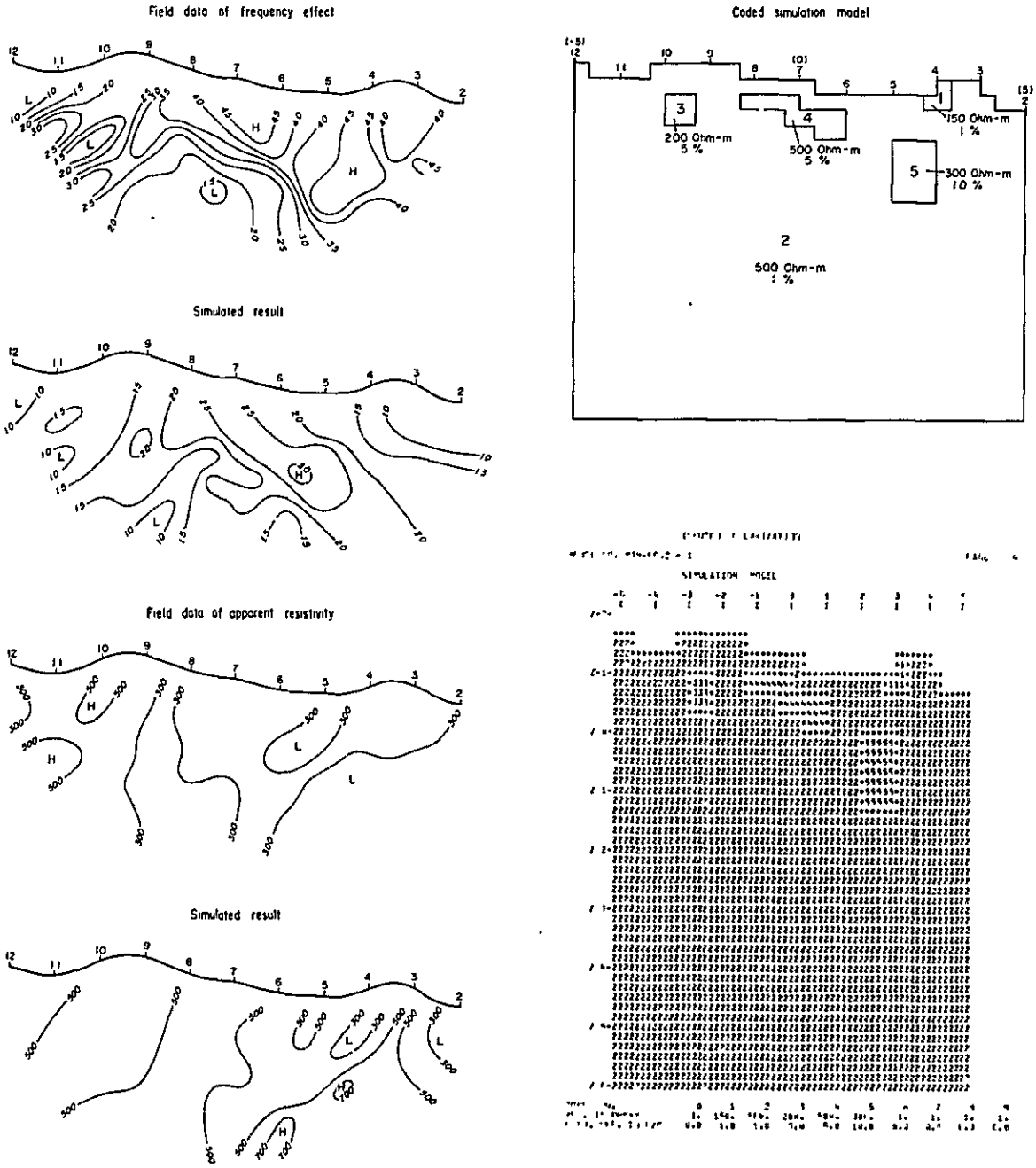

Fig.4-15 Results of sumilation analysis,LineE5(No.2-No.12)

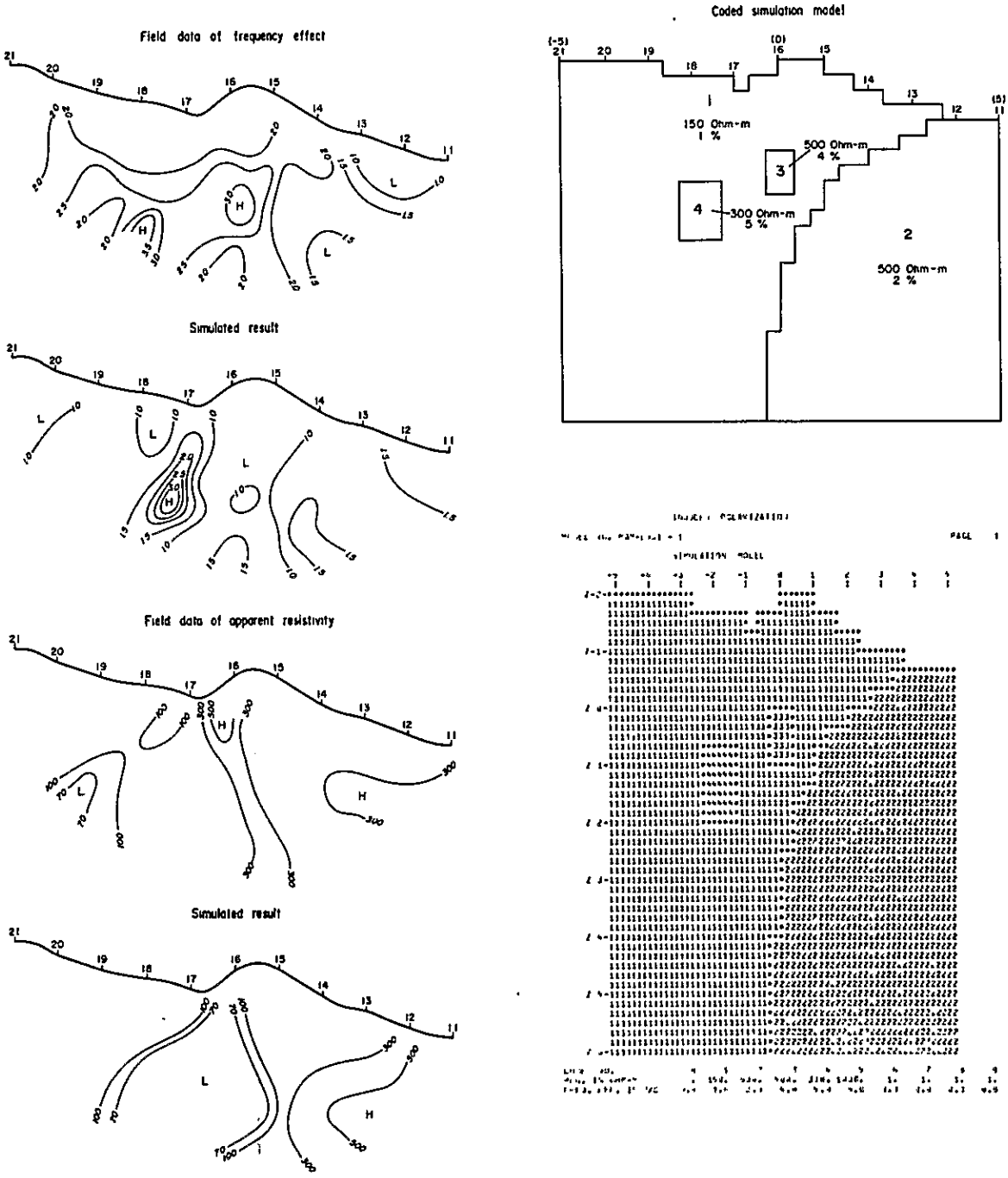

Fig.4-16 Results of sumilation analysis,LineE5(No.11-No.21)

the other is FE 5%, resistivity 300 ohm-m, and code 1 below 200 m from the ground surface at the No. 17-18 stations. Dmd (FE 1%, resistivity 15 ohm-m and code 1) is set. Quartz diorite in northern part is set FE 2%, resistivity 500 ohm-m and code 2.

The following matters are pointed out after simulation; the high FE zones coded 3 and 4 are detected corresponding to field measurements. The new high FE zone at No. 17-18 stations are detected and a background value of FE is lower than field data. Concerning AR, 300 ohm-m zone is distributed. The low AR zone (< 100 ohm-m) at No. 15 - 18 stations where dacite is widely distributed is prominent.

C) FE-1V Anomaly (Fig. 4-17)

This anomaly occurs the southern part of Line W_4, the part from No. 11 station to 21 station where is overlain by dacitic pyrocrastic rocks and the gossan is found at No. 16 station and No. 17 station. The FE distribution is as follows, 2.5% FE zone between No. 14 station and No. 16 station dips south, 4% FE zone at No. 18 station dips north. These anomalies are independent. The former is made by mineralization of Mamlis mine deposit. The latter is due to a high FE source at a shallow part and shows a part of roof pattern. Four models are made to this anomaly that 2.5% FE zone between No. 14 station and No. 16 station dips south, 4% FE zone at No. 18 station dips north. These anomalies are independent. The former is generated by mineralization of Mamlis mine deposit. The latter is due to high FE source at a shallow part and shows a part of roof pattern. According to above terms, four modes are made.

Model A:

A vertical high FE zone (FE 8%, resistivity 500 ohm-m, code 1) is set below No. 19-20 stations and a horizontal high FE zone (FE 6%, resistivity 300 ohm-m, code 2) is set below No. 12-14 stations.

Model B:

A high FE zone (FE 8%, resistivity 500 ohm-m, code 2), dipping north, is set below No. 19-20 stations and a horizontal high FE zone (FE 6%, resistivity 300 ohm-m, code 4) and low resistivity zone (FE 4%, resistivity 100 ohm-m, code 5) are set below No. 12-14 stations.

Model C:

A high FE zone (code 2) dipping south is set below No. 19-20 stations. Another conditions are same in case of Model B.

Model D:

A horizontal high FE zone (FE 10%, resistivity 200 ohm-m, code 2) is set below the shallow part below No. 19-20 stations and a wide 5% zone dipping south is set at No. 12-15 stations.

A dacitic pyroclastic rocks (FE 1%, resistivity 300 ohm-m, code, A:3, B~D:1) and quartz diorite (Model A: FE 2%, resistivity 500 ohm-m, Code 4, Model B~D: FE 1%, resistivity 200 ohm-m, code 3) are set.

The result of simulation is almost similar to field measurements except Model D. Each FE pattern below No. 16-20 stations indicates

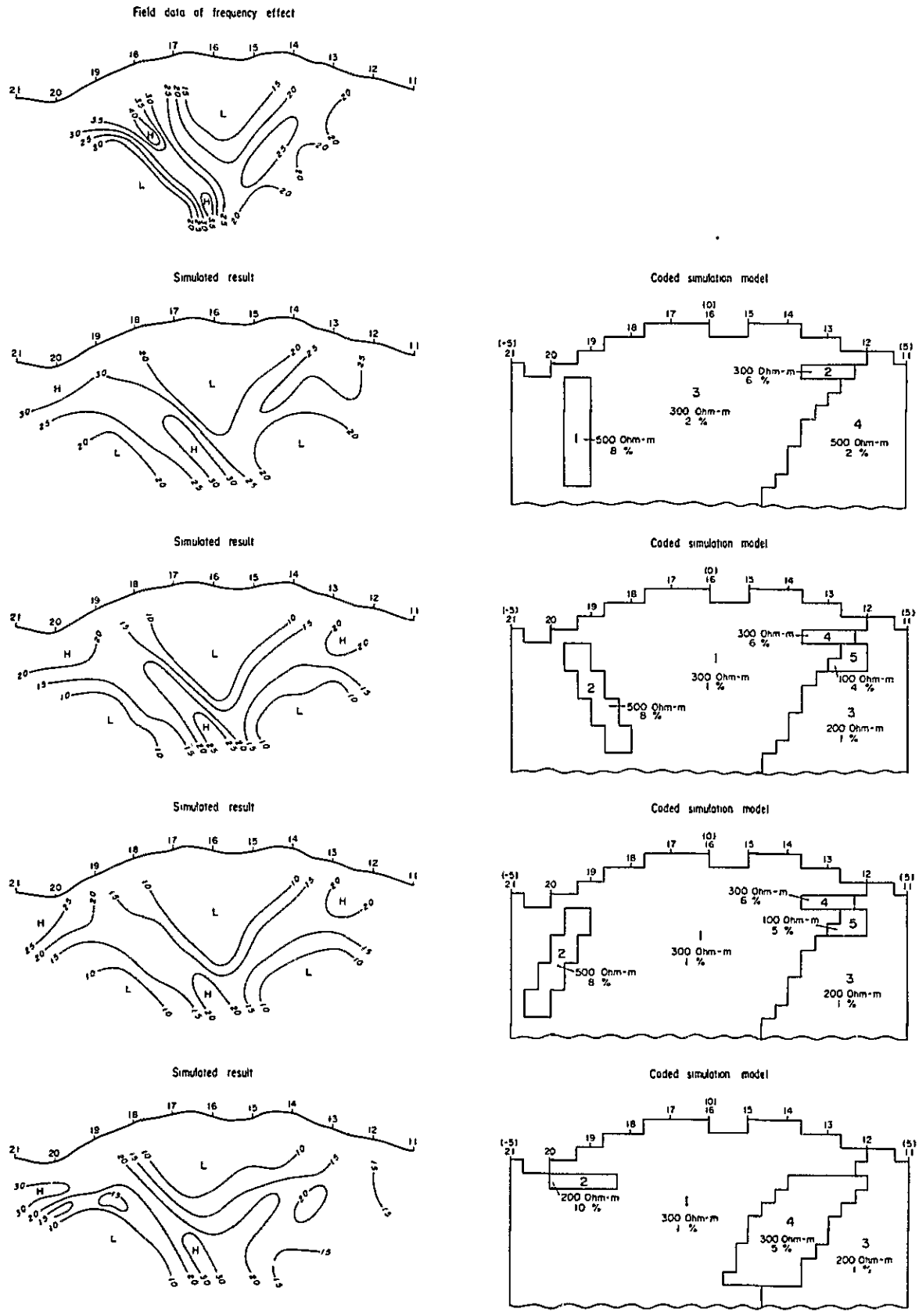

Fig.4-17 Results of sumilation analysis,LineW4(No.11-No.21)

similar with field data, but it is difficult to decide which FE pattern is best, because a full pattern of this anomaly is not caught. An FE pattern of Model A from No. 12 station to 16 station is similar because the assumption of resistivity value to quartz diorite is reasonable.
FE patterns below No. 18-20 and No. 13-16 are different from the field data. The possibility of model D is rare.

4-5-8 Survey remarks

The present survey has succeeded to find five FE anomalies, whose distribution, continuation to deeper bodies and geological evidence has been previously mentioned in 4-5-6. The simulation analyses using a computer has been made to estimate FE, AR and depth of the conducting bodies, as described in 4-5-7. What we have disclosed in the present survey of the Mamlis Area will be briefly summarized again, and the future plan of geophysical exploration will be described below.

A) Aşağı Mamlis Anomaly (FE-I Anomaly)

(1) The wide distribution of the FE-1 anomaly may be caused by the development of mineralized and argillized zones.

(2) The anomalous area of FE 2.5% or higher coincides with a pyrite-disseminated, silicified and argillized zone in quartz diorite. The fact that the field AR measured on Line E_6 is lower than the result of laboratory test of a quartz diorite specimen may indicate the extension of an alteration zone east of this line.

(3) The fact that this anomaly trends NW-SE may also indicate the northern extension.

(4) The downward continuation of this anomalous body cannot be expected.

B) North Sivri kaya Anomaly (FE-II Anomaly)

(1) The area surrounded by a FE 3% contour corresponds to gossan outcrops of dacitic pyroclastics. In the eastern part of this anomaly, the downward continuation to a deeper conductor can be expected.

(2) The primary sulfide minerals cannot be expected to be found at the bottom of the gossan.

C) Southeast Haydar Tepe Anomaly (FE-III Anomaly)

(1) This anomaly is related to the gossan. Among Line E_2 and E_6 it trends in the E-W direction.

(2) The depth of the anomaly source is thought to be shallow-seated beneath Lines E_2, E_3 and E_6, but relatively deep beneath Lines E_4 and E_5. Although the geological survey results prospect the source structure is gently-sloped southwards the simulation analysis do not find such a tendency.

(3) The most promising gossan has been found by the geological survey on Lines W_1 and W_2 west of this anomaly. However, there is no geophysical anomaly over the gossan, so that the deeper continuation of the gossan can not be prospected.

(4) The primary sulfide minerals can be expected to be found at the bottom of gossan at Lines E_4 and E_5 No. 16 ~ 17 stations.

D) Southwest Haydar Tepe Anomaly (FE-IV Anomaly)

(1) This anomaly may possibly be continued westwards and southwards beyond the survey area. Unfortunately, the entire picture of this anomaly has not been captured because it is located at the southwest corner of the survey area.

(2) This anomaly may be related to the shallow-seated source, whose continuation downward can not be presumed.

E) Southwest Sivri kaya High AR

(1) The high AR zone, as high as 500 ohm-m, coincides with quartz diorite in the southwest Sivri kaya. However, the corresponding FE anomaly is not found. This may imply that the fresh quartz diorite body without mineralization and alteration is continued downwards.

F) Remarks on the Mamlis Mine Prospectings

(1) The anomaly pattern related to the Mamlis Mine has been clarified by a 50 m-interval electrode configuration but not by a 100 m-interval one. An outstanding clear anomaly has been captured on Line W_3 (8-18), on the other hand, the corresponding anomaly becomes very weak on Line W_4 (8-18). Accordingly, it is not expected a westward extension of this anomaly.

Future Plan of Geophysical Exploration (PL. 4-28)

(1) For the purpose of disclosing the anomaly sources, the following drillings are desired.

Rank	Anomaly	Location of Drilling	Direction	Depth
A	FE-III	Line E_5 No. 16-17	Vertically down	250-300 m
A	FE-I	Line E_5 No. 4-5	Vertically down	100-150 m
B	FE-IV	Line W_4 No. 19-20	Vertically down	200-250 m
B	FE-III	Line E_2 No. 15-16	Vertically down	250-300 m
B	FE-I	Line E_5 No. 7	Vertically down	100-150 m
B	FE-III	Line E_5 No. 18	Vertically down	250-300 m

(2) For the purpose of clarifying the entire picture of the FE-I anomaly found in the northeastern part, the further geophysical prospecting to the north and east of the present survey area is desired.

(3) The western and southern extensions of the FE-IV anomaly should be surveyed because it may be continued in these directions.

4-6 Sin Area

4-6-1 Survey area (PL. 4-29)

Sin area is located about 20 km northwest of Tunceli and the northwest corner of the survey area. It takes about one hour on the gravel road to go the Sin hamlet by jeep. Further, it takes about 20 minutes on foot to go from Sin hamlet to Sin mine (closed) in the central part of the survey area.

The survey covers an area of 1.9 km^2 including 16 survey lines. The total length amounts to 270 km.

No.	Line	Length (m)	No. of Survey stations
1	N_7	1,700	65
2	N_6	"	"
3	N_5	"	"
4	N_4	"	"
5	N_3	"	"

No.	Line	Length (m)	No. of Survey stations
6	N_2	1,700	65
7	N_1	1,600	60
8	00	1,700	65
9	S_1	"	"
10	S_2	"	"
11	S_3	"	"
12	S_4	"	"
13	B(8)	1,100	35
14	B(11)	"	"
15	K_1	2,100	85
16	K_2	2,400	100
Total		27,000 m	1,030

4-6-2 Survey period

Land Survey : June 19 to September 12, 1979

Field IP Measurements : July 4 to September 22, 1979

4-6-3 Outline of geology

The geological feature of this area is characterized with the Düzpelit Formation consisting of dacitic pyroclastics underlaid with the Atadoğdu Formation consisting of mudstone and sandstone as well as the Bentepe Formation of mudstone and sandstone embedded in conglomerate.

The Sin dacite intrusions penetrate complicatedly these Formation. The mineralization is found in the alteration zones around the dacite contact with the surrounding sedimentary rocks. The Sin dacite intrusions are observed widely in the survey area, accompanying with silicified, argillized and pyrite disseminated zones. The silicified zones are conspicuous near the Sin Mine, where malachitestain is observed along an E-W trending fracture zone within the dacite intrusions. The strong silicification is associated with network and quartz vein including sphalerite. See a detailed account in the 1978 Geological Survey Report of Tunceli Area.

4-6-4 Survey apparatus

The field apparatuses used in the survey are as follows:

Transmitter

Type	:	IP square-wave generator Model T 2800
Manufacturer	:	Geotronics Co., USA
Input Voltage	:	95 - 120 V, 400 Hz
Output Voltage	:	95 - 800 V
Output Current	:	0.05 - 2.0 A
Frequency	:	0.1, 0.3, 1, 3 and 10 Hz

Receiver

Type	:	IP Receiver Geomite Model R401
Manufacturer	:	Geotronics Co., USA
Input Voltage	:	9.0 μV ~ 10 V, 6 steps
Input Impedance	:	10 M ohm
Time Constant	:	2, 6, 15, 60, 150 and 600 sec.

Electrode

Current Electrode	:	Stainless steel stick
Potential Electrode	:	Porous electrode pot saturated with copper sulfate solution

Engine Generator

Type	:	Mark 11-400
Manufacturer	:	McCullch, USA
Output	:	115 V, 400 Hz, 2 kw

4-6-5 Results of rock sample tests

FE and AR laboratory tests are made with 27 rock specimens sampled in the Sin area. The sampling locations are illustrated in PL. 4-30. The results of rock specimen tests are tabulated in Table 4-3. The statistical distribution of observed values of resistivity is shown in Fig. 4-18.

Table 4-3 Results of Rock Sample Tests in Sin Area

No.	Rocks	FE (%)	Resistivity (ohm-m)	Metal Factor	Remarks
TSR-324	Zn-Malachite Ore	18.2	1,580	12	
S-6	Siliceous Dacite	3.5	3,280	1	Malachite stain poor
S-10	" "	2.9	1,730	2	Pb-Zn Veinlet with malachite
S-9	Siliceous Dacite	2.6	3,160	1	Py imp.
S-11	" "	3.5	3,500	1	"
S-15	" "	1.0	160	6	Thin Hem-Qtz Vein
TER-257	" "	2.1	316	7	Hem-Qtz Vein, Py imp.
TER-258	" "	1.6	247	6	Malachite stain along fissure
S-13A	Dacite	2.8	420	7	
S-13B	"	2.3	185	12	
S-16	"	3.2	399	8	
TSR-184	"	3.4	863	4	Py imp. (poor)
TWR-141	"	3.7	412	9	
TWR-143	"	2.4	1,940	1	
TSR-186	"	2.2	1,090	2	
TER-263	Siliceous Dacitic Tuff	1.9	217	9	Weathered
TER-264	Dacitic Tuff	1.1	196	6	
S-1	Limestone	2.4	1,810	1	
TER-259	"	1.4	773	2	
S-3	Siliceous Mudstone	1.3	626	2	Py imp.
S-12	" "	9.2	760	12	"
TER-261	" "	2.1	258	8	"
TER-262	" "	0.9	64	14	Weathered
TER-265	" "	0.6	497	1	Py imp. (Poor)
S-14A	Black Mudstone	1.3	8,550	0.2	
S-14B	" "	0.7	1,530	0.5	
TER-265-1	Siliceous Black Mudstone	1.5	808	2	

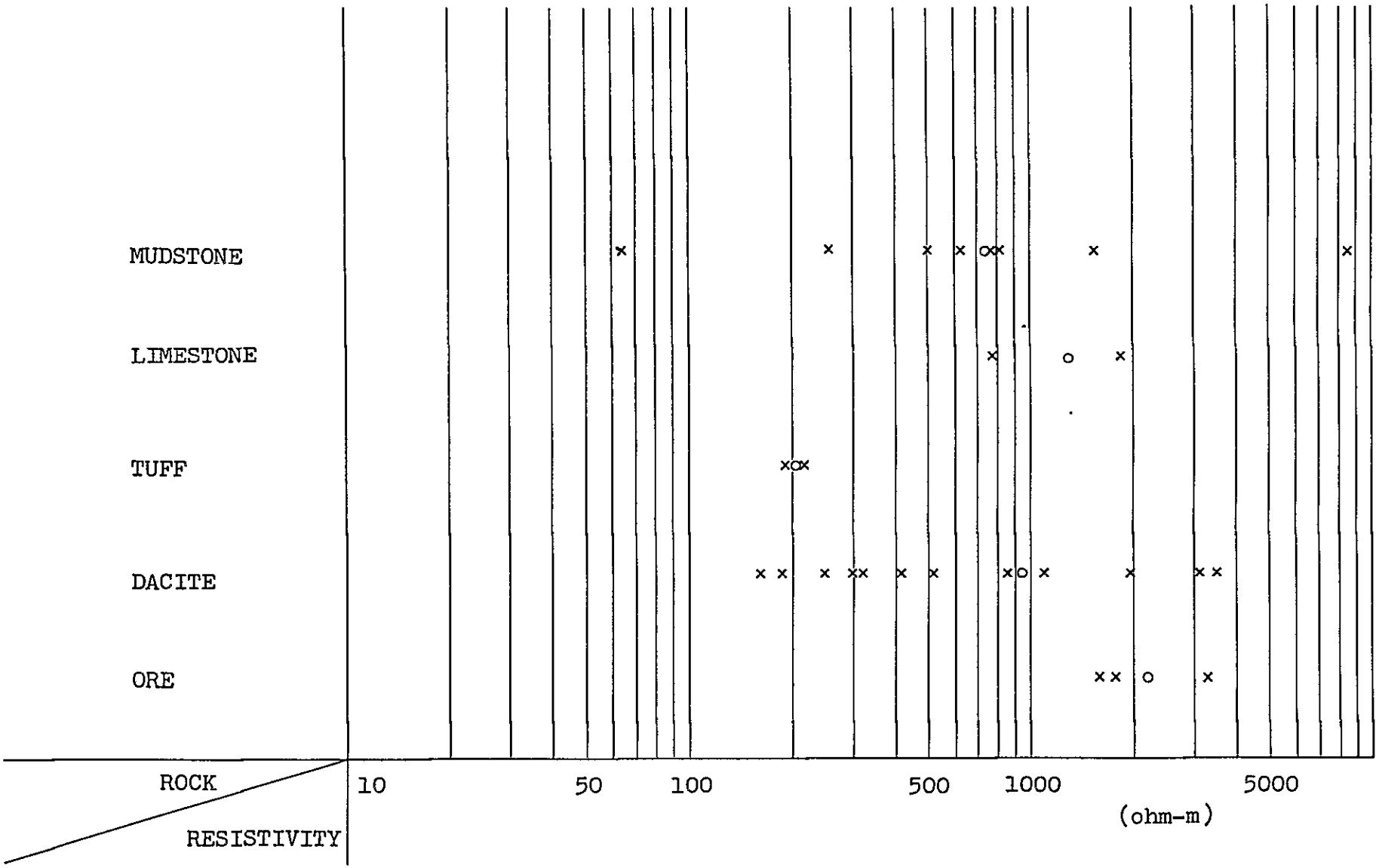

Fig.4-18 Distribution range of resistivity in laboratory measurements (Sin area)

The statistical distribution ranges of FE and resistivity except for both the maximum and minimum values together with its mean values are given below.

Rock	FE (%)	Mean (%)	Resistivity (ohm-m)	Mean (ohm-m)
Ore	2.9 ~ 18.2	8.2	1,580 ~ 3,280	2,200
Dacite	1.6 ~ 3.5	2.6	185 ~ 3,160	903
Tuff	1.1 ~ 1.9	1.5	196 ~ 217	207
Limestone	1.4 ~ 2.4	1.9	773 ~ 1,810	1,290
Mudstone	0.7 ~ 2.1	1.3	258 ~ 1,530	746

The followings can be pointed out from Fig. 4-18.

FE: (1) The FE values of ore specimens range from 2.9 to 18.2%, lower than ore specimens sampled in the Mamlis area. This may be caused by abundance of oxide minerals.

(2) The FE values of dacite, tuff, limestone and mudstone range from 0.7 to 3.5%. The specimens including pyrite- and hematite-bearing quartz vein indicate a slightly higher FE.

Resistivity:

(1) The resistivity values of rock specimens sampled in the Sin area range from 64 to 8,550 ohm-m. Those of dacite and mudstone specimens are statistically distributed in wider ranges.

(2) Ore specimens take resistivity values as high as 1,000 ohm-m. Possible causes of such high resistivities may be the silicification of dacite as host rock and abundance of oxide minerals.

(3) Although we have tested a few specimens of limestone and tuff, we can conclude that limestone has a high resistivity amounting to 1,000 ohm-m in contrast to tuff having a low resistivity amounting to 200 ohm-m.

(4) Judging from the statistical distribution of resistivity values of rock specimens, it may be difficult to classify rocks on the basis of differences in resistivity.

The resistivity and FE values range 100 ~ 4,000 ohm-m and 0 ~ 4%, respectively. These ranges are common to all kinds of rock specimens sampled in this area. Fig. 4-19 shows the FE-resistivity relation.

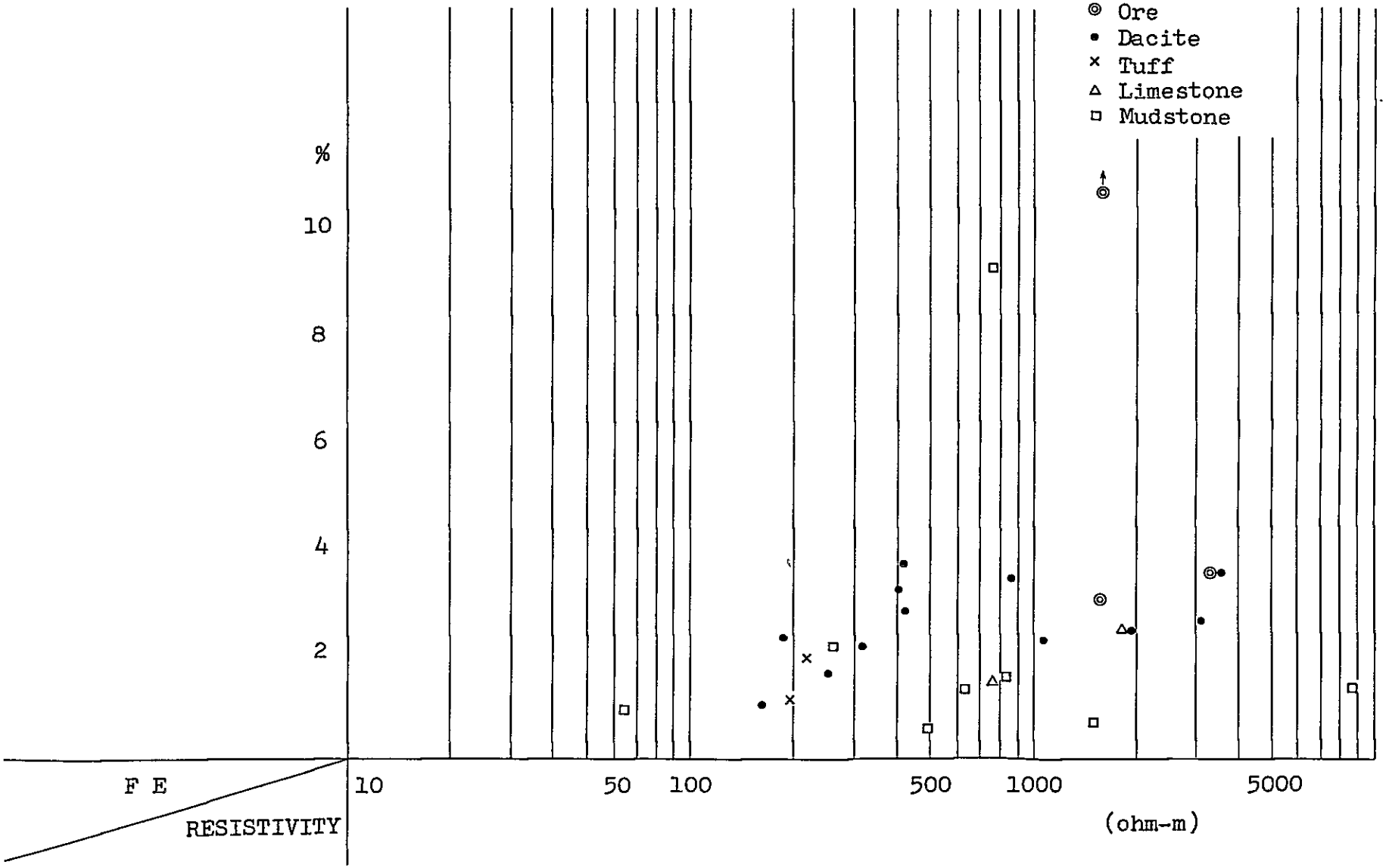

Fig.4-19 Correlation between FE and resistivity in laboratory measurements (Sin area)

4-6-6 Survey results

The cross sections of FE, AR and MF (PL. 4-31 ~ 4-46) are drawn by the use of the field survey data processed by the method as previously mentioned in 4-3. The data are also used for drawing plan maps of FE, AR and MF at various levels of 100 m (n = 1), 200 m (n = 3) and 300 m (n = 5) below the ground surface (PL. 4-47 ~ 4-55). The panel diagrams represent three-dimensional distributions of FE and AR (PL. 4-56, PL. 4-57).

The synthetic considerations of both the geophysical and geological together with the results of rock specimen tests make us a qualitative interpretation as follows.

1) FE

The range of FE values obtained in this survey area is 0.2 ~ 14.2% In a fashion similar to the analyses of the Mamlis area, the statistical treatments are made for the purpose of determining the standard level by which we can discriminate between anomaly and background noise. Figs. 4-20 and 4-21 show the histogram and the cumulative frequency distribution, respectively. It is seen in the histogram that the FE values are statistically governed by the Gaussian distribution law. The standard levels corresponding to background noise, weak anomaly and anomaly are determined as

	Fig. 4-21	Standard value
Background Noise	5.5%	5 ~ 6%
Weak Anomaly	8%	> 8%
Anomaly	11%	> 10%

The above-tabulated values are very high as compared with those of the Mamlis area. This may be caused by the geological fact that the Sin dacite is widely pyrite-disseminated, silicified and argillized in the survey area. In the southwest margin of the survey area, Line K_2 No. 1 ~ 10, where the unaltered Sin dacite is outcropped, FE values range 0.2 ~ 2% under the background noise level of the Mamlis area.

n = 1 Plan Map (PL. 4-47)

(1) The FE values range from 0.2 to 11.4%. The FE ranging from 2 to 4% covers predominantly the northern and western parts of the area.

(2) A small-sized anomaly which exceeds 10% is detected at Line S_1 No. 10 ~ 11 stations. This corresponds to the strong mineralization zone of the Sin Mine, and hereafter called FE-I Anomaly.

(3) Three weak anomalies are detected at Line N_1 No. 6 ~ 9 and Line 00 No. 8 ~ 9 stations (called FE-IV Anomaly). These also coincide with the mineralized and argillized zones although the FE-IV anomaly is somewhat extended eastwards.

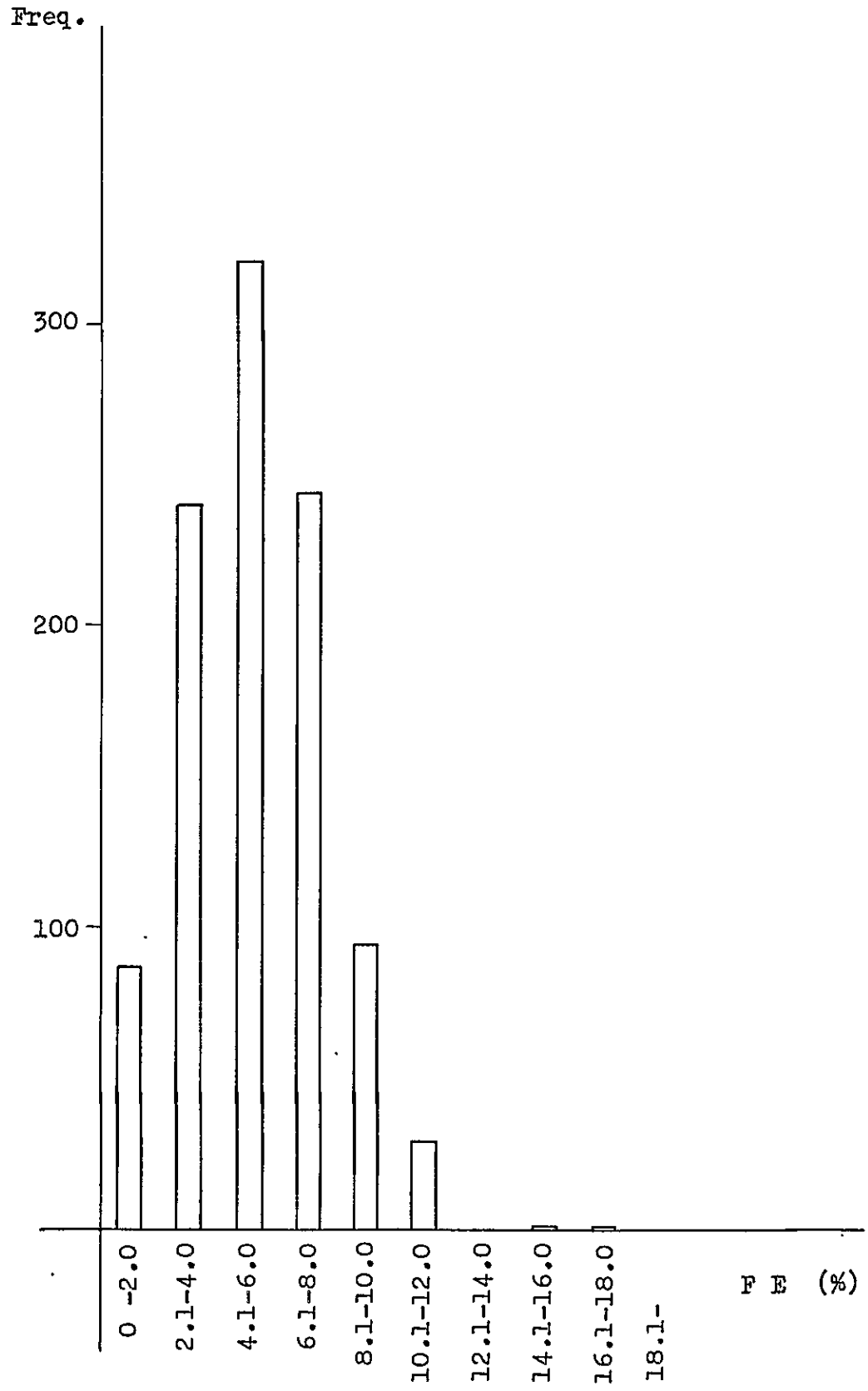

Fig.4-20 Histogram of FE (Sin area)

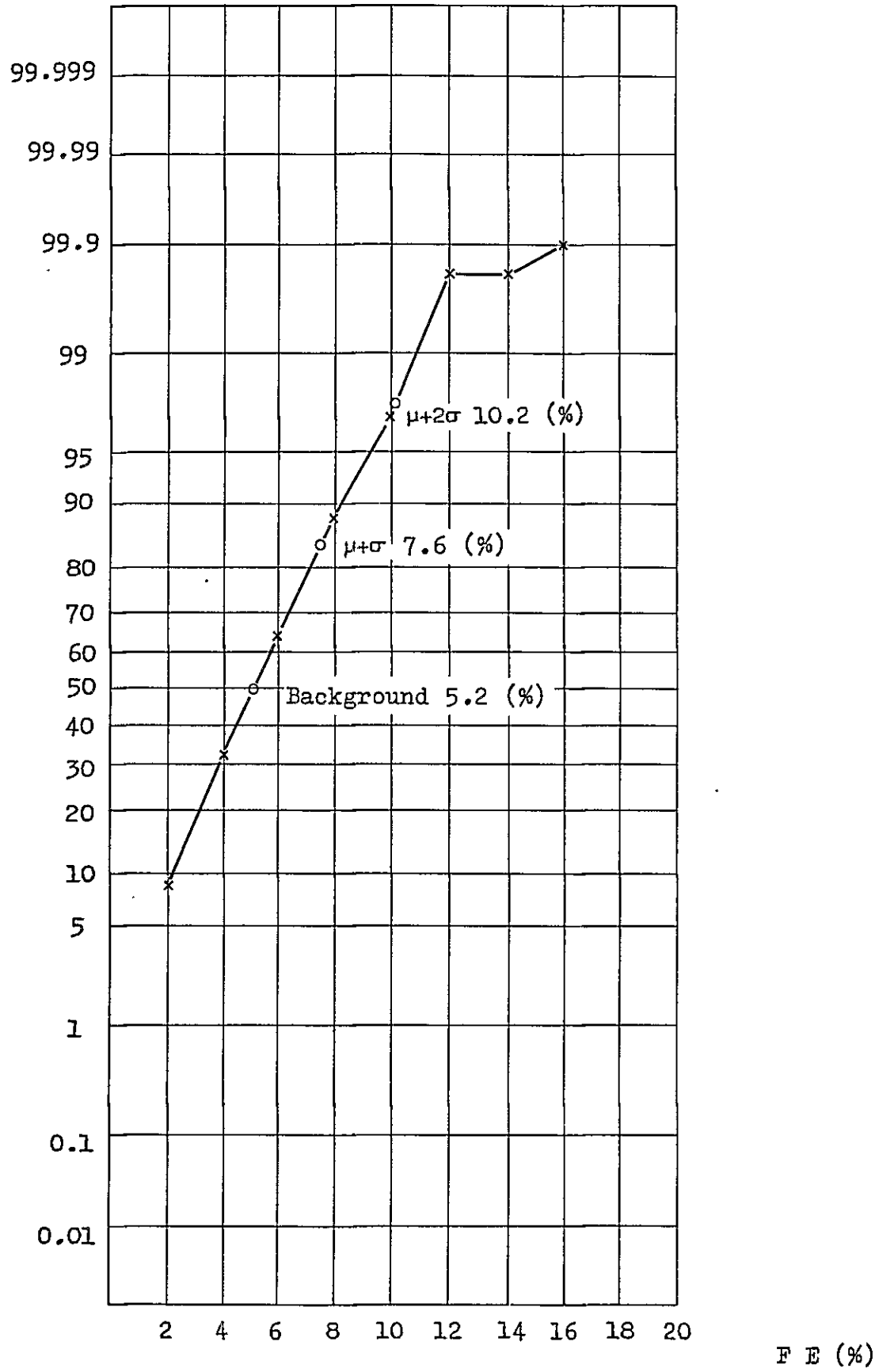

Fig.4-21 Comulative frequency distribution of FE (Sin area)

(4) The FE anomaly distribution over 6% trends NW-SE in the central part and NE-SW in the eastern part of the area. This coincides roughly with the Sin dacite (Dt) outcrops. North of the central part, the percentage of FE falls down to less than 4%.

(5) A NW-SE trending FE pattern, less than 4%, in the southern part of the survey area agrees well with the mudstone and sandstone distribution of the Bentepe Formation (Bem). 2 ~ 4% FE zones are also seen over both the northwestern Aem and the northeastern Bem. The FE values have a tendency to increase over the Dt distribution in the southwestern part of the survey area.

n = 3 Plan Map (PL. 4-48)

(1) The range of FE is from 0.7 to 11.2%. A high FE zone is predominant in the central and southeastern parts of the area. A wedge-shaped low FE zone penetrates the high FE zone.

(2) Three anomalies higher than 10% are found at Line S_1 No. 9 ~ 10 (FE-I Anomaly), Line S_1 No. 12 ~ 13 (FE-II Anomaly) and Line N_1 No. 7 ~ 8 (FE-IV Anomaly).

The FE-I and IV anomalies seem to shift their locations northwards and northwestwards, respectively, as compared with the n = 1 map. The FE-II anomaly is newly detected in the n = 3 map.

(3) Anomalies as high as 8% are found in the areas surrounding the above-mentioned high anomalies. The FE-III anomaly at Line S_1 and S_2 No. 6 ~ 8 stations and another high anomaly at Lines N_2 and N_1 No. 11 station are newly detected in this plan map. The mineralized alteration zone around Line 00 No. 7 station is also surrounded with some weak anomalies.

(4) Anomalies as high as 6% almost coincide with the Dt distribution, although the southwestern Dt has a low FE. FE values are as low as 3 ~ 5% over the Atadoğdu Formation (Aem) in the northwestern part of the survey area, but somewhat higher than what expected from the n = 1 plan map.

n = 5 Plan Map (PL. 4-49)

(1) In the mapped area, FE ranges from 0.1 to 14.3%. A 6% or higher FE zone is much more predominantly expanded south of Line N_5.

(2) A weak anomaly as high as 8% is stretched southwestwards from the central part of the mapped area. The coverage is wider in this map than in the n = 1 and 3 maps.

This may possibly imply that the corresponding mineralized zone has a large-scale root stretching southwestwards.

(3) The northwestern area is dotted with three newly discovered highs of 10% or more along the NW-SE trend. These anomaly located on mudstone and sandstone belonging to the Atadoğdu Formation may reflect the existence of deepseated dacite intrusions.

(4) It is seen in the central part of the survey area that a low FE zone runs parallel to Line Base 8 in the east side. The minimum spot of FE, 1.8%, is found at Line N_1 No. 9 station.

2) AR

Fig. 4-22 and 4-23 are the histogram and the cumulative frequency distribution based on the AR results, ranging from 14 to 9,460 ohm-m, in the survey area. Background noise, low anomaly and high anomaly are defined as the following ranges:

Background noise	160 ohm-m
Low AR anomaly	< 100 ohm-m
High AR anomaly	> 500 ohm-m

According to the above criterions, the AR distribution in the following plan maps is examined.

n = 1 Plan Map (PL. 4-50)

(1) The range of AR is 14 ~ 2,350 ohm-m in this map.

(2) One of low AR zones (< 100 ohm-m) centered at Lines N_4 and N_2, No. 1 ~ 2 and Lines S_1 and S_2, No. 4 ~ 5 stations covers widely the southwestern part of the mapped area. This corresponds to the quaternary deposits extending in the E-W direction. Another low centered at Line 00 No. 11 and Line N_2 and N_3 No. 12 stations covers the central and northeastern parts of the mapped area. The Line 00 No. 11 station is located on the Sin Mine mineralized zone and its northern extension. The Lines N_2 and N_3 No. 12 stations are location on the pyrite-disseminated and silicified zone, and the Line N_2 No. 15 station on the distribution of quartz veins accompanied with chalcopyrite and malachite.

(3) A low AR centered at Line 00 No. 6 ~ 9 stations agrees well with a pyrite-disseminated and argillized alteration zone, which has newly been found by the present geological survey. The corresponding low anomaly seems to be extended eastwards.

(4) A high AR zone (> 500 ohm-m) north of the central parts covers the unaltered Sin dacite (*Dt*).

Fig.4-22 Histogram of AR (Sin area)

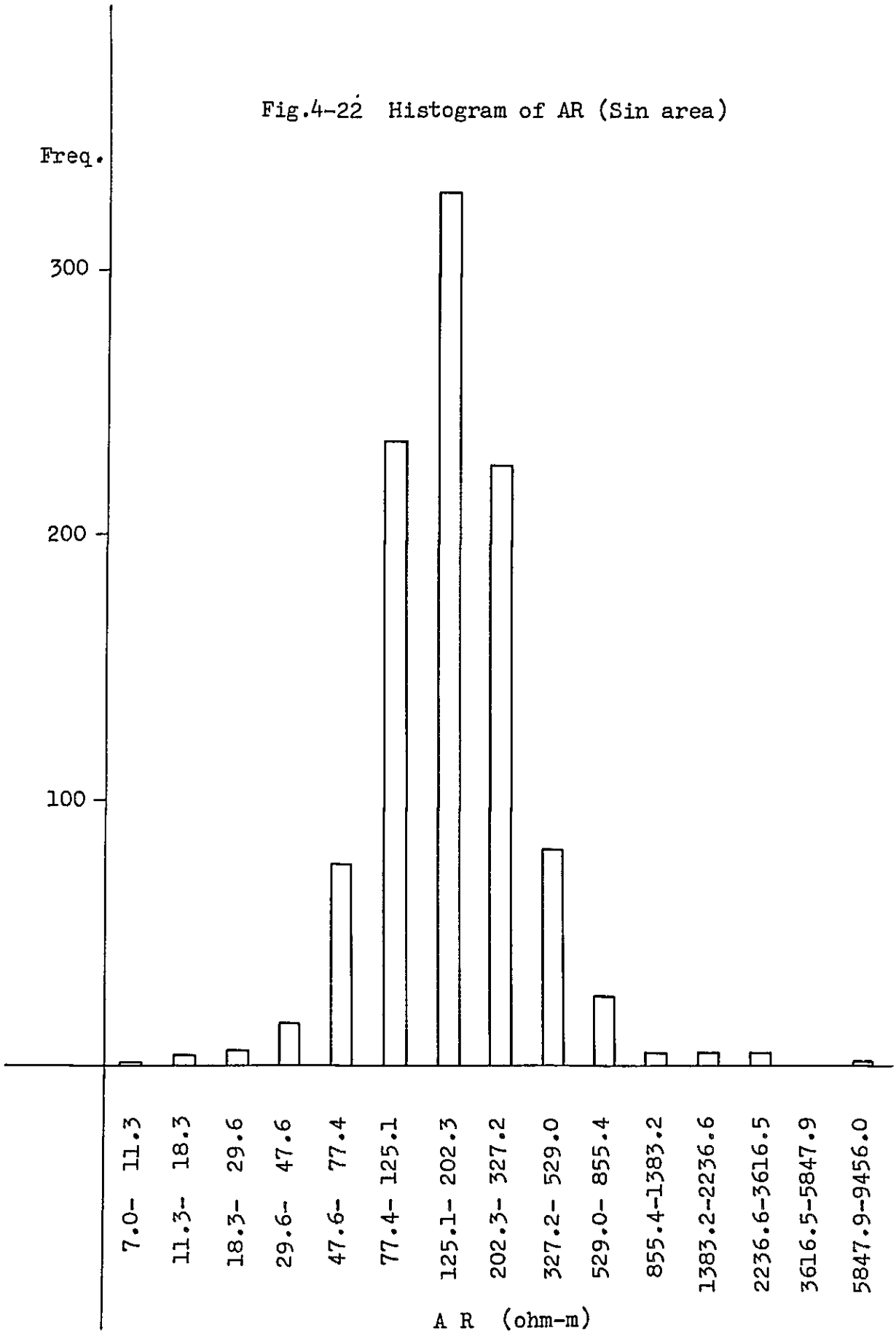

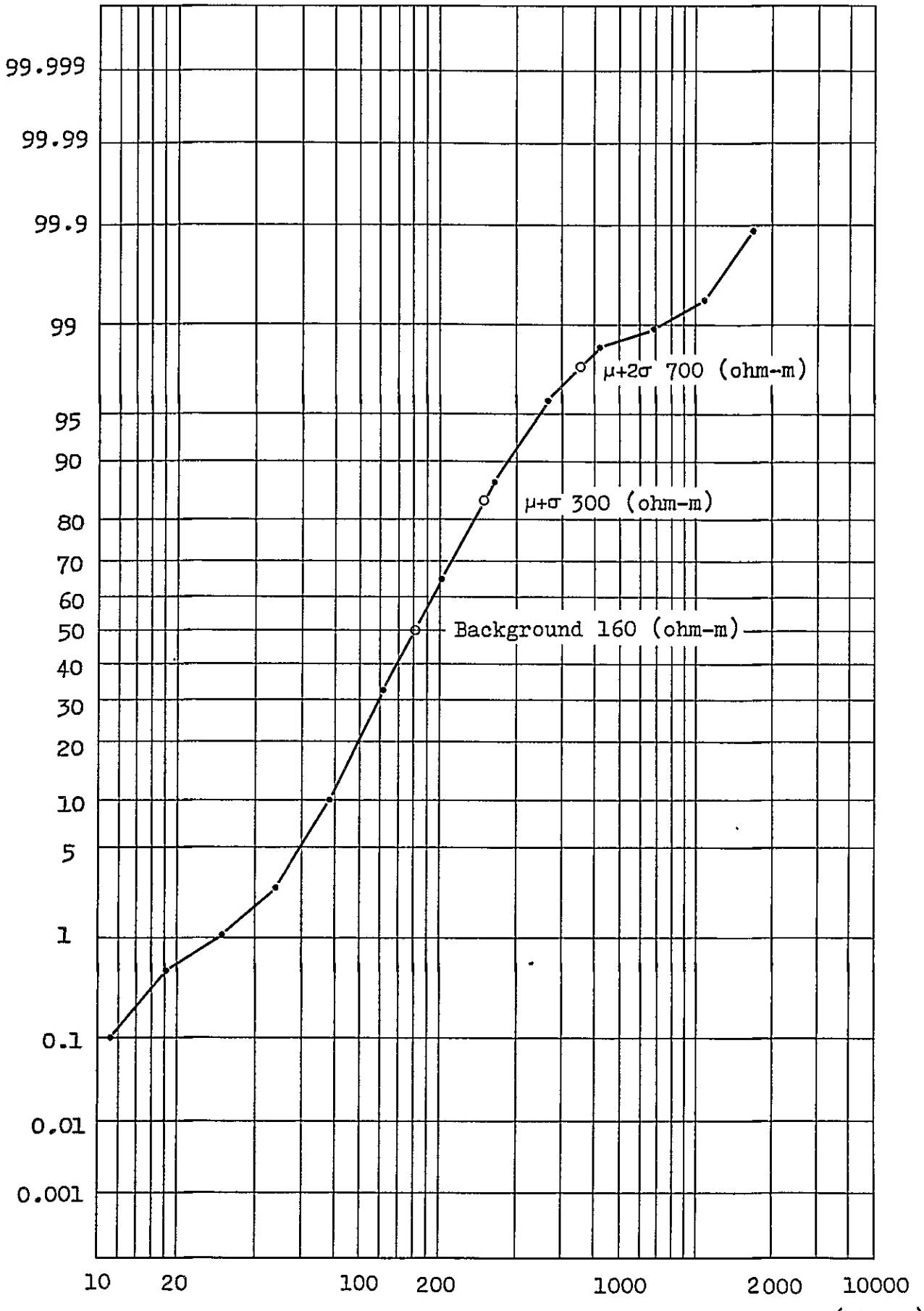

Fig.4-23 Cumulative frequency distribution of AR (Sin area)

n = 3 Plan Map (PL. 4-51)

(1) AR values range from 14 to 646 ohm-m.

(2) The midrange 150 ~ 200 ohm-m is predominant in the n = 3 map. A couple of low AR are found in the margin of this map, but the low AR zone widely covering the southern part of the n = 1 mapped area is vanished away in this case.

(3) The two low anomalies, which are found at Line 00 No. 6 ~ 9 and Line N_1 No. 9 ~ 11 stations, are here combined into a new anomaly NE-SW trending in the central part of this map.

(4) The high AR zone (> 500 ohm-m) is found at the same location as the n = 1 map, but the coverage is somewhat diminished.

n = 5 Plan Map (PL. 4-52)

(1) AR values range from 33 to 2,540 ohm-m in this map.

(2) The range from 150 to 250 ohm-m is predominant.

(3) The small-sized low AR zone is arranged along Line Base (8) north of the central part of the mapped area.

(4) High AR zones are found around Line N_6 No. 6 ~ 7, Line N_5 and N_4 No. 12 ~ 13 and Line N_1 No. 6 ~ 7 stations.

3) MF

Figs. 4-24 and 4-25 are the histogram and the cumulative frequency distribution of MF values, ranging from 1 to 689, of the Sin area. The histogram indicates the log-normal distribution with a peak at a range between 21 and 40. Background noise, low and high MF anomalies are defined in the present report as the ranges lower than 32 (μ = 50%), 60 ($\mu + \sigma$ = 84%) and 144 ($\mu + 2\sigma$ = 98%), respectively. In other words, the MF anomaly is defined as MF $\geqq$ 60. According to these criterions, the plan maps of MF for n = 1, 3 and 5 are examined as follows:

n = 1 Plan Map (PL. 4-53)

(1) MF values range from 1 to 301 in this map.

(2) There are six MF anomalies higher than 80 in the central and northeastern parts of the area.

(3) High MF anomalies, higher than 80, at Line 00 No. 7 station and at Line N_2 No. 9 and Line S_1 No. 10 ~ 12 stations cover the mineralized and silicified zones which are confirmed by the geological survey.

(4) For high MF anomalies distributed over the western and northeastern parts of the mapped area, the patterns of MF = 80 contour are very similar to those of AR = 100 ohm-m contour of the n = 1 plan map of AR.

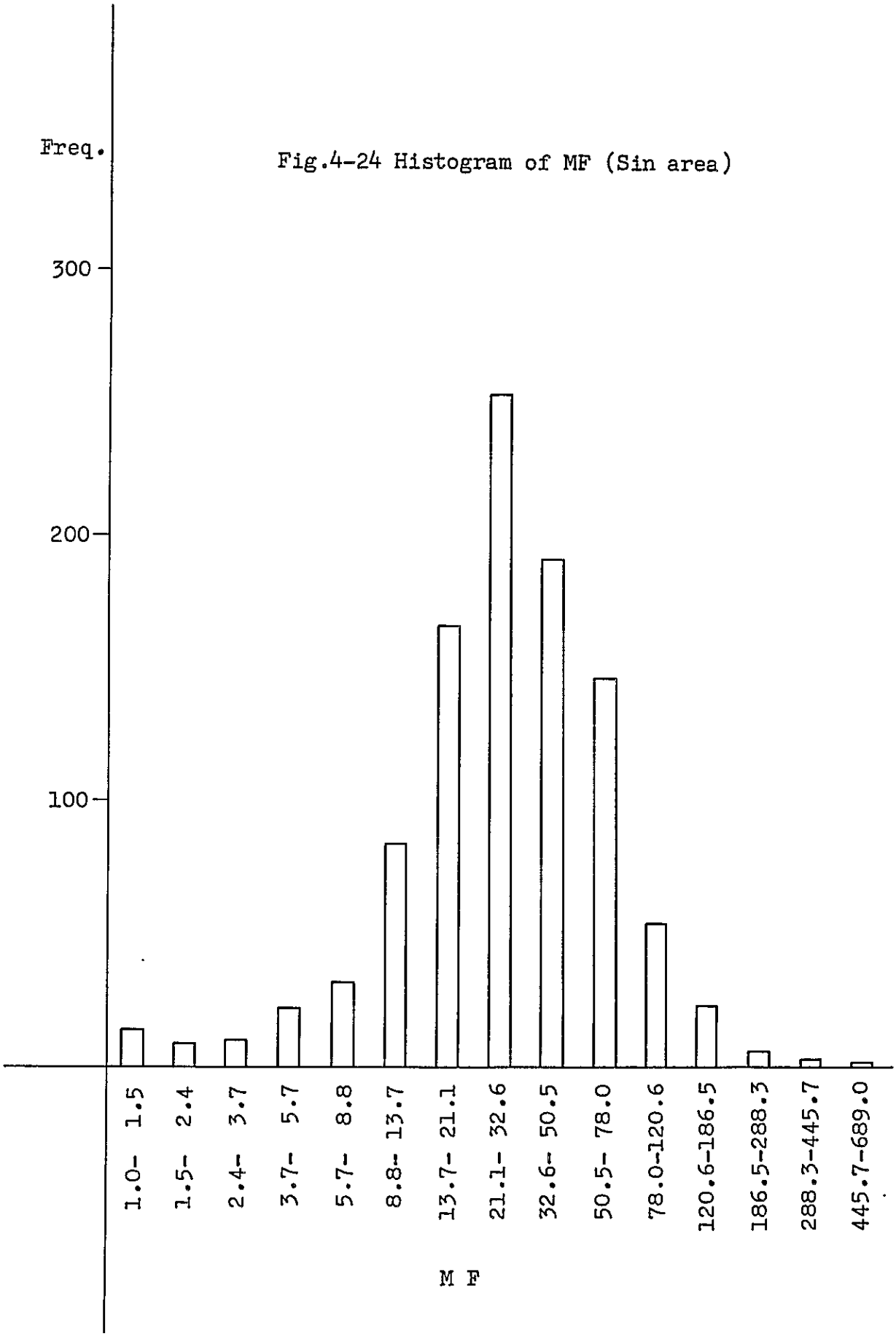

Fig.4-24 Histogram of MF (Sin area)

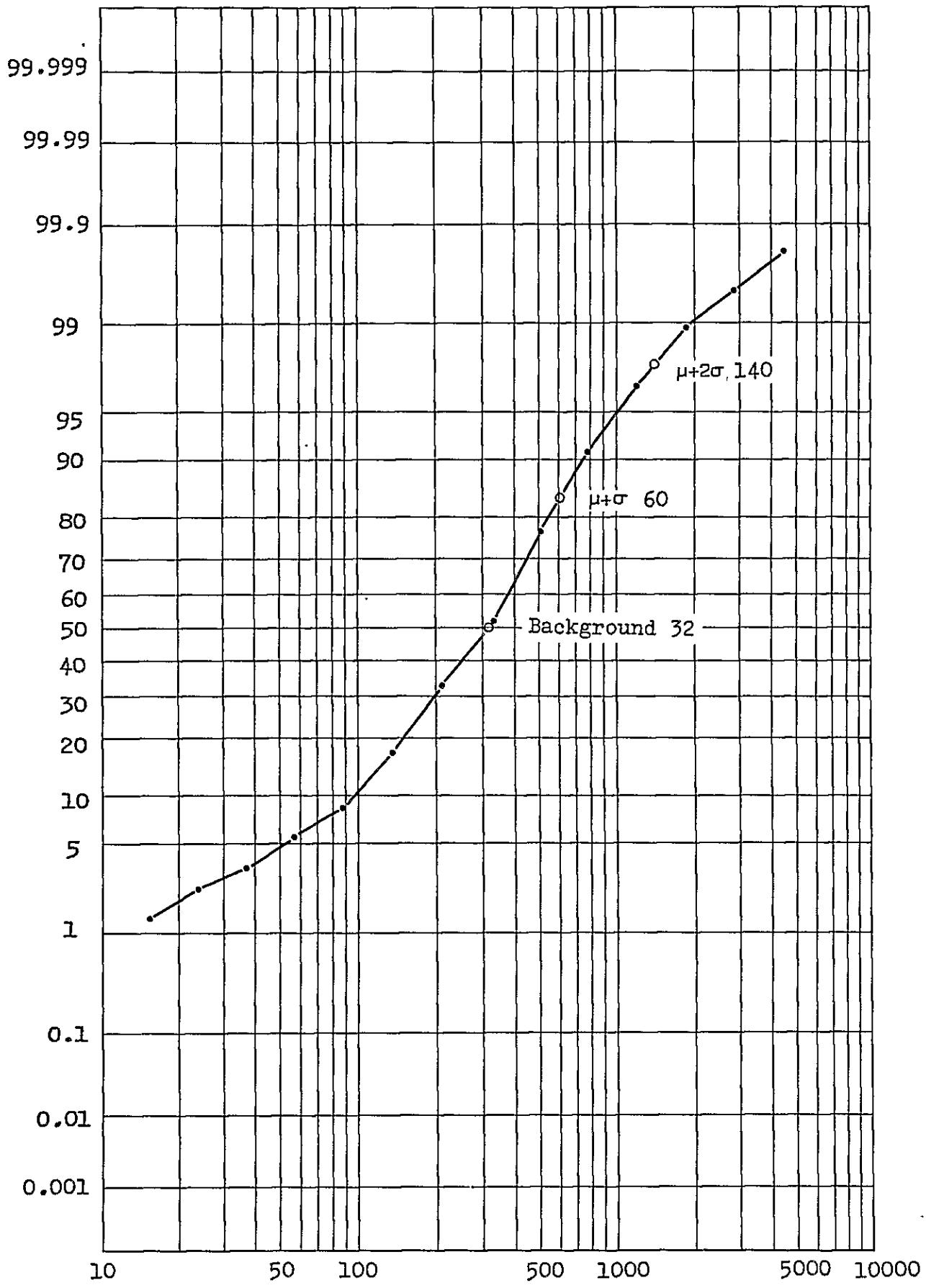

Fig.4-25 Cumulative frequency distribution of MF (Sin area)

This fact indicates that this MF high reflects from the low AR. Another high coincides with the pyrite disseminated and silicified zone around Line N_3 and N_2 No. 12 stations in the northeastern area. The geological survey has discovered malachite stain near the Line N_2 No. 15 station.

n = 3 Plan Map (PL. 4-54)

(1) MF Values range from 4 to 350 in this plan map.

(2) There are three high MF anomalies in the central, the southeastern and the southwestern parts of the area. Conspicuously high MF values are detected Line N_1 No. 7 ~ 8, Line S_1 No. 9 ~ 10 and Line N_3 and N_2 No. 9 ~ 10 stations. The patterns of these anomalies are different from those in the n = 1 map. That is to say, the N-S trending anomaly east of the central part of the n = 1 mapped area changes its trending direction into NE-SW in the northern area, but shifts its location slightly westwards in the southern area.

n = 5 Plan Map (PL. 4-55)

(1) MF values range from 2 to 242 in this plan map.

(2) The ranges from 20 to 40 are predominant as a whole. There are two MF anomalies higher than 80 at Line N_4

No. 9 station and Line S_3 No. 13 ~ 14 stations.

The former is what is newly detected in this map, but the latter corresponds to the n = 3 anomaly although the center of it is shifted slightly northwards.

4-6-7 Results of simulation analyses

In 4-6-5, the qualitative analysis is done with regard to FE, AR and MF plan map. The correlation is discussed between FE anomalies, AR, MF patterns and the distribution of geology and mineralization. The four anomalous zones found by the qualitative analysis are applied a simulation analysis for the purpose of estimating FE and resistivity values and the depth of anomaly source.

A) FE-1 Anomaly (Fig. 4-26)

This anomaly occurs below No. 10-11 stations of Line S_1. The ground surface is covered with Sin decite partly containing malachite at the neighborhood of the open pit of Sin mine. FE pattern on Line S_1 shows that a high FE zone (FE-1) over 10% dips west from No. 11-12 stations, another high FE zone (FE-11) occurs below No. 12-13 stations. The zone over 8% FE surrounds two anomalies above described. The specimens (Nos. S_4 ~ S_{10}) indicates that the distribution of FE is 2.6 ~ 18.2%. Resistivity value spreads highly between 1,730 ~ 3,280 ohm-m because of oxidization and silicification. The following model is made up considering FE pattern of field measurements, geology and rock sample

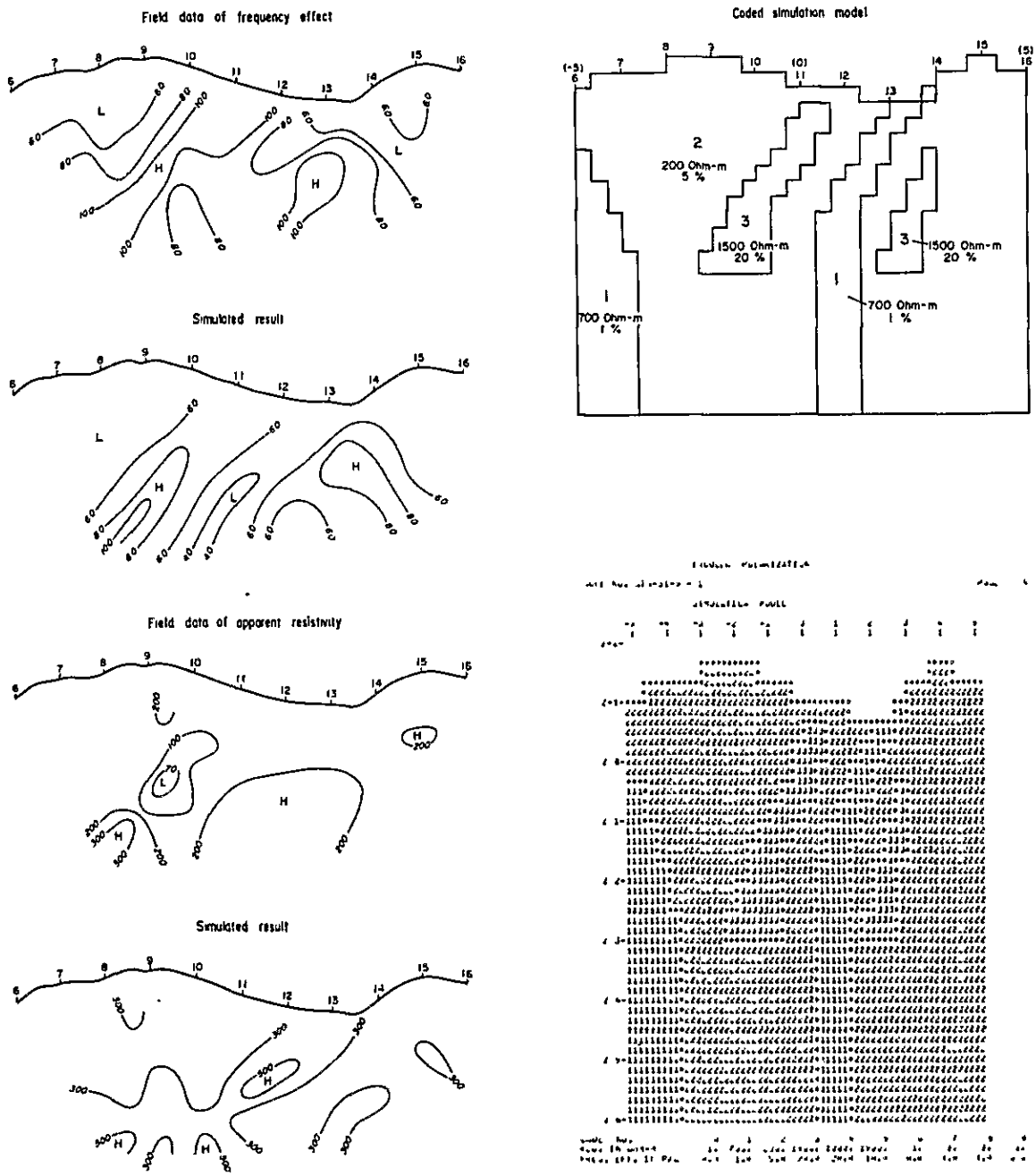

Fig.4-26 Results of sumilation analysis,LineS1(No.6-No.16)

tests. A high FE zone (FE 20%, resistivity 1,500 ohm-m, code 3), dipping west, is assumed below No. 11-12 stations and No. 13-14 stations. Sin dacite which is a host rock is set FE 5%, resistivity 200 ohm-m and code 2. Bentepe Formation (Bem) and Atadoğdu Formation (Aem) at No. 13-14 stations are set FE 1%, resistivity 700 ohm-m and code 1.

The results of simulation: In regard to FE, high FE zones appear below No. 9-11 stations and No. 13-14 stations corresponding to field data. The low FE zone below No. 10-12 stations in field data is detected stronger than field values, because the influences of Bem and Aem are strongly presumed. In regard to AR, the values of AR are generally higher than field values, over 200 ohm-m zone below No. 10-13 stations in field data decreases its distribution area.

B) FE-11 and FE-111 Anomalies (Fig. 4-27)

These are detected at the deep parts below No. 11-13 stations and No. 6-8 stations on the Line S_2. The simulation is applied to the extent of No. 4-14 stations. Geology and modeling are as follows: Sin decite (Dt), which is assumed FE 5%, resistivity 200 ohm-m, code 2 overlies at No. 6-11 stations. Below Dt, Atadoğdu Formation (Aem) is assumed that it has FE 1%, resistivity 700 ohm-m, code 1. At the deeper zone below Aem, Dt (code 2) is assumed as same as the shallow part. The models of FE-11 and FE-111 anomalies are assumed that these have FE 20%, resistivity 1,500 ohm-m, code 3 below No. 6-7 stations (depth 150 m) and No. 12-13 stations (depth 200 m) respectively.

The results of simulation: In regard of FE, the patterns of high and low FE zones is similar to field measurements except of following 6% FE zone widely spreads west below No. 11-13 stations and small 8% zone exists below No. 6-8 stations. In regard of AR, the wide AR zone appears below No. 9-10 stations. The reasons of difference between simulation and field measurements are as follows: The distribution of Aem at the middle deep part is very different from the assumed geological cross section. The resistivity value of FE-111 anomaly may be almost same value of host rock, less than assumed value.

C) FE-IV Anomaly (Fig. 4-28)

This anomaly is detected at the middle deep part between No. 7-8 stations on the Line N_1. Sin dacite (Dt) is widely overlaid on the ground surface, and strongly oxided and argilized to the extend of No. 6-7 stations and malachite stain partly exists. FE pattern of field data is complexly distributed at No. 6-9 stations from shallow part to the middle deep part. The following model is made on the extent of No. 4-14 stations. The two high FE zones below No. 7-9 stations and No. 11 station are assumed FE 20%, resistivity 1,500 ohm-m, code 3. Dt area is assumed FE 5%, resistivity 200 ohm-m, code 2 and Aem area is set FE 1%, resistivity 700 ohm-m, code 1.

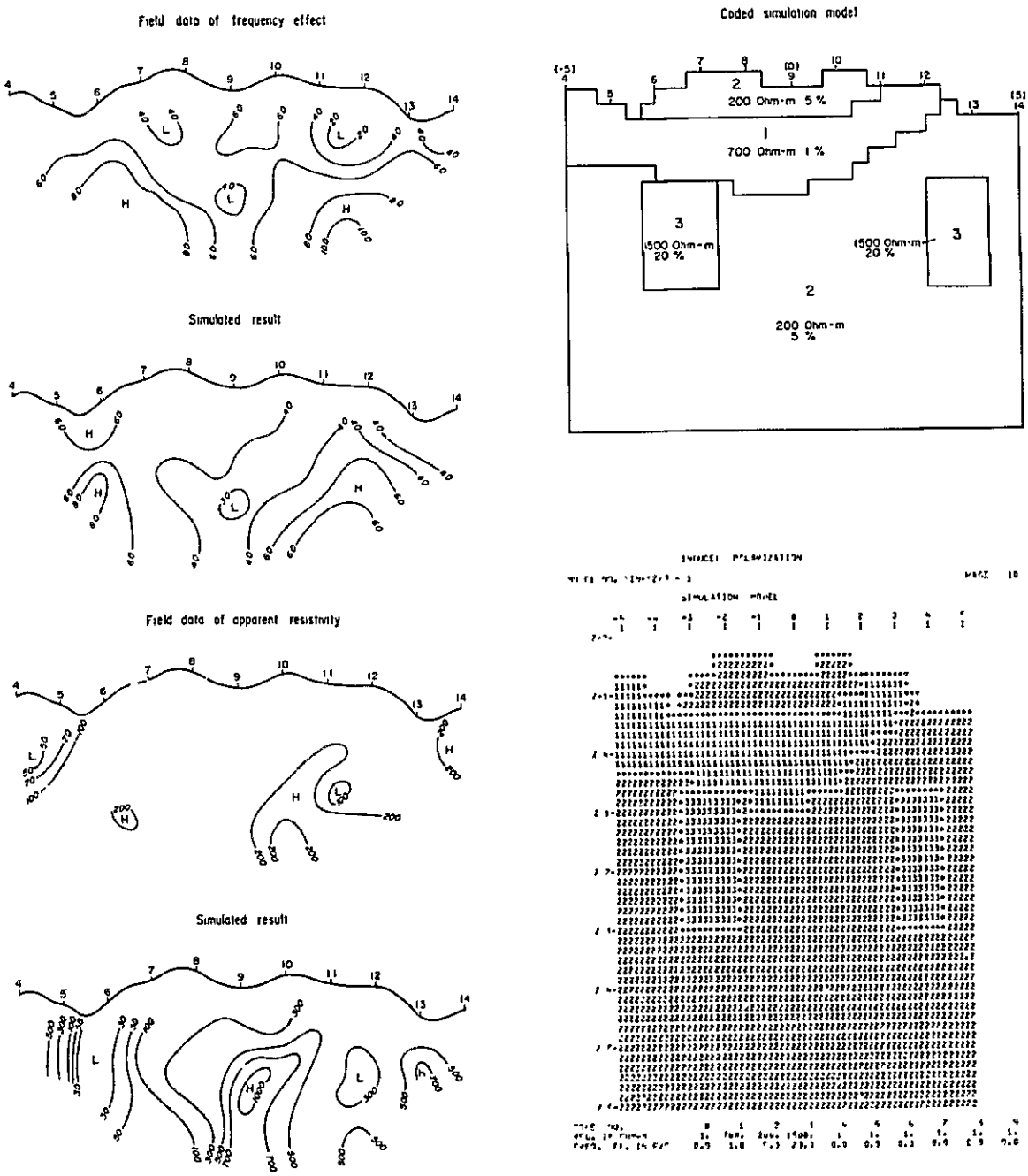

Fig.4-27 Results of sumilation analysis,LineS2(No.4-No.14)

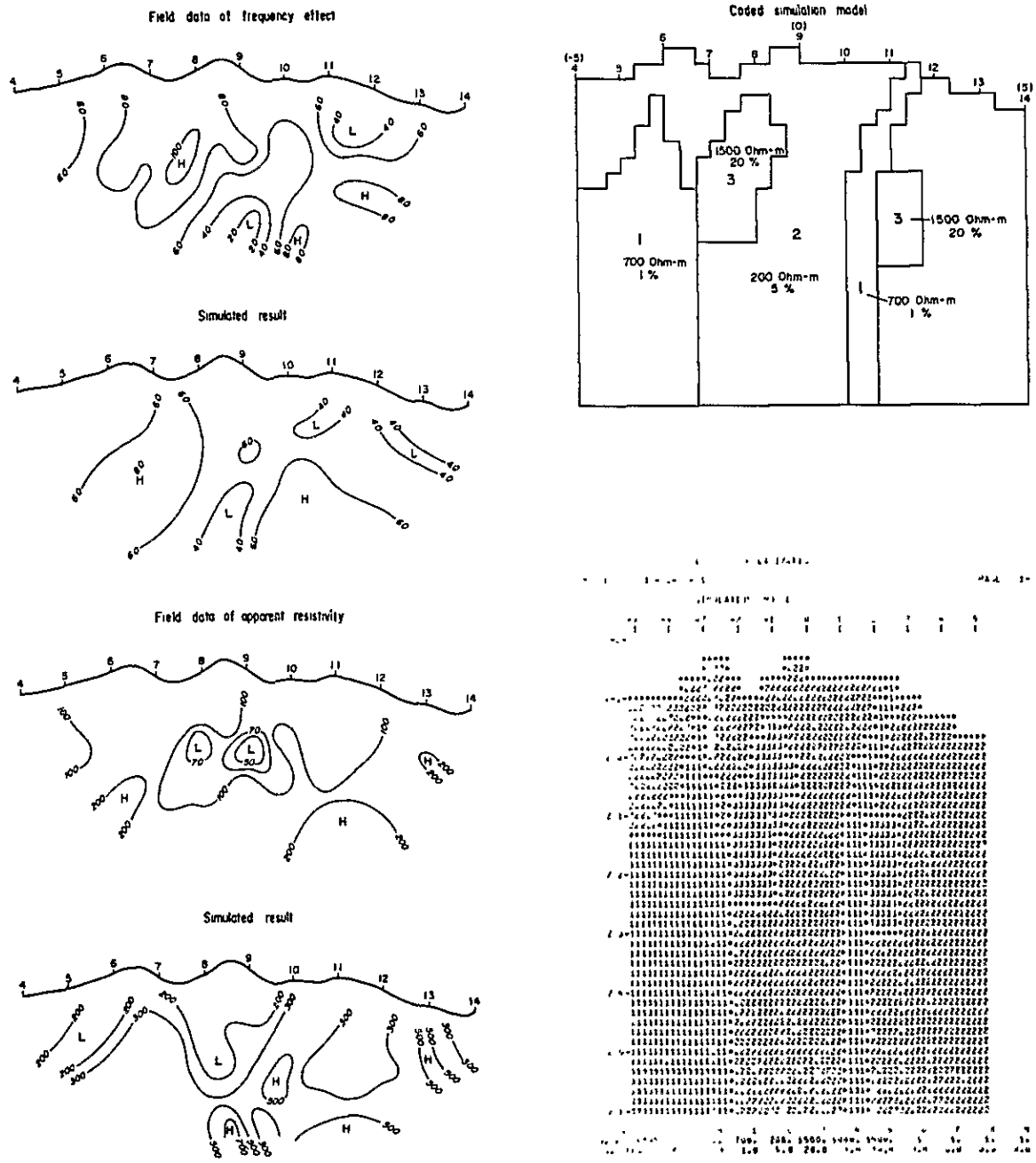

Fig.4-28 Results of sumilation analysis,LineN1(No.4-No.14)

,

The results of simulation: The FE pattern of simulation is as a whole similar to the field measurements except of the followings. The high FE zone (>10%) at No. 7-8 stations changes the place to No. 6-7 stations. The small FE anomaly below No. 11-12 stations moves at the deep part below No. 10-11 stations. AR shows generally higher values than field values.

4-6-8 Survey remarks

The present survey has discovered four FE anomalies, whose locations, trends, downward continuations and geological evidences have been described in 4-6-6. The simulation analyses of these results are made to estimate FE, AR and depths to the resultant sources. What we obtained in the Sin-area survey is briefly summarized as follows. In addition, the future plan of geophysical prospecting will be mentioned later.

A) Central Anomaly (FE-I Anomaly)

(1) This is caused by the mineralized bodies around the open pit of the closed Sin Mine. According to the results of computer simulation analyses, the high FE zone (FE 20%, resistivity 1500 ohm-m) sloping westwards is presumed.

(2) This anomaly continues downwards to the FE-II anomaly as the southern extension. Meanwhile, the western extension of this anomaly is thought to be continued downwards to the FE-III anomaly.

B) Southeast Anomaly (FE-II Anomaly)

(1) This is located right below the anomaly at Line S_2 No. 13 station. The simulation analyses conclude that this is a promising anomaly amounting to 20% FE and 1,500 ohm-m resistivity located at a depth of 200 m below the Nos. 12 and 13 stations.

C) Southwest Anomaly (FE-III Anomaly)

(1) This covers Line S_2 No. 5 ~ 7 and S_3 No. 6 ~ 8 stations.

(2) The simulation analyses point out an anomalous zone of 20% FE and of 1,500 ohm-m resistivity near Line S_2 Nos. 6 and 7 stations.

D) Central West Anomaly (FE-IV Anomaly)

(1) This anomaly is related to the mineralized zone confirmed by the geological survey at Line N_1 No. 5 ~ 9 and Line N_2 No. 6 ~ 9 stations.

(2) According to the results of computer simulation, the FE and resistivity reach up to 20% and 1,500 ohm-m, respectively, around Line N_1 No. 7 ~ 9 stations.

Future Plan of Geophysical Exploration (PL. 4-58)

(1) The following drilling explorations are desired to disclose the anomaly sources.

Rank	Anomaly	Location of Drilling	Direction	Depth
A	FE-II	Line S_2 No. 12-13	Vertically down	250 m
A	FE-III	Line S_2 No. 6-7	"	250 m
B	FE-I	Line S_1 No. 10-12	"	200 m
B	FE-IV	Line N_1 No. 7-8	"	200 m
C	FE-I	Line S_1 No. 13-14	"	200 m

(2) The further geophysical prospecting to the south of the present survey area can be expected to capture the southern extension of the FE-II anomaly.

(3) A precise IP survey with a 50 m-interval electrode configuration may be effective for clarifying the sources related to small-scale network vein which has been confirmed by the geological survey.

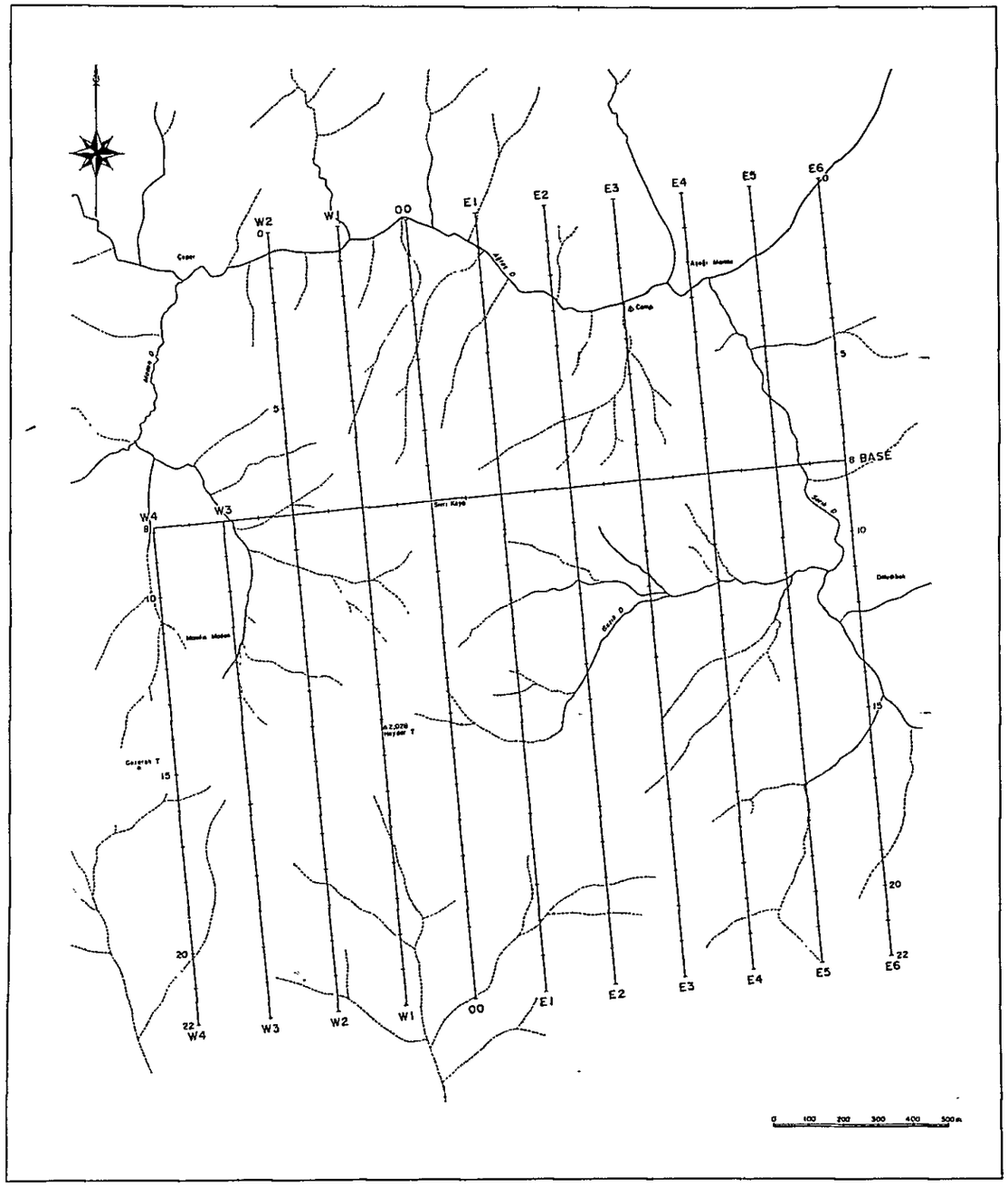

PL.4-1

MINERAL RESEARCH AND EXPLORATION INSTITUTE
GEOLOGICAL SURVEY
OF
TUNCELİ AREA, EASTERN TURKEY
PHASE II

LOCATION MAP OF IP SURVEY IN MAMLIS AREA

LOCATION MAP

Scale 1:5,000

METAL MINING AGENCY OF JAPAN
JAPAN INTERNATIONAL
COOPERATION AGENCY

MADEN TETKİK VE ARAMA
ENSTİTÜSÜ, TURKEY

PL.4-1 Location map of IP survey in Mamlis area

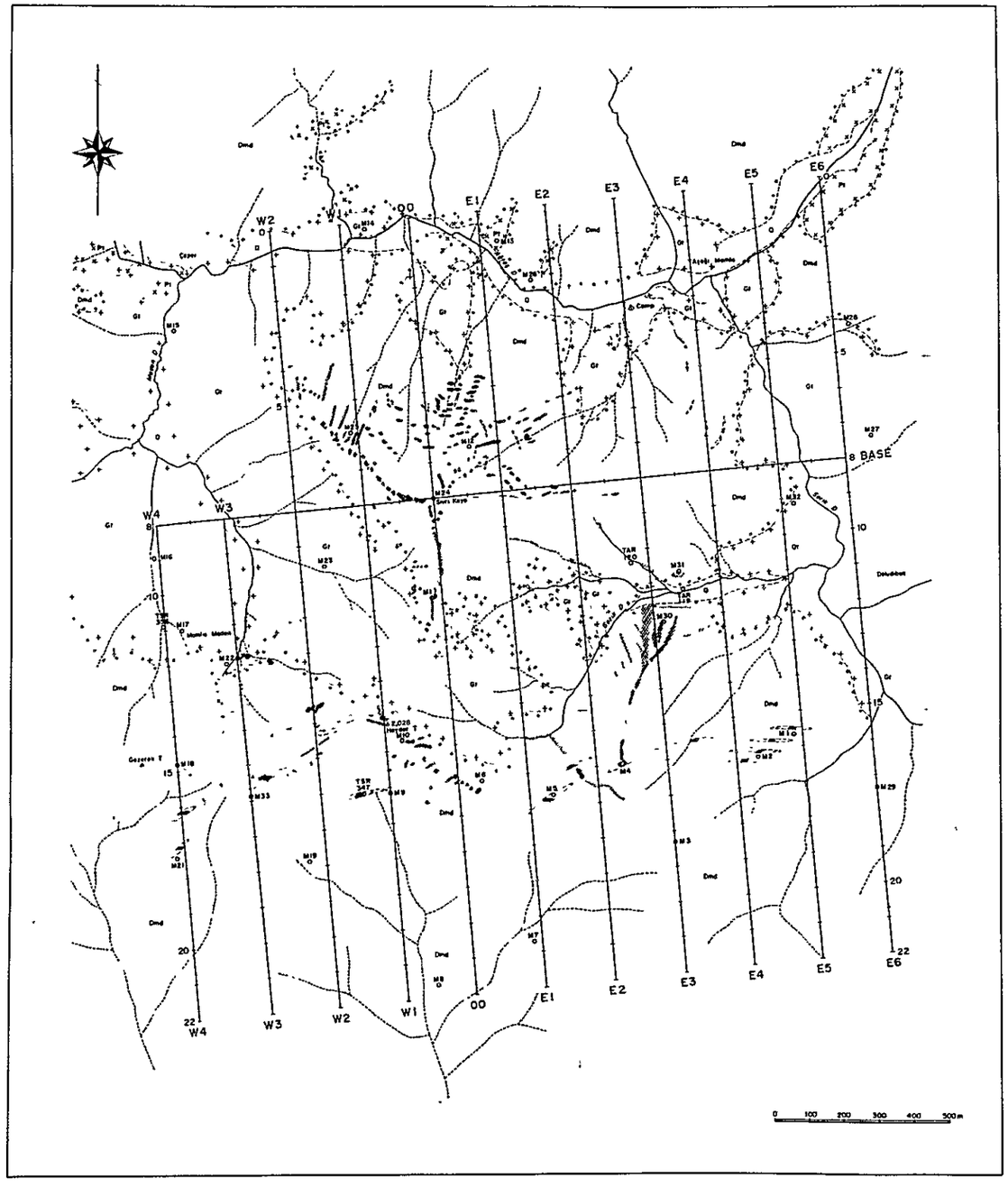

PL.4-2

MINERAL RESEARCH AND EXPLORATION INSTITUTE
GEOLOGICAL SURVEY
OF
TUNCELI AREA, EASTERN TURKEY
PHASE II

GEOLOGICAL MAP & SAMPLING LOCATION MAP IN MAMLIS AREA

LOCATION MAP

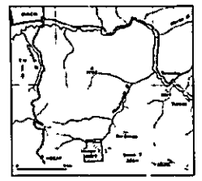

Scale 1:5,000

METAL MINING AGENCY OF JAPAN
JAPAN INTERNATIONAL COOPERATION AGENCY

MADEN TETKIK E ARAMA EN "ITUSU, TURKEY

LEGEND

GEOLOGICAL AGE and FORMATION

MIOCENE — Dutpelé F — Dmd — Dacite lava, Dacite pyroclastics

EOCENE — Benlepe F — Bem — Red mudstone, Calcareous sandstone

EOCENE — Atadağı F — Aem — Mudstone, Sandstone (calcareous)

IGNEOUS ROCKS

Tertiary — Dt — Dacite

Tertiary — Pt — Porphyry

Gt — Granite

ALTERATION and MINERALIZATION

As — Argillization

As — Strong argillization

Si — Silicification

Si — Strong silicification

Lm — Limonitization

Go — Gossan

Vq — Quartz and limonite vein

Vs — Cu, Pb and Zn vein

Do — Disseminated zone (pyrite)

Oxide copper zone

PL.4-2 Geological map and sampling location map in Mamlis area

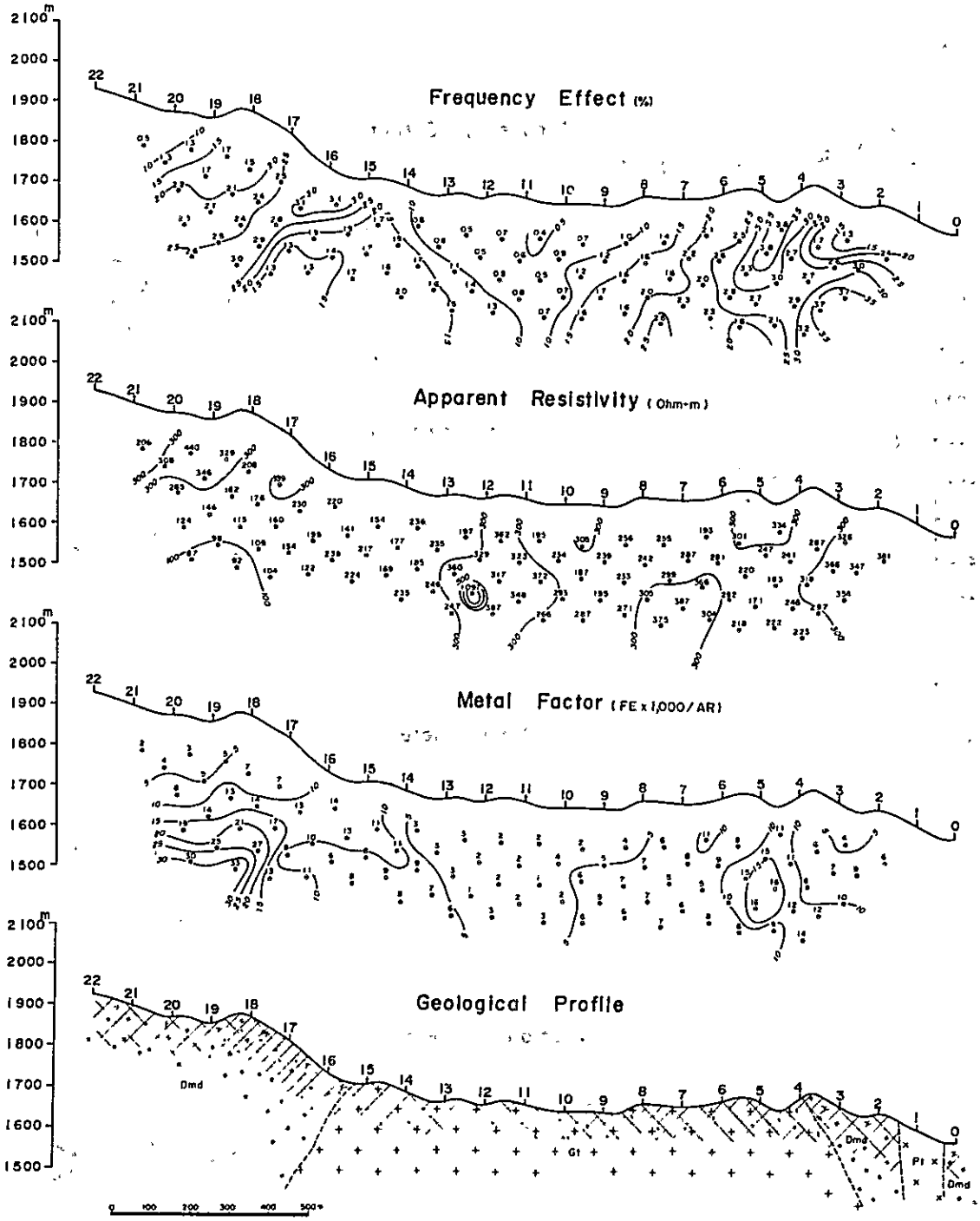

PL.4-3 Profile of IP survey in Mamlis area (Line E_6)

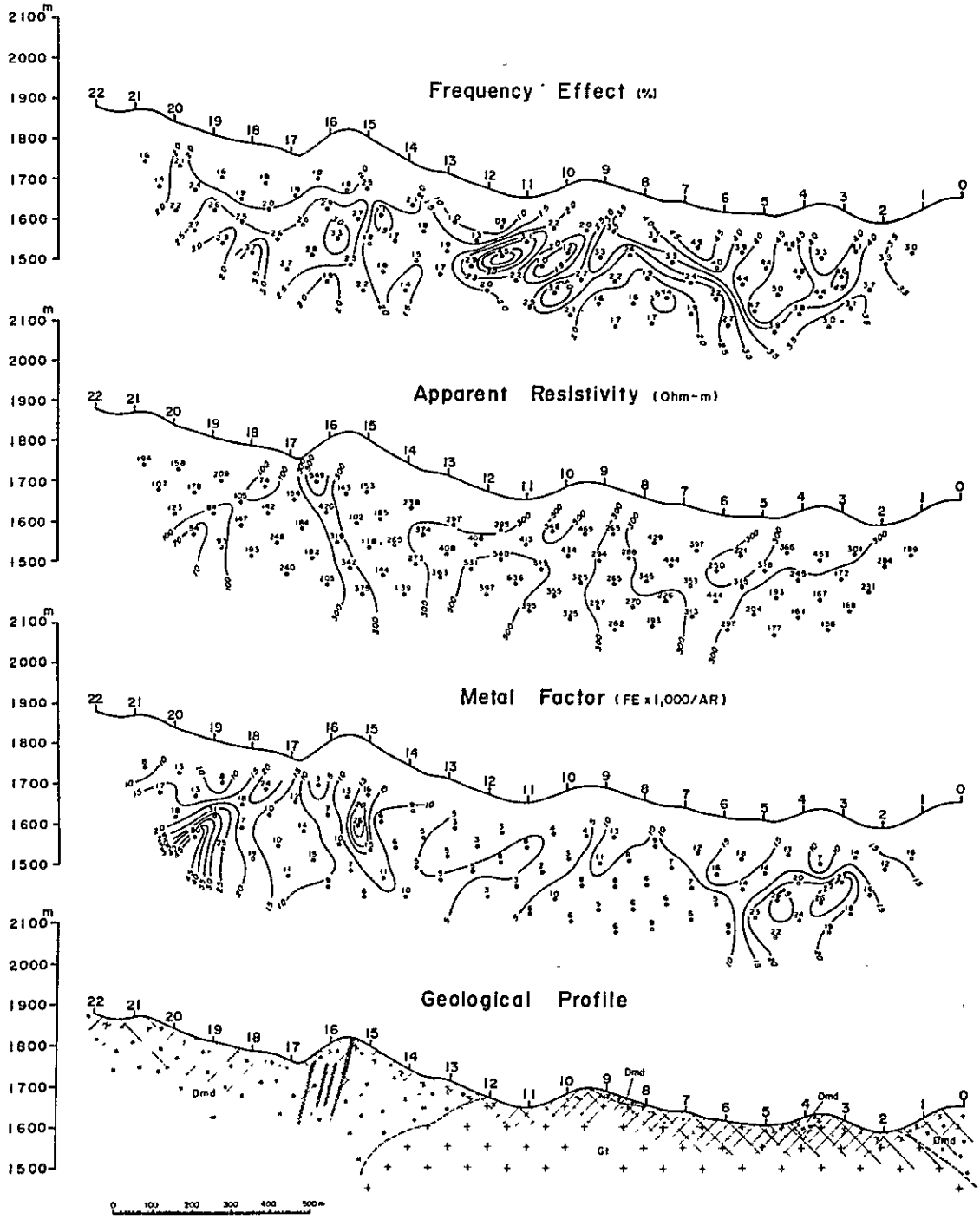

PL.4-4 Profile of IP survey in Mamlis area (Line E_5)

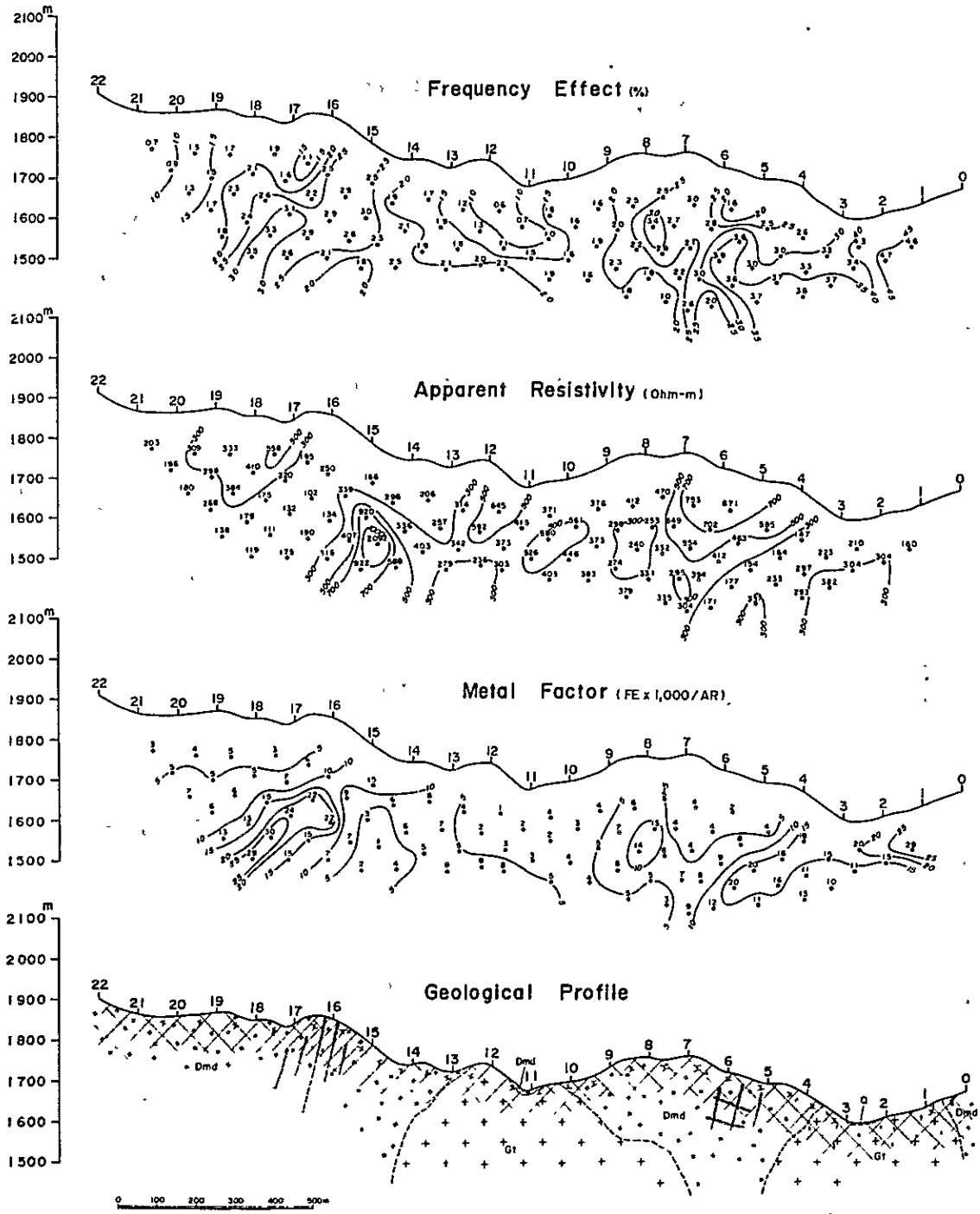

PL.4-5 Profile of IP survey in Mamlis area (Line E_4)

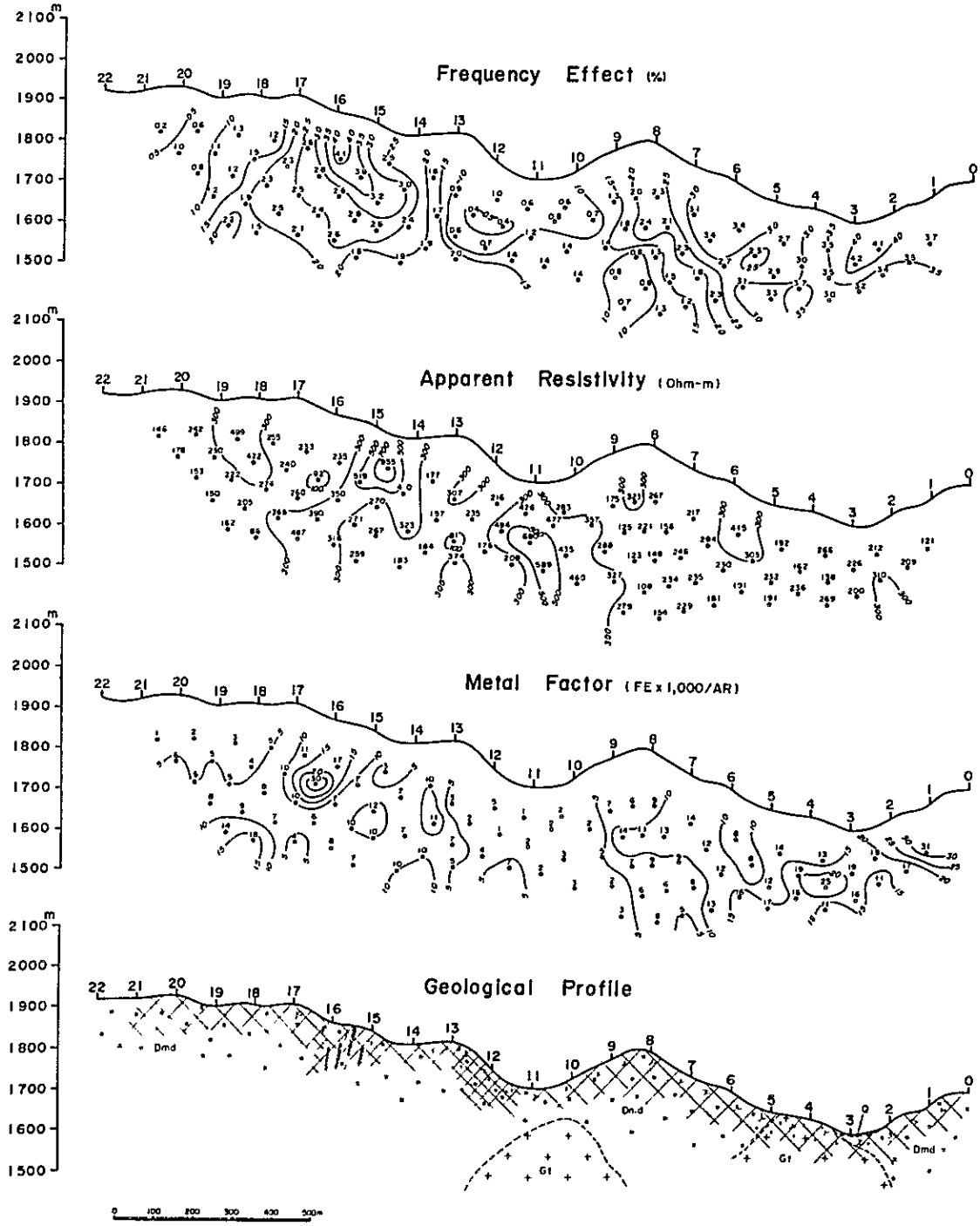

PL.4-6 Profile of IP survey in Mamlis area (Line E_3)

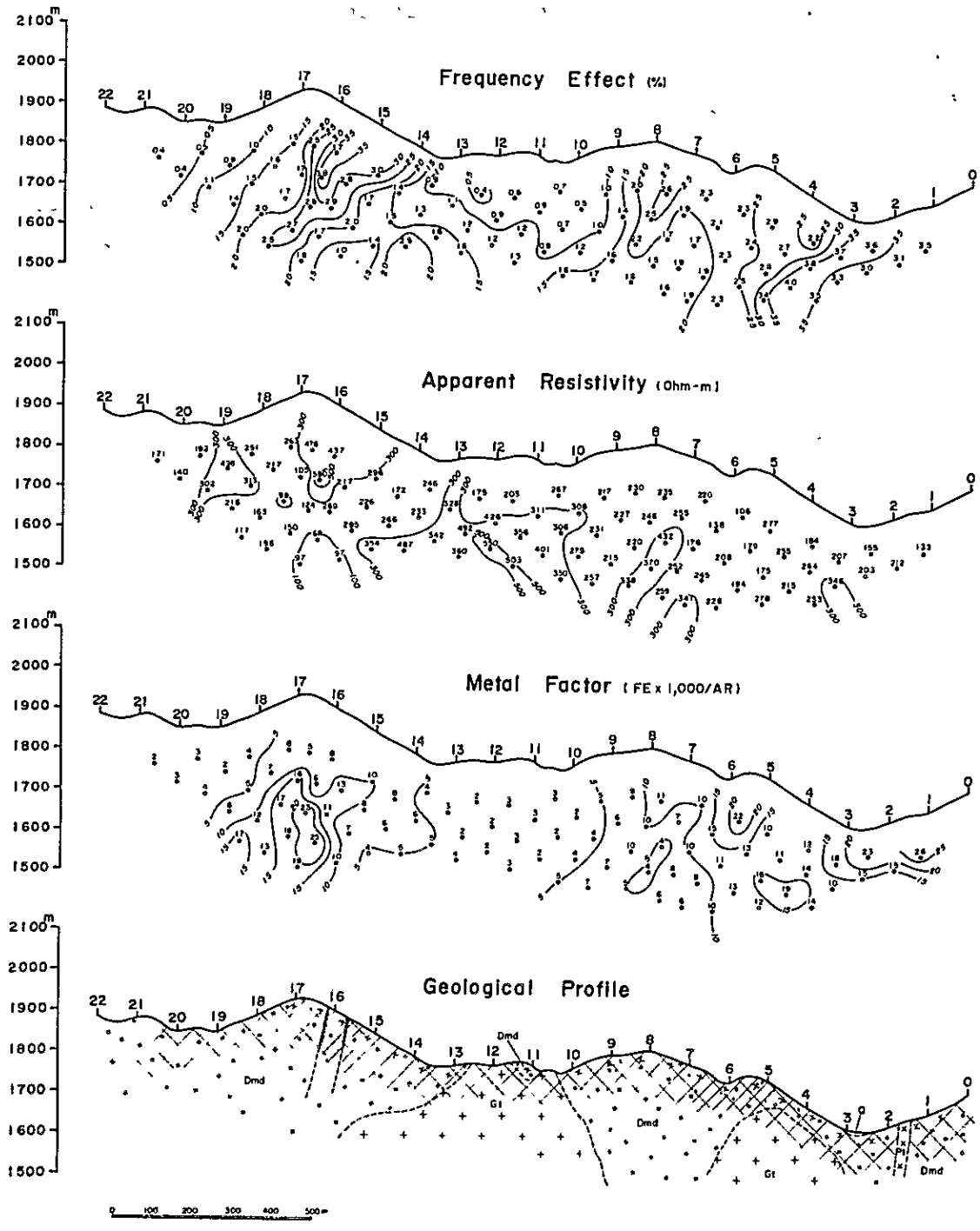

PL.4-7 Profile of IP survey in Mamlis area (Line E_2)

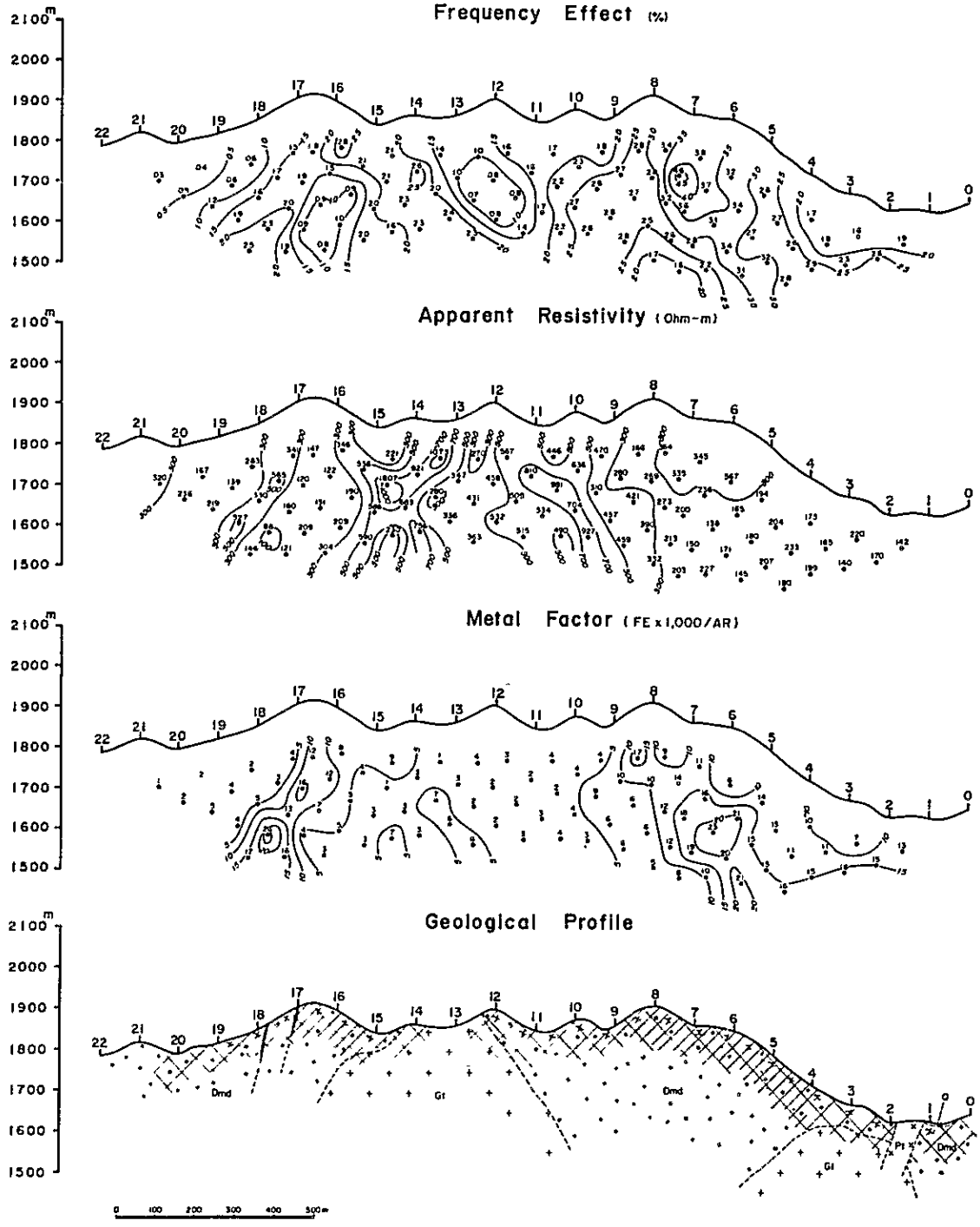

PL.4-8 Profile of IP survey in Mamlis area (Line E_1)

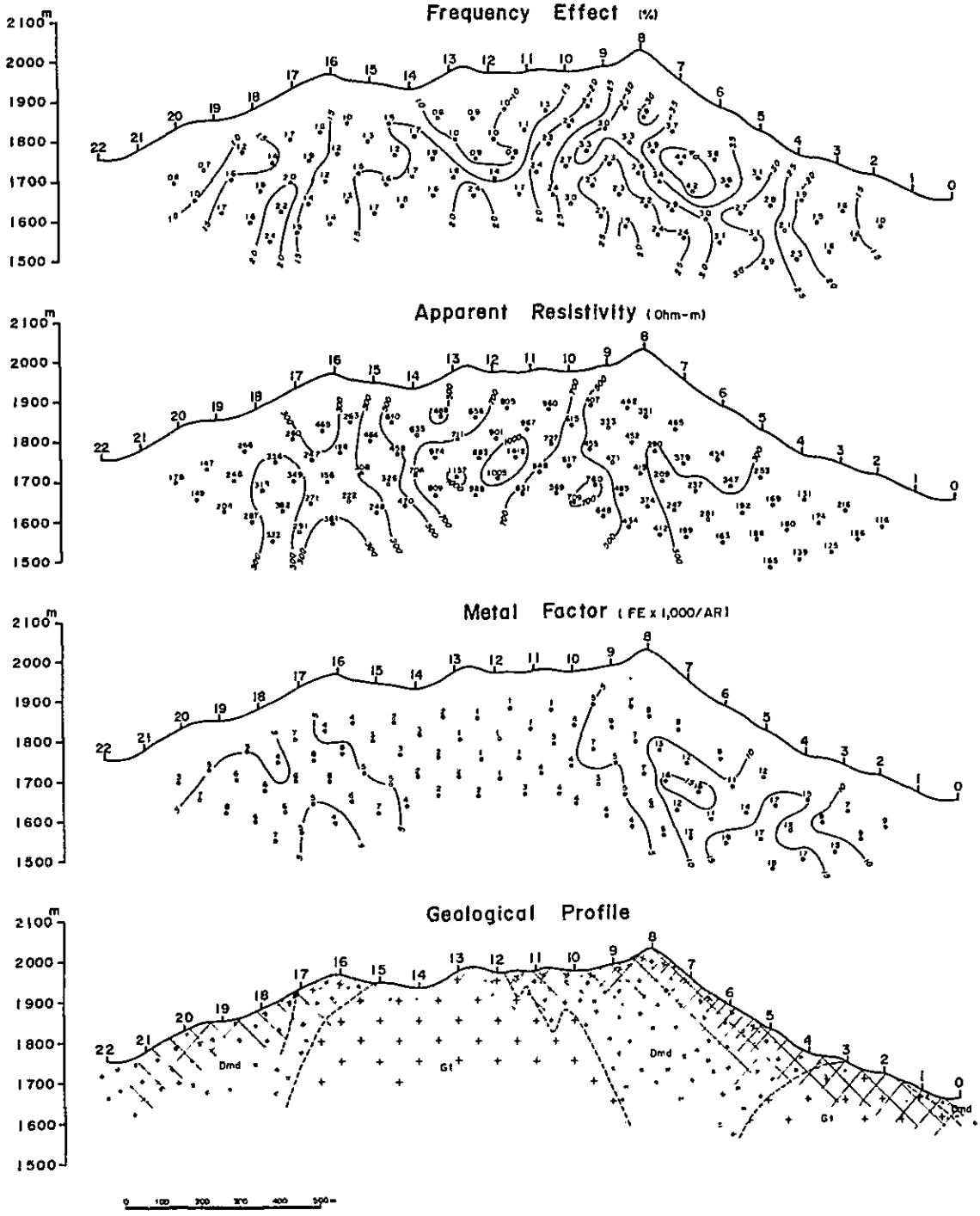

PL.4-9 Profile of IP survey in Mamlis area (Line 00)

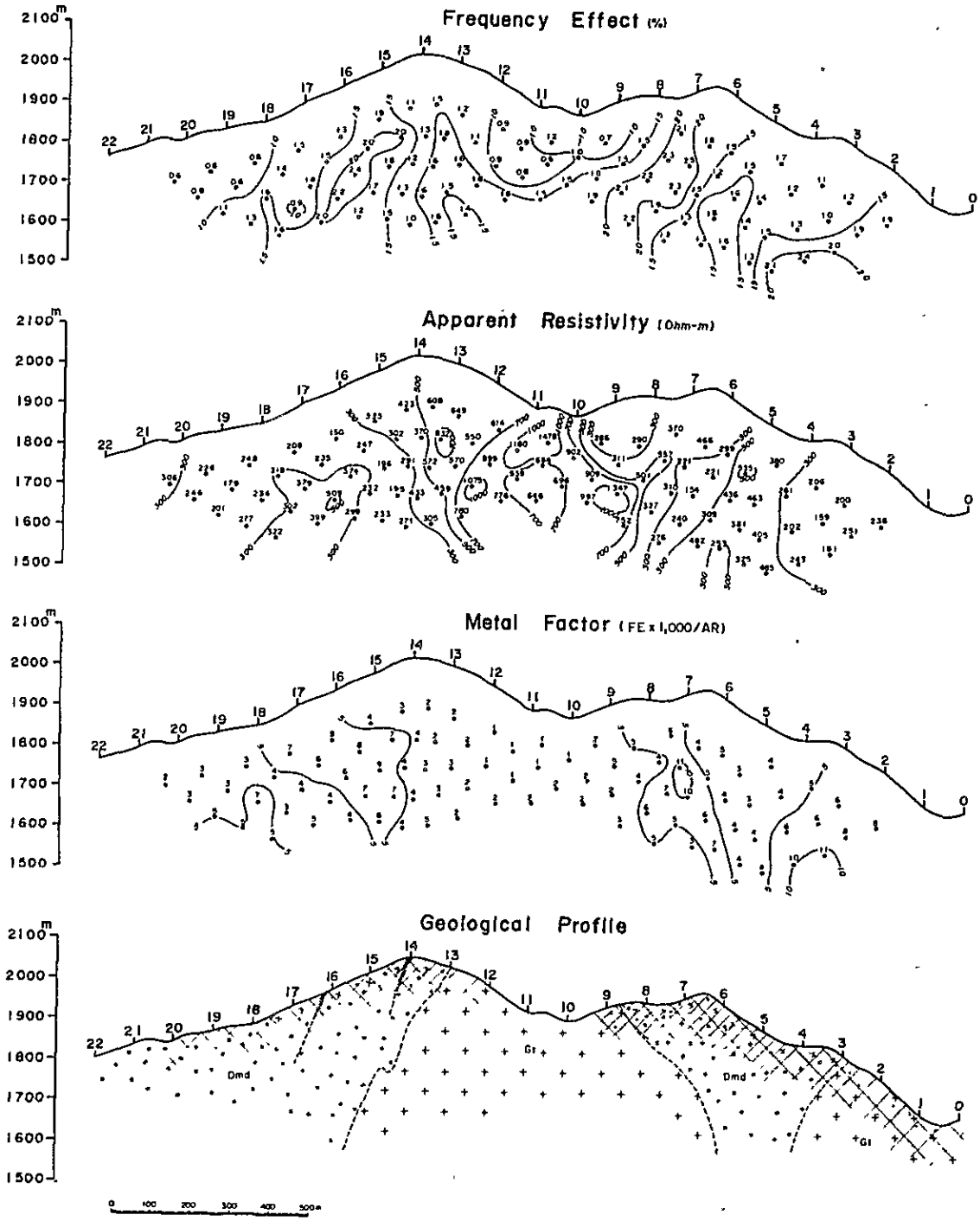

PL.4-10 Profile of IP survey in Mamlis area (Line W_1)

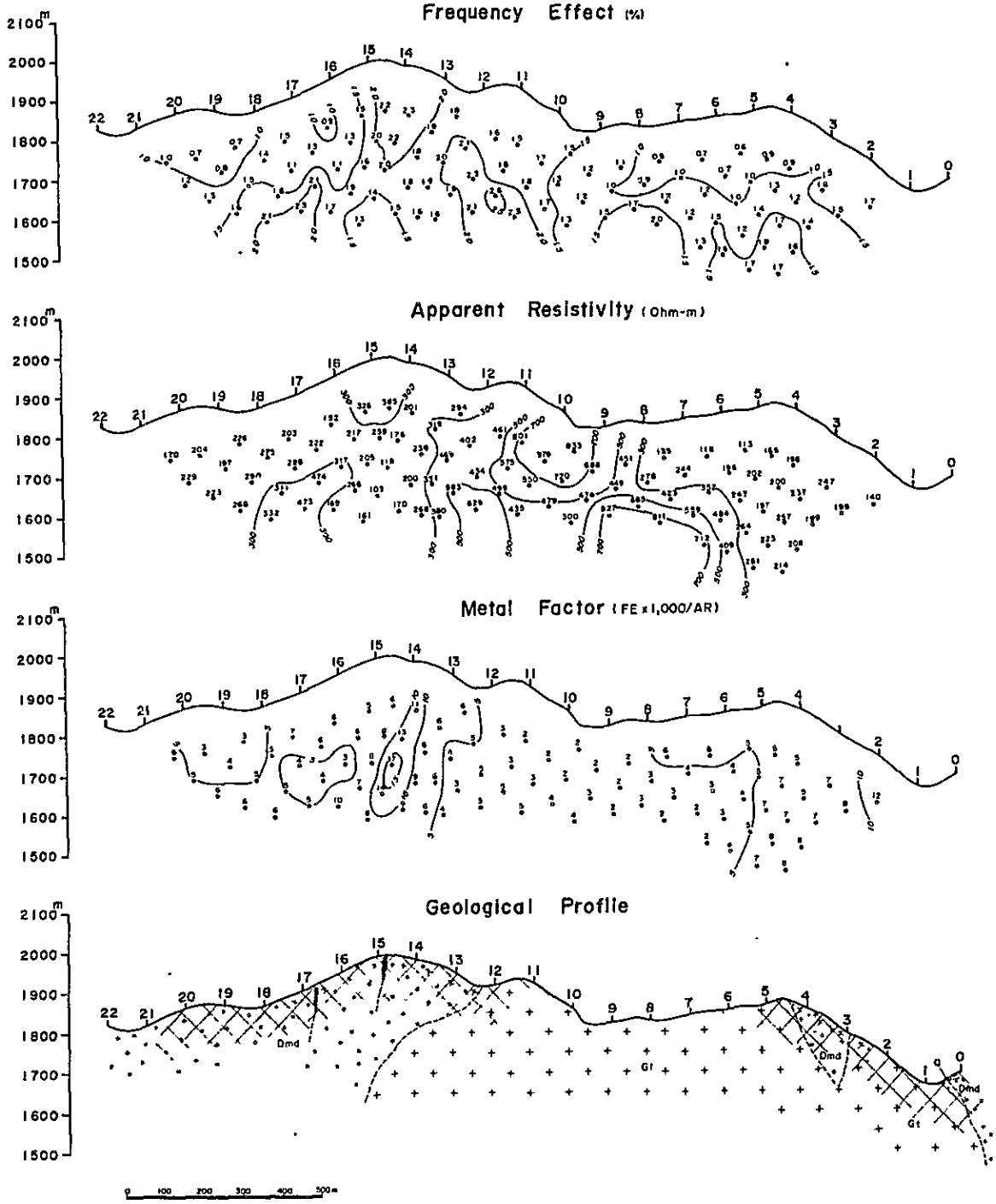

PL.4-11 Profile of IP survey in Mamlis area (Line W_2)

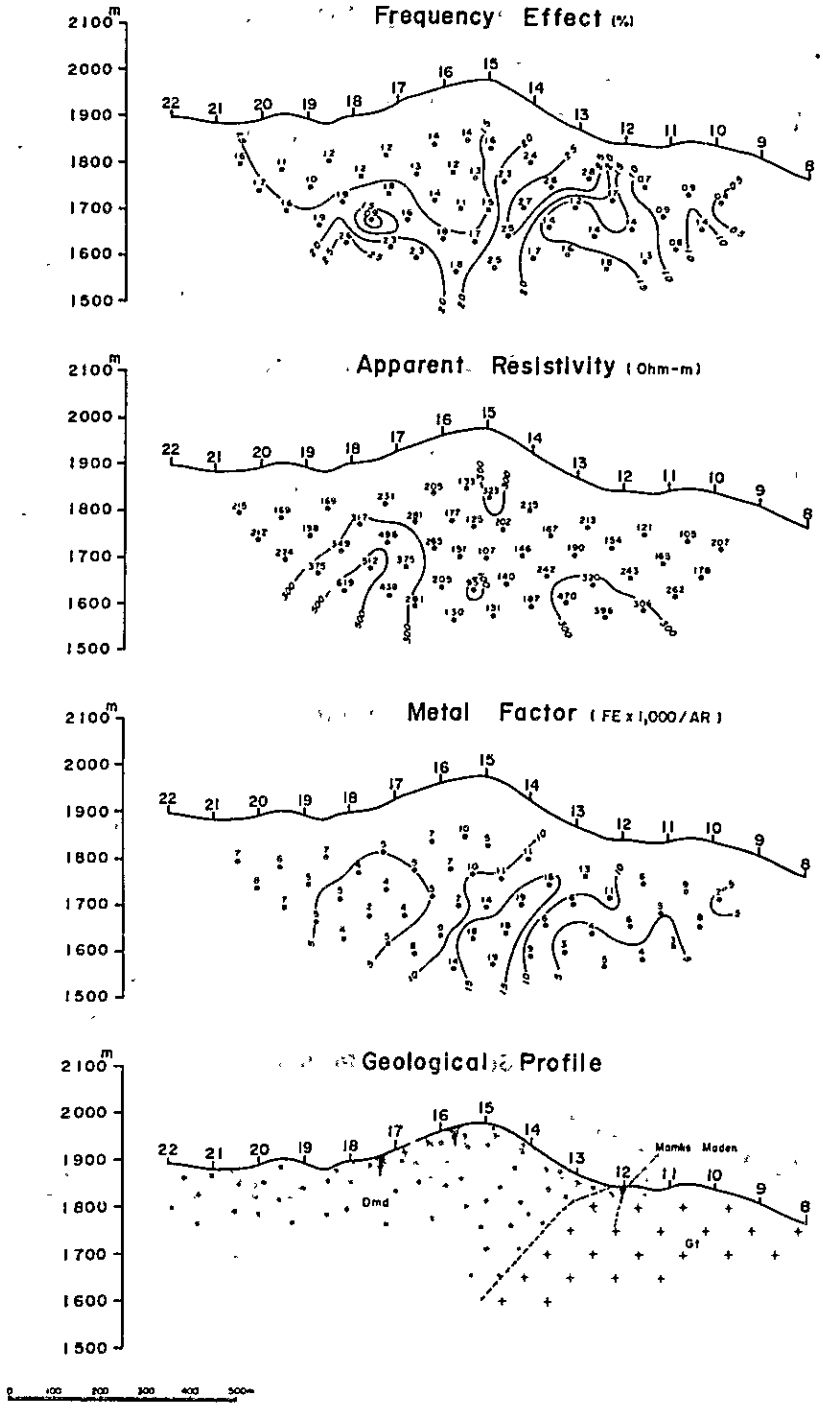

PL.4-12 Profile of IP survey in Mamlis area (Line W_3)

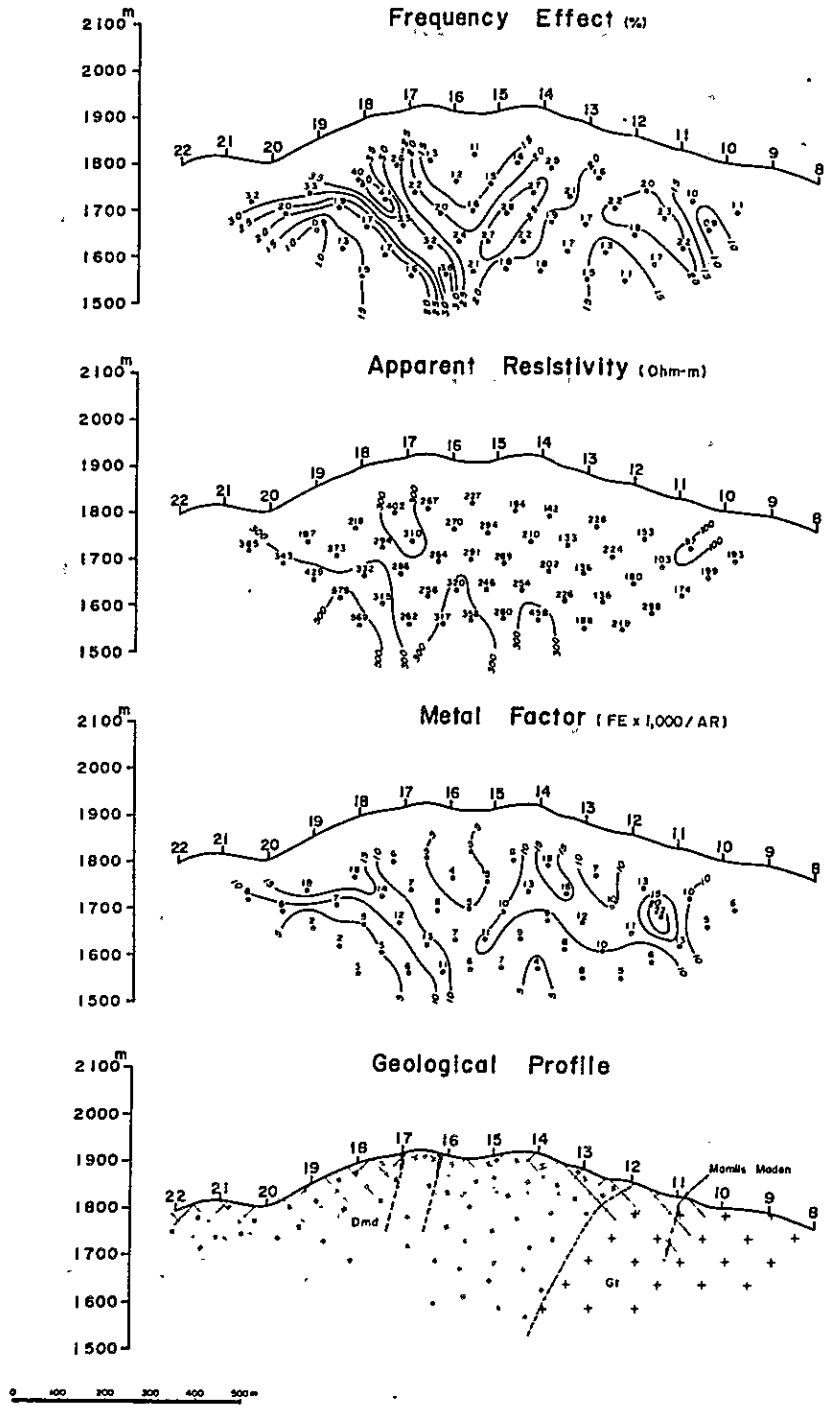

PL.4-13 Profile of IP survey in Mamlis area (Line W_4)

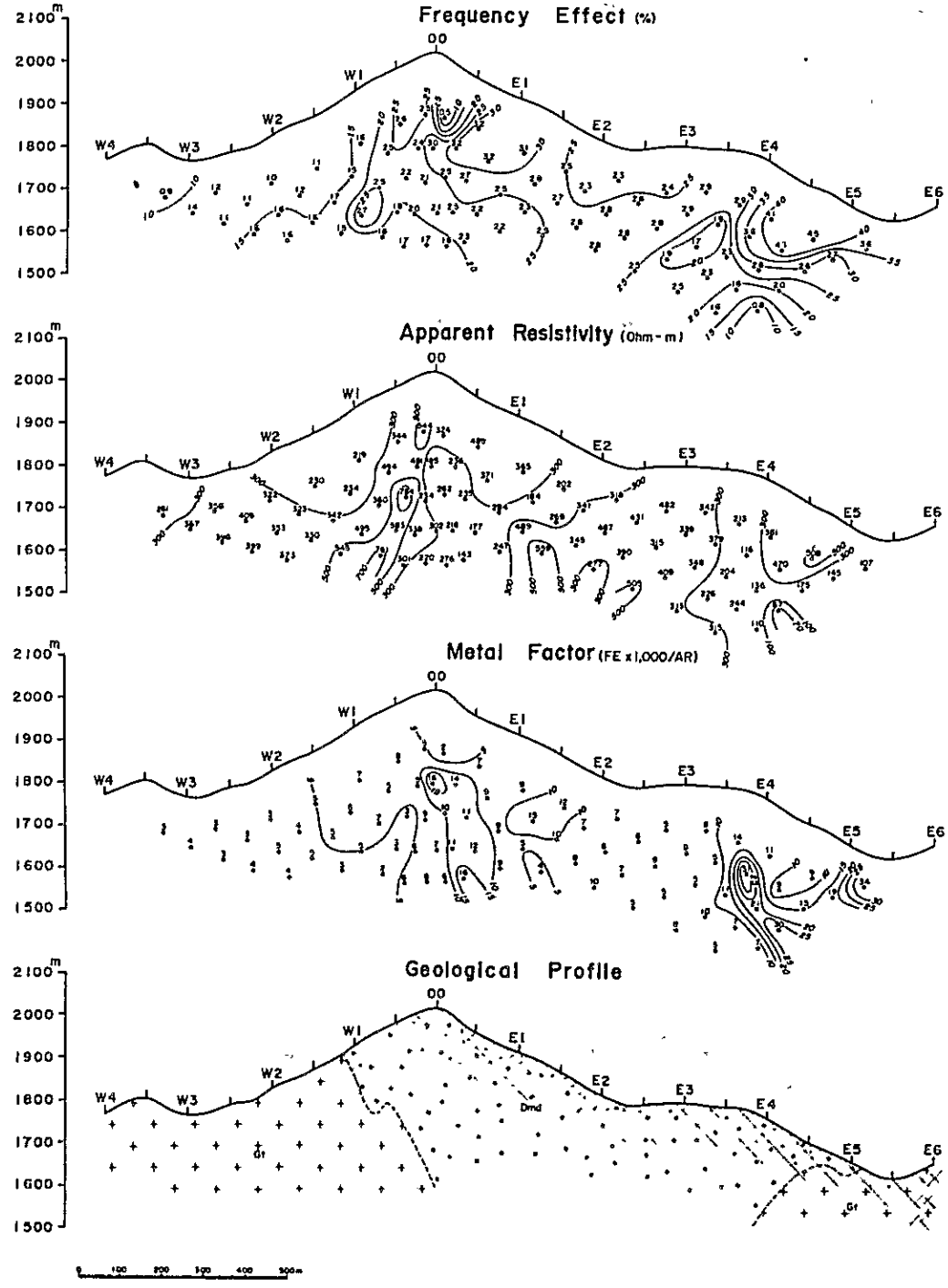

PL.4-14 Profile of IP survey in Mamlis area (Line Base (8))

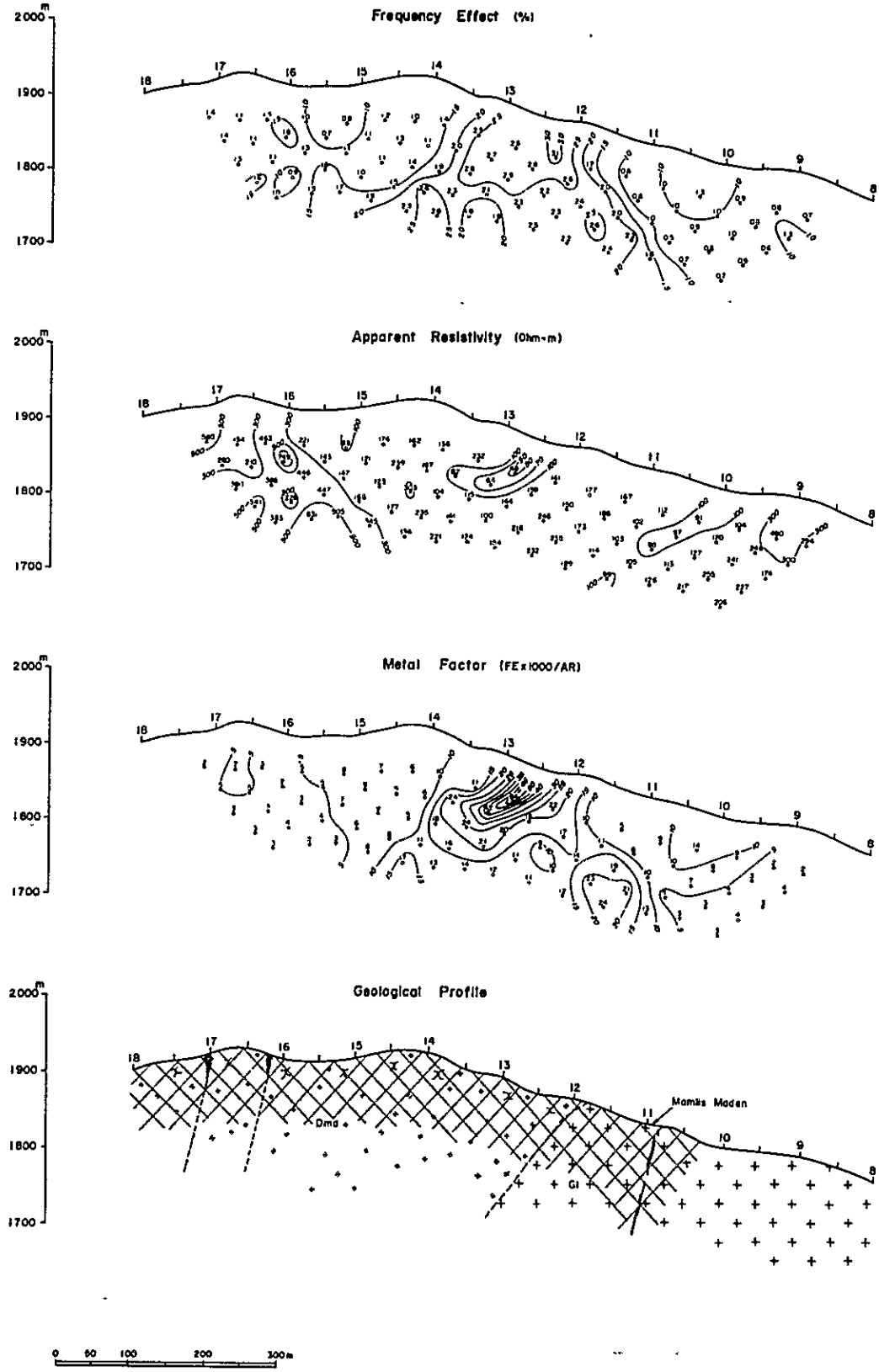

PL.4-15 Profile of IP survey in Mamlis area (Line W_3(8-18))

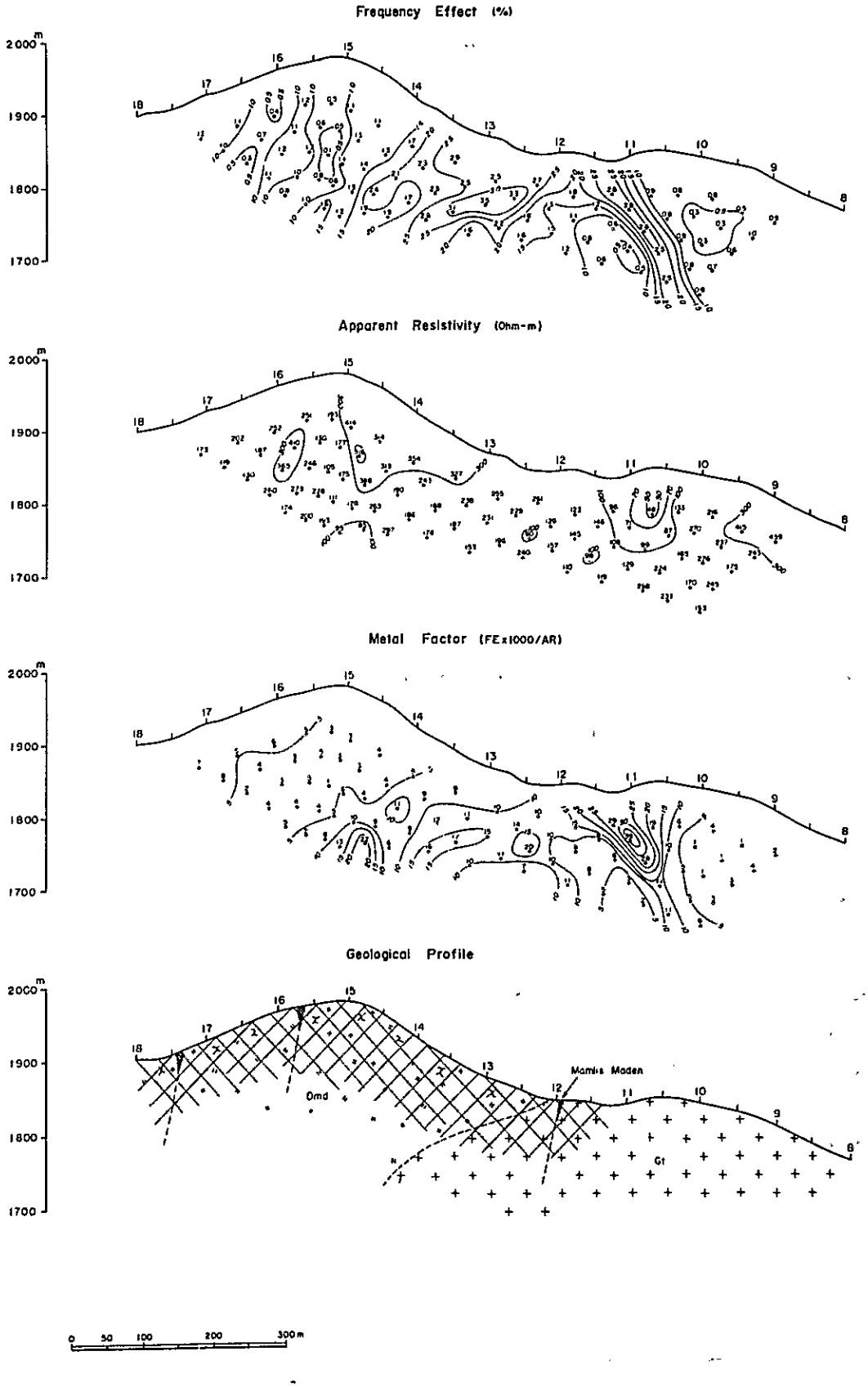

PL.4-16 Profile of IP survey in Mamlis area (Line W_4(8-18))

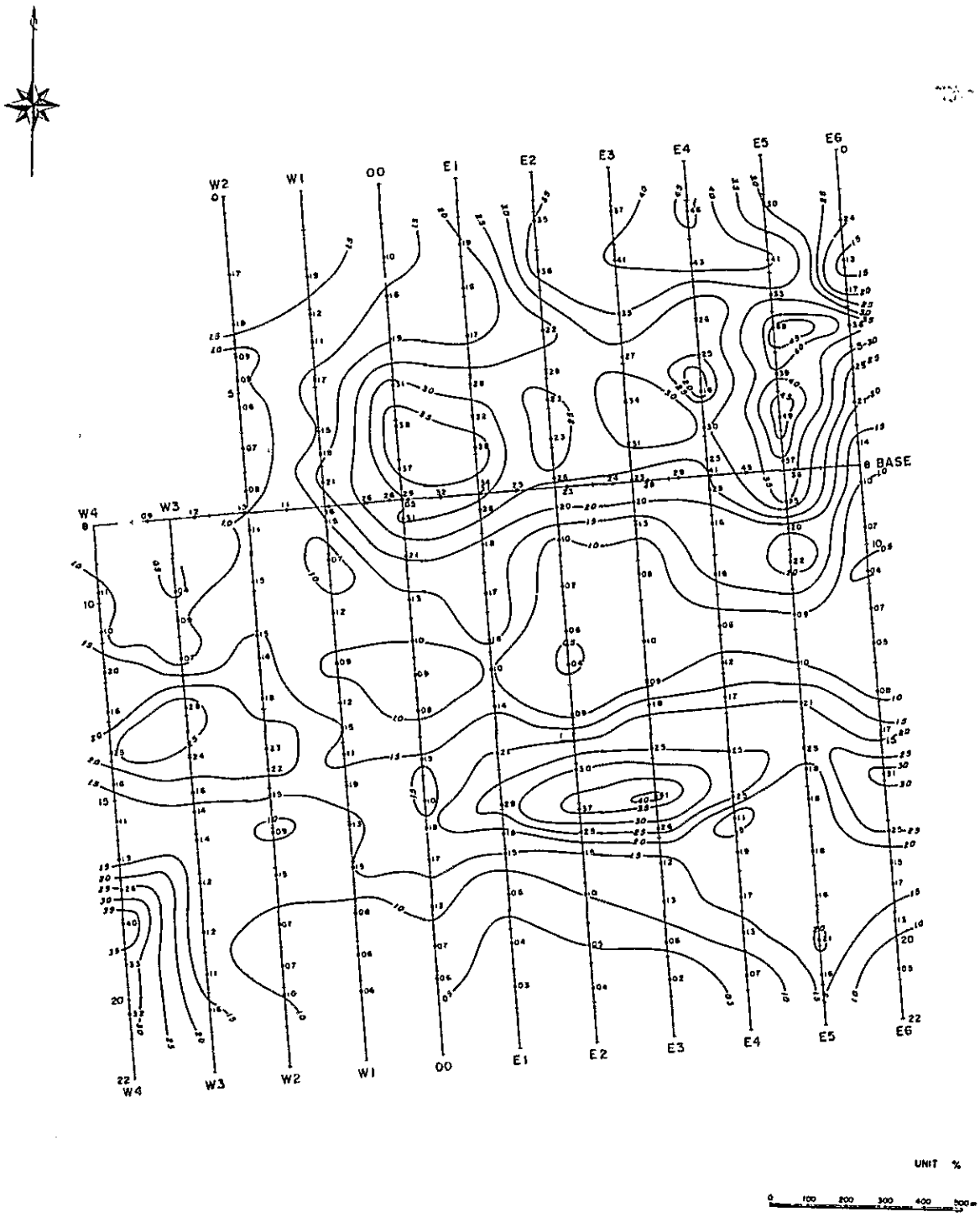

PL.4-17 FE plane map in Mamlis area (n=1)

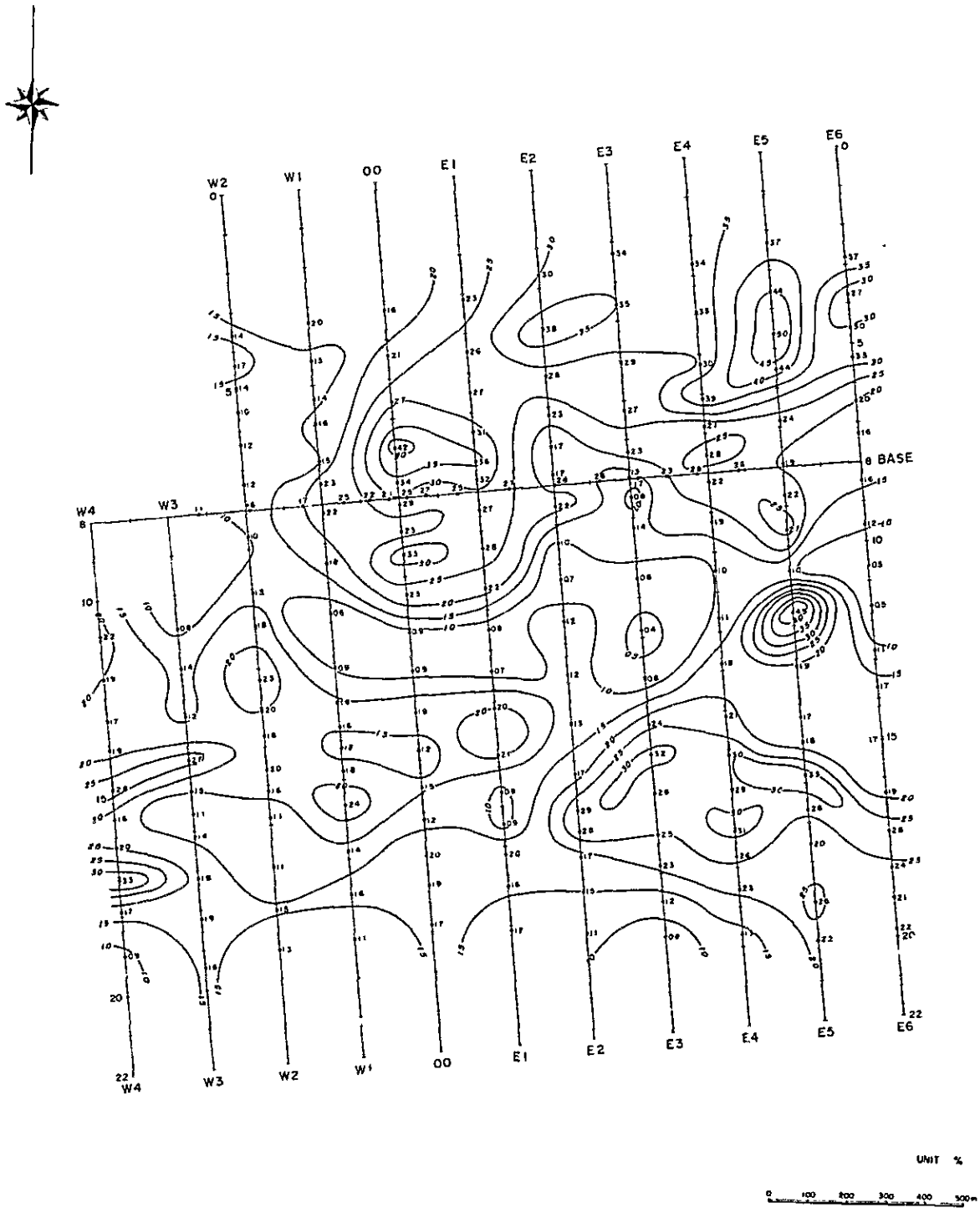

PL.4-18 FE plane map in Mamlis area (n=3)

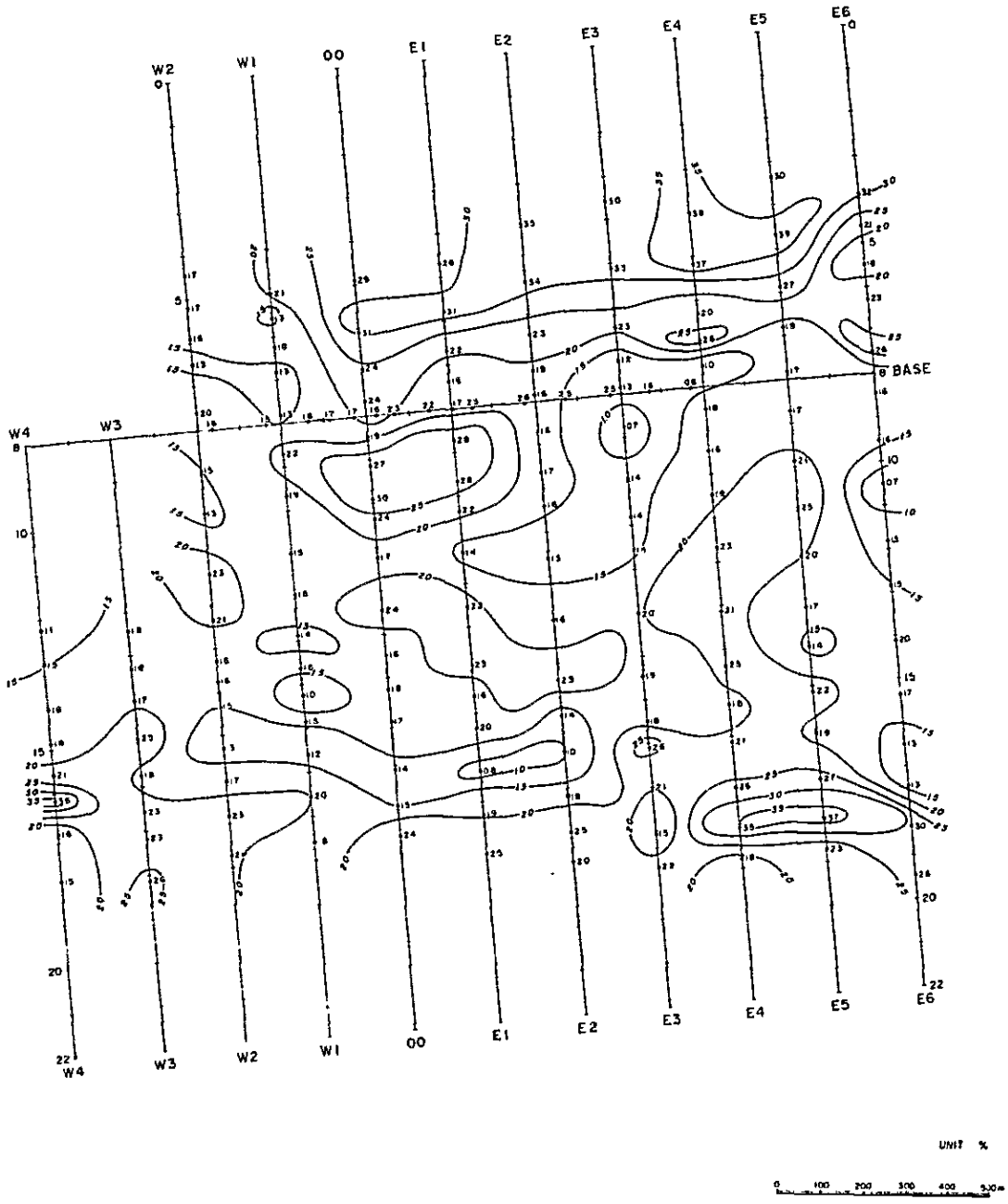

PL.4-19 FE plane map in Mamlis area (n=5)

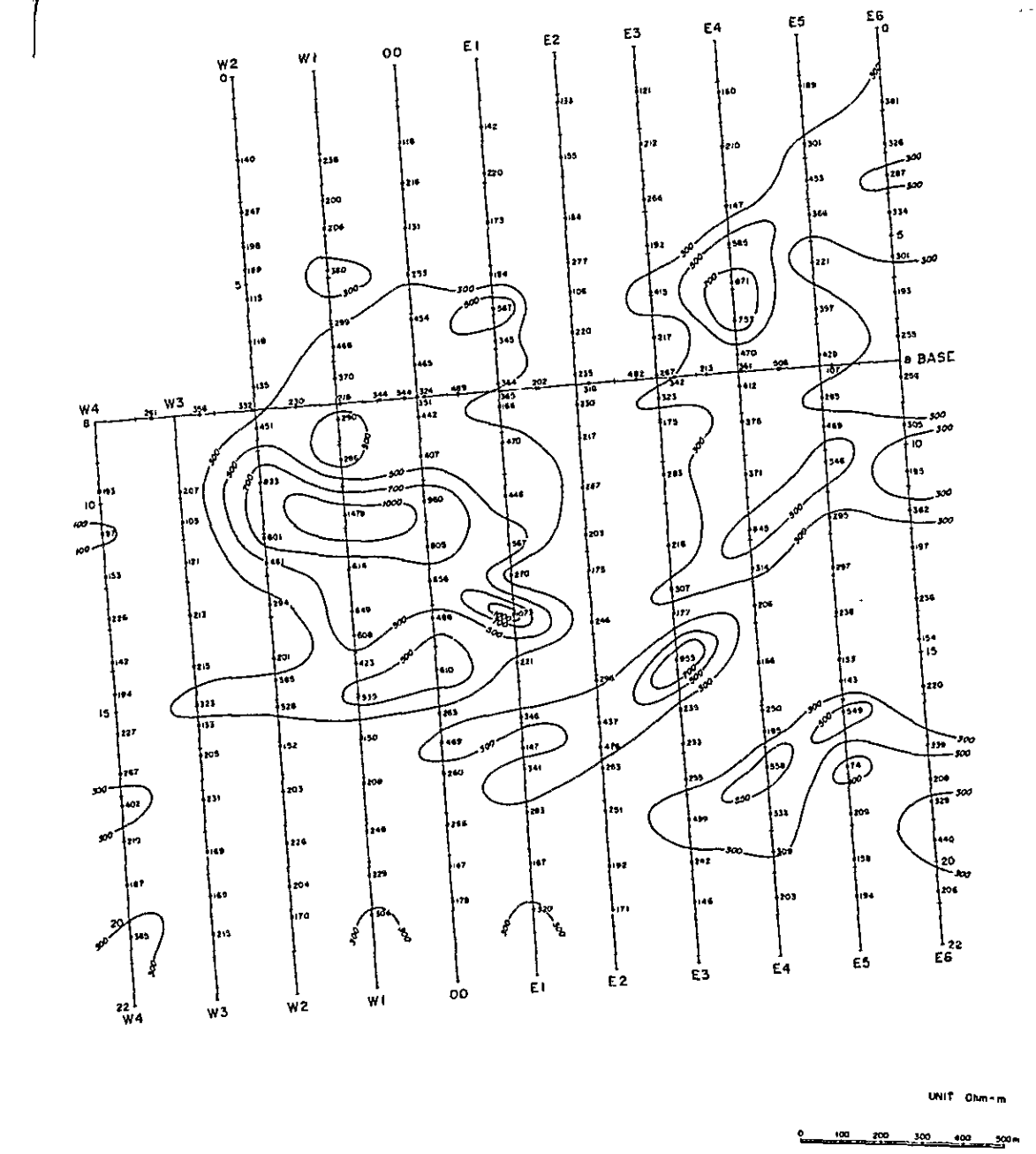

PL.4-20 AR plane map in Mamlis area (n=1)

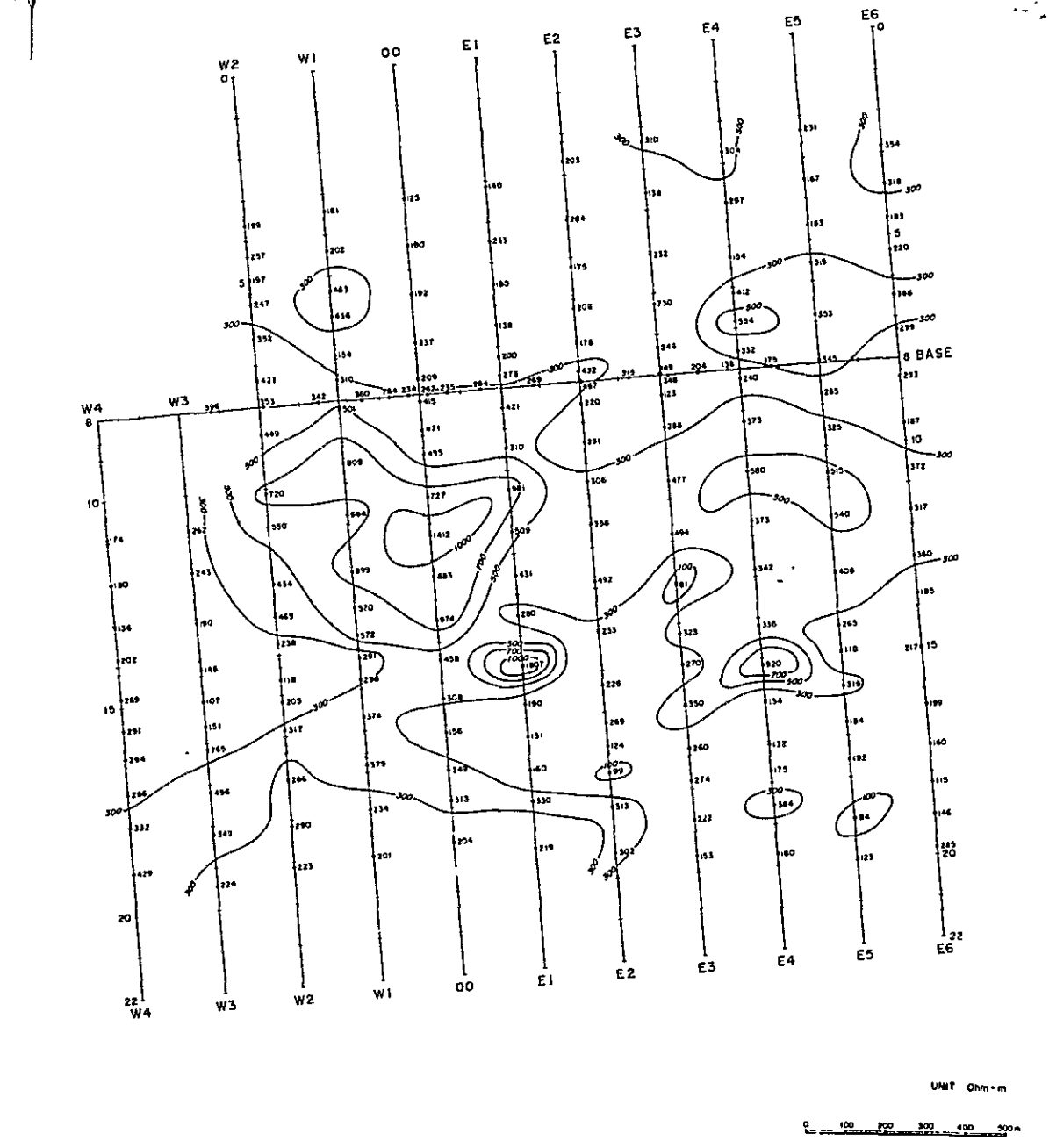

PL.4-21 AR plane map in Mamlis area (n=3)

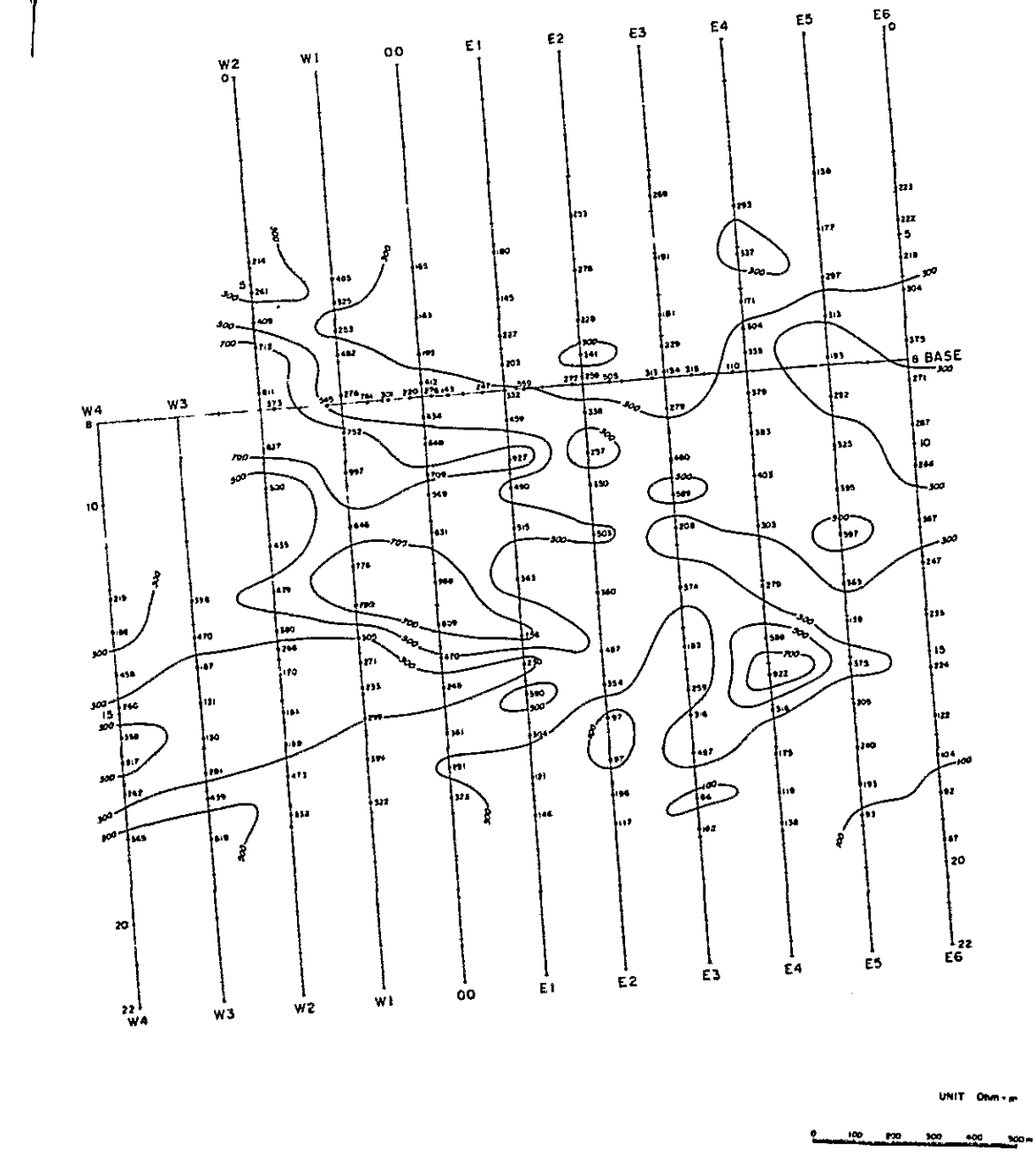

PL.4-22 AR plane map in Mamlis area (n=5)

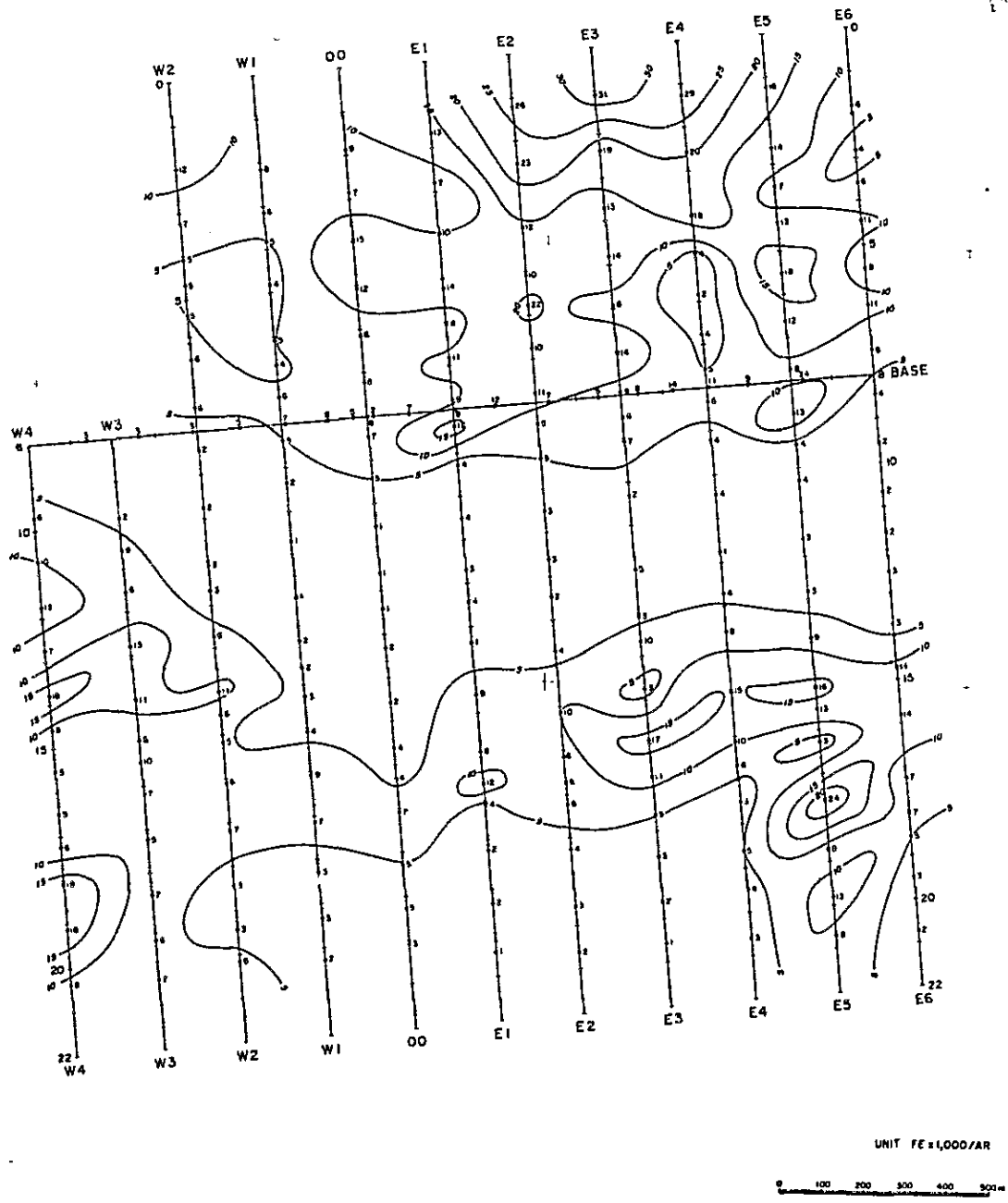

PL.4-23 MF plane map in Mamlis area (n=1)

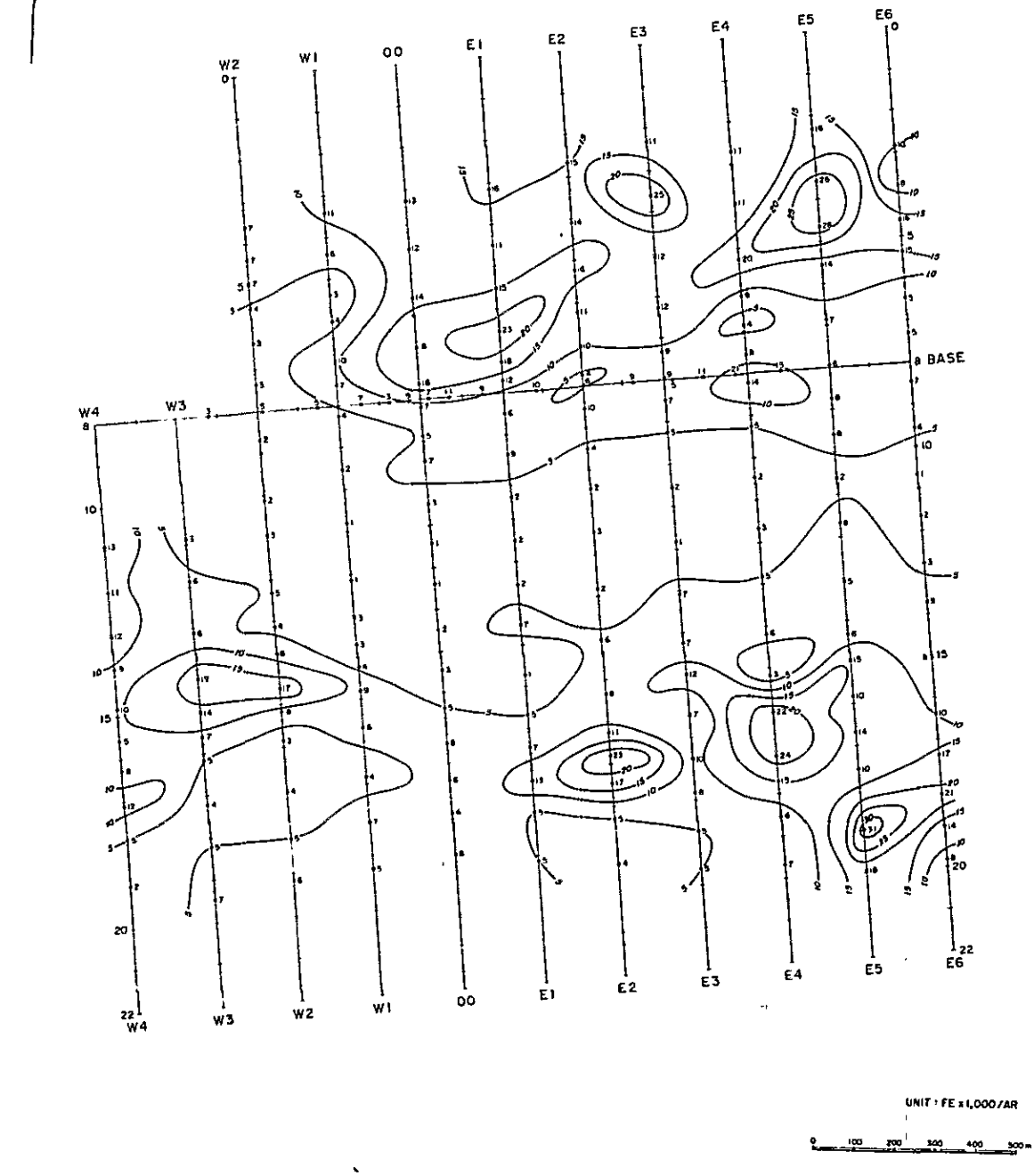

PL.4-24 MF plane map in Mamlis area (n=3)

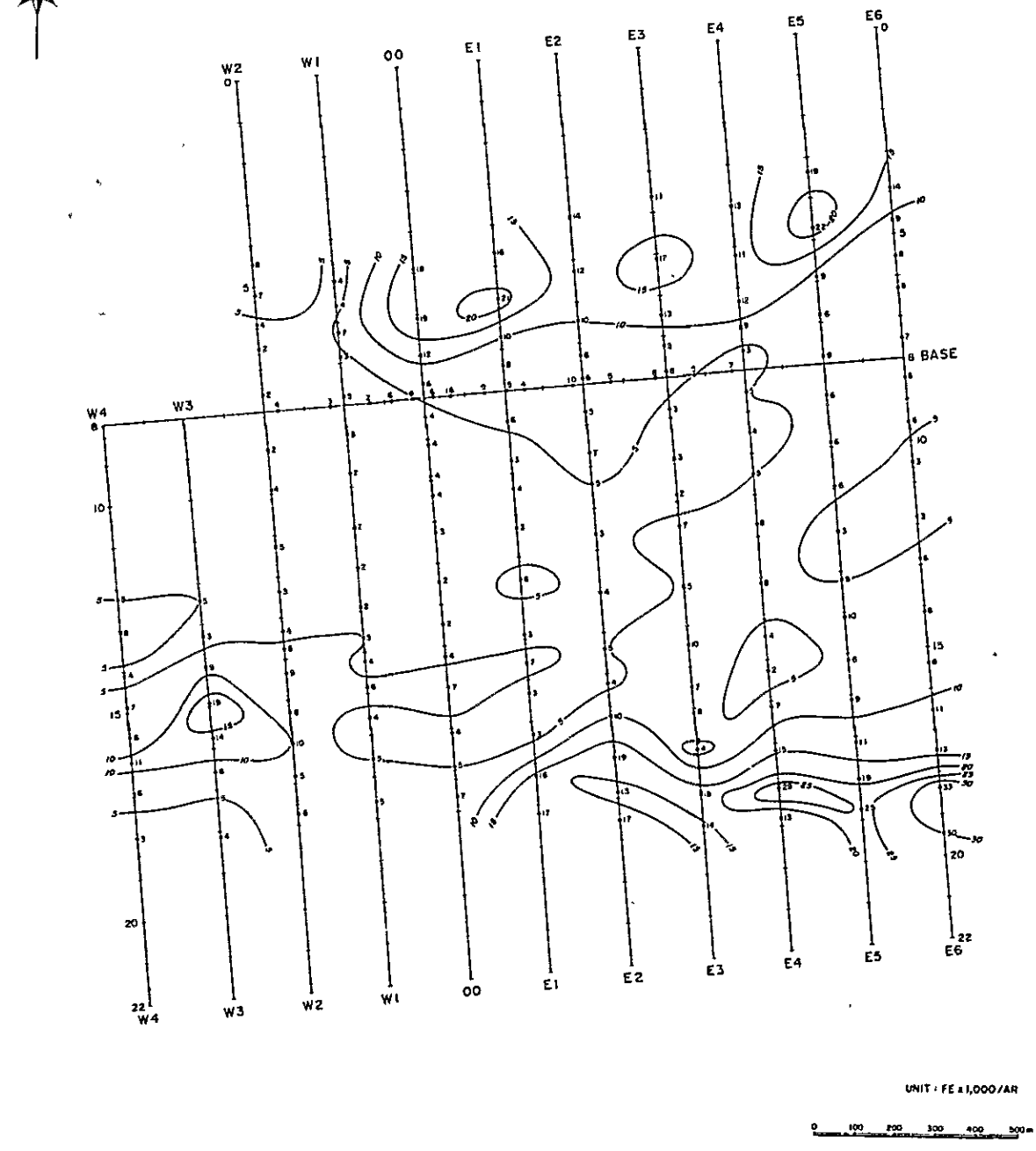

PL.4-25 MF plane map in Mamlis area (n=5)

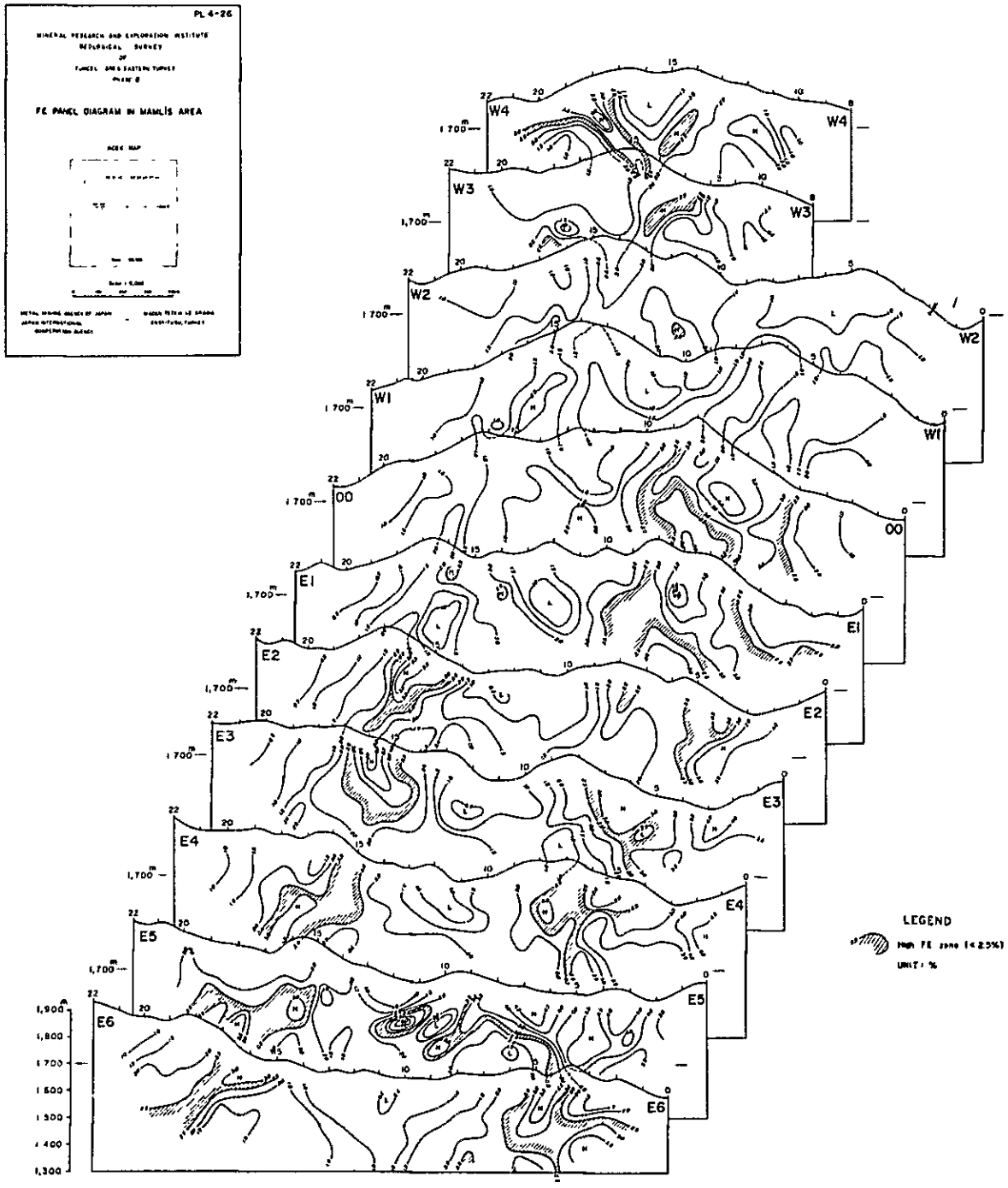

PL.4-26 FE panel diagram in Mamlis area

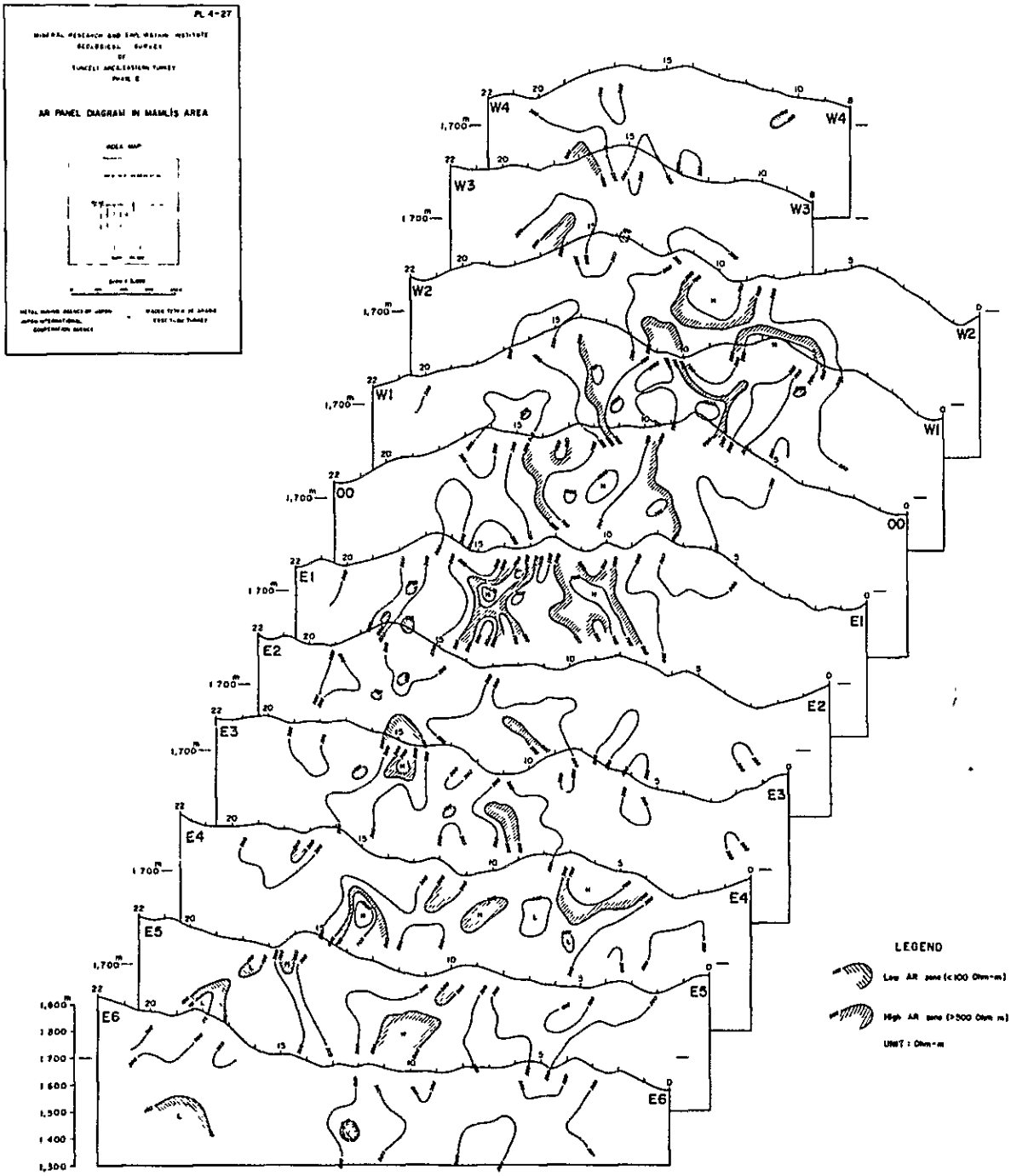

PL.4-27 AR panel diagram in Mamlis area

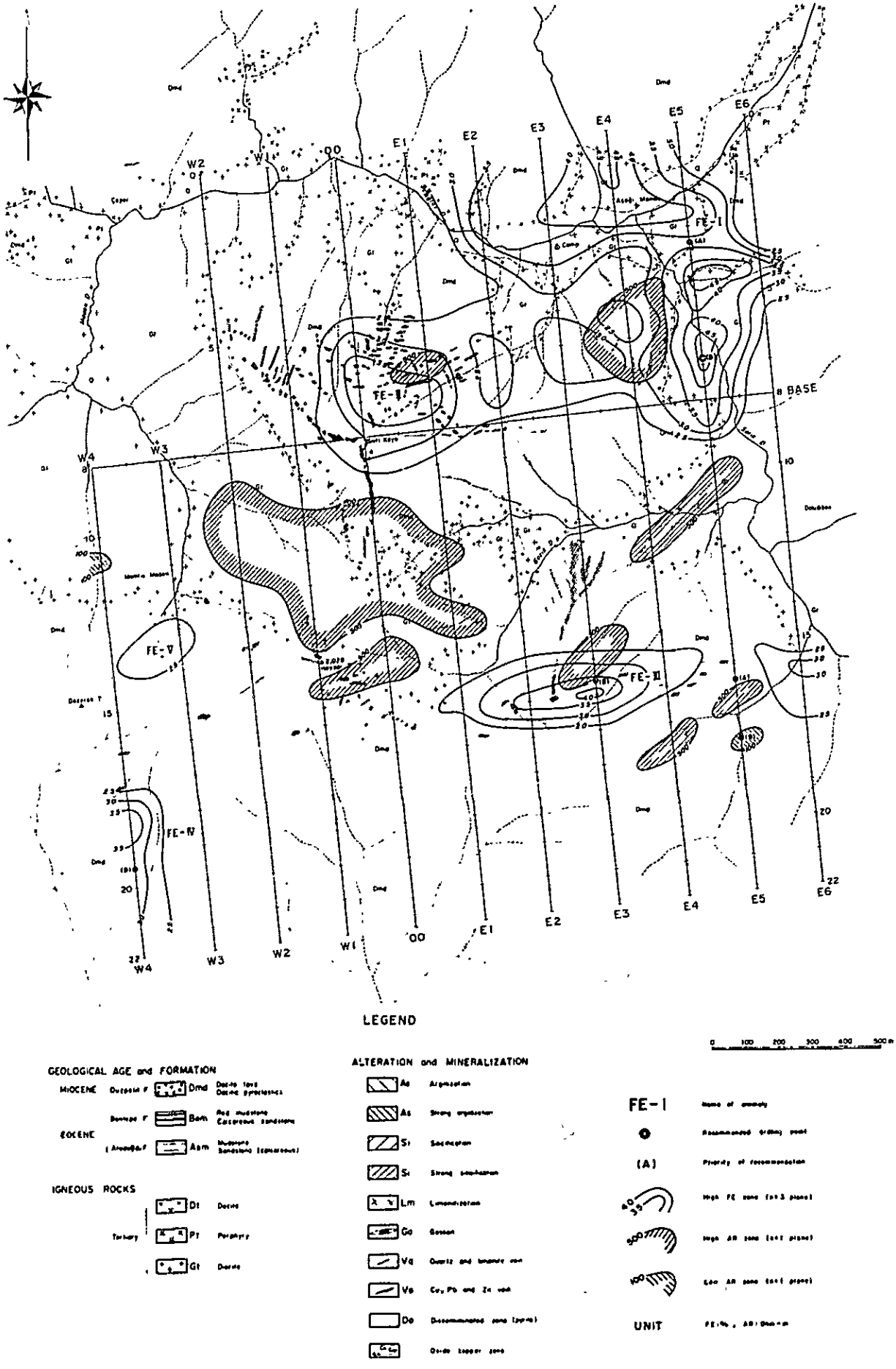

PL.4-28 Interpretation map in Mamlis area

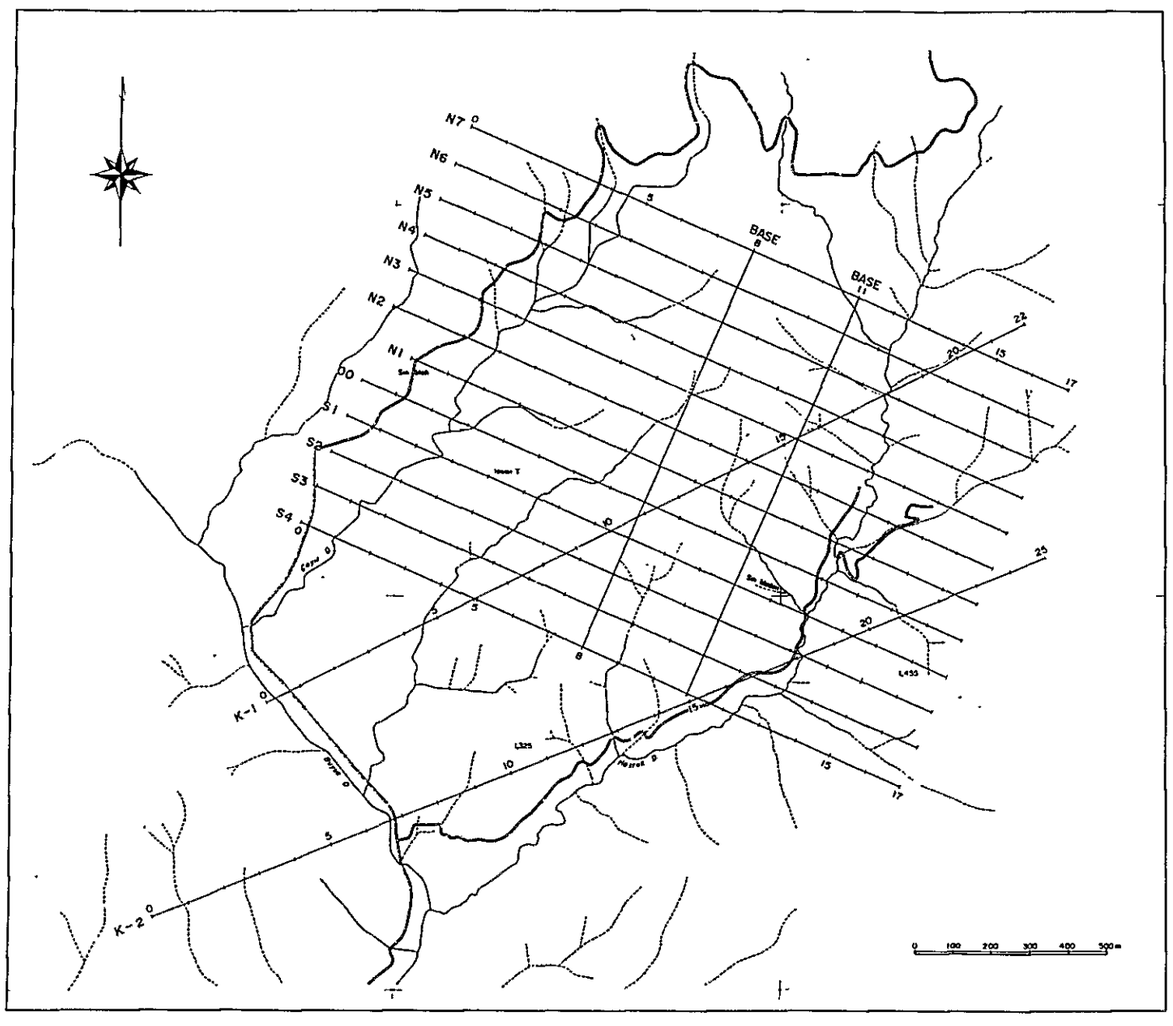

PL 4-29

MINERAL RESEARCH AND EXPLORATION INSTITUTE
GEOLOGICAL SURVEY
OF
TUNCELI AREA, EASTERN TURKEY
PHASE II

LOCATION MAP OF IP SURVEY IN SİN AREA

LOCATION MAP

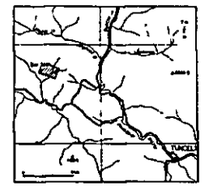

Scale 1:3,000

METAL MINING AGENCY OF JAPAN
JAPAN INTERNATIONAL COOPERATION AGENCY

–

MADEN TETKİK VE ARAMA ENSTİTUSU, TURKEY

PL.4-29 Location map of IP survey in Sin area

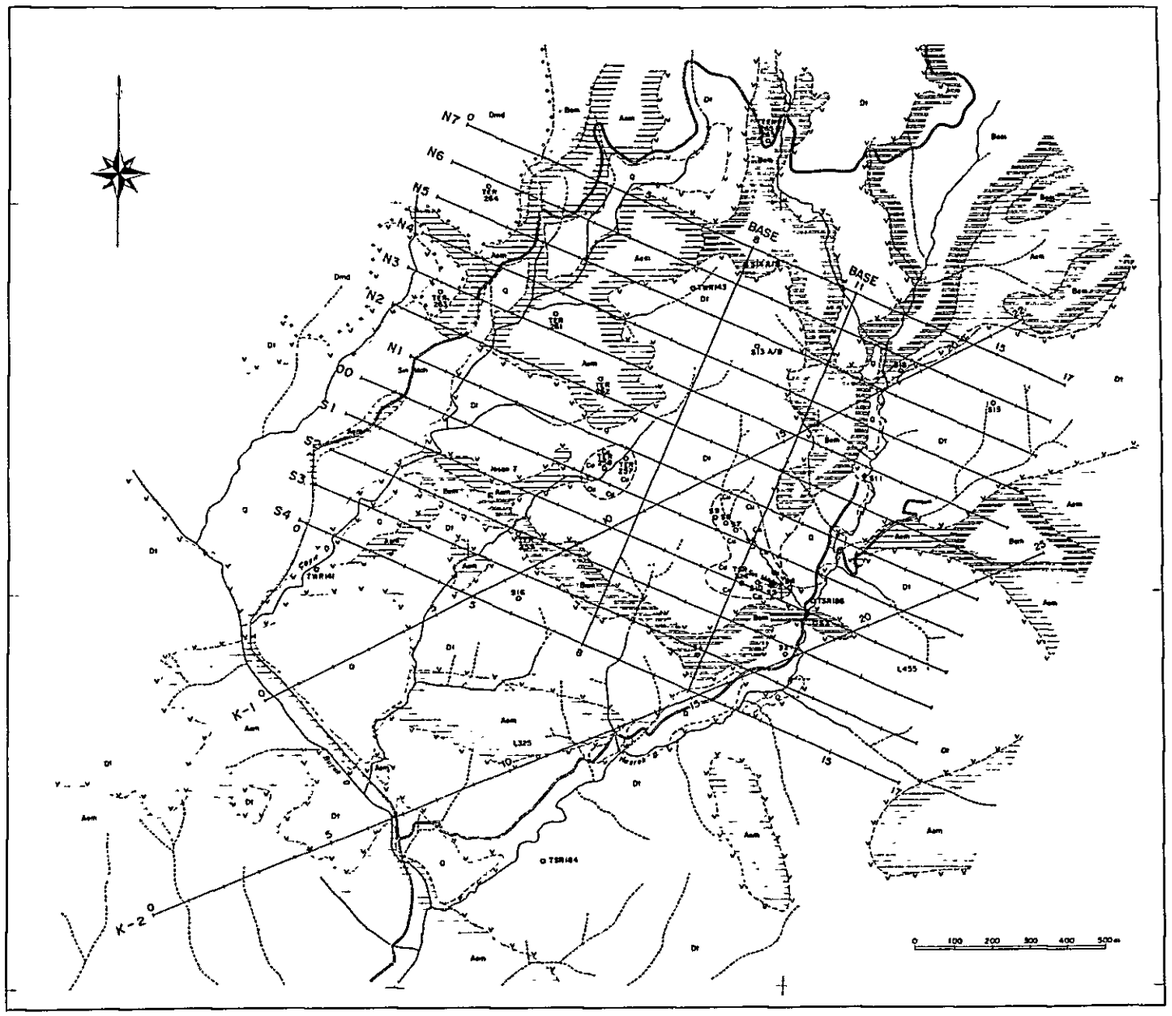

PL.4-30

MINERAL RESEARCH AND EXPLORATION INSTITUTE
GEOLOGICAL SURVEY
OF
TUNCELI AREA, EASTERN TURKEY
PHASE II

GEOLOGICAL MAP & SAMPLING LOCATION MAP IN SİN AREA

LOCATION MAP

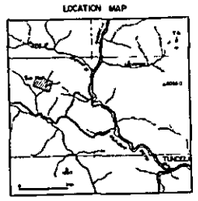

METAL MINING AGENCY OF JAPAN
JAPAN INTERNATIONAL COOPERATION AGENCY

—

MADEN TETKİK VE ARAMA ENSTİTÜSÜ, TURKEY

LEGEND

GEOLOGICAL AGE and FORMATION

MIOCENE
- Dikmetepe F. — Dmd — Dacite tuff, Dacite pyroclastics

EOCENE
- Bentepe F. — Bem — Red mudstone, Calcareous sandstone
- Aladağlar F. — Aem — Mudstone, Sandstone (calcareous)

IGNEOUS ROCKS

Tertiary
- Dt — Dacite
- Pt — Porphyry
- Gt — Granite

ALTERATION and MINERALIZATION
- Ac — Argillization
- As — Strong argillization
- Si — Silicification
- Si — Strong silicification
- Lm — Limonitization
- Go — Gossan
- Vq — Quartz and telanite vein
- Vc — Cu, Pb and Zn vein
- De — Decomposed zone (pyrite)
- Oxide copper zone

PL.4-30 Geological map and sampling location map in Sin area

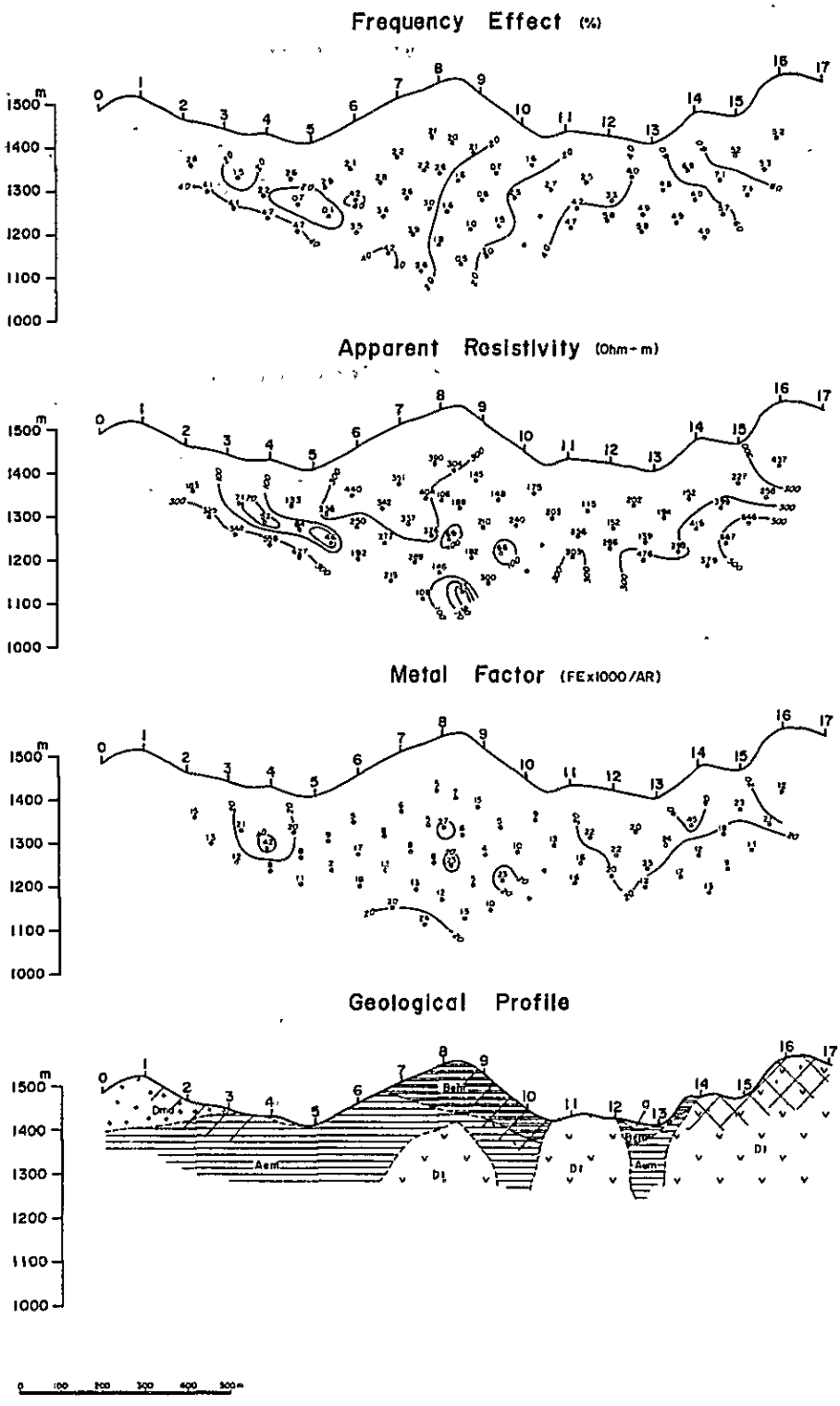

PL.4-31 Profile of IP survey in Sin area (Line N_7)

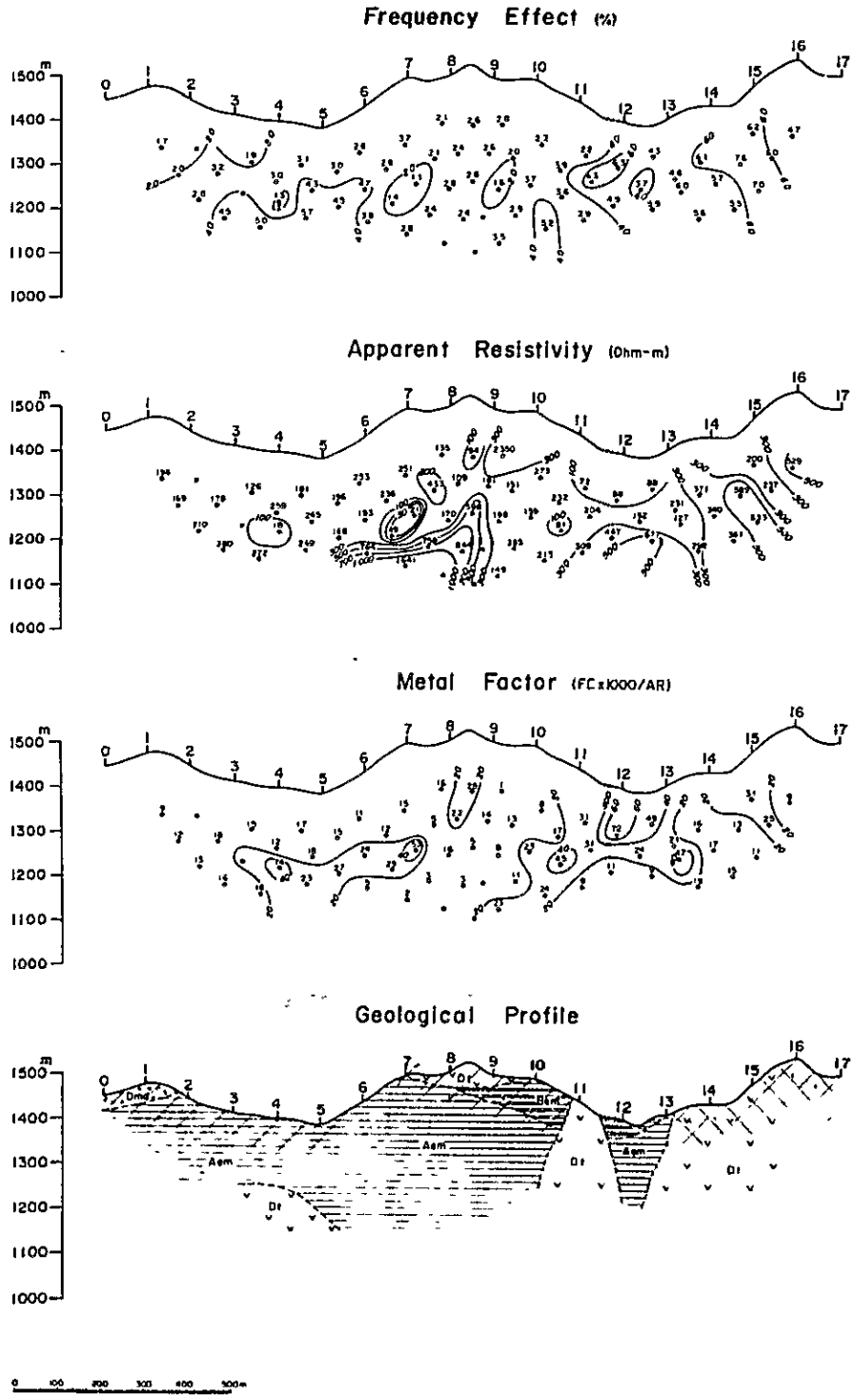

PL.4-32 Profile of IP survey in Sin area (Line N_6)

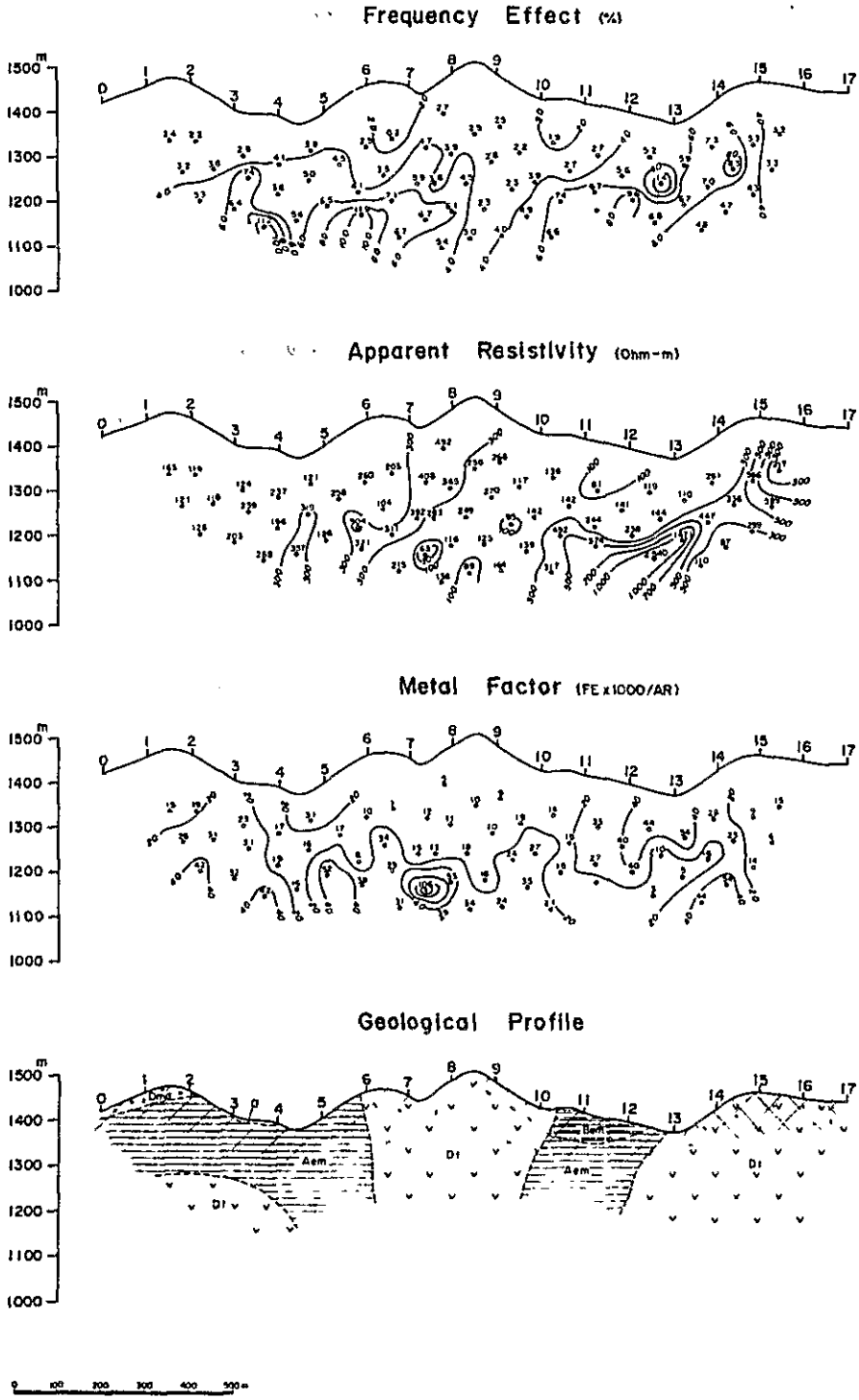

PL.4-33 Profile of IP survey in Sin area (Line N_5)

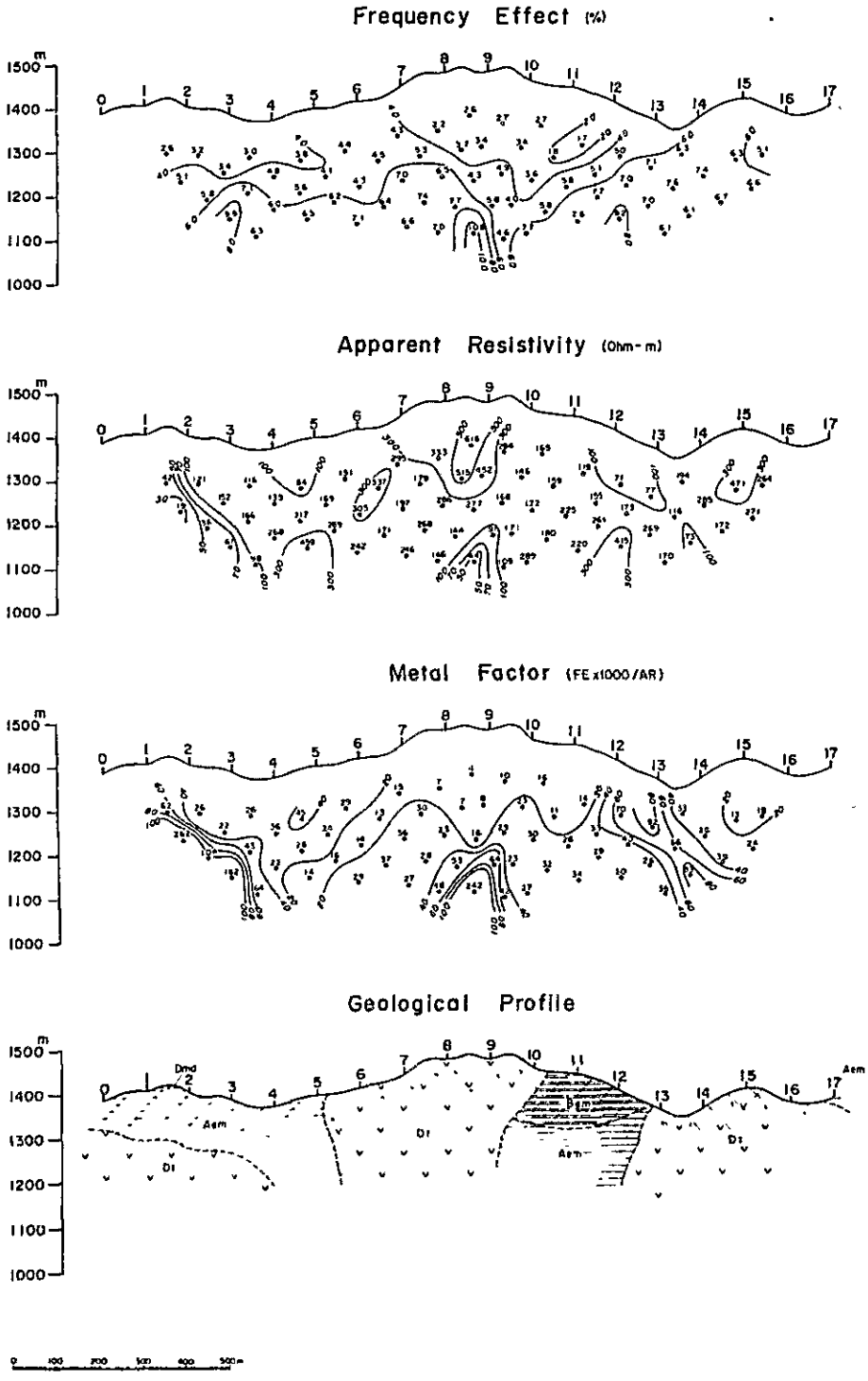

PL.4-34 Profile of IP survey in Sin area (Line N_4)

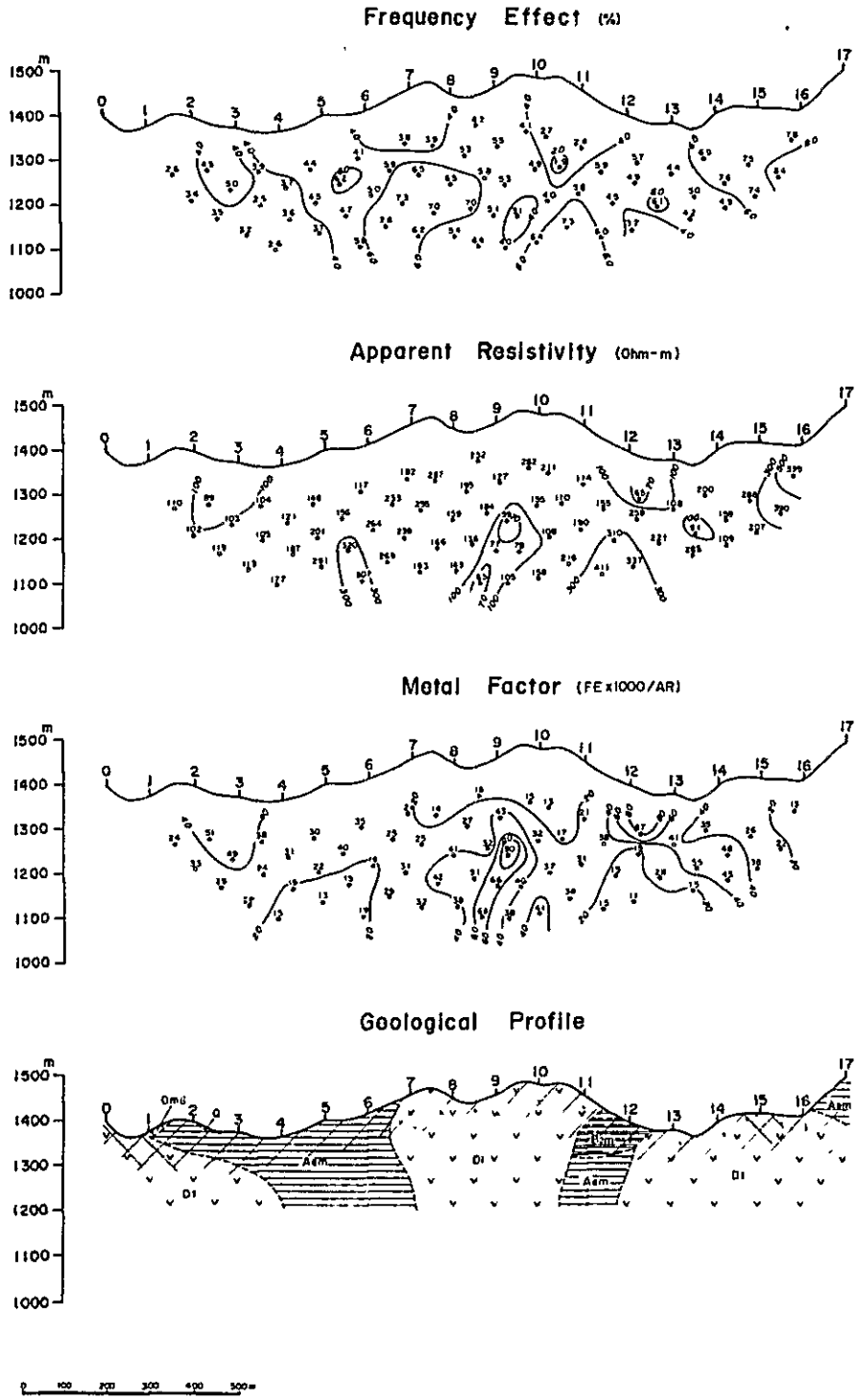

PL.4-35 Profile of IP survey in Sin area (Line N_3)

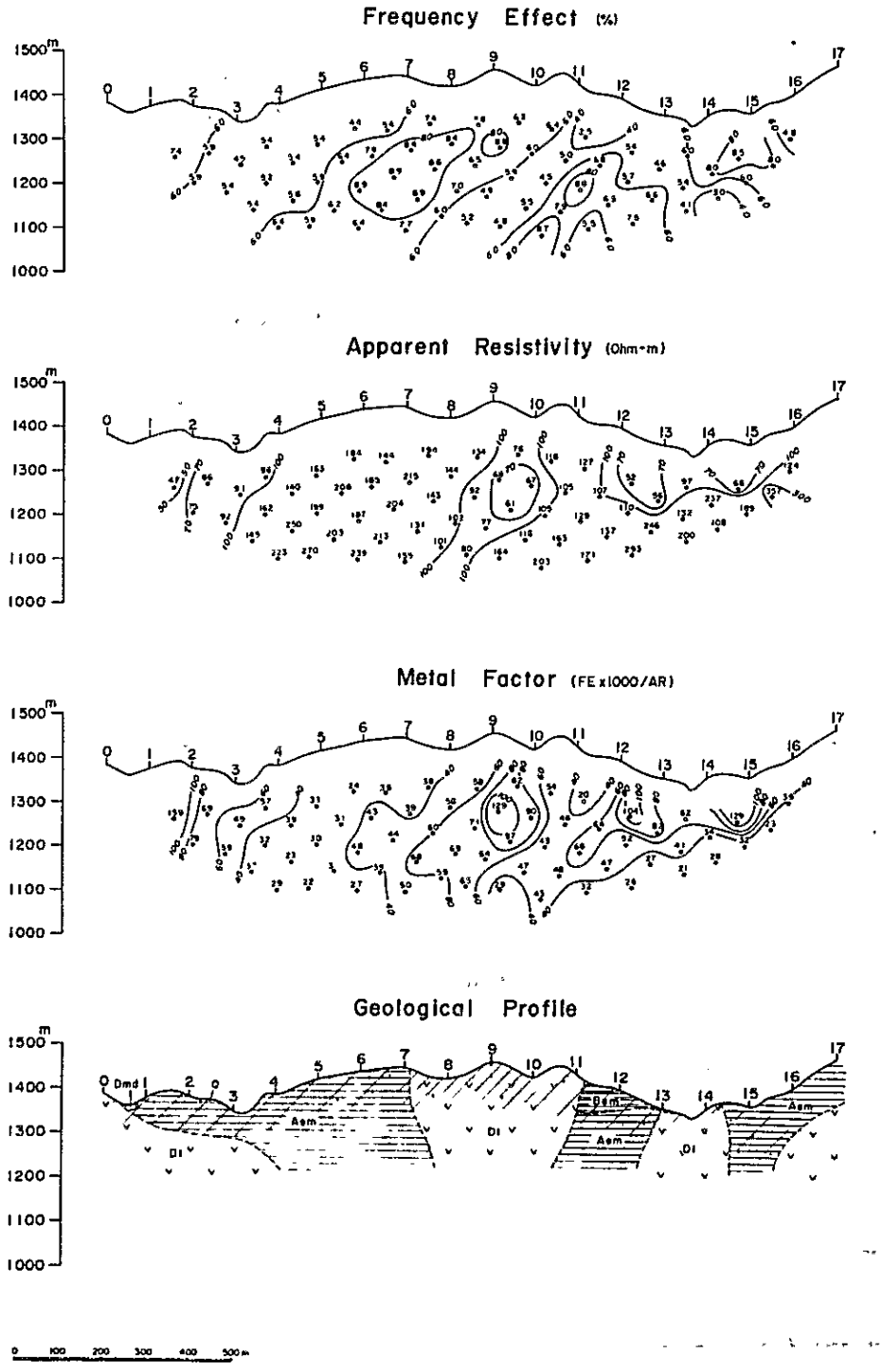

PL.4-36 Profile of IP survey in Sin area (Line N_2)

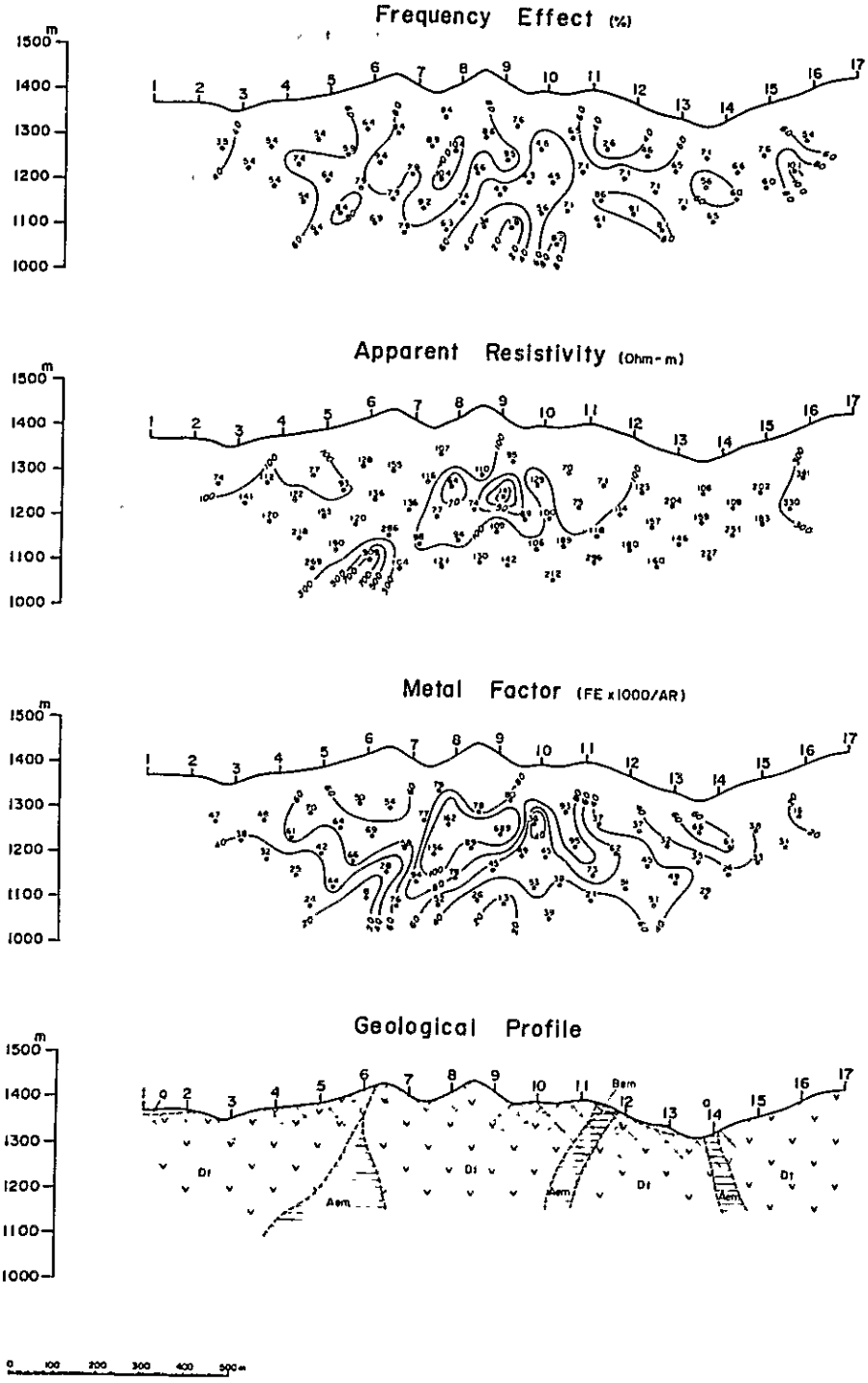

PL.4-37 Profile of IP survey in Sin area (Line N_1)

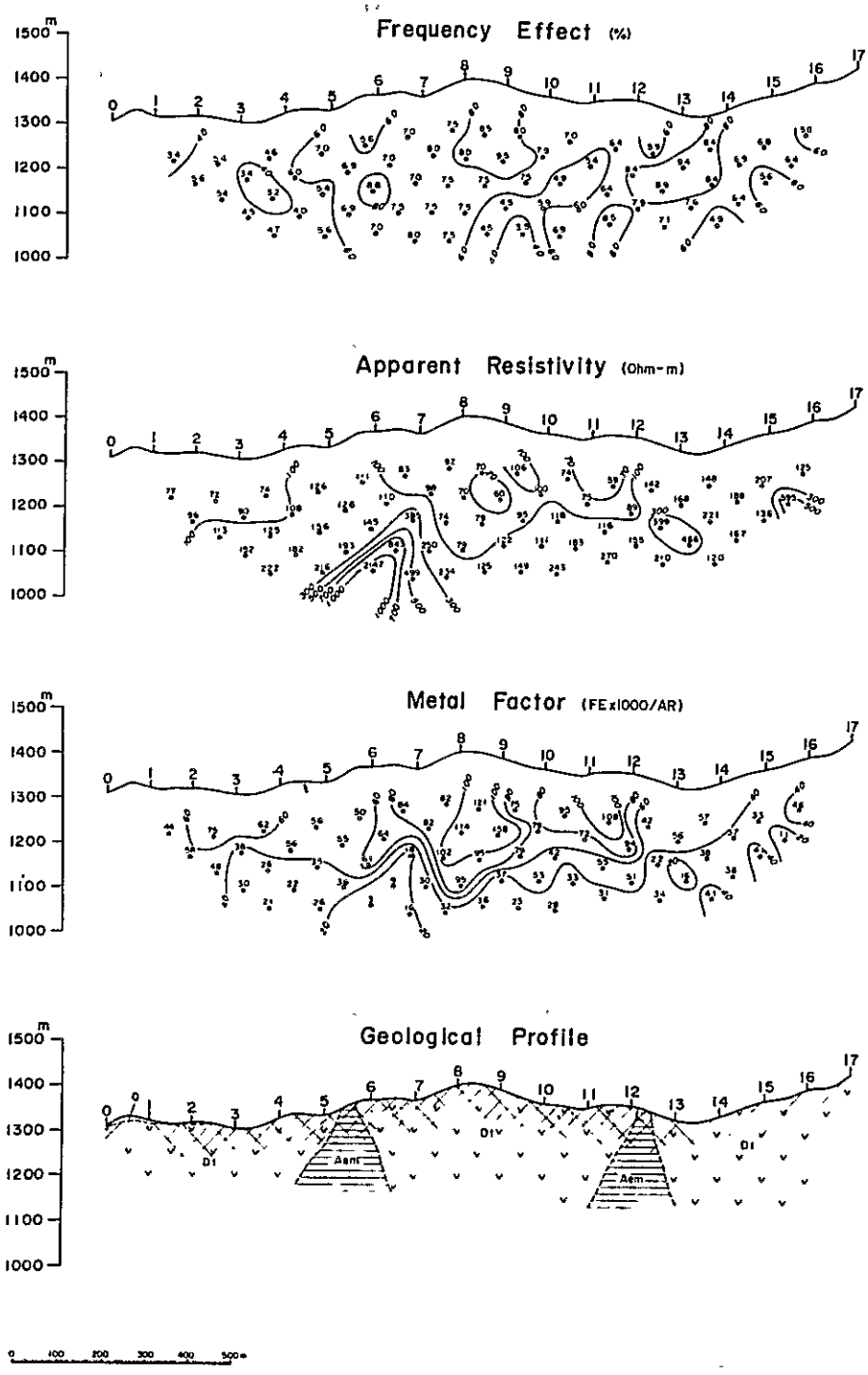

PL.4-38 Profile of IP survey in Sin area (Line.00)

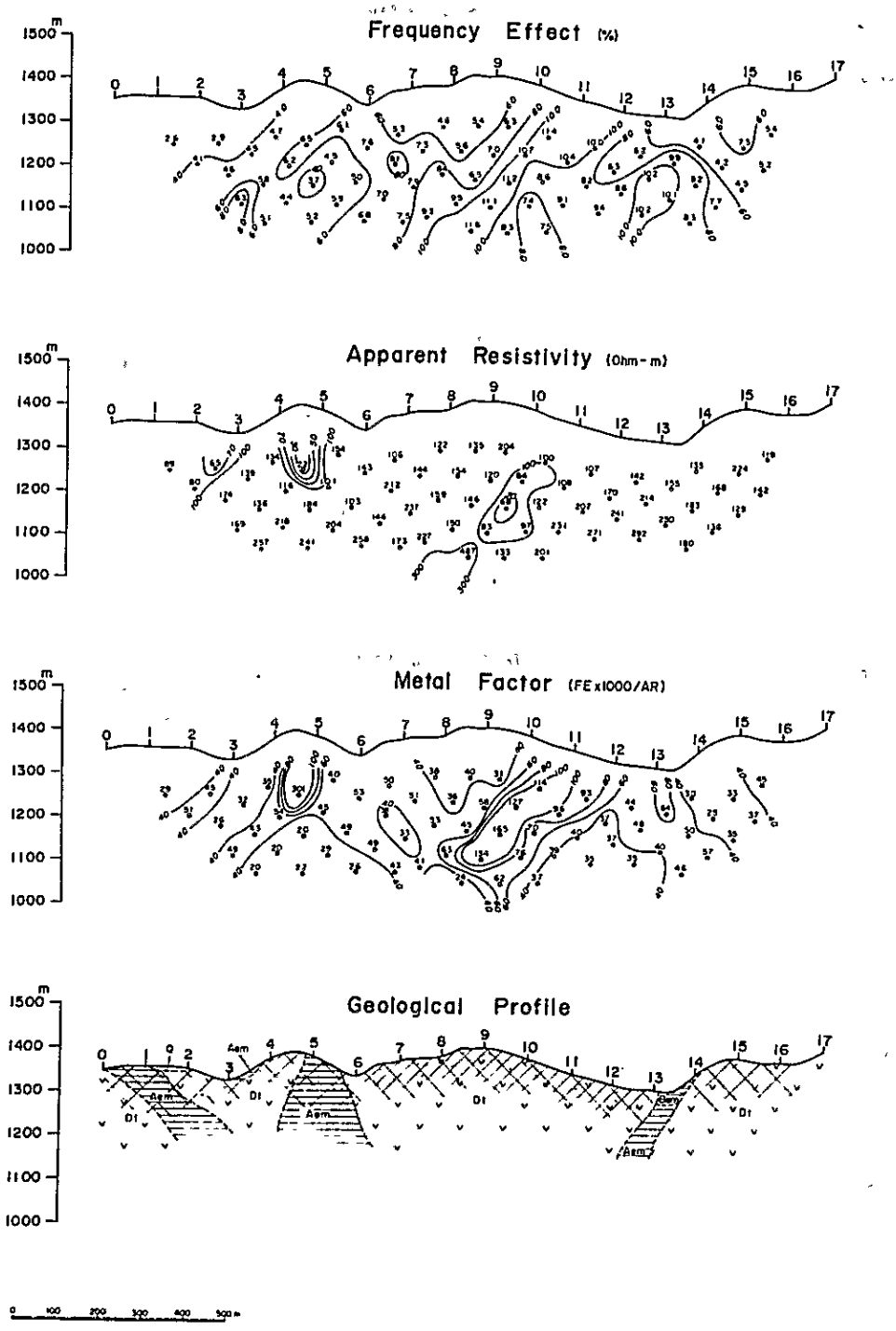

PL.4-39 Profile of IP survey in Sin area (Line S_1)

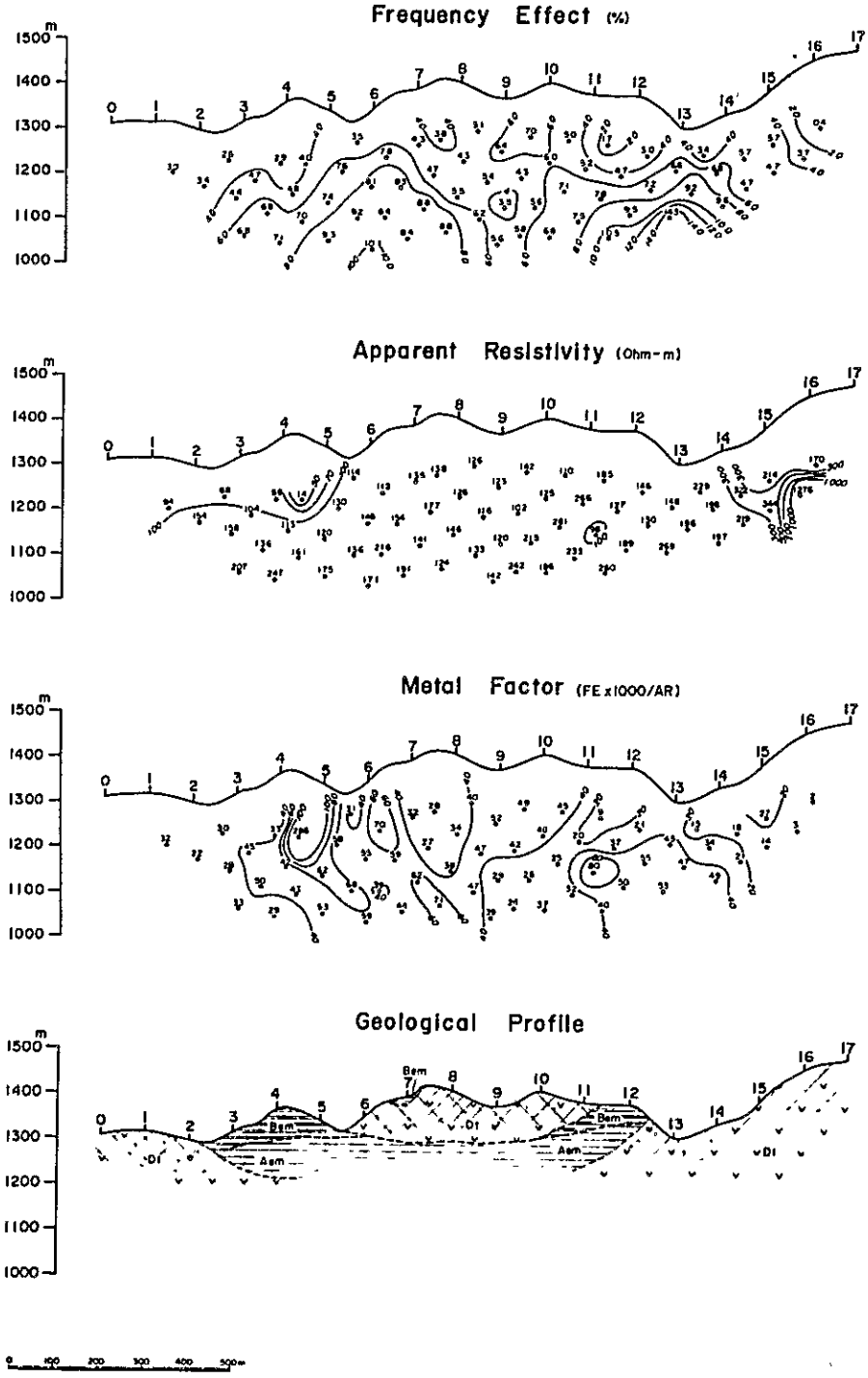

PL.4-40 Profile of IP survey in Sin area (Line S_2)

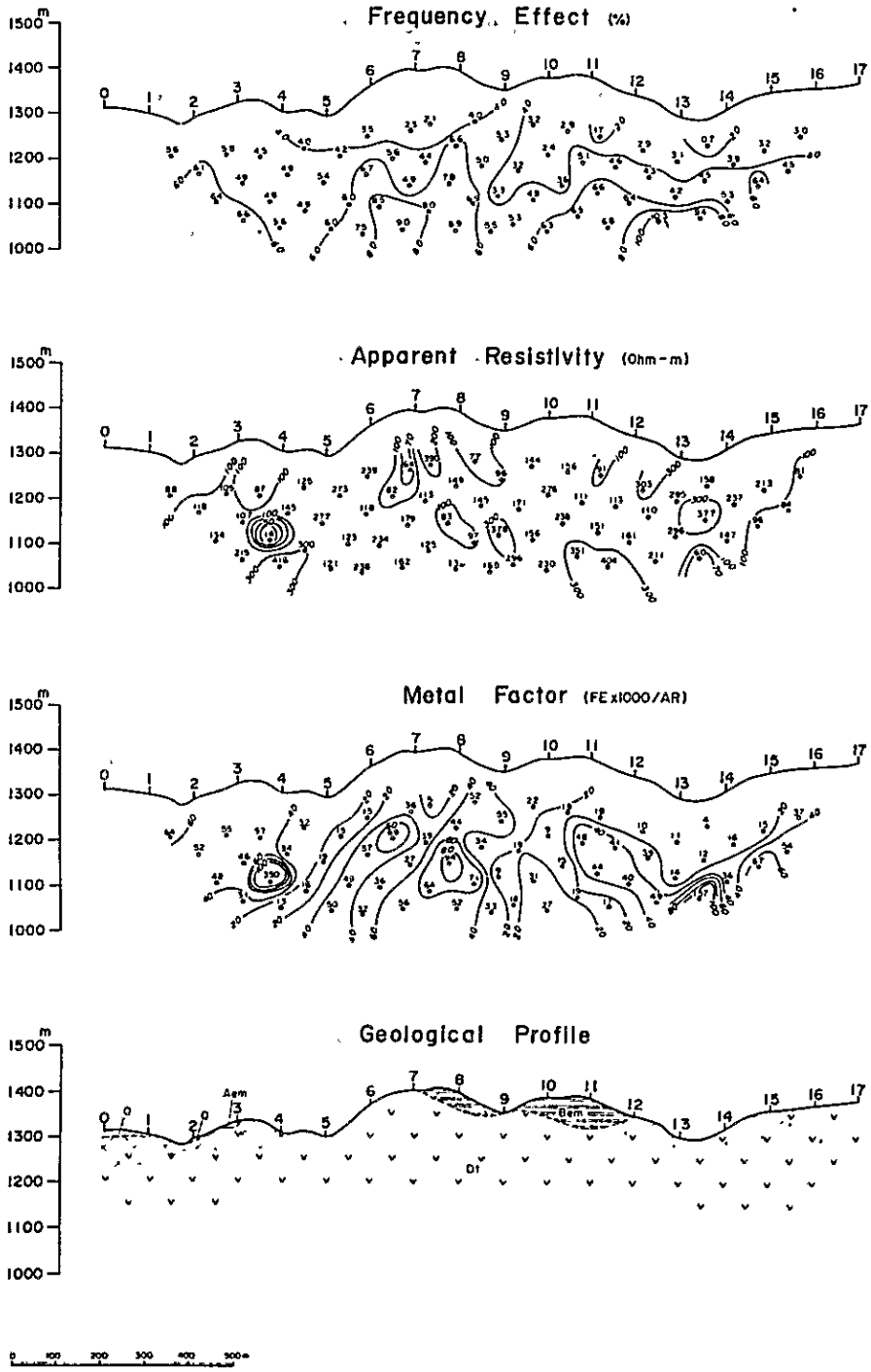

PL.4-41 Profile of IP survey in Sin area (Line S_3)

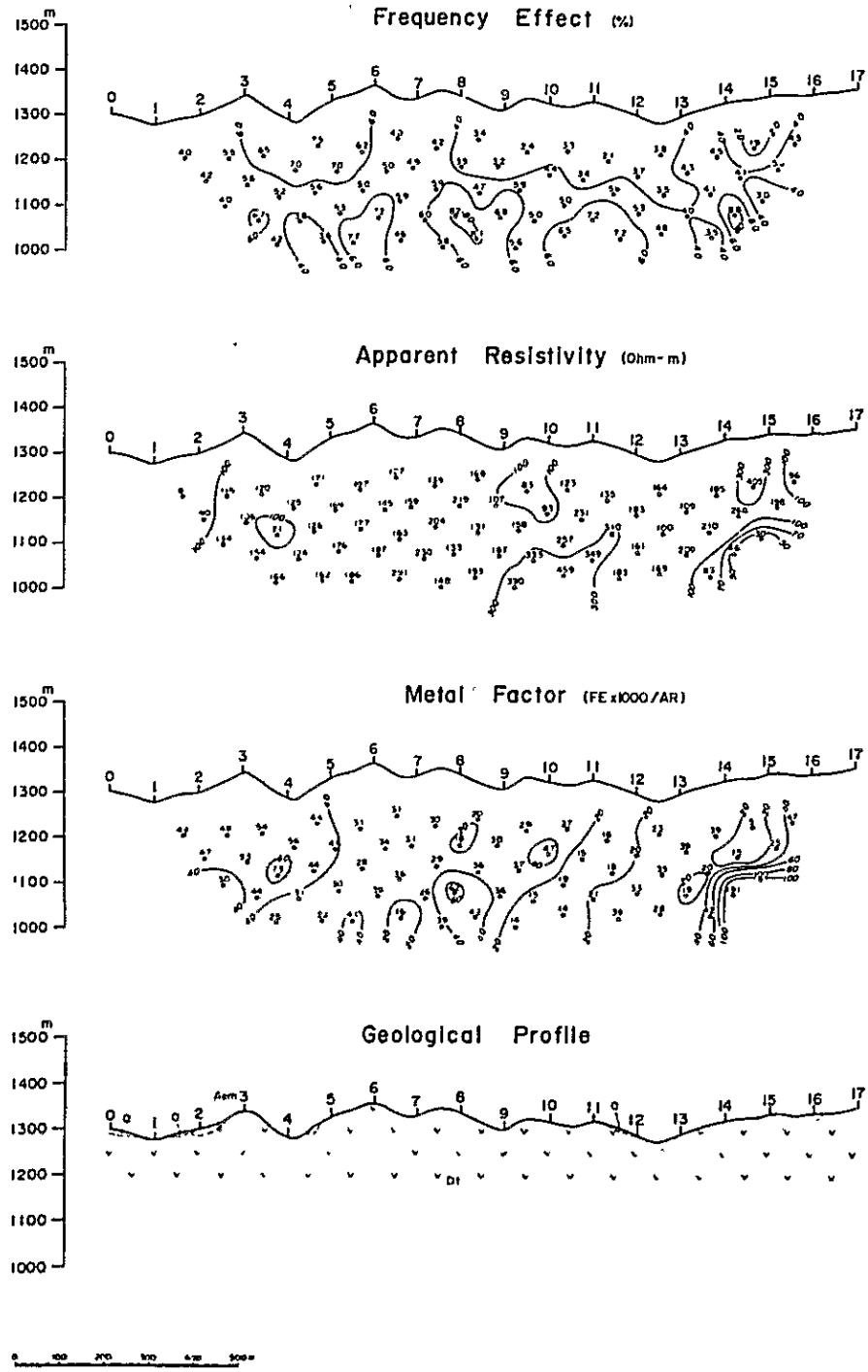

PL.4-42 Profile of IP survey in Sin area (Line S_4)

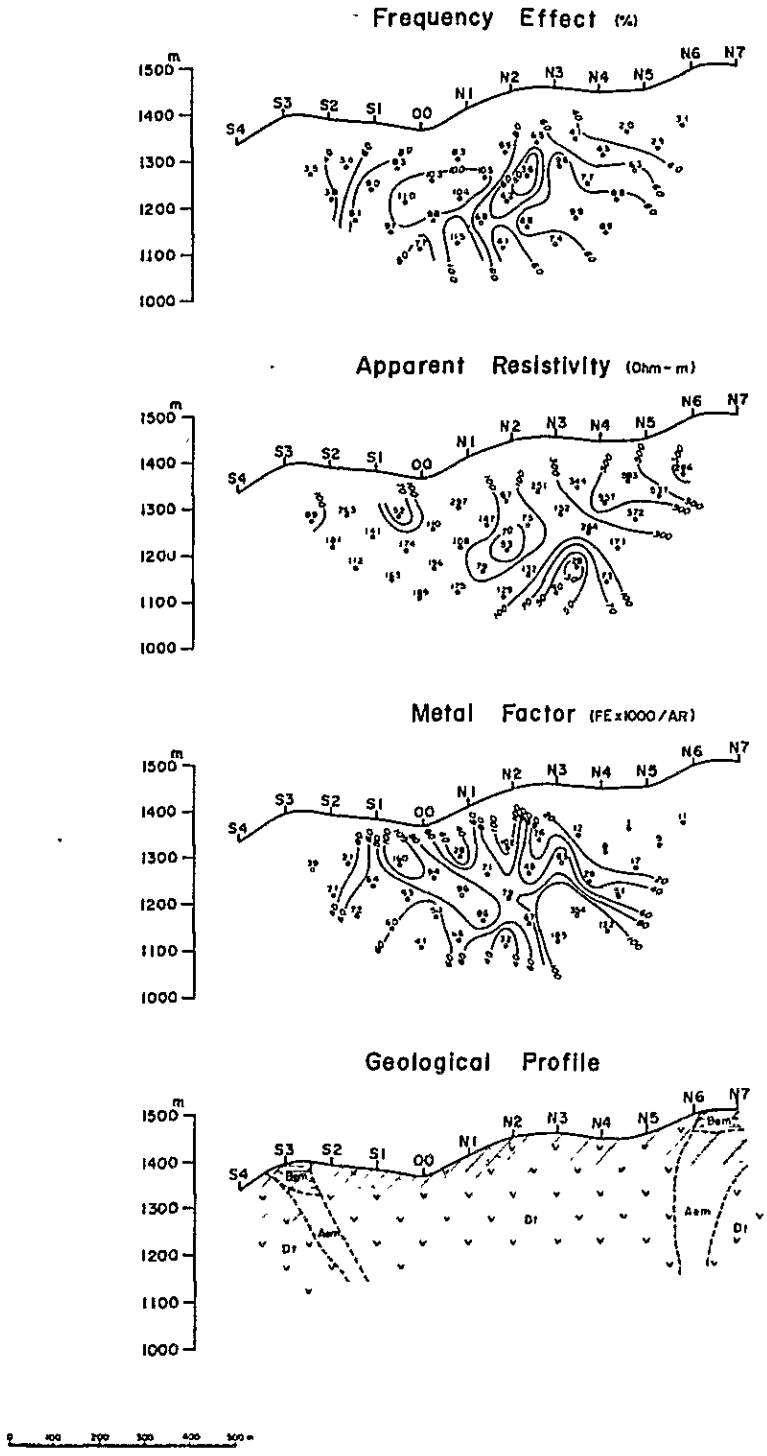

PL.4-43 Profile of IP survey in Sin area (Line Base (8))

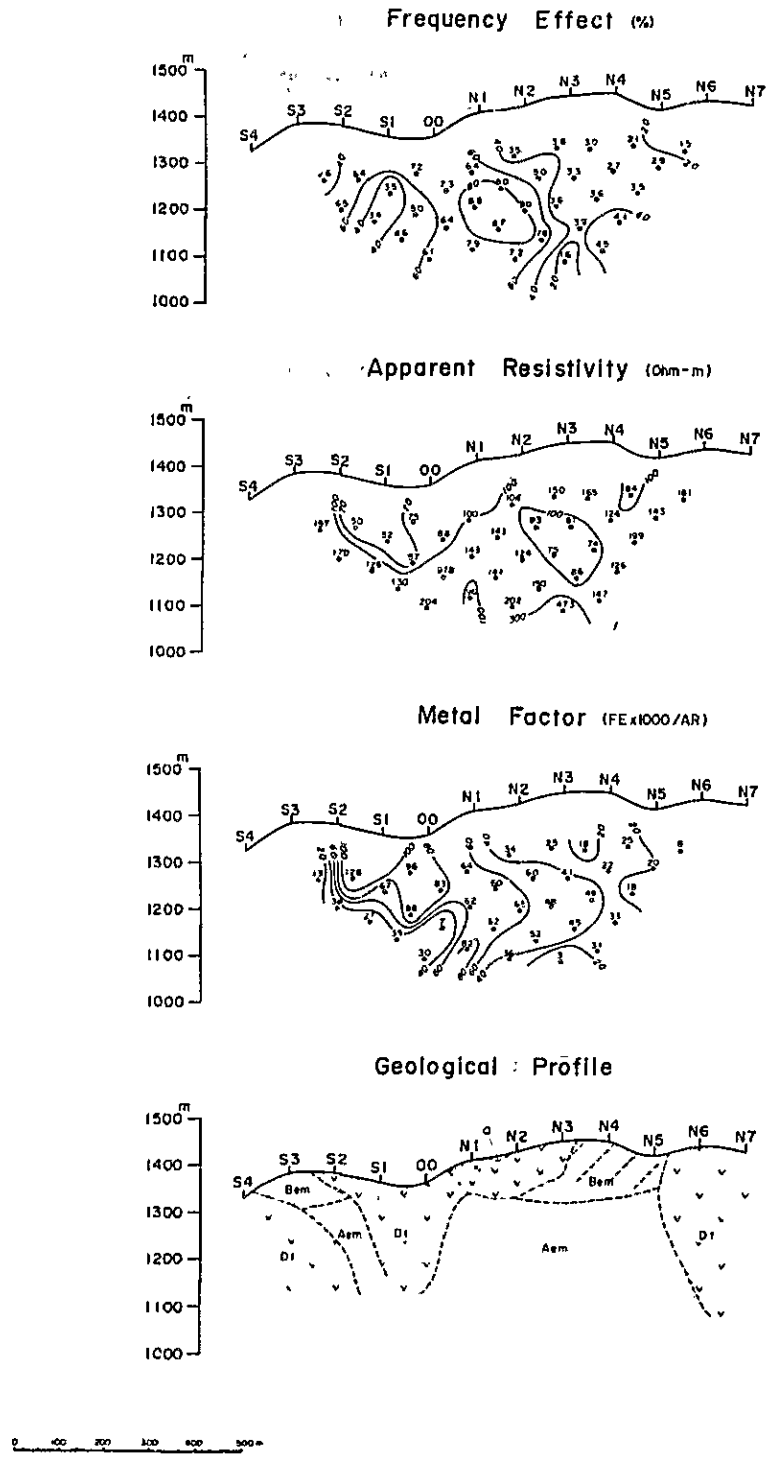

PL.4-44 Profile of IP survey in Sin area (Line Base (11))

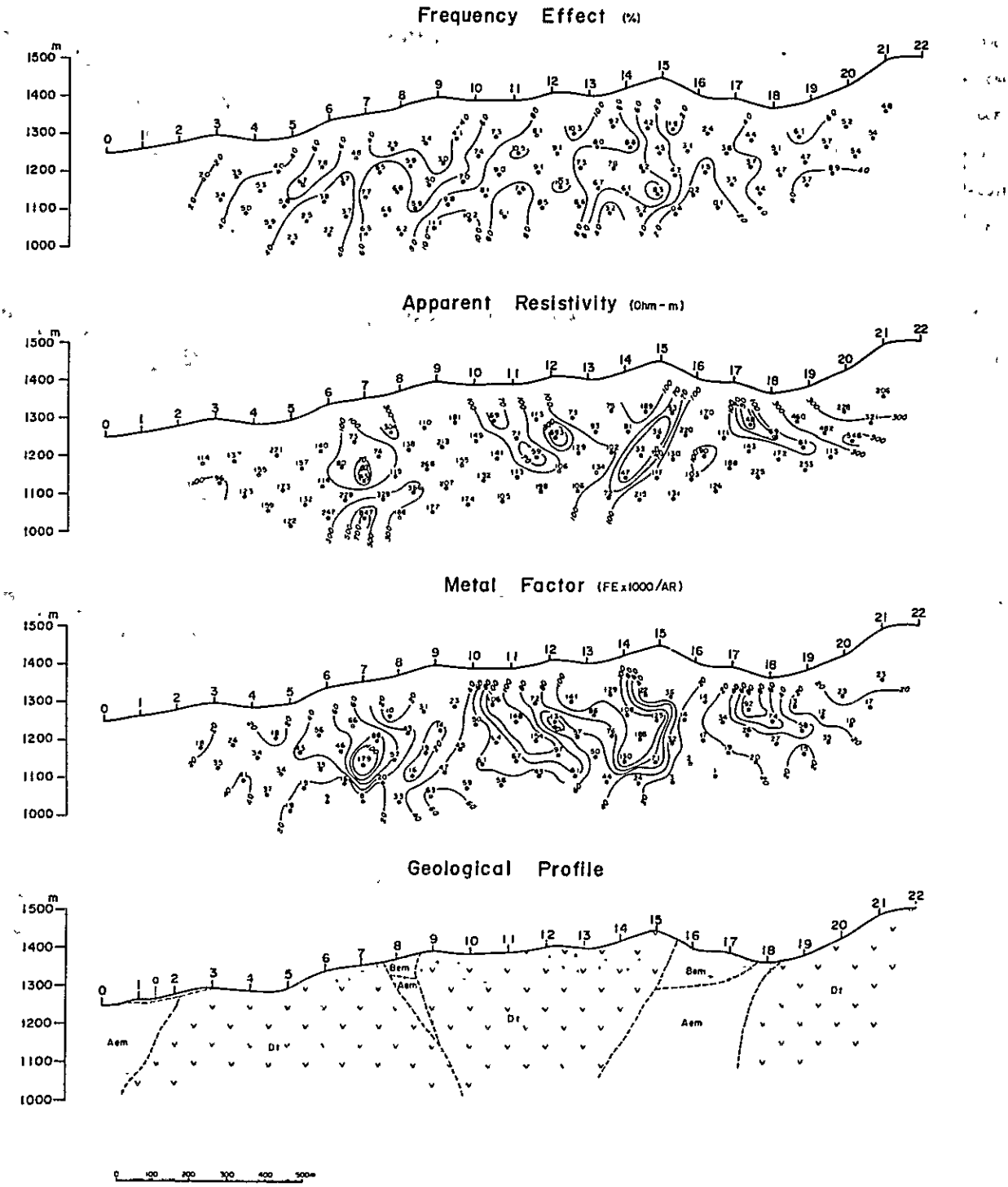

PL.4-45 Profile of IP survey in Sin area (Line K_1)

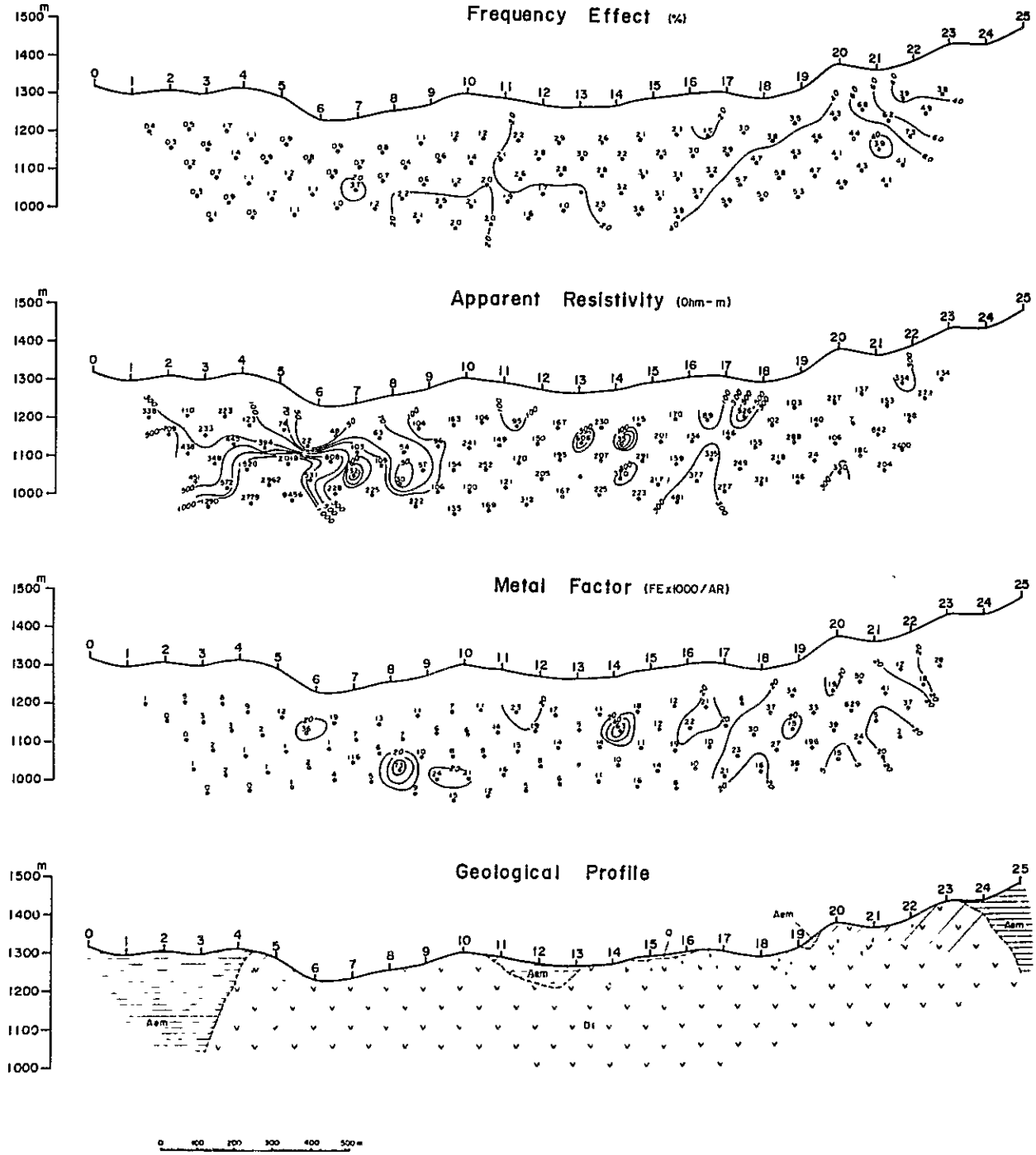

PL.4-46 Profile of IP survey in Sin area (Line K_2)

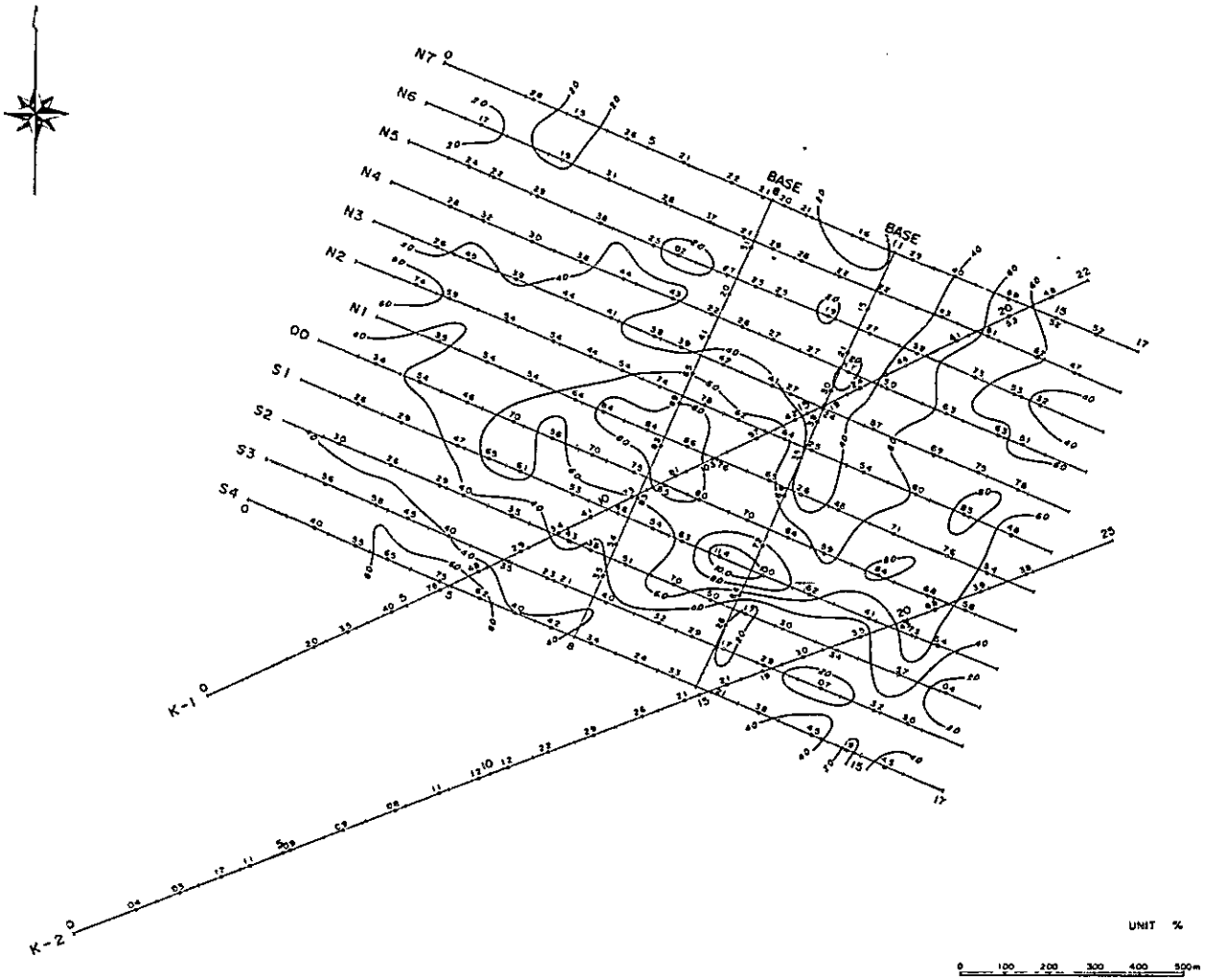

PL.4-47 FE plane map in Sin area (n=1)

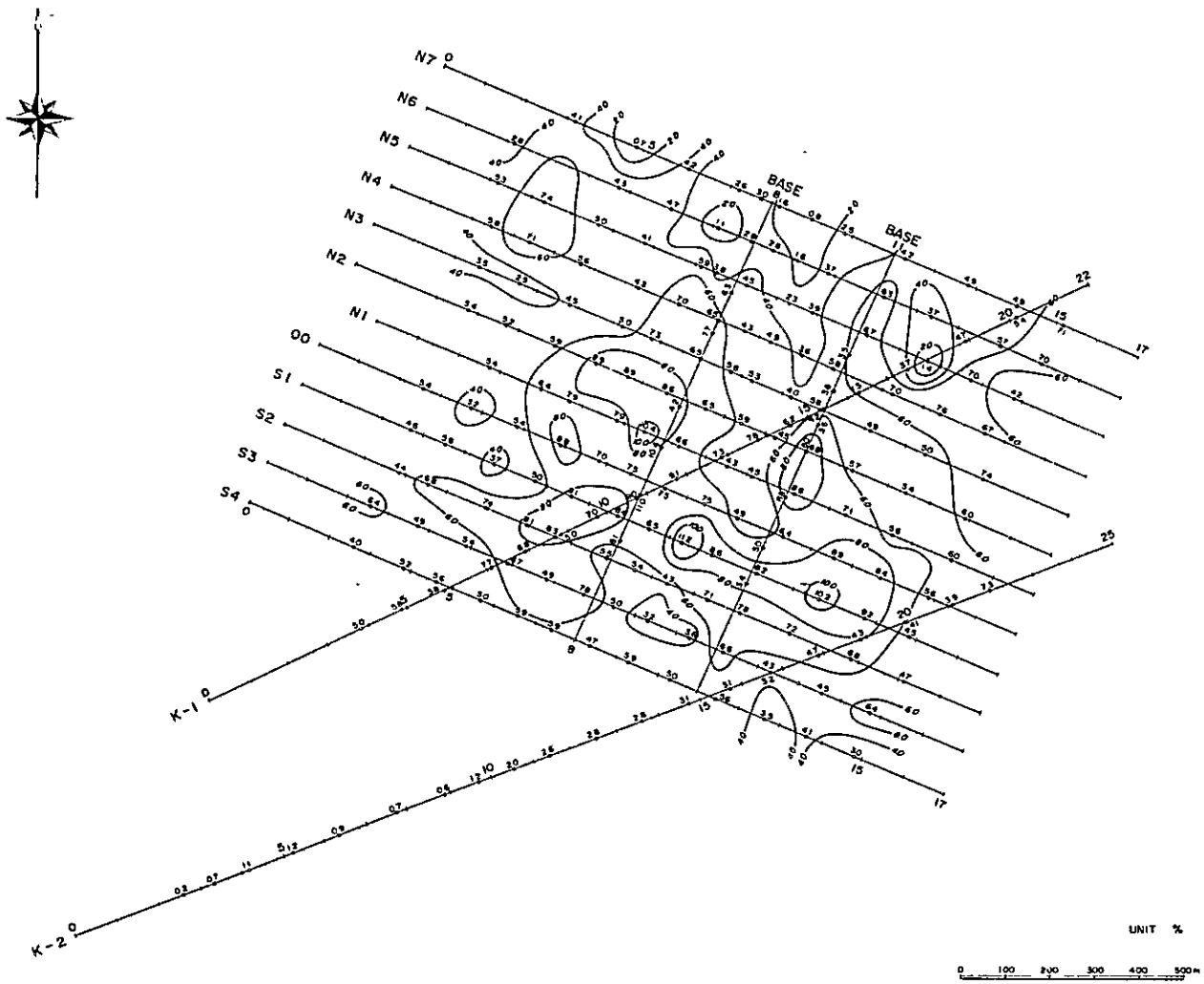

PL.4-48 FE plane map in Sin area (n=3)

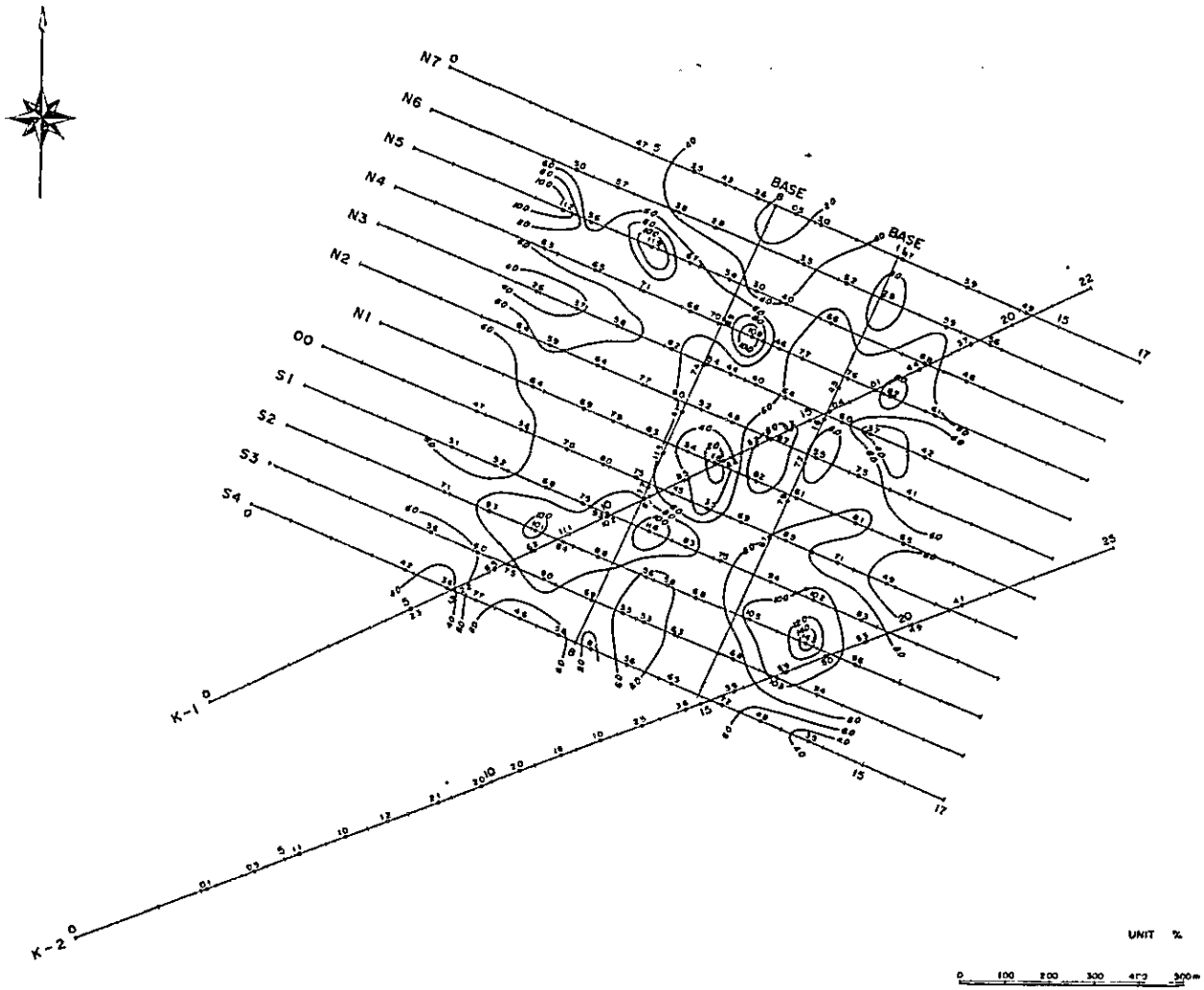

PL.4-49 FE plane map in Sin area (n=5)

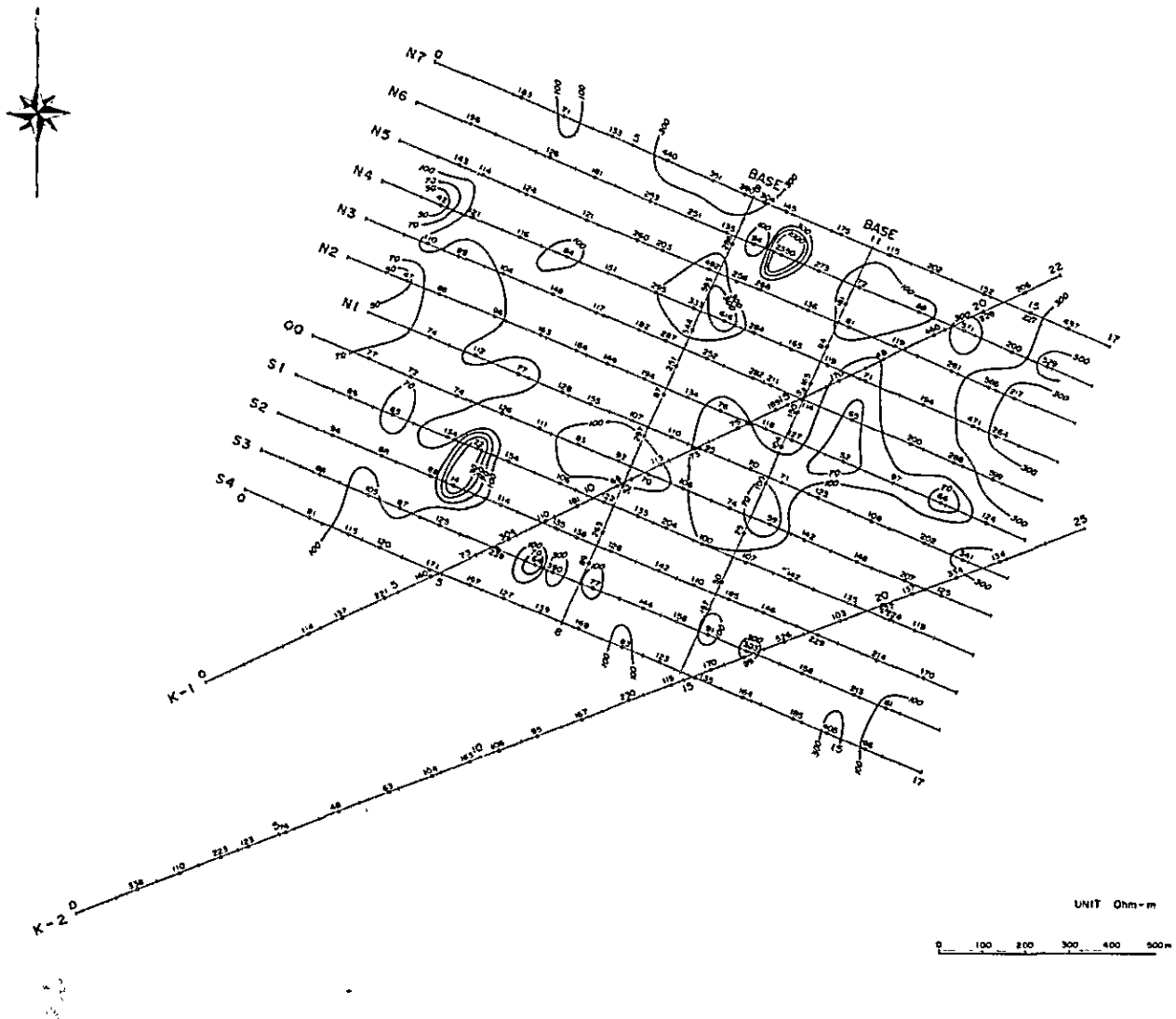

PL.4-50 AR plane map in Sin area (n=1)

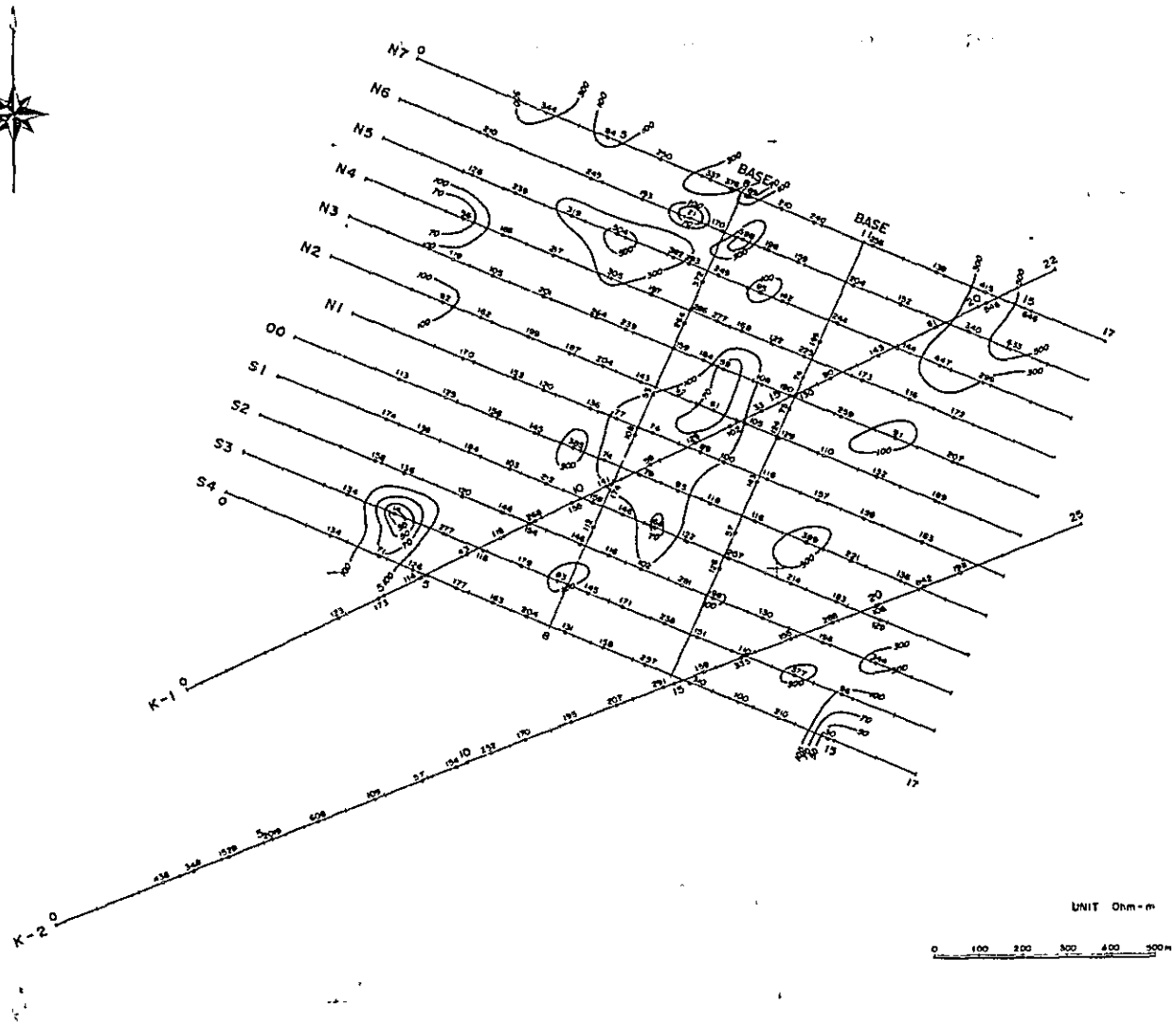

PL.4-51 AR plane map in Sin area (n=3)

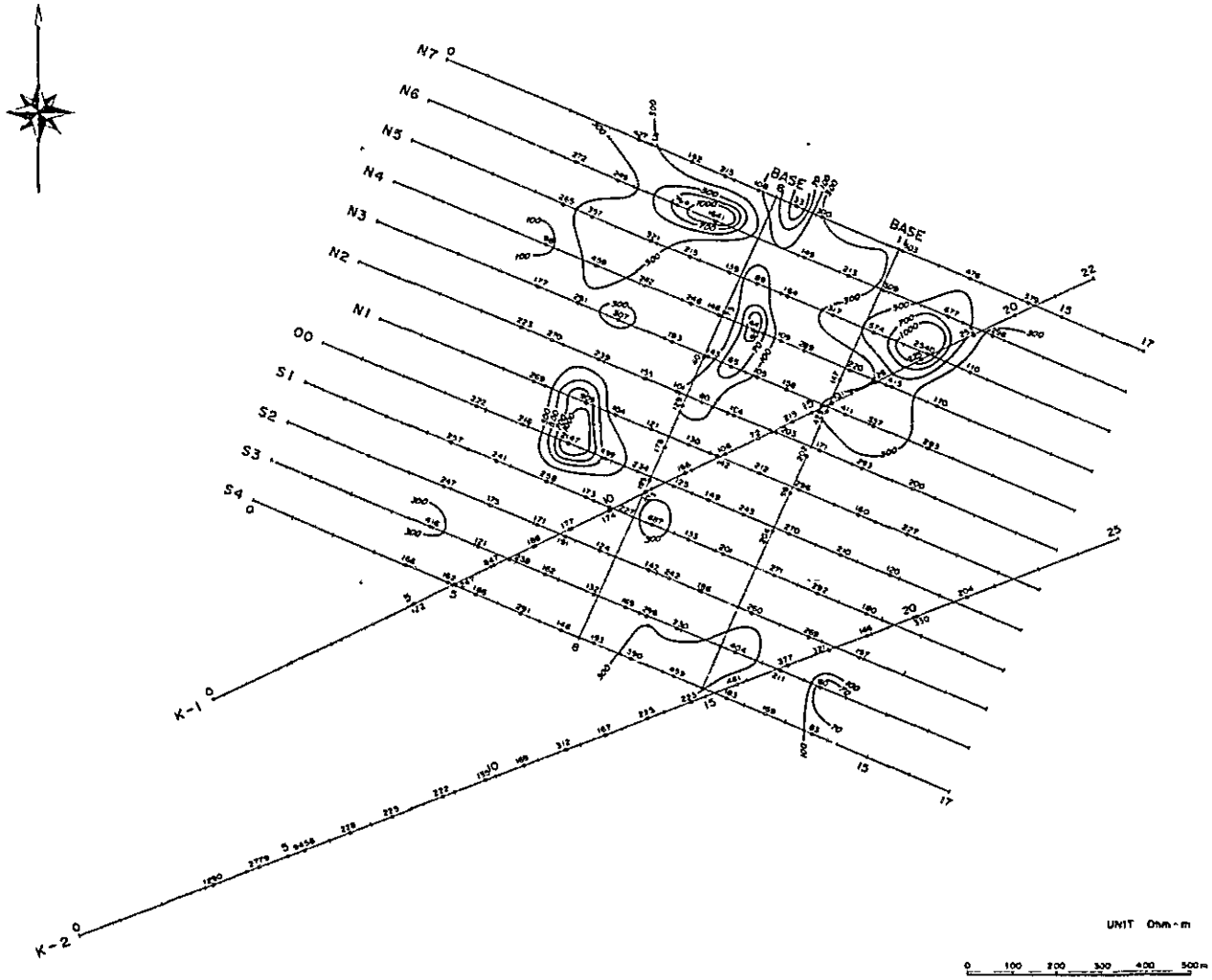

PL.4-52 AR plane map in Sin area (n=5)

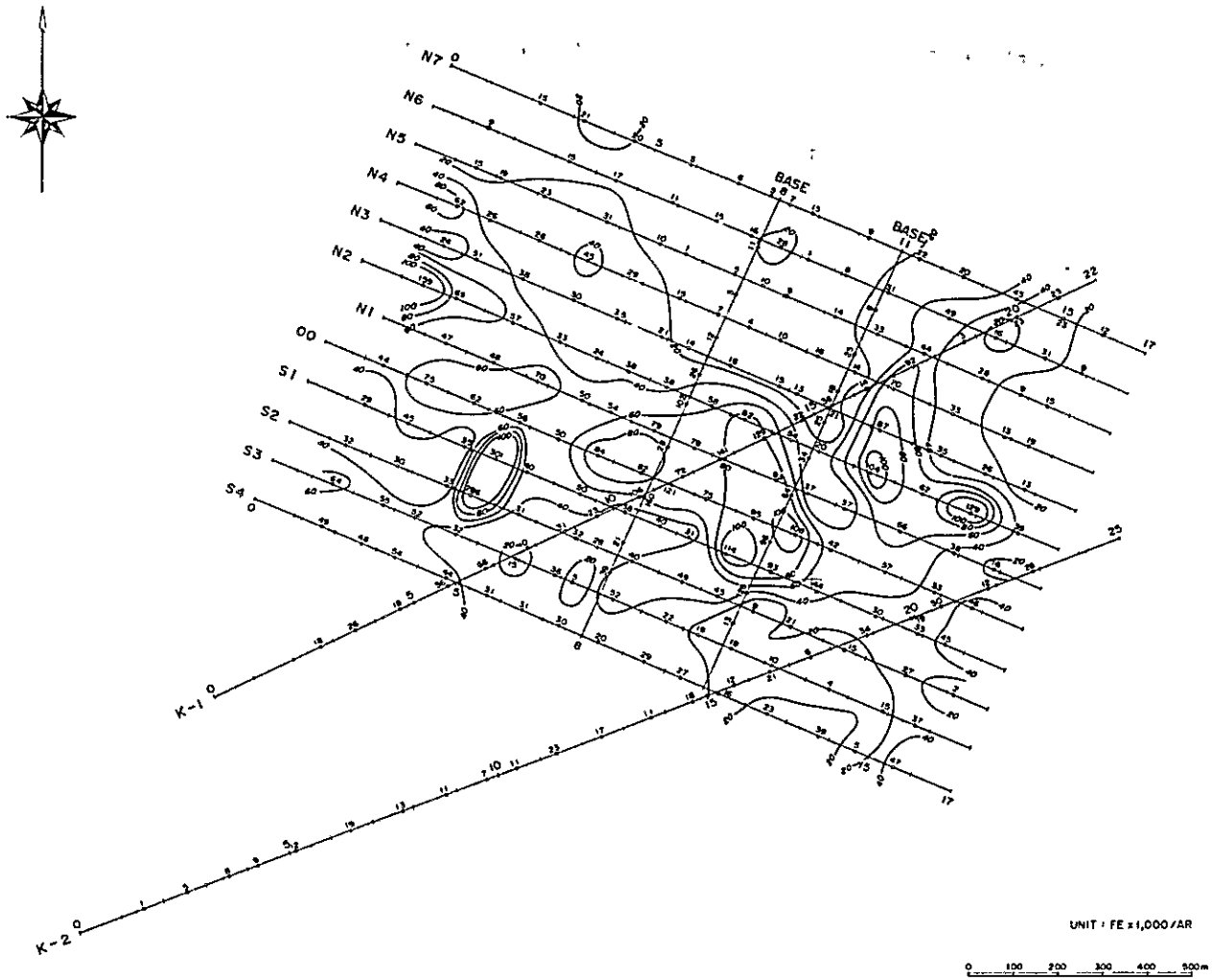

PL.4-53 MF plane map in Sin area (n=1)

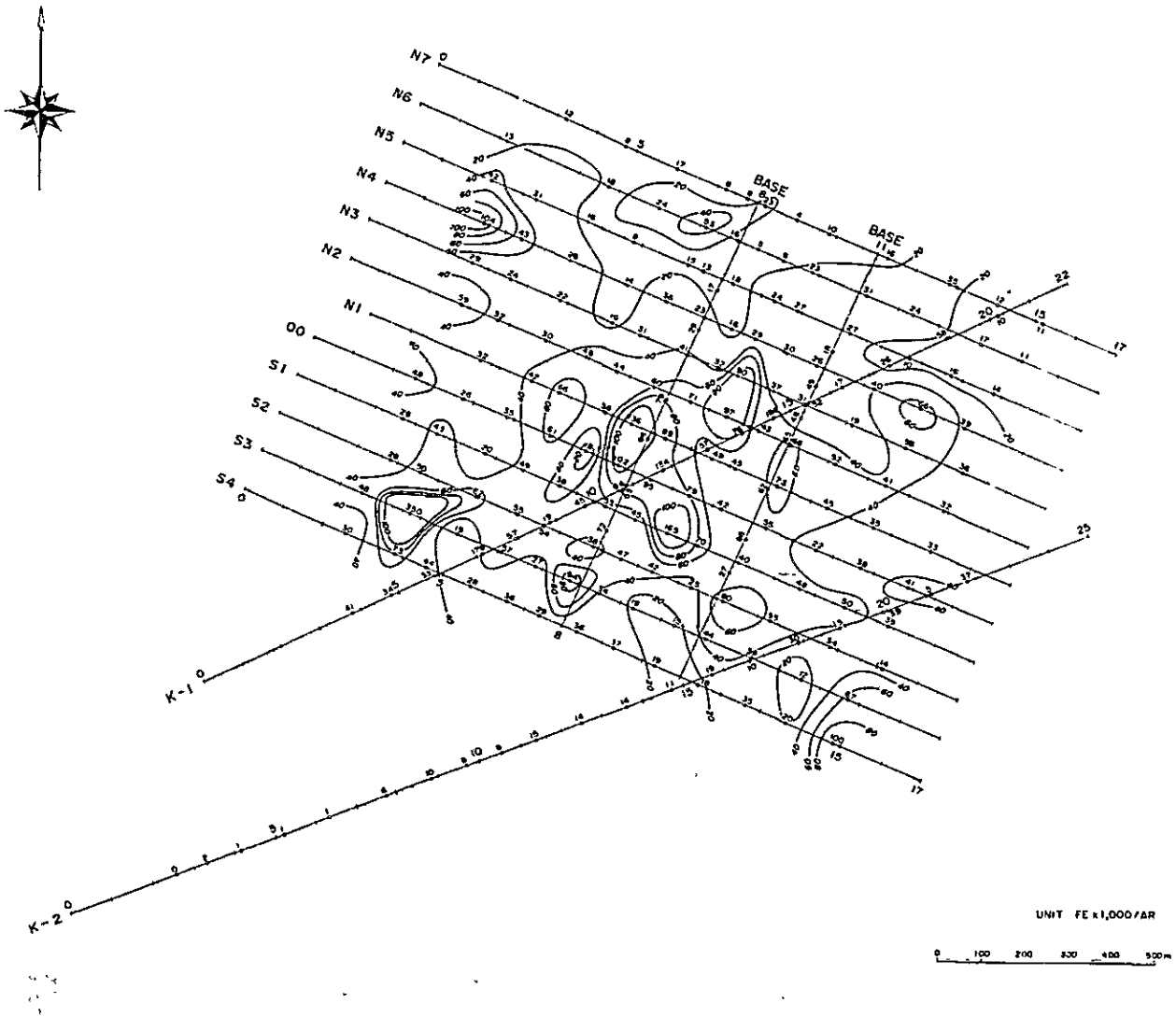

PL.4-54 MF plane map in Sin area (n=3)

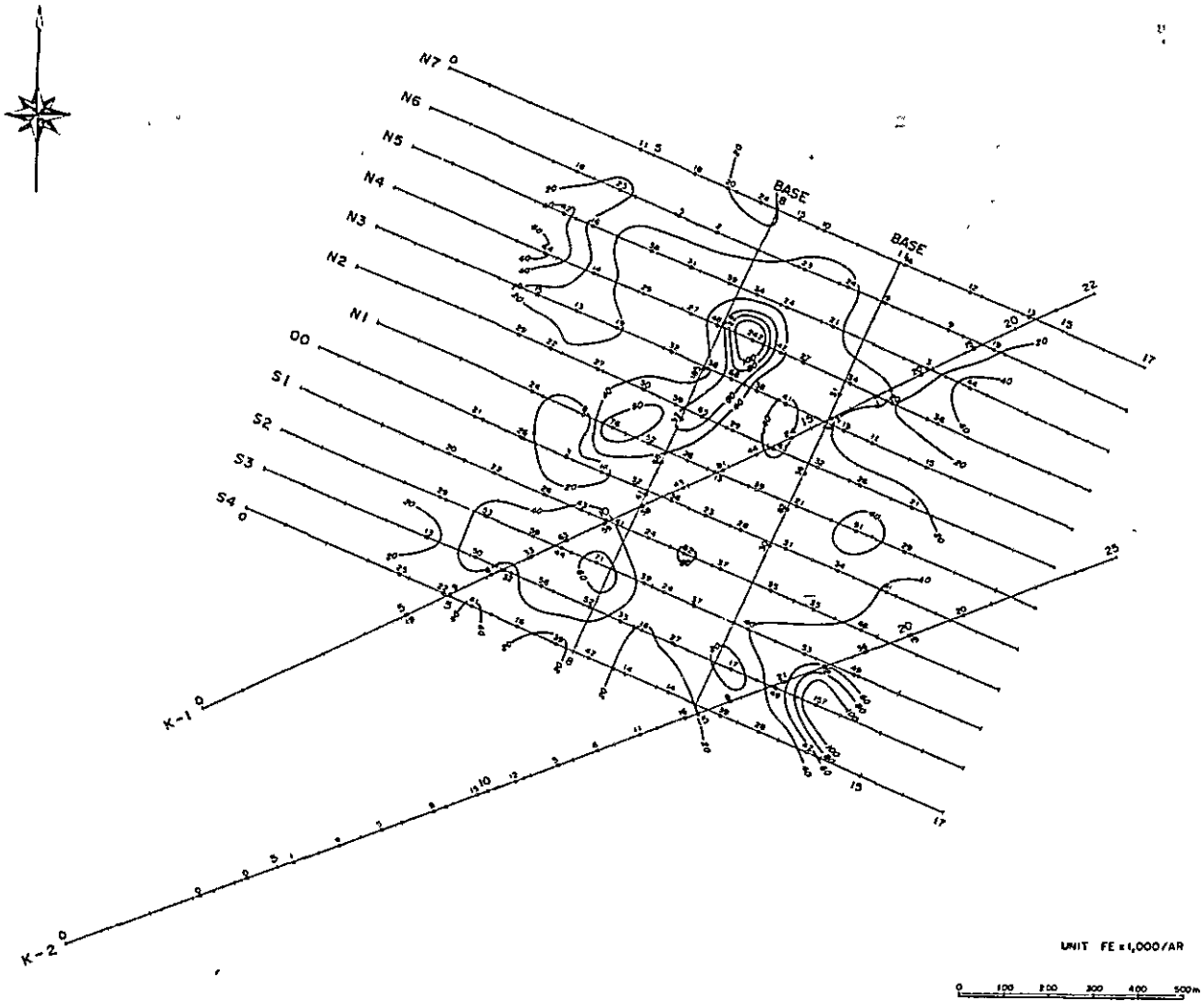

PL.4-55 MF plane map in Sin area (n=5)

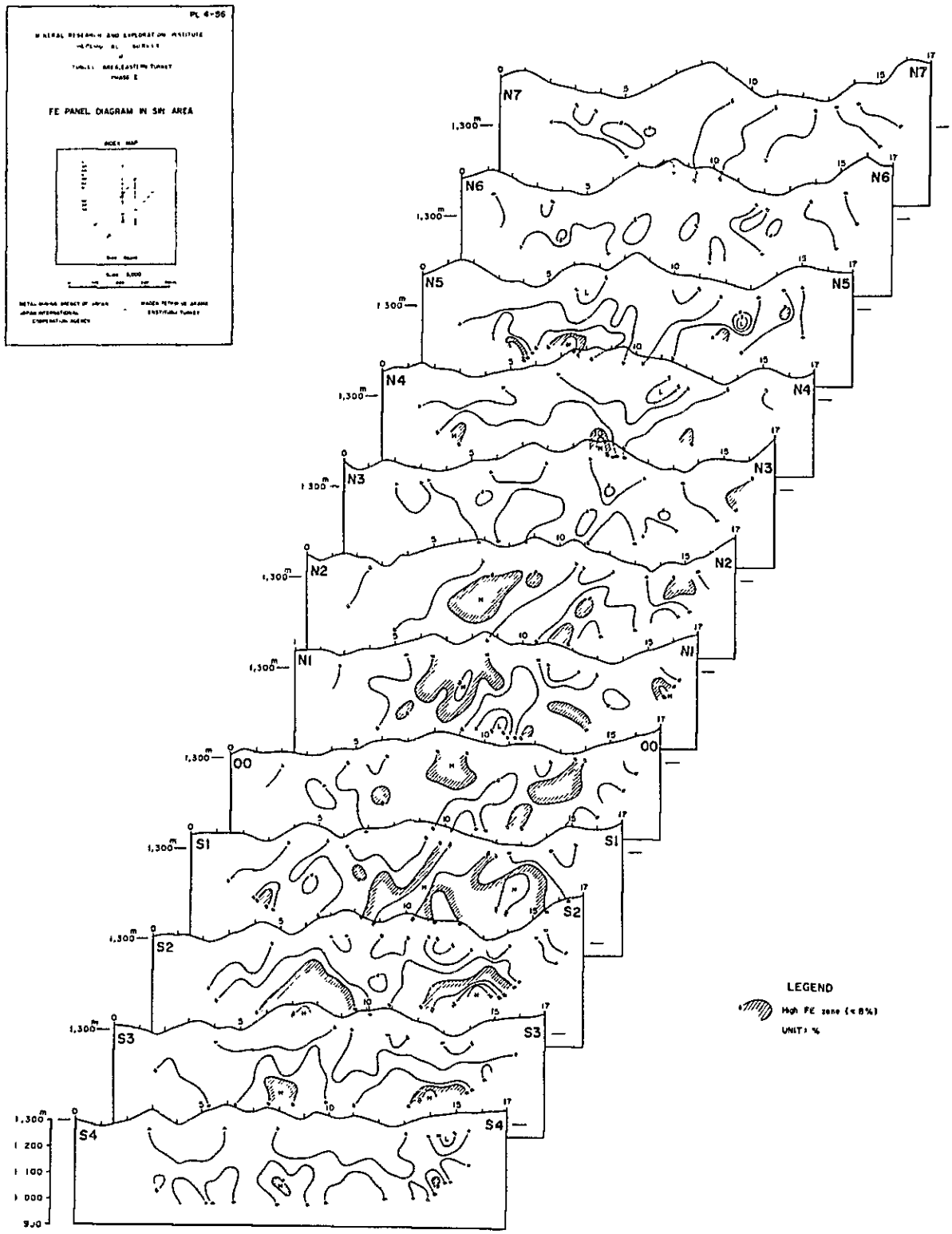

PL.4-56 FE panel diagram in Sin area

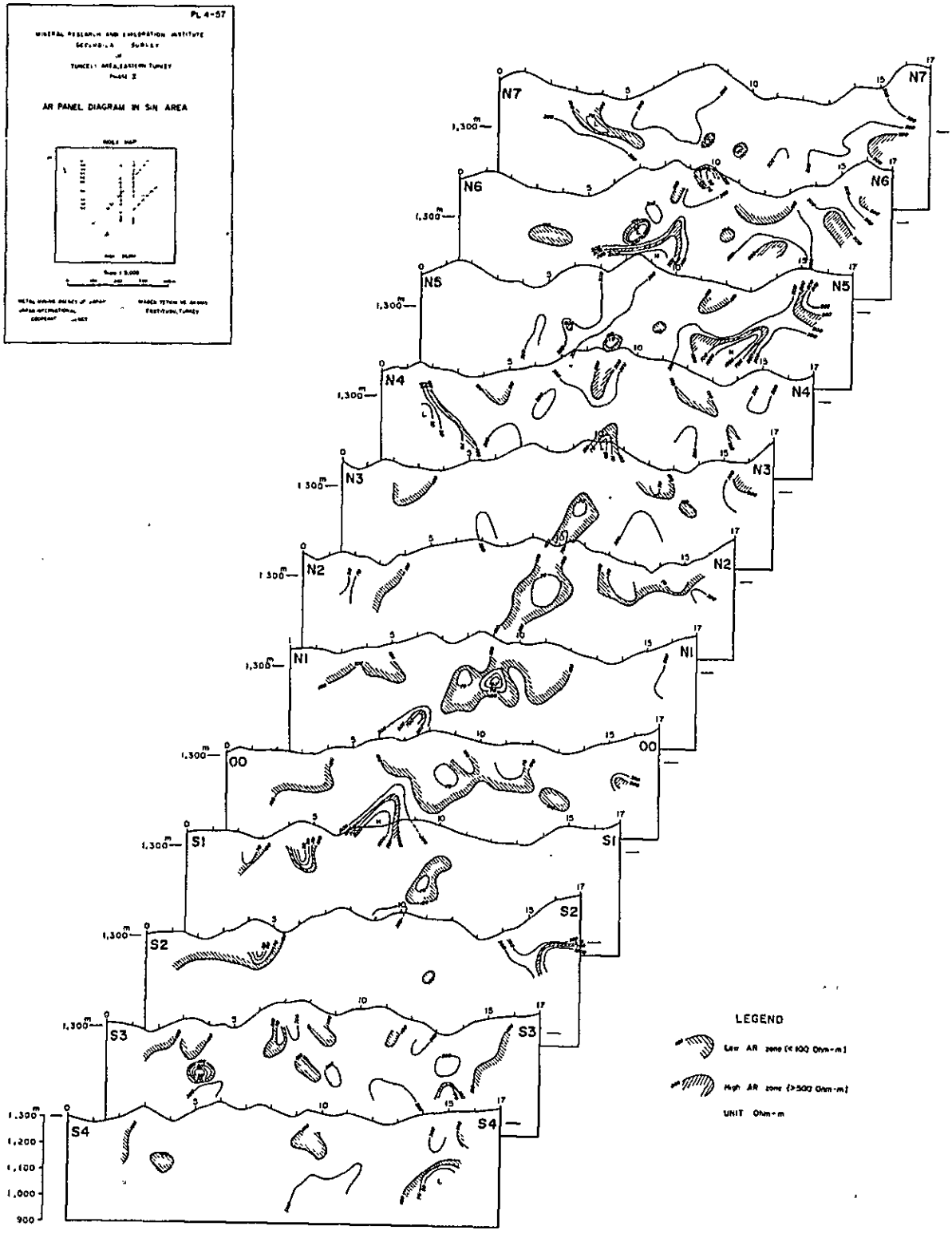

PL.4-57 AR panel diagram in Sin area

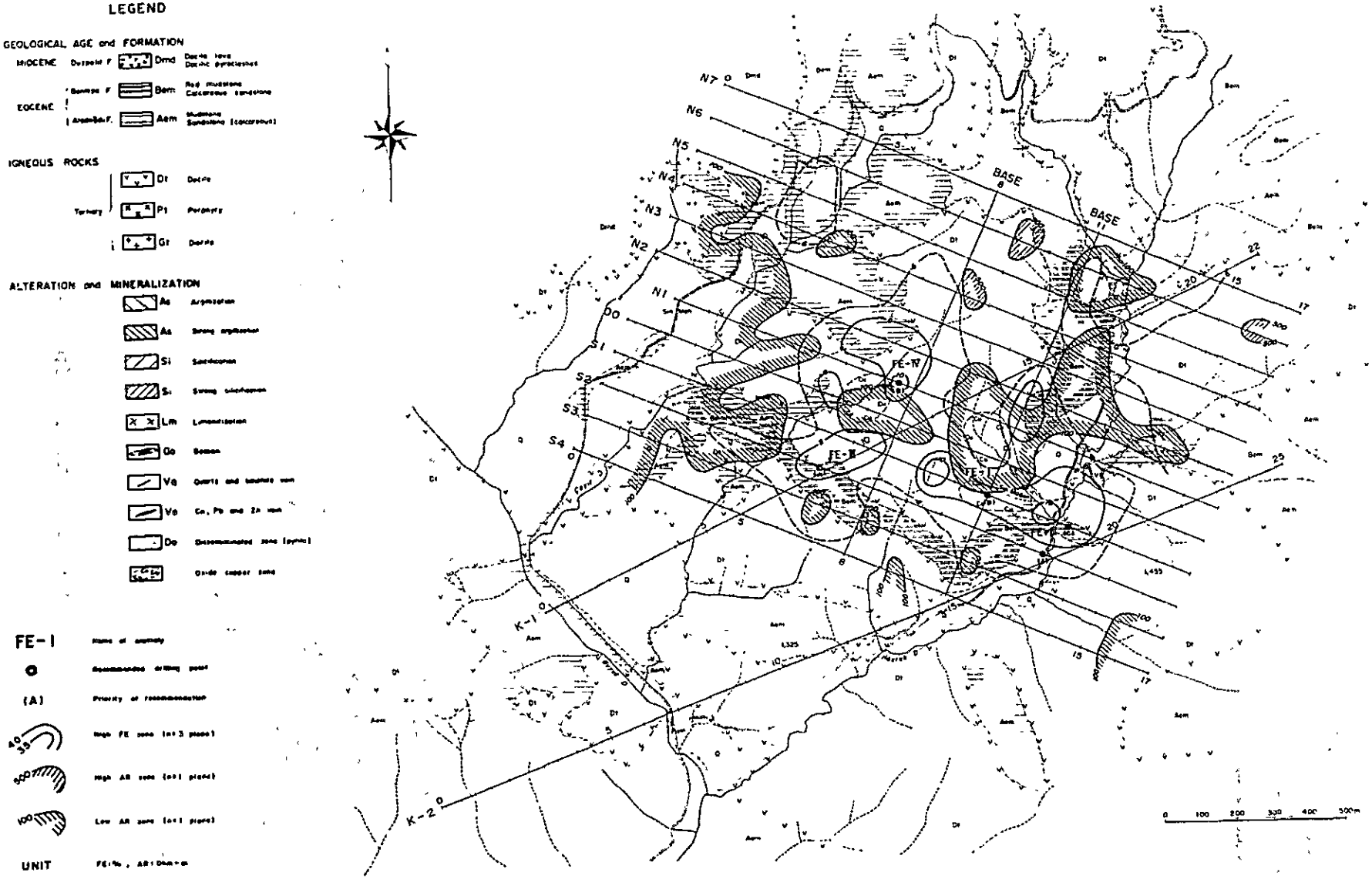

PL.4-58 Interpretation map in Sin area